A new phylogenetic hypothesis of Tanystropheidae (Diapsida, Archosauromorpha) and other “protorosaurs”, and its implications for the early evolution of stem archosaurs (#51657)

First submission

Guidance from your Editor

Please submit by **17 Sep 2020** for the benefit of the authors (and your $200 publishing discount) .

✓ **Structure and Criteria**
Please read the 'Structure and Criteria' page for general guidance.

▦ **Raw data check**
Review the raw data.

🖼 **Image check**
Check that figures and images have not been inappropriately manipulated.

Privacy reminder: If uploading an annotated PDF, remove identifiable information to remain anonymous.

Files

Download and review all files from the materials page.

35 Figure file(s)
1 Table file(s)
2 Raw data file(s)

Structure and Criteria

Structure your review

The review form is divided into 5 sections. Please consider these when composing your review:

1. **BASIC REPORTING**
2. **EXPERIMENTAL DESIGN**
3. **VALIDITY OF THE FINDINGS**
4. General comments
5. Confidential notes to the editor

You can also annotate this PDF and upload it as part of your review

When ready submit online.

Editorial Criteria

Use these criteria points to structure your review. The full detailed editorial criteria is on your guidance page.

BASIC REPORTING

- ✓ Clear, unambiguous, professional English language used throughout.
- ✓ Intro & background to show context. Literature well referenced & relevant.
- ✓ Structure conforms to PeerJ standards, discipline norm, or improved for clarity.
- ✓ Figures are relevant, high quality, well labelled & described.
- ✓ Raw data supplied (see PeerJ policy).

EXPERIMENTAL DESIGN

- ✓ Original primary research within Scope of the journal.
- ✓ Research question well defined, relevant & meaningful. It is stated how the research fills an identified knowledge gap.
- ✓ Rigorous investigation performed to a high technical & ethical standard.
- ✓ Methods described with sufficient detail & information to replicate.

VALIDITY OF THE FINDINGS

- *i* Impact and novelty not assessed. Negative/inconclusive results accepted. *Meaningful* replication encouraged where rationale & benefit to literature is clearly stated.
- ✓ All underlying data have been provided; they are robust, statistically sound, & controlled.
- ✓ Speculation is welcome, but should be identified as such.
- ✓ Conclusions are well stated, linked to original research question & limited to supporting results.

Standout reviewing tips

The best reviewers use these techniques

Tip	***Example***
Support criticisms with evidence from the text or from other sources	*Smith et al (J of Methodology, 2005, V3, pp 123) have shown that the analysis you use in Lines 241-250 is not the most appropriate for this situation. Please explain why you used this method.*
Give specific suggestions on how to improve the manuscript	*Your introduction needs more detail. I suggest that you improve the description at lines 57- 86 to provide more justification for your study (specifically, you should expand upon the knowledge gap being filled).*
Comment on language and grammar issues	*The English language should be improved to ensure that an international audience can clearly understand your text. Some examples where the language could be improved include lines 23, 77, 121, 128 – the current phrasing makes comprehension difficult.*
Organize by importance of the issues, and number your points	*1. Your most important issue* *2. The next most important item* *3. …* *4. The least important points*
Please provide constructive criticism, and avoid personal opinions	*I thank you for providing the raw data, however your supplemental files need more descriptive metadata identifiers to be useful to future readers. Although your results are compelling, the data analysis should be improved in the following ways: AA, BB, CC*
Comment on strengths (as well as weaknesses) of the manuscript	*I commend the authors for their extensive data set, compiled over many years of detailed fieldwork. In addition, the manuscript is clearly written in professional, unambiguous language. If there is a weakness, it is in the statistical analysis (as I have noted above) which should be improved upon before Acceptance.*

A new phylogenetic hypothesis of Tanystropheidae (Diapsida, Archosauromorpha) and other “protorosaurs”, and its implications for the early evolution of stem archosaurs

Stephan N F Spiekman Corresp., 1 , **Nicholas C Fraser** 2 , **Torsten M Scheyer** 1

1 Palaeontological Institute and Museum, University of Zurich, Zurich, Switzerland

2 National Museums Scotland, Edinburgh, United Kingdom

Corresponding Author: Stephan N F Spiekman
Email address: stephanspiekman@gmail.com

The historical clade “Protorosauria” represents an important group of archosauromorph reptiles that had a wide geographic distribution between the Late Permian and Late Triassic. “Protorosaurs” are characterized by their long necks, which are epitomized in the genus *Tanystropheus* and in *Dinocephalosaurus orientalis*. Recent phylogenetic analyses have indicated that “Protorosauria” is a polyphyletic clade, but the exact relationships of the various “protorosaur” taxa within the archosauromorph lineage is currently uncertain. Several taxa, although represented by relatively complete material, have previously not been assessed phylogenetically. We present a new phylogenetic hypothesis that comprises a wide range of archosauromorphs, including the most exhaustive sample of “protorosaurs” to date and several “protorosaur” taxa from the eastern Tethys margin that have not been included in any previous analysis. The polyphyly of “Protorosauria” is confirmed and therefore we suggest the usage of this term should be abandoned. Tanystropheidae is recovered as a monophyletic group and the Chinese taxa *Dinocephalosaurus orientalis* and *Pectodens zhenyuensis* form a new archosauromorph clade, Dinocephalosauridae, which is closely related to Tanystropheidae. The well-known crocopod and former “protorosaur” *Prolacerta broomi* is considerably less closely related to Archosauriformes than was previously considered.

A new phylogenetic hypothesis of Tanystropheidae (Diapsida, Archosauromorpha) and other "protorosaurs", and its implications for the early evolution of stem archosaurs

Stephan N. F. Spiekman[1], Nicholas C. Fraser[2], Torsten M. Scheyer[1]

[1]University of Zurich, Palaeontological Institute and Museum, Karl-Schmid-Strasse 4, 8006 Zurich, Switzerland

[2]National Museums Scotland, Chambers St, Edinburgh EH1 1JF, UK

Corresponding author:
Stephan Spiekman
Karl-Schmid-Strasse 4, 8006 Zurich, Switzerland
Email address: stephanspiekman@gmail.com

Abstract

The historical clade "Protorosauria" represents an important group of archosauromorph reptiles that had a wide geographic distribution between the ~~Late~~ Permian and Late Triassic. "Protorosaurs" are characterized by their long necks, which are epitomized in the genus *Tanystropheus* and in *Dinocephalosaurus orientalis*. Recent phylogenetic analyses have indicated that "Protorosauria" is a polyphyletic clade, but the exact relationships of the various "protorosaur" taxa within the archosauromorph lineage is currently uncertain. Several taxa, although represented by relatively complete material, have previously not been assessed phylogenetically. We present a new phylogenetic hypothesis that comprises a wide range of archosauromorphs, including the most exhaustive sample of "protorosaurs" to date and several "protorosaur" taxa from the eastern Tethys margin that have not been included in any previous analysis. The polyphyly of "Protorosauria" is confirmed and therefore we suggest the usage of this term should be abandoned. Tanystropheidae is recovered as a monophyletic group and the Chinese taxa *Dinocephalosaurus orientalis* and *Pectodens zhenyuensis* form a new archosauromorph clade, Dinocephalosauridae, which is closely related to Tanystropheidae. The well-known crocopod and

former “protorosaur” *Prolacerta broomi* is considerably less closely related to Archosauriformes than was previously considered.

Introduction

Non-archosauriform archosauromorphs lived during the ~~Late~~ Permian and Triassic and belong to the archosaurian stem-lineage, the ancestral lineage of crocodylians and birds. Historically, many members of this group were placed within either “Protorosauria” or “Prolacertiformes”. These two groups generally encompassed the same taxa and the usage of one term over the other depended on the inclusion within the clade of either *Protorosaurus speneri* or *Prolacerta broomi*, or both. Since both names generally apply to the same taxa and are often used interchangeably, and because “Protorosauria” Huxley 1871 predates “Prolacertiformes” Camp 1945, we refer to the members of these groups here as “Protorosauria” (sensu Chatterjee 1986). Apart from the two above mentioned taxa, the terrestrial and aquatic long-necked tanystropheids (e.g. *Tanystropheus*, *Macrocnemus*, *Langobardisaurus*, and *Tanytrachelos*) represent the most important and widely included members of “Protorosauria”. Formerly, the enigmatic arboreal drepanosaurids were also referred to the clade, but they have recently been revealed to represent a separate clade of non-saurian diapsids (Pritchard & Nesbitt 2017; Pritchard et al. 2016). As Permo-Triassic non-archosauriform archosauromorphs, “protorosaurs” represent some of the earliest members of the archosaur-lineage and as such are important both for our understanding of early archosauromorph evolution and the acquisition of traits within the archosaur character complex. For instance, the Chinese dinocephalosaurids represent the only known viviparous archosauromorphs (Li et al. 2017b; Liu et al. 2017).

Recent cladistic studies have extensively dealt with early archosauromorph phylogeny (early Archosauria, Nesbitt 2011; early Archosauromorpha with a focus on proterosuch~~ids~~, Ezcurra 2016; Allokotosauria, Nesbitt et al. 2015; Rhynchosauria, Butler et al. 2015 and Ezcurra et al. 2016; and Tanystropheidae, Pritchard et al. 2015). These, and some earlier analyses, indicate that “Protorosauria” does not form a monophyletic clade as historically considered, but rather represents a paraphyletic or polyphyletic grouping of non-archosauriform archosauromorphs (*Fig. 1*, but for an exception see Simões et al. 2018, who recovered Protorosauria excluding *Prolacerta* as a monophyletic clade outside Archosauromorpha). However, none of these analyses were constructed to specifically address the interrelationships of “Protorosauria” and many recently described taxa (e.g. the genera *Pectodens*, *Fuyuansaurus*, *Dinocephalosaurus*, *Raibliania*, *Elessaurus*, and *Sclerostropheus*) attributed to the group have not been included (Dalla Vecchia 2020; De Oliveira et al. 2020; Fraser et al. 2013; Li et al. 2017a;

Rieppel et al. 2008; Spiekman & Scheyer 2019). Moreover, the two best known tanystropheid genera, *Tanystropheus* and *Macrocnemus*, were recently revised extensively, revealing much additional morphological information, particular with regards to the skull, which has not been incorporated in the abovementioned analyses (Miedema et al. 2020; Spiekman et al. 2020).

Here we present an extensive phylogenetic analysis, focusing on “protorosaur” and other early archosauromorph interrelationships. The new dataset includes 42 operational taxonomic units (OTUs), of which 23 are “protorosaurs”, and employs 307 morphological characters, many of which are new or distinctly revised from previous analyses. Since the definition of “Protorosauria” in the literature is inconsistent, with many taxa having been placed alternately within and outside the group, we first provide a historical overview of “protorosaur” systematics and discuss the taxa that have formerly been included in the group. Several of these are represented by very fragmentary material or have since been identified as belonging to an entirely separate lineage to that of the archosauromorph “protorosaurs”, and they were therefore not included in ~~the~~ phylogenetic analysis.

Historical background of “Protorosauria”

Protorosaurus speneri was one of the earliest known fossil reptiles, first described in Latin by Spener (1710). He considered *Protorosaurus* to be a crocodile, with many similarities specifically to the Nile crocodile, *Crocodylus niloticus* (Gottmann-Quesada & Sander 2009). More than a century later, *Protorosaurus* was recognized as an extinct reptile (Meyer 1830), and subsequently assigned a species definition (Meyer 1832), and covered in an extensive monograph (Meyer 1856). The clade “Protorosauria”, with *Protorosaurus* as the only representative, was erected by Huxley (1871), as part of Sauropsida, then as now considered to be the clade that encompasses all modern birds and reptiles and their direct ancestors. In his classification of the reptiles, Osborn (1903) provided the first definition of “Protorosauria” and assigned *Palaeohatteria*, a synapsid (Fröbisch et al. 2011), and *Kadaliosaurus*, an araeoscelid diapsid (DeBraga & Reisz 1995), to the clade. Therein, the group was closely related to dinosaurs. Williston (1925) placed “protorosaurs” within “Parapsida" alongside squamates, ichthyosaurs, and mesosaurs. Other genera that were included within “Protorosauria” were *Sapheosaurus* and *Pleurosaurus*, now firmly established rhynchocephalians (Hsiou et al. 2019; Rauhut et al. 2012), and *Araeoscelis* and *Aphelosaurus*, now considered to be early non-neodiapsid diapsids (Ezcurra et al. 2014; Reisz et al. 2011b).

After extensive excavations at the Anisian-Ladinian deposits of Monte San Giorgio on the border between Switzerland and Italy, newly discovered specimens allowed for the first comprehensive description of both *Tanystropheus longobardicus* and *Macrocnemus bassanii* (Peyer 1931; Peyer 1937). Initially *Tanystropheus longobardicus* was placed within a newly erected suborder “Tanysitrachelia”, which apart from *Tanystropheus* also included *Trachelosaurus fischeri*, a small, long-necked reptile from the Buntsandstein (Early to Middle Triassic) of Germany (Broili & Fischer 1918). “Tanysitrachelia” was placed within Sauropterygia (Peyer 1931). *Trachelosaurus* is only known from a few disarticulated postcranial elements and therefore its phylogenetic position is uncertain, although it is currently still considered a “protorosaur” (Benton & Allen 1997; Jalil 1997; Rieppel et al. 2003). However, in the later report on *Macrocnemus bassanii*, Peyer (1937) found many comparisons between *Protorosaurus* and both *Macrocnemus* and *Tanystropheus*, and therefore both taxa were reassigned to “Protorosauria”, which was considered closely related to squamates and rhynchocephalians rather than archosaurs therein.

Around the same time *Prolacerta broomi* was described and assigned to the newly erected family “Prolacertidae” (Parrington 1935). “Prolacertidae” was classified as part of “Thecodontia”, a group that was at the time considered either as a “primitive” lineage within Archosauria (Watson 1917), or both ancestral to archosaurs and lepidosaurs (Broom 1914). “Thecodontia” is now unequivocally a paraphyletic grouping and has been abandoned as a clade (Benton 2005). However, based on its incomplete infratemporal bar, *Prolacerta* was considered to be intermediate between “lacertilians” (i.e. squamates) and more “primitive thecodonts” such as *Youngina capensis* (Parrington 1935). The description of a new specimen of *Prolacerta* led to the consideration that it was more closely related to *Protorosaurus* and resulted in the first inclusion of *Prolacerta* into “Protorosauria” (Camp 1945). Camp (1945) favored “Protorosauria” over “Eosuchia” based on seniority, and included taxa placed in “Eosuchia”, “Trachelosauria”, and “Protorosauria” by Williston (1925) within this clade and established it within Lepidosauria. This superorder “Protorosauria” was further subdivided in the orders “Prolacertiformes”, which he synonymized with “Eosuchia” (sensu Broom 1914, meaning it also included Younginiformes), “Trachelosauria” or Tanystropheidae, and, more tentatively, Thalattosauria and “Acrosauria” (the latter containing the rhynchocephalian pleurosaurids).

Kuhn-Schnyder (1954) defined the Middle Triassic *Macrocnemus* and *Tanystropheus* as squamates (German: Eidechsen, which literally translates to lacertids) that were morphologically intermediate between the Jurassic squamates and the supposed “squamate ancestor” *Prolacerta*.

Protorosaurus was not considered, since this interpretation was based mainly on skull anatomy, which was insufficiently understood in *Protorosaurus* at this point. This hypothesis differed from that of Colbert (1945; 1965) and Romer (1956; 1966; 1968), who considered “protorosaurs” as “Euryapsida” (sometimes also called “Synaptosauria”; Cope 1900), a clade which consisted of “protorosaurs” and sauropterygians, thus being similar to Sauropterygia as defined previously by Peyer (1931). This classification, which represented an important systematic paradigm for reptiles, was largely based on the temporal fenestration of the skull. “Euryapsids” were considered as a group that was entirely separate from “anapsids”, synapsids, and diapsids, based on the presence of an upper temporal fenestra, surrounded by the postorbital, squamosal, and parietal, and the absence of a lower temporal fenestra. The inclusion of “protorosaurs” within “euryapsids” was mainly based on *Araeoscelis*, which shows this fenestration type, in contrast to other “protorosaurs” that show the typical diapsid condition. Among others, the “Protorosauria” of Romer (1966) included *Protorosaurus*, *Tanystropheus*, *Trachelosaurus*, and *Trilophosaurus* (currently considered an allokotosaur within non-archosauriform Archosauromorpha; Ezcurra 2016; Nesbitt et al. 2015; Sengupta et al. 2017~~; Spielmann et al. 2008~~) within “Protorosauria”. On the other hand, *Prolacerta* and *Macrocnemus* were assigned to “Prolacertiformes” within “Eosuchia”, interpreted as the ‘basalmost’ order of Lepidosauria (“Eosuchia” was maintained contra Camp 1945). “Euryapsida” has generally not been used as a grouping in recent years, and its former members are now distributed within Diapsida (Benton 2005; Merck 1997). Furthermore, an extensive redescription of *Araeoscelis* has shown various differences with taxa such as *Protorosaurus* and *Prolacerta* (Vaughn 1955), and it is now considered an early diapsid that it is not closely related to “protorosaurs” (Ford & Benson 2020). The hypothesis of “Euryapsida” comprised of Sauropterygia and “Protorosauria” was criticized by Kuhn-Schnyder (1963; 1967; 1974). Kuhn-Schnyder (1967) and Wild (1973) argued that because of the ventrally opened lower temporal bar of *Macrocnemus* and *Tanystropheus*, “Protorosauria”, including *Protorosaurus*, belonged to “Prolacertidae” within Lepidosauria.

Based on new material, *Prolacerta* was extensively redescribed by Gow (1975), which included the first detailed description of postcranial remains. This study was the first to conclude that *Prolacerta*, together with *Macrocnemus* and *Tanystropheus*, was clearly not part of the lepidosaurian lineage, but instead was archosaurian in many of its features. These taxa were grouped in the newly erected order “Parathecodontia”, with *Prolacerta* and *Macrocnemus* being further classified together within “Prolacertidae” and *Tanystropheus* within Tanystropheidae. Nevertheless, the need for a detailed phylogenetic re-examination of these taxa was stressed and this revision did not consider *Protorosaurus*.

In the 1970s and the subsequent two decades, a considerable number of taxa were included within "Protorosauria", further indicating the significance of the group: *Tanytrachelos ahynis* (Olsen 1979), *Langobardisaurus pandolfii* (Bizzarini & Muscio 1995), *Cosesaurus aviceps* (originally considered an avian ancestor; Ellenberger & De Villalta 1974, but later designated as a "protorosaur" by Olsen 1979), *Malerisaurus robinsonae* (Chatterjee 1980), *Kadimakara australiensis* (Bartholomai 1979), *Prolacertoides jimusarensis* (Young 1973), *Malutinisuchus gratus* (Otschev 1986), and *Boreopricea funerea* (Tatarinov 1978). In addition, "Protorosauria" as designated by Evans (1988) included *Megalancosaurus preonensis*, a member of the Drepanosauridae, a family of highly specialized, arboreal diapsids (Calzavara et al. 1980; Pritchard et al. 2016; Renesto et al. 2010). Chatterjee (1980) also included the Carboniferous *Petrolacosaurus kansensis* within "Prolacertiformes", although this view was swiftly disputed (Evans 1988; Reisz et al. 1984), and *Petrolacosaurus* is now widely considered an araeoscelid diapsid instead (Ezcurra et al. 2014; Ford & Benson 2020; Reisz et al. 2011b).

Cladistics became widespread as a method for establishing phylogenetic relationships between taxa during the 1980s and its implementation on diapsid phylogeny quickly led to a relatively clear-cut division between Lepidosauromorpha and Archosauromorpha, with "Protorosauria" firmly established within the latter group (Bennett 1996; Benton 1984; Benton 1985; Evans 1988; Gauthier 1984; Gauthier 1994; Gauthier et al. 1988b). Chatterjee (1986) pointed out the priority of "Protorosauria" over "Prolacertiformes" based on seniority, but since "Protorosauria" had previously often included *Araeoscelis* and was therefore shown to be polyphyletic, many authors since preferred "Prolacertiformes" (see Evans 1988, pages 226-227 for an overview of the use of both terms within the literature between 1945 and 1988). However, although the place of "protorosaurs" among Archosauromorpha became firmly established, the interrelationships of the various "protorosaurs" was not evaluated cladistically except for Chatterjee (1986) and Evans (1988). Olsen (1979) and Wild (1980a) also provided a hypothesis of "protorosaur" interrelationships on a non-cladistic basis.

This issue would soon be addressed in more detail in several papers. One study included 11 "protorosaurs" (excluding the poorly known *Prolacertoides*) and three outgroups and 48 morphological characters (Benton & Allen 1997). In the same year, the description of a new "protorosaur", *Jesairosaurus lehmani*, was accompanied by an analysis including ten protorosaurs and eight outgroup taxa, employing 71 characters (Jalil 1997; the initial analysis also included *Trachelosaurus*, *Prolacertoides*, *Malutinisuchus*, and *Kadimakara*, but these poorly known taxa were excluded from the final analysis, as the inclusion of these taxa left "protorosaurs" unresolved). Another study addressing early archosauromorph phylogeny also included several “protorosaurs” (Dilkes 1998). This analysis included 144 characters and 23 taxa, out of which seven were traditionally considered as “protorosaurs”, including two drepanosaur taxa, which were not included in Benton & Allen (1997) and Jalil (1997). It recovered a monophyletic “Protorosauria” in which *Protorosaurus* formed a sister taxon to two lineages, Drepanosauridae and Tanystropheidae, whereas *Prolacerta* was placed outside the clade as the sister taxon of Archosauriformes. Peters (2000) used the matrices of Evans (1988), Jalil (1997), and Bennett (1996) and reran each of them after adding a number of characters and rescoring some characters for certain taxa, for a total taxon sample that included 11 “protorosaurs”, other non-archosauriform archosauromorphs, the pterosaur *Eudimorphodon*, and two enigmatic and possibly gliding diapsids, *Longisquama insignis* (Sharov 1970) and *Sharovipteryx mirabilis* (Cowen 1981; Sharov 1971). *Sharovipteryx* is an enigmatic gliding reptile with a membrane stretched between the hindlimbs, which represents an entirely unique morphology among gliding reptiles. It has ~~very very tentatively~~ been ascribed to “protorosaurs” or tanystropheids by some authors (Gans et al. 1987; Pritchard & Sues 2019; Tatarinov 1989; Tatarinov 1994; Unwin et al. 2000), but its phylogenetic position is highly uncertain due to its highly specialized, yet very poorly known morphology. Peters (2000) found that the “protorosaurs”, and *Longisquama* and *Sharovipteryx*, to be very closely associated with *Eudimorphodon*, from which a “protorosaurian” ancestry for pterosaurs was concluded. However, the exact topologies varied strongly between the different analyses, and this hypothesis of pterosaur ancestry has widely been rejected by other pterosaur and archosaur studies (e.g. Hone & Benton 2007; Nesbitt 2011; Padian 1997). The datasets of Benton & Allen (1997), Dilkes (1998), and Jalil (1997) were combined into one larger character list of 239 characters by Rieppel et al. (2003), which was used specifically to address “protorosaur” phylogeny, and in particular the question of “protorosaur” monophyly, which had now been put in doubt (Dilkes 1998). This approach included seven “protorosaur” taxa (*Protorosaurus*, *Drepanosaurus*, *Megalancosaurus*, *Prolacerta*, *Macrocnemus*, *Langobardisaurus*, and *Tanystropheus longobardicus*), and four outgroup taxa (*Petrolacosaurus*, *Youngina*, *Rhynchosaurus*, and *Trilophosaurus*). Additional analyses were performed after subsequently including *Euparkeria* and *Proterosuchus*, and the lesser known “protorosaurs” *Boreopricea* and *Jesairosaurus*. Although the first analysis found a monophyletic “Protorosauria”, the other two resulted in a paraphyly. Although Rieppel et al. (2003) concluded that the monophyly of “Protorosauria” as previously regarded (e.g. Benton & Allen 1997; Jalil 1997) could not be maintained, they argued the need for an extensive phylogenetic investigation into “protorosaurs”. Senter (2004) investigated the phylogenetic position of drepanosaurs in an analysis that comprised “protorosaurs“ (*Prolacerta*, *Macrocnemus*, and *Langobardisaurus*), *Longisquama*, non-archosaurian Archosauriformes, birds, a non-avian dinosaur, and a number of early diapsids. This study found drepanosaurs to form a clade with *Longisquama* and *Coelurosauravus*, which was termed "Avicephala", as the sister group to Neodiapsida, which in his analysis encompassed *Youngina*, the rhynchocephalian *Gephyrosaurus*, and several archosauromorphs. The included "protorosaurs" formed a monophyletic clade within Archosauromorpha. However, an analysis using the same character list by Renesto & Binelli (2006) could not reproduce the same topology. Renesto et al. (2010) reaffirmed the position of drepanosaurs among "protorosaurs", whereas Pritchard & Nesbitt (2017) recovered Drepanosauromorpha as a separate clade of non-saurian diapsids. Müller (2004) included four different "protorosaur" taxa in his broad-scale analysis of diapsid relationships, which consisted of 184 characters compiled mainly from Rieppel et al. (1999) and DeBraga & Rieppel (1997). This study also inferred a polyphyletic "Protorosauria", with *Tanystropheus*, *Macrocnemus*, and *Prolacerta* being successive sister taxa to rhynchosaurs and *Trilophosaurus*, whereas drepanosaurs were only quite distantly related to these taxa.

"Protorosaurs" were virtually unknown from China until about 15 years ago, with the exception of the tentative "protorosaur" *Prolacertoides jimusarensis* (Young 1973). However, a number of new finds have been referred to "Protorosauria", including *Tanystropheus* cf. *longobardicus* (Rieppel et al. 2010; now *Tanystropheus* cf. *hydroides*, see Spiekman et al. 2020), *Tanystropheus* sp. (Li 2007), and *Macrocnemus fuyuanensis* (Jiang et al. 2011; Li et al. 2007), forms very similar to European counterparts, as well as completely new taxa, such as *Dinocephalosaurus orientalis* (Li 2003; Li et al. 2004; Liu et al. 2017; Rieppel et al. 2008), *Fuyuansaurus acutirostris* (Fraser et al. 2013), an unnamed taxon closely related to *Dinocephalosaurus* (Li et al. 2017b), and potentially *Pectodens zhenyuensis* (Li et al. 2017a). This has revealed that "protorosaurs" had a Tethys-wide distribution and are considerably more morphologically diverse than previously appreciated. Except for *Dinocephalosaurus orientalis*, which has been included in phylogenetic analyses of Rieppel et al. (2008), Liu et al. (2017), and De Oliveira et al. (2020), none of the Chinese taxa have been phylogenetically assessed so far.

But new "protorosaur" findings have also been reported from outside of China. Fraser & Rieppel (2006) re-examined the *"Tanystropheus antiquus"* material from the Upper Buntsandstein of Baden-Württemberg, Germany, and assigned it to a new taxon, *Amotosaurus rotfeldensis*. Furthermore, Gottmann-Quesada & Sander (2009) provided a monograph on the German *Protorosaurus speneri* material, including the first detailed description and reconstruction of the skull, based on the first discovery of a well-preserved skull in 1972, which previously had only been briefly documented (see

Haubold & Schaumberg 1985 p. 223; Fichter 1995 and references therein). Gottmann-Quesada & Sander (2009) also provided a phylogenetic analysis, which employed the matrix of Dilkes (1998), with several modifications to the character scoring of *Mesosuchus*, *Prolacerta*, and *Protorosaurus*. This resulted in a tree with a polyphyletic "Protorosauria" that recovered *Protorosaurus* as the sister taxon to *Megalancosaurus*. A new species of *Macrocnemus*, *Macrocnemus obristi*, has been described from Alpine Europe (Fraser & Furrer 2013), and a specimen from Monte San Giorgio on the border of Switzerland and Italy was recently assigned to *Macrocnemus fuyuanensis*, the species of *Macrocnemus* which was previously only known from China (Jaquier et al. 2017; Scheyer et al. 2020b). A new species of *Tanystropheus*, *Tanystropheus hydroides*, has also been described from Monte San Giorgio (Spiekman et al. 2020). This new species was previously considered to represent the adult stage of *Tanystropheus longobardicus* (Wild 1973), but long bone histology revealed that the small specimens of *Tanystropheus longobardicus* were skeletally mature, thus representing a separate species from *Tanystropheus hydroides*. Two poorly known new protorosaurs have been reported from Russia based on limited, isolated remains, the large-sized *Vritramimosaurus dzerzhinskii*, considered to be closely related to *Prolacerta* (Sennikov 2005), and *Augustaburiania vatagini*, a medium-sized tanystropheid (Sennikov 2011). From Poland two new, possibly "protorosaur", archosauromorphs have been described. *Czatkowiella harae* has been interpreted as being closely related to *Protorosaurus* (Borsuk-Białynicka & Evans 2009b), whereas the highly gracile, and putative glider, *Ozimek volans* is similar to *Sharovipteryx* (Dzik & Sulej 2016). Ezcurra et al. (2014) re-examined material consisting of five vertebrae, three fragmented forelimb elements, and some indeterminable fragments from the ~~Late~~ Permian of Tanzania previously described by Parrington (1956) and assigned it to the new taxon *Aenigmastropheus*. Following an analysis modified from Reisz et al. (2010), used to address both synapsid and diapsid affiliations, it was recovered among "protorosaurs" as the sister taxon to *Protorosaurus*. In addition, they found *Eorasaurus*, previously assigned as a "protorosaur" by Sennikov (1997), to likely be an archosauriform, which would make *Aenigmastropheus* the second known "protorosaur" and non-archosauriform archosauromorph from the Permian. Two more tanystropheid genera, *Sclerostropheus fossai* and *Raibliania calligarisi* were recently identified, based on partial postcranial remains (Dalla Vecchia 2020; Spiekman & Scheyer 2019). Finally, recent findings have shone more light on the occurrence and distribution of tanystropheids in the Americas. Isolated material from the Middle and Late Triassic North America, largely consisting of cervical vertebrae, as well as some other postcranial remains, indicate that tanystropheids were more widespread and also occurred until more recently than previously thought (Formoso et al. 2019; Lessner et al. 2018; Pritchard et al. 2015; Sues & Olsen 2015).

From South America, some likely tanystropheid remains from the Induan to early Olenekian of Brazil have been reported (De Oliveira et al. 2018; De Oliveira et al. 2020), which, if indeed tanystropheids, would represent among the earliest records of the clade, and would indicate a wide, if not nearly cosmopolitan distribution of the clade during the Early Triassic.

The original phylogenetic matrices by Pritchard et al. (2015) and Ezcurra (2016), and their subsequently modified iterations (e.g. Butler et al. 2019; Ezcurra & Butler 2018; Ezcurra et al. 2017; Nesbitt et al. 2017a; Nesbitt et al. 2015; Pritchard et al. 2018; Pritchard & Nesbitt 2017; Pritchard & Sues 2019; Scheyer et al. 2020a; Sengupta et al. 2017; Stocker et al. 2017), represent the two separate datasets that most comprehensively addressed “protorosaur” relationships. The former focused specifically on tanystropheid relationships. It found *Protorosaurus* as the sister taxon to all other archosauromorphs, whereas *Prolacerta* formed the sister taxon to Archosauriformes. Tanystropheidae was recovered as a monophyletic clade and consisted of *Macrocnemus*, *Amotosaurus*, *Tanystropheus*, *Langobardisaurus*, *Tanytrachelos*, and the new Hayden Quarry material that was presented therein. The character list consisted of 200 characters, including novel characters and characters derived from many previous analyses (Benton 1985; Benton & Allen 1997; Conrad 2008; DeBraga & Rieppel 1997; Dilkes 1998; Gauthier 1984; Gauthier et al. 1988a; Gauthier et al. 1988b; Hutchinson et al. 2012; Jalil 1997; Merck 1997; Modesto & Sues 2004; Müller 2004; Nesbitt 2011; Rieppel 1994). Ezcurra (2016) presented a very extensive analysis of early archosauromorph interrelationships that used 600 characters to analyze 96 taxa. Out of these characters, 96 were new. The remaining characters were compiled from the literature (mainly Desojo et al. 2011; Dilkes 1998; Dilkes & Arcucci 2012; Ezcurra et al. 2015; Ezcurra et al. 2010; Ezcurra et al. 2014; Gower & Sennikov 1996; Gower & Sennikov 1997; Jalil 1997; Nesbitt 2011; Nesbitt et al. 2015; Parrish 1992; Pritchard et al. 2015; Senter 2004; Trotteyn & Ezcurra 2014). Like Pritchard et al. (2015), it found *Protorosaurus* to be the sister taxon to all other archosauromorphs and *Prolacerta* to be the sister taxon to Archosauriformes. *Boreopricea* was found as the sister taxon to *Prolacerta* + Archosauriformes and *Jesairosaurus* formed the sister to a monophyletic Tanystropheidae, ~~made up~~ of *Macrocnemus*, *Amotosaurus*, and *Tanystropheus*.

Overview of “protorosaur” taxa

In the following, an overview is provided of taxa which have been attributed to “Protorosauria”, but which have not been included in the present analysis, since they are either represented by insufficient material for inclusion or because it is now widely considered that they are not closely related to *Protorosaurus speneri*, *Prolacerta broomi*, or Tanystropheidae.

Aenigmastropheus parringtoni Ezcurra, Scheyer & Butler 2014. *Aenigmastropheus parringtoni* is known from one specimen, UMZC T836, from the Wuchiapingian (middle ~~L~~ate Permian) of Tanzania. It comprises five cervical and dorsal vertebrae, the distal part of a right humerus, the proximal part of the right ulna, and a number of small fragments. The specimen was first described by Parrington (1956), and was considered to be insufficiently preserved for a confident taxonomic diagnosis. However, it was noted that its morphology contained both primitive diapsid traits as well as archosaurian characteristics. The specimen was recently revised and assigned to a new taxon, which was recovered as the sister taxon to *Protorosaurus speneri* in a cladistic analysis (Ezcurra et al. 2014).

Kadimakara australiensis Bartholomai 1979. *Kadimakara australiensis* is known from two partial skulls first described by Bartholomai (1979). The holotype is represented by the postorbital region, whereas the other specimen comprises a partial snout. Although both specimens do not have any shared preserved regions, they were attributed to the same taxon based on their similar size and shared close similarity to *Prolacerta broomi*. The validity of *Kadimakara australiensis* has been questioned and Borsuk-Białynicka & Evans (2009b) and Evans & Jones (2010) considered the specimens to be congeneric with *Prolacerta broomi*. Ezcurra (2016) corroborated the close affinity of *Kadimakara australiensis* to *Prolacerta broomi*, but only considered the holotype in the revised diagnosis of the taxon therein, since the lack of overlapping morphology precludes the direct comparison between the holotype and referred specimen. Ezcurra (2016) argued in favour of the validity of *Kadimakara australiensis*, pointing out a medial fossa on the posterior half of the parietals as a distinguishing feature between this species and *Prolacerta broomi*. However, other distinguishing features indicated by Bartholomai (1979) were revealed to result from an erroneous interpretation of the morphology of the postorbital bar. *Kadimakara australiensis* ~~originates~~ from the lower beds of the upper part of the Arcadia Formation, central Queensland, Australia, which are of Induan (earliest Triassic) age.

Megacnemus grandis Huene 1954. *Megacnemus grandis* was described based on one isolated long bone exceeding 20 cm in length, which was identified as a femur (Huene 1954). It is likely from the Gogolin Formation of southwest Poland, which is lower Anisian (Middle Triassic) in age (Skawiński et al. 2017). Skawiński et al. (2015) re-examined the specimen and corroborated its "protorosaurian" affinities. However, they also considered the possibility that the specimen represents a humerus rather than a femur, and therefore only identified the bone as a propodial. It has not been included in any phylogenetic analyses due to its extremely poorly known morphology.

Prolacertoides jimusarensis Young 1973. *Prolacertoides jimusarensis* is known from a single, poorly preserved skull (IVPP V3233) and represents the first described protorosaur from China, which was considered to be closely related to *Prolacerta broomi* (Young 1973). Ezcurra (2016) provided a more detailed osteological description of the holotype in English, but *Prolacertoides jimusarensis* was omitted from the final analysis therein, due to a lack of preserved morphological characters, which resulted in its inclusion reducing the reliability of the analysis. In analyses 1 and 2 of Ezcurra (2016), which included *Prolacertoides* and other poorly represented taxa, *Prolacertoides jimusarensis* was positioned in a large polytomy including most early archosauromorphs with *Protorosaurus speneri* as the sister taxon. *Prolacertoides jimusarensis* has previously been included phylogenetically in Benton & Allen (1997), Evans (198), Jalil (1997), and Rieppel et al. (2003). Notably, Benton & Allen (1997) retrieved *Prolacertoides jimusarensis* as being the sister taxon to *Trilophosaurus buettneri* and to thus fall outside of the traditional "Protorosauria". However, its exact phylogenetic affiliations were questioned by all authors due to a lack of morphological information for the taxon.

Rhombopholis scutulata Owen 1842. *Rhombopholis scutulata* was originally described as an amphibian (Owen 1842). It is represented by a single block that contains a number of postcranial bones, including four vertebrae, a number of ribs, and five limb elements that belong to at least two individuals Benton & Walker (1996). In a revision of the reptile material from the Keuper Sandstone Group of England (Anisian, Middle Triassic), this specimen, as well as a number of other specimens, was considered as being closely related to *Macrocnemus bassanii* (Walker 1969). Benton & Walker (1996) provided a redescription of *Rhombopholis scutulata*, an identified it as a "prolacertiform" metataxon, meaning that no autapomorphies could be ~~assigned to it~~ to distinguish it from other "prolacertiforms" and that the different specimens possibly belong to more than one taxon. Thus, the block attributed to *Rhombopholis scutulata* might also include various ~~"prolacertid"~~ remains that only potentially belong to one taxon.

Sharovipteryx mirabilis Sharov 1971. A virtually complete but poorly preserved specimen with long and gracile hindlimbs with an apparent skin membrane present between the legs was initially described as *Podopteryx mirabilis* and interpreted as a gliding reptile (Sharov 1971). However, because the name *Podopteryx* was already occupied by a genus of damselflies, the taxon was renamed *Sharovipteryx mirabilis* by Cowen (1981). *Sharovipteryx mirabilis* was described in detail by Gans et al. (1987). Although the phylogenetic position of *Sharovipteryx mirabilis* is exceedingly hard to assess due to the lack of visible morphological details, it has been incorporated in "Protorosauria" by various authors (e.g. Ivakhnenko & Kurochkin 2008; Peters 2000; Unwin et al. 2000).

Cosesaurus aviceps Ellenberger & De Villalta 1974. *Cosesaurus aviceps* is known from a single specimen, which represents an impression of a complete skeleton. As such, the outline of the specimen is well-preserved, but the detailed morphology of the taxon is very poorly known. The specimen was found at the Montral-Alcover outcrop (Ladinian, Middle Triassic), Sierra de Prades, Tarragona province, Spain. Due to the lack of morphological information, the phylogenetic affinities of *Cosesaurus aviceps* are unclear. It was initially thought to represent an ancestor to birds (Ellenberger 1977; Ellenberger 1978; Ellenberger & De Villalta 1974). However, the now widely accepted view that birds represent a derived clade of theropod dinosaurs refutes this hypothesis. *Cosesaurus aviceps* was redescribed by Sanz & López-Martínez (1984), and considered to bear many similarities to various "protorosaurs". *Cosesaurus aviceps* has also been found among "protorosaurs" in subsequent phylogenetic analyses (Benton & Allen 1997; Evans 1988; Jalil 1997; Rieppel et al. 2003). In a widely criticized reinterpretation of previous analyses (e.g. Hone & Benton 2007) it was concluded that Pterosauria are a derived lineage with "Prolacertiformes", which was largely based on several morphological characters observed in *Cosesaurus aviceps*, as well as the poorly known, gracile reptiles *Sharovipteryx mirabilis* and *Longisquama insignis* (Peters 2000). Although *Cosesaurus aviceps* might represent a "protorosaur", the lack of morphological information does not allow this taxon to be reliably incorporated in phylogenetic analyses, and recent phylogenetic investigations into archosauromorph or "protorosaurian" affinities did not consider this taxon.

Vritramimosaurus dzerzhinskii Sennikov 2005. The holotype of *Vritramimosaurus dzerzhinskii* is a single cervical vertebra, and referred material comprises another cervical vertebra, a caudal vertebra, and two fragmentary vertebrae. They were originally discovered in 1953 and 1954 by B.P. Vjuschkov. *Vritramimosaurus dzerzhinskii* has been described as a "large, specialized prolacertilian"(Sennikov 2005). The material originates from the Rassypnaya locality of the Petropavlovka Formation, Orenburg Region, Russia, which is of uppermost Olenekian (Early Triassic) age. Its estimated overall body size is at least three meters, making *Vritramimosaurus dzerzhinskii* one of the larger early archosauromorphs and considerably larger than *Prolacerta broomi*, to which it is considered to be closely related (Sennikov 2005). However, the limited and fragmentary material allows for only a very ambiguous comparison with other taxa and the taxon has therefore not been included in phylogenetic analyses.

Malerisaurus robinsonae Chatterjee 1980 and *Malerisaurus langstoni* Chatterjee 1986. *Malerisaurus robinsonae* is known from two individuals that are part of the stomach contents of a specimen of the phytosaur *Parasuchus hislopi* from the Maleri Formation (~~Carnian to Early Norian~~, early Late Triassic) of central India (Chatterjee 1980). Another specimen from the Tecovas Member, lower Dockum Formation of western Texas, US, (Carnian, early Late Triassic) was recognized as representing a taxon that was very closely related to *Malerisaurus robinsonae* and assigned to *Malerisaurus langstoni* (Chatterjee 1986). However, this holotype and only known specimen is actually composed of elements belonging to several diapsid taxa, most notably *Trilophosaurus buettneri* (Spielmann et al. 2006). Therefore, *Malerisaurus langstoni* is no longer considered a valid taxon. Furthermore, the validity of the Indian *Malerisaurus robinsonae* was questioned, as this taxon also showed distinct similarities to *Trilophosaurus buettneri* (Spielmann et al. 2006). Following the original interpretation by Chatterjee (1980; 1986) of *Malerisaurus robinsonae* as a "protorosaur" closely related to *Protorosaurus speneri*, it has been incorporated in phylogenetic analyses (Benton 1985; Benton & Allen 1997; Evans 1988; Jalil 1997; Rieppel et al. 2003). *Malerisaurus robinsonae* was removed from the final analyses due to insufficient character preservation in Benton (1985) and Rieppel et al. (2003), whereas it was retrieved as part of a polytomy within Archosauromorpha by Evans (1988). Benton & Allen (1997) included only *Malerisaurus langstoni* in the final analysis and found it as the sister taxon to all included "protorosaurs" except *Protorosaurus speneri*, *Prolacerta broomi*, and *Boreopricea funerea*. Finally, Jalil (1997) included both *Malerisaurus* species as a single OTU and found it to be the sister taxon to *Jesairosaurus lehmani*. *Malerisaurus* spp. have not been included in any of the recently published phylogenetic analyses of early archosauromorphs. Recently, Nesbitt et al. (2017b) identified both *Malerisaurus* species as separate from *Trilophosaurus buettneri*, and considered them to belong to Allokotosauria, more specifically as a member of Azendohsauridae.

Malutinisuchus gratus Otschev 1986. *Malutinisuchus gratus* is a very poorly known taxon that has been considered a prolacertid. It is known from the Belyaevsky I, Bukobay Svita, Ladinian, Orenburg region, Russia (Otschev 1986; Tverdokhlebov et al. 2003). The known material comprises several fragmentary remains, including an elongated cervical vertebra, two partial limb bones, and likely pectoral girdle elements. *Malutinisuchus gratus* was incorporated into phylogenetic analyses by Jalil (1997) and Rieppel et al. (2003), but in both cases omitted from the final analysis due to lack of morphological information. In one of the trees recovered by Jalil (1997) *Malutinisuchus gratus* formed a polytomy with all other taxa forming the clade "Prolacertiformes" therein.

Boreopricea funerea Tatarinov 1978. *Boreopricea funerea* is known from a nearly complete specimen and an anterior end of a snout, collected from a borehole, number 141, at 1112.3 meters deep at Kolguyev Island in the Barents Sea. This borehole is part of the Vetluzhian Series (Induan, earliest Triassic; Benton & Allen 1997). The referred specimen is likely lost (Benton & Allen 1997). *Boreopricea funerea* was originally considered to represent an intermediate form between *Prolacerta broomi* and *Pricea longiceps* (now considered a junior synonym of *Prolacerta broomi*), and *Macrocnemus bassanii* (Tatarinov 1978). The taxon was later redescribed in more detail by Benton & Allen (1997), who commented on the poor state of the specimen and the absence of certain elements described by Tatarinov (1978) as a consequence of damage that the holotype had sustained after this description, such as the crushing of the skull and the removal and in some cases disappearance of certain postcranial elements. Among these are the interclavicle and ossified sternum, which contained characters that were important in distinguishing *Boreopricea funerea* from other "protorosaurs". Furthermore, because these elements were removed and later placed back on the card on which the specimen is kept, the identification of the tarsal bones is difficult and ambiguous (Rieppel et al. 2003). *Boreopricea funerea* has been included in several phylogenetic analyses (Benton & Allen 1997; Evans 1988; Ezcurra 2016; Jalil 1997; Rieppel et al. 2003) and an emended diagnosis has been provided by Ezcurra (2016). *Boreopricea funerea* was found as nested between *Prolacerta* and a clade comprising *Macrocnemus*, *Cosesaurus*, *Tanystropheus*, and *Tanytrachelos* (Evans 1988). In the phylogenetic analysis accompanying the redescription of the taxon, *Boreopricea funerea* represented the sister taxon to *Prolacerta* (Benton & Allen 1997). In the final tree of Jalil (1997) *Boreopricea funerea* was positioned between *Langobardisaurus* and a clade comprising *Cosesaurus*, *Tanystropheus*, and *Tanytrachelos*. In the various trees produced by Rieppel et al. (2003) the ~~topology~~ of *Boreopricea funerea* varied. In some cases it was positioned as closely related to *Protorosaurus* and in others as being more closely related to *Prolacerta*. Ezcurra (2016) recovered *Boreopricea funerea* as the sister taxon to the clade composed of *Prolacerta* and all Archosauriformes. Because ~~personal observation was not~~ possible due to the badly damaged skull, no cranial characters were scored in which Tatarinov (1978) and Benton & Allen (1997) were in disagreement ~~by Ezcurra (2016)~~.

Eorasaurus olsoni Sennikov 1997. *Eorasaurus olsoni*, one of the very few known Permian archosauromorphs, is known from several vertebrae. The taxon was originally considered to be ~~most~~ closely related to *Protorosaurus* and was therefore placed within "Protorosauridae" (Sennikov 1997). Ezcurra et al. (2014) provided additional observations and an emended diagnosis for *Eorasaurus olsoni*, and it was retrieved as an archosauriform that formed a trichotomy with *Euparkeria capensis* and *Erythrosuchus africanus* in the included phylogenetic analysis. *Eorasaurus olsoni* was also included by Ezcurra (2016) and formed a massive polytomy and the base Archosauriformes in the analyses 1 and 2 therein, but it was pruned from the final analysis due to insufficient morphology being currently known for the taxon.

Hayden Quarry tanystropheid. Recently a large number of postcranial elements with clearly tanystropheid affinities were described, encompassing vertebrae, femora, and a calcaneum (Pritchard et al. 2015). Because the material is represented by isolated elements, it is unclear whether they all belong to the same taxon, and thus it was thus not referred to any specific taxon. The calcaneum was shown to share apomorphies with that of *Tanytrachelos ahynis*, and was therefore assigned to this species. This material currently represents the only known tanystropheid material from western North America and is of approximately middle Norian age (Late Triassic; Irmis et al. 2011), thus being one of the later representatives of the tanystropheid clade. Although it was not concluded that the Hayden Quarry material represents a single taxon, a hypothetical Hayden Quarry taxon was included in the phylogenetic analysis of Pritchard et al. (2015), which recovered it as the sister taxon to the North American *Tanytrachelos ahynis*. Nevertheless, since the material represents only limited postcranial material, which furthermore cannot unequivocally be assigned to a single taxon, it is not considered for phylogenetic analysis here.

Vallesaurus cenensis Wild 1991. *Vallesaurus cenensis* is known from a single, well-preserved and complete specimen that was discovered in the Cene quarry, upper part of the Zorzino Limestone (Revueltian, early-middle Norian, Late Triassic), in Lombardy, Italy (Renesto & Binelli 2006). Wild (1991) mentioned the specimen and assigned it to the genus *Vallesaurus* but did not formally describe the specimen. The specimen (Renesto 2000) and species (Pinna 1993) were further referred to, and a formal description was provided by Renesto & Binelli (2006). *Vallesaurus cenensis* has additionally been compared to other drepanosaurs by Renesto et al. (2010). Therein, the new species *Vallesaurus zorzinensis* was included in the genus, which differs from *Vallesaurus cenensis* in having an opposable hallux with two phalanges, of which the first one is straight. *Vallesaurus cenensis* has been included in phylogenetic analyses (Pritchard & Nesbitt 2017; Pritchard et al. 2016; Renesto et al. 2010; Senter 2004). Drepanosaurs, such as *Vallesaurus cenensis*, are not included in the present analysis because they likely represent a separate lineage of reptiles outside of Archosauromorpha, and are therefore only distantly related to ~~other~~ “protorosaurs” (Pritchard & Nesbitt 2017).

Drepanosaurus unguicaudatus Pinna 1980. *Drepanosaurus unguicaudatus* was first described based on the holotype, which consists of a largely complete, articulated skeleton, missing the skull and anterior cervical vertebrae, and several juvenile specimens (Pinna 1980). This was followed by a more extensive description (Pinna 1984), and these findings were later summarized in English (Pinna 1986). Renesto (1994c) revised the morphology of *Drepanosaurus unguicaudatus*, especially regarding the highly specialized forelimbs, and it was suggested that the juvenile specimens belong to *Megalancosaurus preonensis*. This suggestion was reinforced by Renesto (2000), who considered the holotype as the only known specimen of *Drepanosaurus unguicaudatus*, whilst a juvenile specimen (MCSNB 4783), previously described by Renesto & Paganoni (1995), was attributed to *Drepanosaurus* sp. A revised diagnosis and overview of the provenance of the species was provided in Renesto et al. (2010). Pritchard et al. (2016) described new remains from North America, which were assigned to *Drepanosaurus* sp., which provided new insight into the unique configuration of the grasping forelimb of the taxon. *Drepanosaurus unguicaudatus* has been included in several phylogenetic analyses (Dilkes 1998; Evans 1988; Pritchard & Nesbitt 2017; Pritchard et al. 2016; Renesto et al. 2010; Senter 2004).

Megalancosaurus preonensis Calzavara, Muscio & Wild 1980. *Megalancosaurus preonensis* is known from middle Norian Forni Dolostone of Friuli and Zorzino Limestone of Lombardy, Italy (Renesto et al. 2010). The holotype of *Megalancosaurus preonensis*, which comprises of a complete skull and cervical series, the expanded neural spines of the anterior dorsal vertebrae, several fragments of dorsal ribs, and a right forelimb, was described by Calzavara et al. (1980) and interpreted as an arboreal archosaur. Feduccia & Wild (1993) and Feduccia (1996) suggested that *Megalancosaurus preonensis* was possibly a glider and considered it to be closely related to birds, thus arguing that Triassic archosaurs, rather than theropod dinosaurs, are the sister group to birds. An additional specimen of *Megalancosaurus preonensis* was described, which provided new information on the postcranium of the taxon (Renesto 1994a). Additionally, three specimens that were previously identified as juvenile specimens of *Drepanosaurus unguicaudatus* (Pinna 1980), were re-assigned to the taxon as well (Renesto 1994a). The arboreal lifestyle suggested for *Megalancosaurus preonensis* was questioned by Padian & Chiappe (1998), which considered an aquatic lifestyle for the taxon. The hypothesis that drepanosaurs are the sister group to birds was refuted in a study that also assigned two additional specimens to the species (Renesto 2000). The skull of *Megalancosaurus preonensis* was redescribed in detail by Renesto & Dalla Vecchia (2005). A second species, *Megalancosaurus endennae*, was erected and two specimens that were previously identified as *Megalancosaurus preonensis* were re-assigned to this species (Renesto et al. 2010). *Megalancosaurus endennae* mainly differs from *Megalancosaurus preonensis* in the presence of an opposable hallux in the pes. Another specimen lacking the hindlimb, **MFSN 18443a**, was reassigned to *Megalancosaurus* sp. A functional interpretation of the forelimbs of *Megalancosaurus* spp. was provided by Castiello et al. (2016). *Megalancosaurus preonensis* has been included in several phylogenetic analyses (Benton & Allen 1997; Dilkes 1998; Evans 1988; Pritchard & Nesbitt 2017; Pritchard et al. 2016; Renesto et al. 2010; Senter 2004).

The following taxa are included as operational taxonomic units (OTUs) for the phylogenetic analysis:

Petrolacosaurus kansensis Lane 1945

Age. Late Missourian, late Pennsylvanian, Late Carboniferous.

Occurrence. Garnett Quarry, Rock Lake Member of the Stanton Formation, Kansas, USA (Reisz 1981; Reisz et al. 1982).~~.~~

Holotype. **KUVP 1424**, largely complete right hindlimb.

~~Hypodigm.~~ The referred specimens are listed in (Reisz 1981, p. 4-5).

Diagnosis. The emended diagnosis is provided by Reisz (1981).

Remarks. *Petrolacosaurus kansensis* was first described based on a largely complete hindlimb (the holotype **KUVP 1424**) and pelvis, and identified as a pelycosaur (Lane 1945). Additional postcranial elements from the same locality were assigned to *Podargosaurus hibbardi* in the same study. Additional specimens, including skull material, revealed that *Podargosaurus* was indistinguishable from *Petrolacosaurus kansensis* and therefore its material was reassigned to the latter (Peabody 1952). The systematic position of *Petrolacosaurus kansensis* was disputed, but an additional specimen preserving the skull in more detail revealed it as an early diapsid reptile (Reisz 1977) and it has been described in detail by Reisz (1981). *Petrolacosaurus kansensis* represents one of the best-known Carboniferous diapsids and as such has been widely used as an outgroup in studies on ~~diapsid~~ phylogeny (e.g. Dilkes 1998; Evans 1988; Ezcurra 2016; Ezcurra et al. 2014; Jalil 1997; Pritchard et al. 2015; Simões et al. 2018). A recent phylogenetic hypothesis of early amniot~~es~~ suggests that the diapsid temporal configuration of *Petrolacosaurus kansensis* was likely independently acquired from that of neodiapsids, including saurians (Ford & Benson 2020).

Orovenator mayorum Reisz, Modesto & Scott 2011

Age. Earliest Artinskian, ~~E~~arly Permian (Cohen et al. 2013; Woodhead et al. 2010).

Occurrence. Claystone fissure fills in the Ordovician Arbuckle Limestone, Dolese Brothers Limestone Quarry, Richards Spur, Comanche County, Oklahoma, USA.

Holotype. **OMNH 74606**, a crushed partial skull missing several elements, including large parts of the skull roof and occipital region.

~~Hypodigm~~. **OMNH 74607**, a crushed partial skull preserving most of the skull roof, as well as an axi~~al~~, postaxial, and caudal vertebra.

Diagnosis. The most recent diagnosis was provided by Ford & Benson (2018).

Remarks. *Orovenator mayorum* is an ~~E~~arly Permian reptilian, known from the Richards Spur locality, which represents a unique upland fissure fill deposit (Ford & Benson 2020; MacDougall et al. 2017; Sullivan et al. 2000). Therefore, it was hypothesized that early reptilians from this locality were adapted to an upland environment, and that this in turn would explain their rare occurrence in the fossil record in the ~~E~~arly and ~~M~~iddle Permian (Reisz et al. 2011a). Following the initial description and phylogenetic analysis including *Orovenator mayorum* by Reisz et al. (2011a), in which it was recovered as the sister-taxon to all other known neodiapsids, the taxon was redescribed by Ford & Benson (2018) based on µCT scans. An extensive recent phylogenetic analysis recovered *Orovenator mayorum* as a member of Varanopidae, a clade historically considered to belong to Synapsida, but which was here found on the reptilian lineage outside Neodiapsida (Ford & Benson 2020). The cranial morphology suggests nocturnality and burrowing behavior in *Orovenator mayorum* (Ford & Benson 2018).

Acerosodontosaurus piveteaui Currie 1980

Age. Lopingian (roughly equivalent to the *Dicynodon* AZ of the Karoo Basin), ~~L~~ate Permian (Smith et al. 2012).

Occurrence. Sakamena River Valley, Lower Sakamena Formation, southern Madagascar (Currie 1980).

Holotype. **MNHN 1908-32-57**, a skeleton preserved partially as imprints in two slabs. The posterior half of the skull and mandibles are preserved. Of the postcranium, most of the dorsal vertebral series is preserved, as well as part of the forelimbs, the pelvis and sacral region, and hindlimbs.

Diagnosis. The most recent emended diagnosis is provided by Ezcurra (2016).

Remarks. *Acerosodontosaurus piveteaui* was first described by Currie (1980) and indicated to be closely related to *Youngina capensis*. A redescription of the only specimen of *Acerosodontosaurus piveteaui* revealed that the infratemporal bar is incomplete, in contrast to *Youngina capensis* (Bickelmann et al.

2009). An aquatic lifestyle has been suggested for *Acerosodontosaurus piveteaui*, which is supported by observed skeletal paedomorphosis of the carpal bones. In a phylogenetic analysis addressing the relationships of stem-turtles, *Acerosodontosaurus piveteaui* was recovered in a clade with *Claudiosaurus germaini* within Pantestudines as the sister group to all other members of this clade (Li et al. 2018).

Claudiosaurus germaini Carroll 1981

Age. Lopingian (roughly equivalent to the *Dicynodon* AZ of the Karoo Basin), Late Permian (Smith et al. 2012).

Occurrence. Lower Sakamena Formation near the village of Leoposa, southern Madagascar (Caldwell 1995; Carroll 1981).

Holotype. **MNHN 1978-6-1**, a largely complete skeleton ~~and~~ poorly preserved skull missing the posterior tail section.

~~Hypodigm~~. A list of referred specimens can be found in (Carroll 1981, p. 337-338). Several specimens are located in private ~~specimens~~. Additional undescribed specimens are housed in the SAM (Simões et al. 2018).

Diagnosis. The diagnosis was provided by Carroll (1981).

Remarks. *Claudiosaurus germaini* is a non-saurian diapsid known from various specimens from the Late Permian of southern Madagascar. Its depositional environment, as well as its morphology, as indicated by the enlarged hindlimbs and pedes, and skeletal paedomorphosis, suggest it had an aquatic lifestyle (Caldwell 1995; Carroll 1981).

Youngina capensis Broom 1914

Age. Capitanian to Changhsingian (Rubidge et al. 2013; Smith & Evans 1996)

Occurrence. *Tropidostema*, *Cistecephalus*, and *Dicynodon* AZs (Assemblage Zones), Balfour and Middelton Formations of the Beaufort Group, part of the Karoo Supergroup, South Africa (Broom 1914; Smith & Evans 1996).

Holotype. AMNH 5561, a complete skull and mandibles and a partial articulated vertebral column.

~~Hypodigm~~. The most inclusive hypodigm has been provided by Ezcurra (2016), who supplemented a previous hypodigm of Gow (1975) with specimens found since then.

Diagnosis. The most recent emended diagnosis of *Youngina capensis* was provided by Ezcurra (2016).

Remarks. *Youngina capensis* is a ~~L~~ate Permian non-saurian neodiapsid with a generalized morphology known from a large array of well-preserved specimens. Its morphology has thus been investigated frequently (e.g. Broom 1914; Broom 1922; Currie 1981; Evans 1987; Gardner et al. 2010; Goodrich 1942; Gow 1975; Smith & Evans 1996; Watson 1957). *Youngina capensis* represents an important taxon for phylogenetic analyses that investigate early diapsid and saurian relationships (e.g. Ezcurra 2016; Ezcurra et al. 2014; Ford & Benson 2020; Simões et al. 2018). Specimens that were previously assigned to ~~separate~~ taxa, *Youngoides romeri* (Olson & Broom 1937), *Youngoides minor* (Broom & Robinson 1948), *Youngopsis kitchingi* (Broom 1937), *Youngopsis rubidgei* (Broom & Robinson 1948), and *Acanthotoposaurus bremneri* (Evans & Van Den Heever 1987), have all been shown to be conspecific with *Youngina capensis* (Evans 1987; Gow 1975; Reisz et al. 2000).

Gephyrosaurus bridensis Evans 1980

Age. Hettangian, and possibly Sinemurian, Early Jurassic (Whiteside et al. 2016).

Occurrence. Pontalun and Pant quarries of the St. Bride's fauna, southern Wales (Evans & Kermack 1994; Whiteside et al. 2016).

Holotype. **UCL T.1503**, a right dentary.

~~Hypodigm~~. The material of *Gephyrosaurus bridensis* comprises an extensive amount of isolated remains (over 1,000 specimens following Evans 1980). No complete list of referred specimens is available.

Diagnosis. The diagnosis was provided by Evans (1980, p. 204-205)

Remarks. *Gephyrosaurus bridensis* is exclusively known from extensive isolated remains that have been assigned to a single taxon based on the complementary articulation surfaces between the various elements, as well as their morphology and relative size. *Gephyrosaurus bridensis* has been described in detail in one study addressing the skull (Evans 1980), and another addressing the postcranium (Evans 1981). Although known from younger, Early Jurassic, deposits, *Gephyrosaurus bridensis* is considered the sister taxon to the clade encompassing the Triassic rhynchocephalians *Planocephalosaurus robinsonae*

~~and~~ *Clevosaurus* spp. and more crownward rhynchocephalians (e.g. Hsiou et al. 2015; Scheyer et al. 2020a; Simões et al. 2018). An additional species, *Gephyrosaurus evansae*, was recently described from the Rhaetian (Late Triassic) '*Microlestes*' quarry at Holwell near Bristol, UK (Whiteside & Duffin 2017).

Planocephalosaurus robinsonae Fraser 1982

Age. Early Rhaetian, Late Triassic (Whiteside et al. 2016).

Occurrence. Late Triassic fissure fills of Cromhall and Tytherington quarries, Bristol and Gloucestershire, UK (Fraser 1982; Whiteside & Marshall 2008).

Holotype. **AUP No. 11061**, an isolated left maxilla.

~~Hypodigm~~. As for *Gephyrosaurus bridensis*, *Planocephalosaurus robinsonae* is represented by a large amount of isolated elements (at least 750 specimens from Cromhall quarry according to Fraser 1982), and no complete list of referred specimens is available.

Diagnosis. The diagnosis of *Planocephalosaurus robinsonae* is provided by Fraser (1982, p. 710).

Remarks. Like *Gephyrosaurus bridensis*, *Planocephalosaurus robinsonae* is known from the Late Triassic ~~to Early Jurassic~~ fissure fills of southwestern England and southern Wales. Consequently, its material is also ~~comprised~~ of a large amount of three-dimensionally preserved, isolated remains that can be assigned to a single taxon based on their relative connectivity, morphological similarity, and size (although Simões et al. 2018 considered the assignment of postcranial elements to this taxon only tentative). The skull was described by Fraser (1982), and the postcranium has subsequently been described by Fraser & Walkden (1984). *Planocephalosaurus robinsonae* represents one of the best-known early rhynchocephalians and bears several ~~primitive~~ features compared to more derived rhynhocephalians such as *Clevosaurus* spp. Specimens of *Planocephalosaurus* have also been identified from the Ruthin quarry, southern Wales, but were not assigned to the species level (Whiteside et al. 2016). Small tooth bearing fragments from the ~~L~~ower Tecovas Formation, Chinle Group (late Carnian) in Texas, USA, were assigned to a new species, *Planocephalosaurus lucasi* (Heckert 2004).

Protorosaurus speneri Meyer 1832

Age. Traditionally Tatarian, although conodont data points towards a more specific Wuchiapingian age, ~~L~~ate Permian (Ezcurra et al. 2014; Legler & Schneider 2008).

Occurrence. The Middridge and Quarrington quarries near Durham, Marl Slate, England (Evans & King 1993) and various localities of the Kupferschiefer Formation of ~~Middle~~ Germany (all localities are listed in Table 1 of Gottmann-Quesada & Sander 2009).

~~Holotype.~~ Since no formal holotype had previously been assigned, **NHMW 1943I4**, known as the Swedenborg specimen, was assigned the lectotype by Gottmann-Quesada & Sander (2009).

~~Hypodigm.~~ Table 1 of Gottmann-Quesada & Sander (2009) listed 28 specimens that were included in that study. More specimens that can tentatively be assigned to the species are known, which are distributed among various institutions and private collections across Europe, and a complete hypodigm is missing. Most specimens comprise of postcranial material, whereas skull material is comparatively rare and only known from five different specimens: **RCSHC/Fossil Reptiles 308**, **WMsN P 47361**, **TWCMS S1348(.1 and .2)**, **IGWuG 463016**, and **NMK S 180**. Only **NMK S 180** represents a complete and well-preserved skull.

Diagnosis. Ezcurra (2016) provided the most recent diagnosis for the species.

Remarks. *Protorosaurus speneri* represents the best-known Permian archosauromorph. The first specimen, **RCSHC/Fossil Reptiles 308** or the Spener specimen was described by Spener (1710), and interpreted as a fossil of a Nile crocodile (*Crocodylus niloticus*). *Protorosaurus speneri* was erected and described in detail based on additional material (Meyer 1830; Meyer 1832; Meyer 1856). Additional specimens were described (e.g. Evans & King 1993; Fichter 1995; Haubold & Schaumberg 1985), and recently the taxon was extensively revised (Gottmann-Quesada & Sander 2009). Most of the approximately 40 known specimens are from the Kupferschiefer Formation of Germany, whereas two come from the contemporary Marl Slate of England (Evans & King 1993). Most recent phylogenetic analyses recovered *Protorosaurus speneri* as the sister taxon to all other archosauromorphs (e.g. Ezcurra 2016; Pritchard et al. 2015; for an alternative placement of *Protorosaurus speneri* and tanystropheids outside Archosauromorpha~~,~~ see Simões et al. 2018).

Czatkowiella harae Borsuk-Białynicka & Evans 2009

Age. ~~e~~arliest ~~L~~ate Olenekian (Shishkin & Sulej 2009).

Occurrence. Czatkowice 1, a fissure or cave infill of the Czatkowice quarry near Kraków, Poland.

Holotype. **ZPAL R.V/100**, an isolated, nearly complete right maxilla bearing teeth.

~~Hypodigm~~. A large number of isolated cranial and postcranial elements that could confidently be distinguished from other tetrapod remains of the Czatkowice 1 locality. A large number of these bones are presented and described by Borsuk-Białynicka & Evans (2009b).

Diagnosis. The diagnosis was provided by Borsuk-Białynicka & Evans (2009b).

Remarks. The material now referred to *Czatkowiella harae* was originally discovered in 1978 at Czatkowice 1. It is represented by many isolated and fragmented remains, which were found among similar remains belonging to other small diapsids, such as the euparkeriid *Osmolskina czatkowicensis* (Borsuk-Bialynicka & Evans 2003; Borsuk-Białynicka & Evans 2009a; Borsuk-Białynicka & Sennikov 2009), the lepidosauromorph *Sophineta cracoviensis* (Evans & Borsuk-Białynicka 2009), the kuehneosaurid *Pamelina polonica* (Evans 2009), and three distinct procolophonids (Borsuk-Białynicka & Lubka 2009). Apart from the most diagnostic elements, bones were assigned to *Czatkowiella harae* largely based on size and fitting individual elements together. The morphology of *Czatkowiella harae* corresponds to that of many early archosauromorphs. Its most distinguishing feature is the presence of three-headed anterior dorsal ribs. It has only been considered phylogenetically by Borsuk-Białynicka & Evans (2009b), who recovered *Czatkowiella harae* as the sister taxon to *Protorosaurus speneri*. The taxon is somewhat problematic for inclusion in phylogenetic analyses, since it cannot be fully demonstrated that the isolated and fragmented remains all represent a single taxon. Here, we follow the identification by Borsuk-Białynicka & Evans (2009b) in all but the most tentatively assigned bones (e.g. the squamosal) and as for all other taxa scored, the reference specimen(s) for each scoring are provided in the Supplementary Material. This allows subsequent workers to critically evaluate scorings, as well as exclude certain specimens that further investigation might find belong to a different taxon. Because the inclusion of potentially composite taxa can negatively influence the accuracy of phylogenetic analyses, *Czatkowiella harae* is omitted from the analyses 3 and 4 here.

Tanystropheus longobardicus Bassani 1886

Age. latest Anisian-Ladinian (Spiekman et al. 2020; Spiekman & Scheyer 2019; Stockar 2010).

Occurrence. Besano Formation and the Cassina beds, Meride Limestone, of Monte San Giorgio, Switzerland and Italy.

Neotype. The holotype specimen was destroyed during WWII in Milan (Nosotti 2007; Spiekman & Scheyer 2019; Wild 1973). Neotype established by Wild (1973): **PIMUZ T 2791** – Almost complete and largely articulated, bituminous specimen, lacking the distal half of the tail.

~~Hypodigm~~. **PIMUZ T 2779**, **PIMUZ T 2781**, **PIMUZ T 2795**, **PIMUZ T 2485**, **PIMUZ T 2482**, **PIMUZ T 2484**, **PIMUZ T 3901**, **PIMUZ T 1277**, **MSNM BES SC 265**, and **MSNM BES SC 1018**.

Diagnosis. The most recent diagnosis for the taxon was provided by Spiekman et al. (2020, Methods S1).

Remarks. *Tanystropheus longobardicus* was first described based on a single, partially articulated specimen from the Besano Formation of Monte San Giorgio. It was interpreted as a pterosaur and assigned to *Tribelesodon longobardicus*, with the generic name referring to the tricuspid teeth that were present in the jaws (Arthaber 1922; Bassani 1886; Nopsca 1923). This specimen has unfortunately been lost, but it has been figured in Arthaber (1922). The discovery of additional specimens from the Besano Formation revealed that the elements ~~which~~ were interpreted as elongated phalanges represented elongate cervical vertebrae that were similar to those that were known from the Upper Muschelkalk of the Germanic Basin, which had been assigned to *Tanystropheus conspicuus* (Peyer 1930; Peyer 1931). Therefore, the species was re-assigned to *Tanystropheus longobardicus*. Wild (1973) described the species in detail, and assigned **PIMUZ T 2791** as the neotype. Additional specimens were described in Wild (1980a), including a specimen from the slightly younger Meride Limestone, which was assigned to the separate species *Tanystropheus meridensis*. However, this specimen, as well as an additional specimen that was found from the Meride Limestone (Renesto 2005), were shown to be morphologically indistinguishable from the specimens from the Besano Formation, and therefore *Tanystropheus meridensis* was considered a junior synonym of *Tanystropheus longobardicus* (Nosotti 2007; Spiekman & Scheyer 2019). The functional morphology and configuration of the neck of *Tanystropheus longobardicus* was treated extensively by Tschanz (1986). A small-sized *Tanystropheus* skeleton lacking the skull from the Falang Formation of China was identified as *Tanystropheus* sp., and might represent the only known occurrence of *Tanystropheus longobardicus* from China, indicating a Tethys-wide distribution of the species (Li 2007). Nosotti (2007) described in detail specimens from the Italian side of the Besano Formation and revised the species. Recently, a combined morphological and palaeohistological study revealed that the small-sized specimens of *Tanystropheus* from Monte San Giorgio, which bear distinct tricuspid marginal teeth, are skeletally mature (Spiekman et al. 2020). This indicates that the small-sized specimens represent a separate species from the large-sized specimens, and the former were re-assigned to the new species *Tanystropheus hydroides*. *Tanystropheus longobardicus* was therefore a relatively small-sized *Tanystropheus* species, likely not exceeding 2 metres in total length, which fed on small prey, including soft-shelled invertebrates.

Tanystropheus hydroides Spiekman, Neenan, Fraser, Fernandez, Rieppel, Nosotti & Scheyer 2020

Age. Latest Anisian-earliest Ladinian (Spiekman et al. 2020; Stockar 2010).

Occurrence. Besano Formation of Monte San Giorgio, Switzerland and Italy.

Holotype. **PIMUZ T 2790**, a compressed skull and anterior eight cervical vertebrae in semi-articulation.

~~Hypodigm.~~ **PIMUZ T 2787**, **PIMUZ T 2793**, **PIMUZ T 2818**, **PIMUZ T 2819**, **PIMUZ T 183**, **SNSB-BSPG 1953 XV 2**, and **MSNM V 3663**.

Diagnosis. The diagnosis for *Tanystropheus hydroides* has been provided in Spiekman et al. (2020, p. 2).

Remarks. Specimens of *Tanystropheus hydroides* were previously considered as the adult morphotype of *Tanystropheus longobardicus*, but they were recently shown to represent a separate, large-sized species (Spiekman et al. 2020). Specimens of *Tanystropheus hydroides* were described as *Tanystropheus longobardicus* in Peyer (1931), Kuhn-Schnyder (1947; 1959), and Wild (1973). A *Tanystropheus* specimen has been described from China that attained a size similar to *Tanystropheus hydroides* (Rieppel et al. 2010). Although the postcranial skeleton of this specimen cannot be distinguished from *Tanystropheus hydroides*, the absence of a skull has not allowed the specimen to be assigned to this species with certainty[illegible]owever, it is clear that the genus, and possibly the species *Tanystropheus hydroides*, had a Tethys-wide distribution (Spiekman & Scheyer 2019). *Tanystropheus hydroides* was an aquatic ambush predator that employed its long-neck and a laterally directed snapping bite to catch its prey, which consisted of fish and cephalopods (Spiekman et al. 2020).

GMPKU P 1527

Age. Earliest Carnian (Rieppel et al. 2010).

Occurrence. The upper part of the Zhuganpo Member of the Falang Formation of Nimaigu near Xingyi City, Wusha District, Guizhou Province, southwestern China.

Remarks. A large-sized *Tanystropheus* skeleton from China that is largely complete, but lacking the skull, anterior segment of the neck, the distal end of the tail, and most of the pedes, was identified as *Tanystropheus* cf. *longobardicus* (Rieppel et al. 2010). Recently, it was shown that the large-sized specimens of *Tanystropheus* from Monte San Giorgio represent a separate species from the small-sized specimens, and have been assigned to *Tanystropheus hydroides* (Spiekman et al. 2020). Therefore, the assignment of **GMPKU P 1527** has consequently been altered to *Tanystropheus* cf. *hydroides*. However, because this specimen is known from the eastern side of the Tethys Ocean, whereas the referred specimens of *Tanystropheus hydroides* derive its western margin, this specimen cannot be unequivocally assigned to the species, particularly because cranial morphology appears to be more variable than that of the postcranium within the genus. Because of the biogeographical importance of this specimen as the best-known *Tanystropheus* remains from the eastern Tethys it was incorporated as a separate OTU here.

Tanystropheus “conspicuus” Meyer 1855

Age. Late Anisian to Ladinian (Menning & Hendrich 2016; Spiekman & Scheyer 2019).

Occurrence. Various localities of the Upper Muschelkalk and Lettenkeuper of Central Europe. An overview of all known localities can be found in Supplementary Table 1 of Spiekman & Scheyer (2019).

Lectotype. U-MO BT 740, an isolated, three-dimensionally preserved cervical vertebra.

~~Hypodigm~~. The referred specimens of *Tanystropheus “conspicuus”* are listed in Supplementary Table 1 of Spiekman & Scheyer (2019).

Remarks. A number of elongate bones from the Upper Muschelkalk of Bayreuth, Germany, were identified as reptilian vertebrae and assigned to *Tanystropheus “conspicuus”* by Meyer (1855). These bones had previously also been described by Count Georg zu Münster, who had interpreted these bones as limb bones of a saurian reptile, which he had named “*Macroscelosaurus*”. However, since this work has been lost and this generic name has fallen into disuse (*nomen oblitum*), the generic name *Tanystropheus* has received precedence (Wild 1973, p. 148). Following the description of the semi-articulated specimens of *Tanystropheus longobardicus* (Peyer 1930; Peyer 1931), Huene (1931) considered material previously identified as “*Thecodontosaurus latespinatus*”, “*Thecodontosaurus primus*”, and “*Procerosaurus cruralis*” from the Upper Muschelkalk of Europe to very likely belong to *Tanystropheus “conspicuus”*. Wild (1973) provided a systematic palaeontology section in which these taxa were synonymized with *Tanystropheus conspicuus*. Fragmentary and isolated remains of *Tanystropheus “conspicuus”* are known from the Upper Muschelkalk and Lettenkeuper throughout Central Europe (late Anisian to Ladinian; Menning & Hendrich 2016). This material comprises isolated cervical, dorsal, sacral, and caudal vertebrae, two femora, and an ischium. Peyer (1931) refrained from providing a detailed comparison of *Tanystropheus longobardicus* with *Tanystropheus “conspicuus”* and *“Tanystropheus antiquus”* from the Germanic Basin. Wild (1973) distinguished *Tanystropheus “conspicuus”* from *Tanystropheus longobardicus* on the basis of comparatively wider rib attachment sites and a concavity on the anterior end of the neural spine of the cervical vertebrae. Although he considered these minor differences to be insufficient for a species definition, the distinction between the two taxa was maintained in expectation of additional specimens that would allow for a more complete comparison. A recent revision of *Tanystropheus* spp. revealed that no distinct morphological differences could be identified between *Tanystropheus “conspicuus”*, *Tanystropheus hydroides* (therein the large morphotype of *Tanystropheus longobardicus*), and *Tanystropheus haasi* (Spiekman & Scheyer 2019). However, since the referred material of both *Tanystropheus “conspicuus”* and *Tanystropheus haasi* is insufficient for a detailed comparison and both are only known from fragmentary and isolated postcranial elements, these taxa were considered as nomina dubia.

“Tanystropheus antiquus” Huene 1905

Age. Latest Olenekian to middle Anisian (Menning & Hendrich 2016; Spiekman & Scheyer 2019).

Occurrence. Lower Muschelkalk of Silesia, Poland (Gogolin Formation), Germany (Schaumkalk Formation), and the Netherlands (Vossenveld Formation) (see also Supplementary Table 1 of Spiekman & Scheyer 2019).

Syntype. **SMNS 16687**, **SMNS 10110**, **MGUWr 3872s**, **MGUWr 3888s**, **MGUWr 3895s**, **MGUWr 3902s** and some uncatalogued **MGUWr** specimens, all consisting of single cervical vertebrae. Wild (1973) had assigned **SMNS 10110** as the lectotype, but considered the **MGUWr** specimens to have been lost.

~~Hypodigm~~. All specimens assigned to “*Tanystropheus* (c.f.) *antiquus*” are listed in Supplementary Table 1 of Spiekman & Scheyer (2019).

Diagnosis. Recent diagnoses were provided for this taxon by Sennikov (2011) for "*Protanystropheus antiquus*" and Fraser & Rieppel (2006) for "*Tanystropheus antiquus*".

Remarks. Following the description of the syntype of "*Tanystropheus antiquus*" from the Lower Muschelkalk of Gogolin and Krapkowice, Silesia, Poland (Huene 1905), other isolated *Tanystropheus*-like remains from the Lower Muschelkalk were attributed to the species (e.g. Huene 1931; Kuhn 1971; Schmidt 1928; Schmidt 1938; Spiekman et al. 2019). Ortlam (1966) referred material of the uppermost Buntsandstein (Anisian) to *Tanystropheus longobardicus* and *Macrocnemus bassanii*, but this material was later assigned to "*Tanystropheus antiquus*" by Wild (1980b). The Buntsandstein precedes the Muschelkalk and in contrast to the latter represents largely fluvial sediments (Feist-Burkhardt et al. 2008), and Wild (1980b) concluded that the discovery of "*Tanystropheus antiquus*" from the Buntsandstein, indicated that at least the juvenile individuals had a terrestrial lifestyle. Both Wild (1987) and Evans (1988) later suggested that "*Tanystropheus antiquus*" might belong to a separate genus, based on the large morphological discrepancy between this taxon and other *Tanystropheus* species. Fraser & Rieppel (2006) revised the Buntsandstein specimens and concluded that it represented a separate taxon from "*Tanystropheus antiquus*" and assigned it to the new taxon *Amotosaurus rotfeldensis*. Despite a lack of diagnostic characters in the material, Fraser & Rieppel (2006) tentatively maintained the assignment of the Lower Muschelkalk specimens to "*Tanystropheus antiquus*". Sennikov (2011) compared "*Tanystropheus antiquus*" to *Augustaburiania vatagini*, and also concluded that the former was generically distinct from *Tanystropheus* spp. and renamed the taxon "*Protanystropheus antiquus*".

The relative length of the cervical vertebrae might indeed indicate that "*Tanystropheus antiquus*" is more closely related to *Augustaburiania vatagini* or *Amotosaurus rotfeldensis* than to other *Tanystropheus* species. However, the taxonomic status of "*Tanystropheus antiquus*" is currently unclear, since many specimens of the syntype material (Huene 1902; Huene 1905) were long considered to have been lost (Fraser & Rieppel 2006; Sennikov 2011; Wild 1973; Wild 1980b). However, these specimens have recently resurfaced and were briefly discussed by Skawiński et al. (2017). Any taxonomic evaluation of this taxon would first require a detailed revision of this type material to assess whether subsequently referred specimens of "*Tanystropheus antiquus*" from other localities represent the same species (Spiekman et al. 2019; Spiekman & Scheyer 2019; Wild & Oosterink 1984). Such a revision is currently underway (Szczygielski, personal commun. 2019), and therefore the taxonomic status of "*Tanystropheus antiquus*" is not addressed here. However, we include a preliminary "*Tanystropheus antiquus*" OTU in our analyses based on the strong morphological similarity of the tanystropheid cervical vertebrae from the Lower

Muschelkalk of Central Europe. Our scoring of this OTU is based on two complete cervical vertebrae, **SMNS 16687** and **Coll. Oosterink A638**. The former specimen comes from the Lower Muschelkalk of Krapkowice, Poland, and constitutes part of the syntype of “*Tanystropheus antiquus*”, and the latter derives from the Lower Muschelkalk of Winterswijk, the Netherlands (Spiekman et al. 2019; Wild & Oosterink 1984).

Sclerostropheus fossai Wild 1980

Age. Late Norian (Rigo et al. 2009; Tackett & Tintori 2019).

Occurrence. N-slope of Canto Alto, near Poscante in Val Brembana, Bergamo Province, Italy (Wild 1980a).

Holotype. **MCSNB 4035**, a partial, articulated cervical column.

Diagnosis. The diagnosis was recently provided by Spiekman & Scheyer (2019).

Remarks. *Sclerostropheus fossai* is known from a single specimen, which constitutes a partial, semi-articulated cervical column, and was previously considered within the genus *Tanystropheus* (Wild 1980a). However, the morphology of the cervical vertebrae and ribs differs distinctly from that of other *Tanystropheus* species, which was briefly indicated by Renesto (2005), and it was recently assigned to the new genus *Sclerostropheus* (Spiekman & Scheyer 2019). ~~Together with~~ *Langobardisaurus pandolfii*, *Sclerostropheus fossai* represents a second tanystropheid taxon known from the Norian of northern Italy.

Macrocnemus bassanii Nopsca 1930

Age. latest Anisian-Ladinian.

Occurrence. Besano Formation and Meride Limestone of Monte San Giorgio, Switzerland and Italy (Jaquier et al. 2017; Peyer 1937; Renesto & Avanzini 2002; Rieppel 1989; Stockar 2010).

Holotype. **MSNM 14624**, ~~A~~ cast of MSNM specimen Besano I, a poorly preserved specimen ~~which~~ was destroyed in Milan during WWII (Fraser & Furrer 2013).

~~Hypodigm~~. Rieppel (1989, p. 374) provided the hypodigm for the *Macrocnemus bassanii* material housed at PIMUZ. ~~The~~ specimen listed there as A 111/208 is now catalogued as **PIMUZ T 4822**. Additionally, two specimens of *M. bassanii* are housed in the MSNM: **MSNM BES SC 111**; a complete and fully articulated juvenile including skin remains; **MSNM V 457**, a disarticulated adult specimen, in which a number of skull and jaw bones are preserved, as well as several cervical, dorsal, and caudal vertebrae, gastralia, ribs, and both pelvic girdles and both hindlimbs, excluding the feet.

Diagnosis. The most recent diagnosis was provided by Jaquier et al. (2017).

Remarks. *Macrocnemus bassanii* is the type species of the genus and is known from the Middle Triassic of Switzerland and Italy. It was first described by Nopsca (1930), based on the poorly preserved, and now lost holotype, of which a cast has been preserved. The taxon was described in more detail following the discovery of multiple well-preserved specimens (Peyer 1937). Further details of the skull were provided by Kuhn-Schnyder (1962) and Rieppel & Gronowski (1981). The postcranium and its functional considerations were discussed by Rieppel (1989), which indicated that *Macrocnemus bassanii* was facultatively bipedal. An excellently preserved juvenile specimen, preserving soft tissue was described by Premru (1991) and Renesto & Avanzini (2002). The skull of *Macrocnemus bassanii* was recently redescribed in detail aided by synchrotron tomography, which revealed many similarities in the cranial configuration of the skull with *Prolacerta broomi* (Miedema et al. 2020). *Macrocnemus bassanii* is currently firmly established as a tanystropheid (e.g. Ezcurra 2016; Pritchard et al. 2015).

Macrocnemus fuyuanensis Li, Zhao & Wang 2007

Age. Late Anisian-Ladinian.

Occurrence. Besano Formation of Monte San Giorgio, Switzerland and Zhuganpo Member of the Falang Formation, Yun-nan Province, China (Jaquier et al. 2017; Jiang et al. 2011; Li et al. 2007; Scheyer et al. 2020b).

Holotype. **IVPP V15001** - Mostly complete and largely articulated skeleton missing most of the skull.

~~Hypodigm~~. **GMPKU-P-3001**, almost complete and fully articulated specimen, missing almost the complete tail; **PIMUZ T 1559**, virtually complete and disarticulated specimen, missing parts of the skull, almost the complete tail, and missing the hindlimbs.

Diagnosis. The most recent diagnosis for the species was provided by Scheyer et al. (2020b).

Remarks. *Macrocnemus fuyuanensis* was first described based on the holotype specimen by Li et al. (2007), and distinguished from *Macrocnemus bassanii* based on the limb ratios as well as the number of dorsal vertebrae. Jiang et al. (2011) described another specimen of *Macrocnemus fuyuanensis* with a completely preserved skull, **GMPKU-P-3001**, and concluded that it differed from *Macrocnemus bassanii* in a number of characters. A specimen from the upper Besano Formation was described by Jaquier et al. (2017). This specimen was more similar in limb proportions to *Macrocnemus fuyuanensis* than to *Macrocnemus bassanii*, and also differed from the latter in the morphology of the interclavicle, and identified as *Macrocnemus* aff. *fuyuanensis*. Furthermore, these authors revised the cranial morphology of *Macrocnemus fuyuanensis* specimen **GMPKU-P-3001**, indicating that it did not substantially differ from that of *Macrocnemus bassanii*. The holotype **IVPP V15001** was redescribed and revealed new anatomical details for the taxon, particularly with regards to the palate and pectoral girdle (Scheyer et al. 2020b). The morphology of the interclavicle of the holotype was in correspondence with that of the Swiss specimen **PIMUZ T 1559**, and distinctly differed from that of specimens assigned to *Macrocnemus bassanii*. Therefore, **PIMUZ T 1559** was re-assigned to *Macrocnemus fuyuanensis* and the species thus occurred on both the eastern and western margins of the Tethys Ocean. *Tanystropheus* sp., another well-known tanystropheid, also had a Tethys-wide distribution. However, it is currently uncertain whether the Chinese specimens of this genus represent the same species as the European forms (Spiekman et al. 2020; Spiekman & Scheyer 2019).

Macrocnemus obristi Fraser & Furrer 2013

Age. Early Ladinian.

Occurrence. Prosanto Formation of Ducanfurgga near Davos, canton Graubünden, Switzerland (Fraser & Furrer 2013).

Holotype. **PIMUZ A/III 1467** (housed in the Bündner Naturmuseum, Chur, Switzerland), an articulated partial skeleton, which consists of the posterior dorsal vertebrae, pelvic girdle and hindlimbs, and most of the tail.

~~Hypodigm~~. **PIMUZ A/III 722**, a right pes preserved in dorsal view.

Diagnosis. The diagnosis was provided by Fraser & Furrer (2013, p. 200)

Remarks. *Macrocnemus obristi* is known from two specimens from the Prosanto Formation (Fraser & Furrer 2013). It differs from *Macrocnemus bassanii* and *Macrocnemus fuyuanensis* based on the ratio of the femur and tibia (Fraser & Furrer 2013; Jaquier et al. 2017). Due to its recent description and only partially known morphology, *Macrocnemus obristi* has previously not been included in any phylogenetic analysis.

Tanytrachelos ahynis Olsen 1979

Age. Late Carnian

Occurrence. Virginia Solite Quarry B, Upper member of the Cow Branch Formation, part of the Dan River Group (Newark Supergroup), USA (Casey et al. 2007; Liutkus-Pierce et al. 2014; Olsen 1979).

Holotype. **YPM 7496**, a largely complete, articulated specimen.

~~Hypodigm~~. Hypodigm listed by Olsen (1979, p. 4-5, and note on p. 13), most specimens currently housed in the VMNH.

Diagnosis. The diagnosis for *Tanytrachelos ahynis* was provided by Olsen (1979)

Remarks. *Tanytrachelos ahynis* was described by Olsen (1979) and is known from hundreds of specimens from Solite Quarry B in Virginia (Casey et al. 2007). However, many detailed morphological features are unknown for *Tanytrachelos ahynis*, due to the poor preservation of the specimens. Recently, the authors subjected a relatively well-preserved specimen (**NMS G.2017.11.1**) to synchrotron radiation micro-computed tomography. This revealed the inner anatomy of the cervical vertebrae in some detail, highlighting that as in *Tanystropheus* spp. and *Macrocnemus bassanii* the neural canal passes through the vertebral centrum in *Tanytrachelos ahynis*. However, morphological details could not be observed due to the poor preservation of the specimen, which is likely attributable to diagenetic factors (Liutkus-Pierce et al. 2014). The Solite Quarry B is represented by lacustrine deposits (Fraser et al. 1996), and *Tanytrachelos ahynis* had an aquatic lifestyle (Casey et al. 2007; Olsen 1979). As in *Tanystropheus longobardicus* and *Tanystropheus hydroides*, the presence of paired heterotopic bones parallel to the anterior caudal vertebrae in approximately half of the articulated specimens preserving this region indicates sexual dimorphism.

AMNH FARB 7206

Age. Carnian, Late Triassic (Colbert & Olsen 2001)

Occurrence. Lockatong or Stockton Formation of Hudson County, New Jersey.

Remarks. Small reptilian specimens from the approximately contemporaneous Lockatong Formation of New Jersey have been compared to *Tanytrachelos ahynis*, and although it could not be excluded that some of these specimens might represent *Tanytrachelos ahynis*, not enough diagnostic features were preserved to positively identify any of these specimens to this taxon (Olsen 1979). However, one of these specimens, **AMNH FARB 7206**, was recently referred to *Tanytrachelos ahynis* by Pritchard et al. (2015). This specimen was here scored separately from the specimens from the Solite Quarry B to test this hypothesis and shown to differ in the shape of the cervical vertebrae and the curvature of the femur, raising doubts as to whether this specimen can be referred to *Tanytrachelos ahynis*. Additionally, Pritchard et al. (2015) referred a single calcaneum from the middle Norian Hayden Quarry locality of New Mexico to this species based on the striking similarities in morphology between this element, and the calcaneum of **AMNH FARB 7206**. Since it is currently uncertain whether the latter can be referred to *Tanytrachelos ahynis*, we also consider the assignment of the Hayden Quarry calcaneum to *Tanytrachelos ahynis* as equivocal. Therefore, only specimens from the Solite Quarry B can currently be confidently assigned to *Tanytrachelos ahynis*.

Amotosaurus rotfeldensis Fraser & Rieppel 2006

Age. Early Anisian.

Occurrence. Quarry Kossig (Upper Buntsandstein) of Baden-Württemberg, Germany (Fraser & Rieppel 2006; Ortlam 1966).

Holotype. **SMNS 50830**, a largely disarticulated skeleton, including an articulated cervical series, maxilla, parabasisphenoid, scapulacoracoids, ~~and~~ pelvic girdle~~s~~, and scattered dorsal vertebrae.

~~Hypodigm~~. Many specimens housed in the SMNS, some of which are unprepared or unaccessioned, including: **SMNS 54783 a and b**, a slab and counterslab preserving two largely disarticulated skeletons, including a poorly preserved skull roof, cervical vertebrae, an articulated dorsal vertebral series, three articulated hindlimbs including pedes, and a partial forelimb including manus; **SMNS 50691**, three slabs, preserving a partial pes, a coracoid and maxilla, and a partial skull in ventral view, ilium, and dorsal vertebrae, respectively; **SMNS 54784a and b**, a slab and counterslab preserving the palatal region of a skull and a partial cervical series; **SMNS 54810**, disarticulated skeletons, including both cranial and extensive postcranial remains; **SMNS 90600**, posterior part of the vertebral column, including sacral and anterior caudal vertebrae; **SMNS 90601**, articulated maxilla and jugal; **SMNS 90540**, two skulls in palatal view; **SMNS unnumbered (1)**, partial mandible and cervical vertebrae and ribs; **SMNS unnumbered (2)**, disarticulated cranial elements and a partial cervical series; **SMNS unnumbered (3)**, skull in palatal view, three anterior cervical vertebrae; **SMNS unnumbered (4)**, sacral region.

Diagnosis. The diagnosis of *Amotosaurus rotfeldensis* was provided by Fraser & Rieppel (2006, p. 867).

Remarks. Several specimens of associated skeletons from the Buntsandstein of Baden-Württemberg were assigned to *Macrocnemus bassanii* and *Tanystropheus longobardicus* by Ortlam (1966). However, Wild (1980b) considered this material to represent juvenile specimens of "*Tanystropheus antiquus*", which is known from several isolated remains, mostly cervical vertebrae, from the Lower Muschelkalk of the Germanic Basin (Spiekman & Scheyer 2019). Fraser & Rieppel (2006) re-examined the specimens from the Buntsandstein and assigned it to the new taxon *Amotosaurus rotfeldensis*. The genus was named in honour of R. Wild (amoto = wild in Latin). Ezcurra (2016) and Pritchard et al. (2015) incorporated *Amotosaurus rotfeldensis* in their phylogenetic analyses and provided several new morphological observations for the taxon.

Augustaburiania vatagini Sennikov 2011

Age. Latest Olenekian.

Occurrence. Donskaya Luka locality, right slope of the Don River valley, Lipovskaya Formation, Ilovlyanskii District, Volgograd Region, Russia (Sennikov 2011).

Holotype. **PIN 1043/587**, an isolated middle cervical vertebra.

~~Hypodigm~~. The referred specimens are listed in Sennikov (2011, p. 98).

Diagnosis. The diagnosis was provided by Sennikov (2011).

Remarks. *Augustaburiania vatagini* is known from the latest Olenekian (Early Triassic) of Donskaya Luka of the Don River valley, Russia, and thus represents one of the earliest known tanystropheids together with likely tanystropheid material from the Sanga do Cabral Formation (Induan–early Olenekian) of Brazil (De Oliveira et al. 2018; De Oliveira et al. 2020). Like other tanystropheids, such as "*Tanystropheus antiquus*" and *Tanystropheus "conspicuus"*, *Augustaburiania vatagini* is solely known from isolated postcranial remains, largely represented by cervical vertebrae. The relative length of the mid-cervical vertebrae of *Augustaburiania vatagini* is longer than that of “*Tanystropheus antiquus*” and *Amotosaurus rotfeldensis*, but shorter than that of other *Tanystropheus* species. Furthermore, the cervical vertebrae of *Augustaburiania vatagini* can be distinguished by a distinct concave margin of the centrum of the cervical vertebrae, although the expression of this character in the referred material is subject to much intraspecific variation. Furthermore, the number of cervical vertebrae of *Augustaburiania vatagini*, which was considered to be eight or nine, cannot be established, since no articulated cervical vertebrae have been preserved. Species differentiation based on isolated remains, particularly when relying on cervical vertebrae, is problematic, as their morphology is subject to intraspecific variation and their relative position in the cervical column (Spiekman & Scheyer 2019). As such, although *Augustaburiania vatagini* is known from older deposits than any other European tanystropheid~~s~~, and the morphology of the cervical vertebrae shows minor differences from those of other taxa, the taxonomic status of *Augustaburiania vatagini* remains hard to assess.

Raibliania calligarisi Dalla Vecchia 2020

Age. Early Carnian (Julian).

Occurrence. Predil Limestone near Prasnig Brook, Tarvisio, Udine Province, Italy (Dalla Vecchia 2020).

Holotype. **MFSN 27532**, a partial skeleton comprising the thoracic part of the vertebral column, a single partial cervical vertebra, sacral vertebrae, part of the pelvic girdle and left femur, and a purported tooth.

Diagnosis. The diagnosis was provided by Dalla Vecchia (2020).

Remarks. *Raibliania calligarisi* was recently described from a single specimen from the early Carnian of northern Italy. It is closely related to *Tanystropheus longobardicus* and is slightly younger than the known occurrence of this species (Spiekman et al. 2020). *Raibliania calligarisi* can be distinguished from other tanystropheids based on the morphology of neural spines of the dorsal vertebrae, the pleurapophyses of the posterior dorsal vertebrae, the iliac blade, the anterior portion of the pubis, and a single, disarticulated tooth (Dalla Vecchia 2020). The identification of the single, isolated tooth is somewhat equivocal, as it is located far from where the head would have been preserved. *Raibliania calligarisi* is here considered in a phylogenetic context for the first time. Another specimen discovered in the vicinity of the holotype of *Raibliania calligarisi*, **MFSN 13228**, consisting of three articulated caudal vertebrae, represents the only other described tetrapod remains from the locality. This specimen has not been referred to *Raibliania calligarisi* due to the lack of overlapping morphology between it and the holotype (Dalla Vecchia 2020). Although the relative size of the vertebrae corresponds to that of the holotype of *Raibliania calligarisi*, the morphology of the neural spine differs distinctly from that of *Tanystropheus longobardicus*, to which *Raibliania calligarisi* is closely related.

Prolacerta broomi Parrington 1935

Age. Induan.

Occurrence. Middle Beaufort beds, *Lystrosaurus* AZ, Katberg Formation, South Africa; Transanctartic Mountains, Fremouw Formation, Antarctica (Groenewald & Kitching 1995; Peecook et al. 2019).

Holotype. **UMZC 2003.40** - A partial skull and mandible.

~~Hypodigm.~~ The referred specimens are listed in Spiekman (2018, p. 4-5).

Diagnosis. The latest diagnosis of *Prolacerta broomi* was provided by Spiekman (2018).

Remarks. *Prolacerta broomi* was first described by Parrington (1935) based on a crushed partial skull found in the Katberg Formation, *Lystrosaurus* Zone, near Harrismith, South Africa. *Prolacerta broomi* has played an important role in discussions on the evolutionary origin of modern reptile groups, and has been considered both as an ancestral lepidosaur (e.g. Camp 1945; Parrington 1935) and archosaur (e.g. Romer 1956). *Prolacerta broomi* was first identified as a “protorosaur” by Camp (1945). Following the discovery of more specimens, the complete morphology of *Prolacerta broomi*, including the postcranium was described (Gow 1975). This revealed that *Pricea longiceps* Broom & Robinson 1948 represented a junior synonym of *Prolacerta broomi*. The braincase of *Prolacerta broomi* was described by Evans (1986). Based on new specimens as well as a reappraisal of previously described South African material, Modesto & Sues (2004) provided a redescription of the skull of *Prolacerta broomi*. Specimens of *Prolacerta broomi* have also been described from Antarctica, consisting of several smaller, likely juvenile specimens, and a single, large-sized specimen, which is slightly larger than the specimens known from South Africa (Colbert 1987; Spiekman 2018). Although previously considered a member of the “protorosaurs”, recent phylogenetic analysis indicate that *Prolacerta broomi* is more closely related to Archosauriformes than *Protorosaurus speneri* and tanystropheids are (e.g. Dilkes 1998; Ezcurra 2016; Modesto & Sues 2004; Pritchard et al. 2015; Rieppel et al. 2003). *Prolacerta broomi* has been used widely as an outgroup in phylogenetic analyses on Archosauriformes and early crown-archosaurs (e.g. Butler et al. 2015; Desojo et al. 2011; Dilkes & Sues 2009; Nesbitt 2011; Sookias 2016).

Ozimek volans Dzik & Sulej 2016

Age. Late Carnian or early Norian (Dzik & Sulej 2016; Szulc et al. 2017).

Occurrence. Grabowa Formation (Silesian Keuper) of Krasiejów, Upper Silesia, Poland.

Holotype. **ZPAL AbIII/2512**, partial skeleton missing the skull.

~~Hypodigm.~~ A complete hypodigm can be found in Dzik & Sulej (2016).

Diagnosis. The diagnosis was provided in Dzik & Sulej (2016).

Remarks. *Ozimek volans* was recently described based on several partial and disarticulated skeletons (Dzik & Sulej 2016). An elongate vertebra now referred to this taxon was previously linked to either pterosaurs or *Tanystropheus* due to its extreme elongation (Dzik & Sulej 2007). It is considered a close relative of the gliding reptile *Sharovipteryx mirabilis* and was possibly also a glider, although a comparison is limited due to the poorly known morphology of *Sharovipteryx mirabilis*. The morphology of *Ozimek volans* is highly derived and differs distinctly from other "protorosaurs" in the relative length and gracile construction of the limb bones and the configuration of the pectoral girdle, which includes an enlarged coracoid and possibly ossified sternum. Although formally assigned to the family Sharovipterygidae, *Ozimek volans* was considered a "protorosaur" based on the presence of elongate cervical vertebrae, the posterior curvature of the scapula, and the procoelous articulation surfaces of the cervical vertebrae (which occur in *Tanytrachelos ahynis* and *Langobardisaurus pandolfii* among tanystropheids, but which is widespread ~~in~~ diapsids, e.g. drepanosaurs; Dzik & Sulej 2016). Unfortunately, the skull morphology of *Ozimek volans* is only partially known and identification of many cranial bones is uncertain due to their disassociation and peculiar morphology. *Ozimek volans* has been included in the phylogenetic analysis of Pritchard & Sues (2019), in which it was recovered within Tanystropheidae as the sister taxon to a clade comprising *Langobardisaurus pandolfii* and *Tanytrachelos ahynis*.

Elessaurus gondwanoccidens De Oliveira, Pinheiro, Da Rosa, Dias da Silva & Kerber 2020

Age. Induan-Olenekian (De Oliveira et al. 2020; Dias-da-Silva et al. 2017).

Occurrence. Bica São Tomé, Sanga do Cabral Formation, São Francisco de Assis, Rio Grande do Sul, southern Brazil.

Holotype. **UFSM 11471**, a left hindlimb, partial pelvis, a single sacral vertebra and three caudal vertebrae.

Diagnosis. The diagnosis was provided by De Oliveira et al. (2020).

Remarks. *Elessaurus gondwanoccidens* is known from a single hind limb, partial pelvis, and a few sacral and caudal vertebrae, and has been identified as a tanystropheid (De Oliveira et al. 2020). Several isolated cervical vertebrae with a typical tanystropheid morphology have also been described from the Sanga do Cabral Formation, from which *Elessaurus gondwanoccidens* is known (De Oliveira et al. 2018). ~~However, due to the limited morphological information currently available for *Elessaurus gondwanoccidens*, its identification as a tanystropheid is somewhat uncertain.~~ The phylogenetic analysis presented by De Oliveira et al. (2020) that excludes *Jesairosaurus lehmani* and *Dinocephalosaurus orientalis* recovered *Elessaurus gondwanoccidens* as the sister taxon to ~~all other~~ tanystropheids. However, the analysis that includes both *Jesairosaurus lehmani* and *Dinocephalosaurus orientalis* ~~did not~~ recover *Elessaurus gondwanoccidens* within Tanystropheidae (Supplementary Material of De Oliveira et al. 2020). Instead, *Elessaurus gondwanoccidens* formed a large polytomy with most of the included archosauromorphs. The lack of overlapping morphology between the described material of *Elessaurus gondwanoccidens* and the non-archosauriform archosauromorph *Teyujagua paradoxa*, which are both known from the same locality, implies that it cannot be ruled out that these taxa are synonymous.

Jesairosaurus lehmani Jalil 1997

Age. Late Olenekian-early Anisian (Jalil 1999).

Occurrence. Site 5003 of Busson, at the base of the Zarzaitine Formation, Algeria.

Holotype. **ZAR 06**, a nearly complete skull and mandibles, the neural arches of the five distalmost cervical vertebrae, the complete left and partial right pectoral girdle, and the proximal end of the left humerus.

~~Hypodigm.~~ The hypodigm was provided by Jalil (1997) and Ezcurra (2016).

Diagnosis. The most recent diagnosis was provided by Ezcurra (2016).

Remarks. The material now assigned to *Jesairosaurus lehmani* was originally considered as procolophonid remains (Lehman 1971). However, detailed observation was hampered by the specimens being covered by a hard hematite layer. Additional preparation revealed the diapsid affinity of the material (Jalil 1990), and the material was later described in detail and assigned to *Jesairosaurus lehmani* (Jalil 1997). Ezcurra (2016) provided a morphological redescription of *Jesairosaurus lehmani*. Jalil (1997) identified *Jesairosaurus lehmani* as a "protorosaur" and in a phylogenetic analysis, found it to be the sister taxon to *Malerisaurus langstoni*, whereas the clade they formed, plotted as the sister group to a tanystropheid clade ~~which~~ included *Boreopricea funerea* and *Cosesaurus aviceps*. In a re-analysis of this matrix by Rieppel et al. (2003) *Jesairosaurus lehmani* formed a polytomy with other "protorosaurs", including drepanosaurs, and archosauriforms. In the recent analysis by Ezcurra (2016), *Jesairosaurus lehmani* was recovered as the sister taxon to Tanystropheidae. The unstable position of *Jesairosaurus lehmani* might be related to the poorly resolved relationships of former "protorosaurs" and the difficulty of confident character assessment for this taxon because the specimens are encrusted in hematite, severely hampering their preparation (Jalil 1997).

Langobardisaurus pandolfii Renesto 1994

Age. Middle Norian (Alaunian/Revueltian)

Occurrence. The uppermost section of the Zorzino Limestone Cene quarry, Lombardy, Italy (Renesto 1994b), lower member of the Forni Dolostone of Friuli, Italy (Renesto & Dalla Vecchia 2000), and the Seefeld Formation, near Innsbruck, Austria (Saller et al. 2013).

Holotype. **MCSNB 2883** ~~— A~~n articulated partial skeleton, missing both forelimbs completely, as well as parts of the skull, feet, and tail.

~~Hypodigm~~. **MCSNB 4860**, complete and articulated juvenile preserved in ventral view, with the skull covered by the neck and trunk in external view; **MFSN 1921**, a virtually complete and articulated adult specimen, including a well-preserved skull. Only the posterior part of the tail and part of the left forelimb are missing; **MFSN 26829**, a partial articulated adult specimen, preserving a nearly complete right hindlimb, a partial left hindlimb~~s~~, and some poorly visible parts of the vertebral column and potentially of the pelvic girdle; **P 10121**, a nearly complete impression of an articulated adult, only missing part of the tail, with some fragments of the limb bones and teeth preserved.

Diagnosis. The latest emended diagnosis for *Langobardisaurus pandolfii* was provided by ~~(~~Saller et al. 2013).

Remarks. Renesto (1994b) was the first to describe the genus *Langobardisaurus* based on two specimens originally found in 1974, which were assigned to *Langobardisaurus pandolfii* and considered to be closely related to known tanystropheids, specifically *Macrocnemus bassanii*. It was interpreted as a terrestrial insectivore based on the presence of three cusped teeth, which are quite distinct to the teeth of other archosauromorphs. Bizzarini & Muscio (1995) proposed a new species, *Langobardisaurus rossii*, based on a new but poorly preserved specimen from the Forni Dolostone of Friuli, Italy. This specimen was later considered as a probabl~~y~~ rhynchocephalian lepidosauromorph, mainly inferred from its body proportions, particularly the relative size of the ~~head,~~ cervical ~~region,~~ and trunk region (Renesto & Dalla Vecchia 2007). However, the poor preservation of this specimen prevents an unequivocal taxonomic determination. Another species, *Langobardisaurus*? *tonelloi*, was tentatively ascribed to the genus based on a complete specimen (**MFSN 1921**) by Muscio (1996). The species was considered to differ from *Langobardisaurus pandolfii* in its phalangeal formula and dentition. However, Renesto & Dalla Vecchia (2000) could not find any differences between the phalangeal formula in these two taxa and considered the minor differences in dentition to be attributable to ontogenetic variation, and thus considered *Langobardisaurus tonelloi* to likely represent a junior synonym of *Langobardisaurus pandolfii*, which was later corroborated by Saller et al. (2013). **MFSN 1921** allowed ~~for~~ the first detailed description of the skull of *Langobardisaurus pandolfii* and revealed a unique dentition among archosauromorphs, consisting of an edentulous premaxilla and anterior margin of the maxilla, followed by tricuspid teeth more ~~posteriorly~~ on the maxilla and dentary, and terminating in a very large, molar-like crushing ~~posterior~~most tooth on both the maxilla and dentary. Renesto & Dalla Vecchia (2000) hypothesized that *Langobardisaurus pandolfii* used this highly specialized dentition to feed on large insects, crustaceans, and small scaly fishes. Renesto et al. (2002) described another specimen, **MFSN 26829**, and considered facultative bipedal locomotion for *Langobardisaurus pandolfii*, which has also been proposed for *Macrocnemus bassanii* (Rieppel 1989). **P 10121**, a poorly preserved specimen of *Langobardisaurus pandolfii* consisting of the impression, as well as bone fragments, of a nearly complete skeleton, was described from the Seefeld Formation of Austria, thus extending the biogeographic range of the taxon outside Italy (Saller et al. 2013).

Dinocephalosaurus orientalis Li 2003

Age. Anisian.

Occurrence. Xinmin, Panxian,~~ and~~ Luoping, Guanling Formation, Guizhou Province, China~~.~~ (Li 2003; Liu et al. 2017; Rieppel et al. 2008).

Holotype. **IVPP V13767**, an almost complete skull and the three anteriormost cervical vertebrae and associated ribs.

~~Hypodigm~~. **ZMNH M8752**, an undescribed specimen of which the pelvic morphology was briefly mentioned in comparison to that of *Fuyuansaurus* by Fraser et al. (2013); **LPV 30280**, a partial, articulated skeleton including some disarticulated skull bones, most of the cervical column, parts of the thorax, hindlimbs, and ~~proximal~~ tail. Within the thorax some elements belonging to an embryo are preserved, which indicates that this specimen was pregnant when it died (Liu et al. 2017), **IVPP V13898**, a relatively complete skeleton including a skull preserved in ventral view, a complete cervical series, and parts of the thorax including an articulated fore and hindlimb (Rieppel et al. 2008).

Diagnosis. The most recent diagnosis of *Dinocephalosaurus orientalis* was provided by Rieppel et al. (2008).

Remarks. *Dinocephalosaurus orientalis* was first described based on the holotype which only preserves the skull and three anteriormost cervical vertebrae (Li 2003). The discovery of a specimen preserving much of the postcranial skeleton subsequently revealed a striking convergence between *Dinocephalosaurus orientalis* and *Tanystropheus* spp. (Li et al. 2004). *Dinocephalosaurus orientalis* shares the extreme elongation of the neck with *Tanystropheus* spp., but achieved this elongation through different means, since its neck is ~~made up~~ of comparatively much shorter cervical vertebrae and the neck consists of at least 33 vertebrae, whereas that of *Tanystropheus hydroides* and *Tanystropheus longobardicus* was made up of 13 (Li et al. 2017b; Rieppel et al. 2010; Rieppel et al. 2008). Additionally, the postcranial morphology of *Dinocephalosaurus orientalis* shows clear adaptations to a fully aquatic lifestyle, most notably the paddle-like front and hindlimbs. As for *Tanystropheus* spp., the unique morphology of *Dinocephalosaurus orientalis* has led to various hypotheses regarding its lifestyle and feeding method. Li et al. (2004) tentatively suggested suction feeding for *Dinocephalosaurus orientalis*, which was refuted by Peters (2005) and Demes & Krause (2005). The former argued that *Dinocephalosaurus orientalis* was a benthic ambush predator and a very poor swimmer. This suggestion was in return repudiated by LaBarbera & Rieppel (2005). A general anatomical description of *Dinocephalosaurus orientalis* was provided by Rieppel et al. (2008). This study included a phylogenetic analysis in which *Dinocephalosaurus orientalis* was incorporated into the combined dataset provided by Rieppel et al. (2003), which found a polytomy formed by *Jesairosaurus lehmani*, *Dinocephalosaurus orientalis*, drepanosaurs, and tanystropheids. Liu et al. (2017) described a new *Dinocephalosaurus* specimen, which preserves articulated remains of a ~~juvenile~~ *Dinocephalosaurus* within the thorax of the adult, indicating the first example of vivipary in an archosauromorph reptile. This study also provided an updated version of the phylogenetic analysis of Rieppel et al. (2008), in which they recovered *Dinocephalosaurus orientalis* as the sister taxon to Tanystropheidae. Another embryo bearing close similarities to *Dinocephalosaurus orientalis* was described by Li et al. (2017b). It represents a separate taxon, since it differs distinctly from *Dinocephalosaurus orientalis* in its relative limb proportions and in having 24 rather than at least 33 cervical vertebrae. However, it has not been assigned to a separate species due to the very early ontogenetic stage of the specimen and it was instead referred to as a “dinocephalosaur”, indicating the presence of multiple closely related *Dinocephalosaurus*-like taxa.

Fuyuansaurus acutirostris Fraser, Rieppel & Li 2013

Age. Ladinian (Dong et al. 1997; although the conodont *Paragondolella polygnathiformis* indicates an earliest Carnian age; Jiang et al. 2009).

Occurrence. Zhunganpo Member of the Falang Formation, Guizhou Province, China (Fraser et al. 2013).

Holotype. **IVPP V17983**, a partial skeleton preserving a skull, cervical vertebral column, a few dorsal vertebrae, and ~~a~~ pectoral and pelvic girdle.

Diagnosis. The only diagnosis of *Fuyuansaurus acutirostris* so far was provided by Fraser et al. (2013).

Remarks. *Fuyuansaurus acutirostris* is a small archosauromorph with a long neck and an elongate rostrum, known from a single, possibly juvenile, specimen. It has been interpreted as an aquatic taxon and bears clearly tanystropheid features in the presence of a long neck, ~~made up~~ of elongated cervical vertebrae and corresponding ribs, and the shape of the scapula (Fraser et al. 2013). It can be distinguished from other tanystropheids by its elongate and tapered snout and a pelvic girdle that lacks a thyroid fenestra between the pubis and ischium. *Fuyuansaurus acutirostris* has ~~previously~~ not ~~previously~~ been included in a phylogenetic analysis.

Pectodens zhenyuensis Li, Fraser, Rieppel, Zhao & Wang 2017

Age. Anisian.

Occurrence. Member II of the Guanling Formation, Luoping, Yunnan Province, China (Li et al. 2017a).

Holotype. **IVPP V18578**, a nearly complete and articulated skeleton including ~~skeleton~~.

Diagnosis. The diagnosis was provided by (Li et al. 2017a).

Remarks. *Pectodens zhenyuensis* is a small, highly gracile archosauromorph with an elongate neck, tail, and limbs. It bears certain characteristics typical of "protorosaurs", most notably in having a long neck with elongate cervical vertebrae and ribs. Li et al. (2017a) addressed the similarities of *Pectodens zhenyuensis* to "Protorosauria", but considered its inclusion in this group only tentative, since it lacks several diagnostic features, such as the presence of a hooked fifth metatarsal and a thyroid fenestra between the pubis and ischium, and because it differed from other "protorosaurs" in the shape of its skull and marginal dentition. Most carpal bones are missing in the only known specimen, even though the manus is fully articulated, possibly because these bones had not yet ossified due to the early ontogenetic stage of the specimen. The phylogenetic position of *Pectodens zhenyuensis* has previously not been tested.

Mesosuchus browni Watson 1912

Age. Early Anisian.

Occurrence. Burgersdorp Formation of the Beaufort Group near Aliwal North, Subzone B of the Cynognathus Z, Eastern Cape Province, South Africa (Dilkes 1998; Hancox 2000).

Holotype. **SAM-PK-5882**, a partial skull consisting of the snout, braincase, and palatal regions, mandibles, a partial vertebral column, an incomplete scapula and pelvic girdle, and partial fore and hindlimbs.

~~Hypodigm~~. The hypodigm of *Mesosuchus browni* was provided by Dilkes (1998) and also listed by Ezcurra (2016).

Diagnosis. The most recent diagnosis was provided by Dilkes (1998).

Remarks. *Mesosuchus browni* is considered the best known non-rhynchosaurid rhynchosaur (Butler et al. 2015; Hone & Benton 2008). Like the other early rhynchosaurs *Howesia browni* and *Eohyosaurus wolvaardti*, as well as the archosauriforms *Euparkeria capensis* and *Erythrosuchus africanus*, it is known from the Burgersdorp Formation near Aliwal North in the Eastern Cape, South Africa (Butler et al. 2015; Ezcurra et al. 2016; Rubidge 2005). *Mesosuchus browni* has been studied several times (Broom 1913a; Broom 1913b; Broom 1925; Haughton 1922; Haughton 1924a; Watson 1912), and has been most comprehensively described by Dilkes (1998). In many ways *Mesosuchus browni* shows a morphology ~~which~~ is intermediate between that of rhynchosaurids and other early archosauromorphs. **SAM-PK-6536** represents a particularly informative specimen, as it includes a complete, virtually undistorted skull. The braincase of this specimen was recently described in detail by Sobral & Müller (2019), and revealed a pneumatic sinus between the basal tubera. Pneumatization of the braincase was previously considered a derived archosaur trait, but its presence in *Mesosuchus browni* indicates it had evolved much earlier in the archosauromorph lineage.

Howesia browni Broom 1905

Age. Early Anisian.

Occurrence. Burgersdorp Formation of the Beaufort Group near Aliwal North, Subzone B of the Cynognathus AZ, Eastern Cape Province, South Africa (Dilkes 1995; Hancox 2000).

Holotype. **SAM-PK-5884**, a flattened partial skull missing the snout and occipital regions, and lower jaw~~s~~.

~~Hypodigm~~. **SAM-PK-5885**, a flattened partial skull missing the snout, and lower jaw~~s~~, and an atlas-axis complex; **SAM-PK-5886**, a postcranial skeleton consisting of a partial vertebral column, an incomplete pelvic girdle and left hindlimb, and a complete right tarsus.

Diagnosis. The most recent diagnosis was provided by Dilkes (1995).

Remarks. *Howesia browni* is a non-rhynchosaurid rhynchosaur closely related to *Mesosuchus browni* that was first described by Broom (1905a). Following additional preparation of the three known specimens, *Howesia browni* was extensively described by Dilkes (1995).

Eohyosaurus wolvaardti Butler, Ezcurra, Montefeltro, Samanthi & Sobral 2015

Age. Early Anisian

Occurrence. Burgersdorp Formation of the Beaufort Group near Aliwal North, Cynognathus AZ, Subzone B (Butler et al. 2015).

Holotype. **SAM-PK-K10159**, skull and mandibles missing the anterior part of the snout.

Diagnosis. The diagnosis was provided by Butler et al. (2015).

Remarks. Butler et al. (2015) described *Eohyosaurus wolvaardti* and included it in a phylogenetic analysis. It was recovered as the sister taxon to rhynchosaurids and was thus found to be more closely related to this clade than *Mesosuchus browni* and *Howesia browni*. In another phylogenetic analysis focusing on rhynchosaurs, it was found in a polytomy with rhynchosaurids, *Mesosuchus browni*, *Howesia browni*, and *Noteosuchus colletti*, the last being a poorly known early rhynchosaur from the Induan of South Africa (Ezcurra et al. 2016).

Pamelaria dolichotrachela Sen 2003

Age. Anisian (Lucas 2010).

Occurrence. Yerrapalli Formation, Gondwana Supergroup, Pranhita–Godavari Basin, southern India.

Holotype. **ISIR 316**, a partial skeleton including a largely complete skull.

~~Hypodigm~~. The referred specimens are listed in Sen (2003) and Ezcurra (2016).

Remarks. *Pamelaria dolichotrachela* is known from three specimens originating from the Yerrapalli Formation (Middle Triassic) of India and was originally identified as a “protorosaur” (Sen 2003). However, recent phylogenetic analyses have revealed that *Pamelaria dolichotrachela* is an allokotosaur, closely related to *Azendohsaurus* spp. and *Shringasaurus indicus* (Ezcurra 2016; Nesbitt et al. 2015; Sengupta et al. 2017; and subsequent modifications of these matrices).

Azendohsaurus madagaskarensis Flynn, Nesbitt, Parrish, Ranivoharimanana & Wyss 2010~~)~~

Age. Late Ladinian to early Carnian.

Occurrence. Locality M-28 close to the eastern bank of the Malio River, west of Isalo National Park, southern Madagascar, Isalo II ~~of~~ the Makay Formation (Nesbitt et al. 2015).

Holotype. **UA 7-20-99-653**, partial skull and five anterior cervical vertebrae.

~~Hypodigm~~. A list of referred specimens can be found in appendix 1 of Nesbitt et al. (2015).

Diagnosis. The most recent diagnosis was provided in Nesbitt et al. (2015).

Remarks. *Azendohsaurus madagaskarensis* is the best-known species of the genus, but the first described species is *Azendohsaurus laaroussii*. The latter taxon was originally described from a few teeth and dental fragments and interpreted as an ornithischian dinosaur (Dutuit 1972), and later a sauropodomorph dinosaur (e.g. Gauffre 1993). Postcranial remains from the type locality of *Azendohsaurus laaroussii* can likely also be referred to this species, and indicate that the taxon did not belong to Dinosauria (Cubo & Jalil 2019; Jalil & Knoll 2002). Comprehensive three-dimensionally preserved remains of various individuals from the late Middle Triassic to early Late Triassic of southern Madagascar, which closely resembled the known material of *Azendohsaurus laaroussii*, were assigned to *Azendohsaurus madagaskarensis*. The skull and mandibles were initially described by Flynn et al. (2010). A description of the postcranium and a phylogenetic hypothesis for *Azendohsaurus madagaskarensis* was provided by Nesbitt et al. (2015). This revealed a new clade of non-archosauriform archosauromorphs, Allokotosauria, that includes *Azendohsaurus* spp., *Trilophosaurus* spp., *Pamelaria dolichotrachela*, *Spinosuchus caseanus*, *Shringasaurus indicus*, and *Teraterpeton hrynewichorum*. This clade has subsequently been recovered in other analyses (e.g. Ezcurra 2016; Sengupta et al. 2017), confirming it as one of the three major lineages of non-archosauriform archosauromorphs, together with Rhynchosauria and Tanystropheidae. *Azendohsaurus madagaskarensis* represents one of the best-known non-archosauriform archosauromorphs. It was herbivorous and has a relatively large body size among early archosauromorphs, being approximately 2 to 3 metres in length.

Trilophosaurus buettneri Case 1928

Age. Carnian (Parker & Martz 2010; Spielmann et al. 2008).

Occurrence. *Trilophosaurus* site 1 and *Trilophosaurus* quarries 1-3, Colorado City Formation; Walker's Tank and lower Kalgary site, Tecovas Formation, western Texas, USA (Spielmann et al. 2008).

Holotype. **UMMP 2338**, an incomplete right dentary bearing teeth.

~~Hypodigm~~. A list of referred specimens can be found in appendix 1 of Spielmann et al. (2008).

Diagnosis. The most recent diagnosis is provided by Spielmann et al. (2008, p. 11)

Remarks. *Trilophosaurus buettneri* was first described based on a dentary fragment bearing teeth (Case 1928) and interpreted to be closely related to procolophonids. Additional specimens that gave a much more complete account of the taxon were described by Gregory (1945). Gregory (1945) referred *Trilophosaurus buettneri* to “Protorosauria”. The skull of *Trilophosaurus buettneri* was later redescribed by Parks (1969). Another species referred to the genus, “*Trilophosaurus jacobsi*”, was proposed to represent a junior synonym of *Spinosuchus caseanus* by Nesbitt et al. (2015). *Trilophosaurus buettneri* was redescribed and reinterpreted as a non-archosauriform archosauromorph outside “Protorosauria” by Spielmann et al. (2008). *Trilophosaurus buettneri* was later found within the newly erected clade Allokotosauria (e.g. Ezcurra 2016; Nesbitt et al. 2015). The manus of *Trilophosaurus buettneri* was redescribed by Nesbitt et al. (2015). *Trilophosaurus buettneri* was herbivorous and has a remarkable dentition, characterized by an edentulous, beak-like snout and ~~transversely or~~ labiolingually very wide tricuspid teeth further ~~posterior~~ in the jaws. An arboreal lifestyle has been suggested for *Trilophosaurus buettneri* by Spielmann et al. (2005), based on the relative proportions of the appendicular skeleton and the presence of large curved claws. Although similar claws occur in other allokotosaurs (e.g. *Azendohsaurus madagaskarensis*), a similar interpretation has not been made for these taxa Nesbitt et al. (2015).

Teyujagua paradoxa Pinheiro, França, Lacerda, Butler & Schultz 2016

Age. Induan-Olenekian (Dias-da-Silva et al. 2017; Pinheiro et al. 2019).

Occurrence. Bica São Tomé, Sanga do Cabral Formation, São Francisco de Assis, Rio Grande do Sul, southern Brazil.

Holotype. **UNIPAMPA 653**, a nearly complete skull and mandibles, as well as parts of the first five cervical vertebrae.

Diagnosis. The most recent diagnosis was provided by Pinheiro et al. (2019).

Remarks. *Teyujagua paradoxa* was first described by Pinheiro et al. (2016) and subsequently described in more detail with the aid of µCT data by Pinheiro et al. (2019). The skull and mandible~~s~~ of *Teyujagua paradoxa* exhibit a remarkable combination of plesiomorphic features, typical of non-archosauriform archosauromorphs (e.g. absence of the antorbital fenestra), and derived features ~~which~~ represent synapomorphies for Archosauriformes (e.g. the presence of an external mandibular fenestra). This is also reflected in the position of *Teyujagua paradoxa* in previous phylogenetic analyses including this species, in which it was recovered as the sister taxon to Archosauriformes (Pinheiro et al. 2016; Pinheiro et al. 2019).

Euparkeria capensis Broom 1913

Age. Early Anisian

Occurrence. Burgersdorp Formation of the Beaufort Group near Aliwal North, Subzone B of the Cynognathus AZ, Eastern Cape Province, South Africa (Ewer 1965; Hancox 2000; Sookias 2016).

Holotype. **SAM-PK-5867**, a complete skull and mandible~~s~~ and a largely complete and articulated postcranial skeleton, only missing most of the hands and feet and the majority of the tail.

~~Hypodigm.~~ A complete hypodigm is listed in Sookias (2016)

Diagnosis. An emended diagnosis was recently provided in Sookias (2016).

Remarks. *Euparkeria capensis* is a small, carnivorous archosauriform that has received a lot of interest due to its morphology and phylogenetic position, as it represents a well-known early archosauriform that is closely related to Archosauria. The most extensive morphological description of *Euparkeria capensis* was provided by Ewer (1965). Recently, a detailed revision of the Euparkeriidae, a monophyletic clade comprising *Euparkeria capensis* and its closest relatives, included a morphological reevaluation of this taxon (Sookias 2016; Sookias & Butler 2013; Sookias et al. 2014). The braincase has recently been described in detail by Sobral et al. (2016).

Erythrosuchus africanus Broom 1905

Age. Early Anisian (Abdala et al. 2005).

Occurrence. Various localities in South Africa, most notably near Aliwal North and Burgersdorp, Eastern Cape Province, and Rouxville, Free State Province, Burgersdorp Formation of the Beaufort Group, *Cynognathus* AZ subzone B, Karoo Supergroup (Abdala et al. 2005; Gower 2003).

Holotype. **SAM-PK-905**, an incomplete postcranial skeleton, mainly consisting of the pectoral and pelvic girdles, partial forelimb, and vertebrae.

~~Hypodigm~~. A list of the referred specimens is provided in Appendix 1 of Gower (2003).

Diagnosis. The most recent diagnosis for *Erythrosuchus africanus* is provided by Ezcurra (2016).

Remarks. *Erythrosuchus africanus* is a large-sized carnivorous archosauriform with a skull that is particularly large compared to the postcranium. It was first described based on a partial postcranial skeleton by Broom (1905b). A new and more completely preserved specimen, including a partial skull, was described by Huene (1911). *Erythrosuchus africanus* was more recently described extensively by Gower (2003), and separate studies addressed the morphology of the pes (Gower 1996), and braincase (Gower 1997).

Material and Methods

To resolve the phylogenetic relationships of tanystropheids and other “protorosaurs”, a new comprehensive character matrix was constructed consisting of 307 characters. These include 42 new characters, with the remaining characters having been compiled and modified from the literature (mainly from Ezcurra 2016 and Pritchard et al. 2015, but also sourced from Benton & Allen 1997; Dilkes 1998; Jalil 1997; Pritchard et al. 2018; Senter 2004; Simões et al. 2018; and Sookias 2016). The matrix contains 23 ratio characters, and 48 multistate characters are ordered as they are considered to form a transformational series in which at least one state represents a clear intermediate between two other states. Currently there is ongoing debate whether discrete characters should be ordered and whether to discretize continuous data by using ratios (Grand et al. 2013; Simões et al. 2016), but their application has been considered phylogenetically informative in previous studies of archosauromorph relationships (Ezcurra 2016; Nesbitt 2011). To test for the influence of ordered and ratio characters for our dataset, one round of analyses was performed including the ratio characters and with characters indicated as ordered treated as such, and another round without ratio characters and with all remaining characters unordered. A total of 42 OTUs are included, the large majority of which were scored based on personal observations of relevant specimens. *Petrolacosaurus kansensis* was assigned as the outgroup. Poorly represented or problematic taxa were pruned for the final analyses (these are taxa with less than 25% of characters scored, in addition to *Czatkowiella harae*, which was pruned because this taxon could possibly represent a chimera, see Table 1), resulting in final trees consisting of 32 OTUs. A full list of all character scorings and the specimens and literature that have been employed are provided in the Supplementary Information. The specimens that were scored are specified for each character individually for future assessment and comparison. The analyses were performed in TNT 1.5 (maximum parsimony criterion; Goloboff & Catalano 2016), using several rounds of equally weighted 'New Technology Search' algorithms to adequately explore tree space and maximize the likelihood of finding the global optimum. Initial trees were calculated with 'Sectorial Search', 'Ratchet', 'Drift' and 'Tree Fusing' algorithms using 100 iterations each and 1000 random addition sequences (RAS). Relative fit difference was set at 0.1 and up to 10 suboptimal trees were retained. The saved trees were subsequently put through two separate analyses of three rounds each. One analysis applying 'Sectorial search', 'Ratchet', and 'Ratchet', in that order; and the other 'Ratchet', 'Sectorial search', and 'Ratchet'. All rounds ran 1000 iterations and additionally included 1000 iterations of 'Tree fusing'. At this stage suboptimal trees were discarded, and the strict consensus tree was calculated from the remaining trees. Bremer and Bootstrap support values were calculated, the latter using 'Traditional search' at 1000 iterations.

Character sampling and formulation

Following detailed investigations of early archosaur phylogenetic relationships (e.g. Nesbitt 2011), the phylogeny of non-archosaurian archosauromorphs has received much attention in recent years and several detailed character lists for this group exist, with one analysis focusing on tanystropheids (Pritchard et al. 2015) and another on allokotosaurs (Nesbitt et al. 2015). However, the most comprehensive analysis, consisting of 600 characters, was provided by Ezcurra (2016), in which characters of these previous analyses were included, as well as those of many other studies. Furthermore, for many of the characters included at least one of the character states was figured, limiting subjective interpretation of the characters by the reader. Several subsequent studies have used and slightly modified the matrix provided by Ezcurra (2016) depending on the clade that was focused on in each respective study (e.g. Butler et al. 2019; Ezcurra et al. 2019; Sengupta et al. 2017; Stocker et al. 2017).

Due to its comprehensiveness and well-explained characters, the character list of Ezcurra (2016) was used as the main source for our characters. However, only those characters that were relevant to the sampled taxa were included, as many characters in the original list were used to differentiate between taxa not included herein, such as proterochampsids, archosaurs, and choristoderes. Additional characters were incorporated mainly from the character list of Pritchard et al. (2015), and supplemented by characters from Pritchard et al. (2018), Nesbitt et al. (2015), Nesbitt (2011), Sookias (2016), Simões et al.

(2018), Dilkes (1998), Jalil (1997), Benton & Allen (1997), and Senter (2004). Certain characters taken from the literature were modified to fit more precisely with the specific morphologies observed in the sampled taxa. Finally, new characters were constructed based on detailed morphological comparisons of the included taxa. Autapomorphies of a single species were also incorporated into characters as they represent important morphological information and since these characters might prove phylogenetically relevant after future findings. New characters and characters that have been distinctly modified from previous analyses are discussed and figured.

All characters were critically assessed on their logical construction and whether character states represent valid tests of similarity or primary homology. Issues regarding character construction, specifically how to optimize the construction of characters as to represent similarity tests, are a continuing source of debate (e.g. Brazeau 2011; Kearney & Rieppel 2006; Rieppel & Kearney 2007). Criteria for character construction to minimalize “non-meaningful” character scorings have been suggested by Simões et al. (2016) and examples of problematic characters have also been pointed out by Nesbitt (2011). We assessed all our characters in light of these suggestions, as these criteria provide important considerations for character construction. However, we find that the application of each criterion is dependent on various factors. The taxa included in our analysis all represent Permo-Triassic non-archosaur members of the archosauromorph lineage, as well as early lepidosauromorphs and non-saurian diapsids. This phylogenetically relatively narrow sample is expected to exhibit less morphological variation and cases of homoplasy than larger scale analyses (e.g. both extant and extinct Lepidosauromorpha and closely related taxa as in Simões et al. 2018). Therefore, in certain cases, characters that might otherwise not follow the criteria proposed in Simões et al. (2016) (e.g. the shape of the orbit, Type I A.7, or the use of continuous characters, Type II of Simões et al. 2016) are maintained when, based on detailed comparisons and careful consideration, the character states therein were deemed to likely represent valid similarity tests to the taxa involved. We pose that although these criteria as formulated represent useful tools, the complexity of morphological variation entails that careful observation and logical assessments of similarity by experts on the taxonomic sample at hand should be leading in character construction (Kearney & Rieppel 2006; Rieppel & Kearney 2007). Therefore, a character which might be problematic as a test of homology when applied to one set of taxa, might still be valid when looking at a different taxonomic sample. Following Brazeau (2011) the presence or absence of a feature was formulated as a separate character from its morphology for unordered characters. In these cases, the character describing the morphology of this feature was scored as inapplicable in taxa in which the character is absent.

Character list

1) Ezcurra (2016) ch. 20. *~~Snout,~~ antorbital length (anterior tip of the skull to anterior margin of the orbit) versus total length of the skull: 0.29-0.40 (0); 0.43-0.62 (1); 0.70-0.76 (2), ORDERED RATIO (Ezcurra 2016: Figs. 17 and 18).*

This character was considered to be interdependent with character 76 of Ezcurra (2016). Since this character 20 could be applied to more taxa than character 76, the former was preferred and the latter excluded.

2) Modified from Ezcurra (2016) ch. 21. *~~Snout,~~ dorsoventral height at the level of the anterior tip of the maxilla versus dorsoventral height at the level of the anterior border of the orbit: 0.15-0.27 (0); 0.32-0.51 (1); 0.56-0.80 (2), ORDERED RATIO (Ezcurra 2016: Figs. 17 and 19).*

Character states were defined after comparison of all the different measured ratios.

3) Ezcurra (2016) ch. 22. *~~Snout,~~ proportions at the level of the anterior border of the orbit: transversely broader than dorsoventrally tall or subequal (0); dorsoventrally taller than transversely broad (1) (Ezcurra 2016: Fig. 16).*

4) Modified from Ezcurra (2016) ch. 27. *Premaxilla, main body size: length of the tooth bearing margin in lateral view (in edentulous taxa the ventral margin of the premaxilla contributing to the ventral margin of the upper jaw; =main body) versus the length of the ~~snout~~ (anterior tip of the skull to the anterior border of the orbit): 0.08-0.18 (0); 0.20-0.38 (1); 0.44-0.60 (2), ORDERED RATIO (Ezcurra 2016: Fig. 17).*

The original distinction between the character states was not considered to be phylogenetically relevant, and therefore it was decided here to distinguish the states based on ratios that were discretized a posteriori.

5) Ezcurra (2016) ch. 29. *Premaxilla, downturned main body: absent, alveolar margin sub-parallel to the main axis of the maxilla (0); slightly, in which the alveolar margin is angled at approximately 20 degrees to the alveolar margin of the maxilla (1); strongly, prenarial process obscured by the postnarial process in lateral view (if the postnarial process is long enough) and postnarial process parallel or posteroventrally orientated with respect to the main axis of the premaxillary body (2), ORDERED (Ezcurra 2016: Figs. 16-19).*

6) Ezcurra (2016) ch. 30. *Premaxilla, angle formed between the alveolar margin and the anterior margin of the premaxillary body in lateral view: acute or right-angled (0); obtuse (1) (Ezcurra 2016: Figs. 20 and 21). This character is inapplicable in taxa with a hooked premaxilla.*

7) Modified from Ezcurra (2016) ch. 34. *Premaxilla, prenarial process: absent or incipient (0); present and less than the anteroposterior length of the main body of the premaxilla (1); present and longer than the anteroposterior length of the main body of the premaxilla (2), ORDERED (Ezcurra 2016: Figs. 17 and 21). This character is scored as inapplicable in taxa with confluent external nares.*

An absent or incipient state was added and the character was ordered, since the character is considered a transformational series and state 1 represents a clear intermediate between states 0 and 2. Furthermore, the inapplicability criterion was included, since confluent external nares preclude the presence of a prenarial process.

8) Modified from Ezcurra (2016) ch. 35. *Premaxilla, base of the prenarial process: anteroposteriorly shallow, being not much wider at its base than further distally on the process (0); anteroposteriorly deep, being much wider at its base than further distally on the process (1). (Ezcurra 2016: Figs. 12, 17, 20 and 21). This character is inapplicable in taxa that lack a prenarial process.*

This character was further clarified in its description and an inapplicability criterion was included.

9) Modified from Ezcurra (2016) ch. 36 and 40. *Premaxilla, postnarial process (= posterodorsal process, = maxillary process, = subnarial process): absent (0); short, ends well anterior to the posterior margin of the external naris (1); well-developed, forms most of the ventral border of the external naris or excludes the maxilla from participation in the external naris but process does not contact prefrontal (2); well-developed, forms most of the ventral border of the external naris and postnarial process of premaxilla contacts prefrontal (3), ORDERED (Ezcurra 2016: Figs. 17 and 19).*

Characters 36 and 40 of Ezcurra (2016) were combined here because a contact between the premaxilla and the prefrontal always requires the premaxilla to exclude the maxilla from the external nares. Thus, these conditions can be considered as part of the same transformational series.

10) Ezcurra (2016) ch. 37. *Premaxilla, postnarial process (= posterodorsal process, = maxillary process, = subnarial process): wide, plate-like (0); thin (1). This character is not applicable to taxa that lack a postnarial process (Ezcurra 2016: Fig. 20).*

11) Modified from Ezcurra (2016) ch. 41, and Nesbitt et al. (2015): ch. 247. *Premaxilla, plate-like palatal shelf or process on the medial surface (contribution to secondary palate by premaxillae): absent (0); present (1) (Ezcurra 2016: Figs. 12, 20 and 21)*

The character was redescribed to indicate that the “process” referred to represents a rather wide shelf-like structure. For further explanation, see character 247 of (Nesbitt et al. 2015).

12) Modified from Pritchard et al. (2015) ch. 1. *Premaxilla, distinct posterodorsally to anteroventrally directed grooves terminating at the ventral margin of the bone: absent (0); present (1).*

This character describes the presence of posterodorsally to anteroventrally directed grooves present in *Langobardisaurus pandolfii* MFSN 1921 that were previously mistakenly identified as premaxillary teeth (Saller et al. 2013). This character was reformulated here to describe this feature more specifically.

13) Modified from Ezcurra (2016) ch. 42. *Premaxilla, number of tooth positions: 8 or more (0); 5 or 6 (1); 4 (2); 3 (3); 2 (4); 1 or edentulous (5) ORDERED (Ezcurra 2016: Figs. 16 and 17).*

The states of this character were modified since the original distinction did not cover all observed variation and because state 1 partially covered the same number of teeth as state 0 in the original description. Characters 69 and 278 of Ezcurra (2016) were omitted here, because they were considered to be strongly interdependent with this character.

14) Modified from Ezcurra (2016) ch. 43. *Premaxilla, orientation of the tooth series or the occlusal surface of premaxilla in ventral view: approximately parasagittal (0); strongly transverse and (in case of tooth-bearing premaxillae) anterior teeth covering each other in lateral view (1). This character is inapplicable in taxa with a hooked and beak-like premaxilla (Ezcurra 2016: Fig. 21).*

The inapplicability criterion of this character was modified. It was previously scored as inapplicable in taxa with an edentulous premaxilla. However, we consider that the differentiating morphology addressed by this character can also occur in taxa that lack premaxillary teeth. However, a hooked or beak-like shape morphology does not allow for a transverse occlusal surface.

15) Ezcurra (2016) ch. 24. *Premaxilla-maxilla, suture: simple continuous contact (0); notched along the ventral margin (1) (Ezcurra 2016: Figs. 17 and 19).*

This character was also illustrated and discussed in Supplementary Figure 10 of Pritchard et al. (2018). However, we prefer this character formulation over that of Pritchard et al. (2018).

16) Modified from Ezcurra (2016) ch. 25. *Premaxilla-maxilla, subnarial foramen between the elements: absent (0); present (1) (Nesbitt 2011: Figs. 14, 17 and 19). Not applicable to taxa that have a ventral notch on the suture of the premaxilla and maxilla.*

The inapplicability criterion was included because the presence of a ventral notch on the border between the premaxilla and maxilla precludes the possibility of a subnarial foramen. Character states 1 and 2 of the previous iteration of this character were fused because the distinction between these two states is hard to establish confidently. Furthermore, this distinction is most likely irrelevant to the taxon sample included in this analysis.

17) New, similar to ch. 33 of Ezcurra (2016), ch. 6 of Pritchard et al. (2015), ch. 17 of Dilkes (1998), and ch. 6 of Pritchard et al. 2018. *Premaxilla-maxilla, contact between the premaxilla and maxilla: simple abutting contact (0); overlapping contact in which the premaxilla overlaps the maxilla laterally (1); overlapping contact in which the maxilla overlaps the premaxilla laterally (2); contact in which the premaxilla has a posteriorly directed peg on its posterolateral margin articulating with the maxilla, often accompanied by a groove (3); complicated connection in which the premaxilla has posteriorly projected peg on its medial surface which locks the maxilla against the premaxilla medially (4) (Fig. 2).*

The connection between the premaxilla and maxilla in early archosauromorphs has been discussed in depth and is considered phylogenetically informative. We have reformulated this character based on recent new findings with regards to the articulation between these elements in *Tanystropheus hydroides* (state 1) and *Macrocnemus bassanii* (state 4; Miedema et al. 2020; Spiekman et al. 2020). Among the taxa sampled here, most taxa have a simple abutting contact between premaxilla and maxilla, with neither bone distinctly overlapping the other (state 0; the sampled non-archosauromorph diapsids, *Czatkowiella harae*, *Prolacerta broomi*, *Trilophosaurus buettneri*, *Euparkeria capensis*, and *Proterosuchus fergusi*). In the sampled rhynchosaurs, the maxilla overlaps the premaxilla laterally (state 2; *Mesosuchus browni*). Certain taxa bear a small peg, meaning a short pin or bolt, on the posterolateral end of their premaxilla, which connects to the lateral surface of the maxilla (state 3; *Azendohsaurus madagaskarensis* and *Erythrosuchus africanus*). The configuration of *Macrocnemus bassanii*, in which a peg is present on the medial side of the premaxilla that interlocks with an anteriorly facing peg on the medial side of the maxilla (Miedema et al. 2020), is considered to be non-homologous with the pegs on the posterolateral end of the premaxilla described for state 3, and is therefore scored as a separate state here.

18) Ezcurra (2016) ch. 45. *Septomaxilla: present (0); absent (1) (Ezcurra 2016: Fig. 16).*

The presence of this small element in the anterior ~~snout~~ region is hard to establish, and therefore we were not able to confidently consider it as absent for any taxon. Therefore, this character is not phylogenetically informative for the present analysis, but it is nevertheless maintained as it presents an overview of the presence of the septomaxilla among early archosauromorphs. Contrary to previous interpretations, we were able to identify a septomaxilla in the rhynchosaur *Mesosuchus browni* (SAM-PK-6536).

19) Ezcurra (2016) ch. 52, and Nesbitt et al. (2015): ch. 203. *Maxilla, anterior maxillary foramen: absent (0); present (1) (Ezcurra 2016: Fig. 17).*

20) Modified from Nesbitt et al. (2015): ch. 202. *Maxilla, dorsal portion, shape: obtuse angle between the dorsal and posterior margin of the maxilla, which is straight or slightly convex (0); the dorsal apex of the maxilla ends abruptly and its posterior margin is concave (1)* (*Fig. 3*).

The description of state 0 was modified to more precisely describe the condition observed in *Prolacerta broomi* and *Protorosaurus speneri*. The character as described by Nesbitt et al. (2015) was preferred over character 58 of Ezcurra (2016), since state 2 of the latter implies the presence of an antorbital fenestra, which is scored here already in a separate character (22). In the description of character 202 of Nesbitt et al. (2015) it was pointed out that in *Azendohsaurus madagaskarensis* and *Azendohsaurus laaroussii* the posterodorsal margin of the maxilla is concave, similar to that of Archosauriformes, in which this forms the anterior margin of the antorbital fenestra. A curved posterodorsal margin of the maxilla occurred in many non-archosauriform archosauromorphs (see also character 58 of Ezcurra 2016 and its scoring). The presence of a distinct ascending process of the maxilla, considered to be a saurian trait, (sensu the scoring of character 57 in Ezcurra 2016) is considered to be too ambiguous as a phylogenetic character in the sampled taxa. For instance, the maxillae of *Youngina capensis* (AMNH FARB 5561), *Protorosaurus speneri* (NMK S 180), and *Prolacerta broomi* (BP/1/5880) do not bear a clearly defined process and the maxillae are approximately equally tall relative to their respective snouts in all three taxa. Nevertheless, the former two taxa were previously considered to bear an ascending process, in contrast to *Youngina capensis*. Furthermore the presence of a process-like dorsal portion of the maxilla is strongly dependent on the relative height of the anterior portion of the snout at the level of the anterior margin of the orbit, and this morphology is already covered by character 10 here.

21) Modified from Ezurra (2016) ch. 59. *Maxilla, anterior part of the dorsal margin: convex (0); straight (1); concave (2) (Ezcurra 2016: Fig. 22).*

The anterior part of the dorsal margin is convex in *Prolacerta* (BP/1/5880; Spiekman 2018), *Trilophosaurus* (TMM 31025-207), *Protorosaurus speneri* (NMK S 180), *Mesosuchus browni* (SAM-PK-6536), *Youngina capensis* (SAM-PK-K7578), *Orovenator mayorum* (OMNH 74606), *Petrolacosaurus kansensis* (KUVP 9951), and *Gephyrosaurus bridensis* (Evans 1980). It is completely straight in *Macrocnemus bassanii* (PIMUZ T 4822) and *Proterosuchus fergusi* (RC 846; Ezcurra & Butler 2015b), which is here considered as a separate state, as it is homologous to neither the concave nor convex state, but instead represents an intermediate state.

22) Ezcurra (2016) ch. 13, and Pritchard et al. (2015): ch. 13. *Antorbital fenestra: absent (0); present (1).*

23) New *Maxilla, antorbital fossa: absent (0); or present (1)* (*Fig. 4*). *This character is inapplicable in taxa that have an antorbital fenestra.*

A large circular concavity is present on the lateral margin of the maxilla of *Dinocephalosaurus orientalis* (IVPP V13767) as described by Rieppel et al. (2008). This character is clearly different from the antorbital fossa as described for *Erythrosuchus* (Gower 2003), which refers to a depression within which the large antorbital fenestra is located. Because of the clear affinities with the antorbital fenestra, this fossa is considered to represent a separate structure and the fossa described here, which does not occur in congruence with an antorbital fenestra, is currently only known to be present in *Dinocephalosaurus orientalis.*

24) Ezcurra (2016) ch. 64 *Maxilla, posterior end of the horizontal process distinctly ventrally deflected from the main axis of the alveolar margin: absent (0); present (1) (Ezcurra 2016: Figs. 17 and 22).*

25) Modified from Ezcurra (2016) ch. 68 *Maxilla, alveolar margin in lateral view: straight (0); concave (1); convex (2); sigmoid, anteriorly concave and posteriorly convex (3); sigmoid, anteriorly convex, starting close to mid-length, and posteriorly concave (4) (Ezcurra 2016: Figs. 16 and 19)* (*Fig. 5*).

This character was modified to distinguish between a concave, straight, or convex margin, since it was considered that these distinctions might be phylogenetically informative for this sample of taxa.

26) Modified from Ezcurra (2016) ch. 75. *Maxilla, number of tooth positions: 11-17 (0); 19-40 (1). This character is inapplicable in taxa with multiple tooth rows in the maxilla.*

Character states were defined after determining the tooth count in all included taxa.

27) Ezcurra (2016) ch.47. *Maxilla-jugal, anguli oris crest: absent (0); present (1) (Ezcurra 2016: Fig. 16).*

28) New, combination of ch. 47 of Ezcurra (2016) and part of ch. 8 of Pritchard et al. (2015). *Maxilla-jugal, anguli oris crest: both the jugal and the maxilla are distinctly laterally offset (0); only the jugal is distinctly laterally offset (1) (Ezcurra 2016: Fig. 16). This character is scored as inapplicable in taxa that lack an anguli oris crest.*

The term anguli oris crest is typically used to describe the very conspicuous lateral offset of the jugal seen in rhynchosaurid rhynchosaurs (e.g. Butler et al. 2015; Langer & Schultz 2000; Montefeltro et al. 2010). This crest might have facilitated a muscular cheek (Benton 1983). A much less conspicuous anguli oris crest, which is partially formed by the posterolateral end of the maxilla, was recently described for the non-rhynchosaurid rhynchosaur *Eohyosaurus wolvaardti* (Butler et al. 2015). A similar lateral offset of the maxilla as seen in this taxon, which creates a substantial space between the lateral margin of the crest and the posterior portion of the maxillary tooth row, was considered for the trilophosaurid allokotosaurs *Trilophosaurus buettneri* and *Teraterpeton hrynewichorum* in Pritchard et al. (2015) character 8. We consider the description of this character to address the same morphological structure as seen in *Eohyosaurus wolvaardti* and therefore fused the characters. Although state 1 could possibly represent an intermediate morphology between states 0 and 2, this cannot be ascertained, and therefore this character is not ordered here. A similar lateral offset might also be present in *Langobardisaurus pandolfii*. However, scoring this character for *Langobardisaurus pandolfii* is currently ambiguous, since the preservation of this region is poor in the only specimen in which it is visible (MFSN 1921).

29) Ezcurra (2016) ch. 9. *External nares, confluent: absent (0); present (1) (Ezcurra 2016: Fig. 16, 17 and 20).*

30) Modified from Ezcurra (2016) ch. 12. *External naris, shape: sub-circular (0); oval (1) (Ezcurra 2016: Fig. 19). This character is inapplicable in taxa with confluent external nares.*

An inapplicability criterion was added to this character.

31) New *External naris: located close to the anterior end of the skull (0); a thick anterior margin of the premaxilla results in the external nares being posteriorly displaced (1)* (*Fig. 6*).

In most taxa scored, the anterior margin of the external naris is closely positioned towards the anterior end of the snout. However, in the tanystropheids *Tanystropheus hydroides* (PIMUZ T 2790), *Tanystropheus longobardicus* (MSNM BES SC 1018), *Macrocnemus bassanii* (PIMUZ T 2477), *Pectodens zhenyuensis* (IVPP V18578), *Dinocephalosaurus orientalis* (IVPP V13767) and the archosauriform *Erythrosuchus africanus* (BP/1/5207), the anterior margin of the external naris is separated considerably from the anterior end of the snout by the main body of the premaxilla.

32) Modified from Ezcurra (2016) ch. 78 *Nasal, shape of anterior margin at midline: strongly convex with anterior process and nasal forming an internarial bar (0); transverse with little convexity (1) (Ezcurra 2016: Fig. 16). This character is inapplicable in taxa in which the external nares are completely separated by an internarial bar.*

This character is scored as inapplicable in taxa with a complete internarial bar, since this is always formed, at least in part, by an anterior process of the nasal. Thus, scoring taxa with a complete internarial bar for this character would result in overscoring this trait, as it is already addressed in character 5. Among the taxa with confluent external nares, only the nasals of *Azendohsaurus madagaskarensis* bear anterior processes on the anteromedial margin of the nasal.

33) New *Nasal, antorbital recess: absent (0); or present (1)* (*Fig. 7*).

The antorbital recess is described for *Dinocephalosaurus orientalis* by Rieppel et al. (2008). It is a large gully posterior to the external naris that is largely formed in the nasal bone, but the maxilla and possibly the prefrontal also contribute to it. This recess is non-homologous to the depression of the nasal described by character 80 of Ezcurra (2016). This recess has recently also been identified in *Tanystropheus hydroides* (Jiang et al. 2011; Spiekman et al. 2020).

34) Modified from Pritchard et al. (2018) ch. 311. *Nasal, lateral surface: meets dorsoventrally short length of medial surface of dorsal process/portion of the maxilla (0); meets entire dorsoventral height of medial surface of supra-alveolar portion of maxilla (1). This character is inapplicable in taxa with an antorbital fenestra.*

See character description of character 311 of Pritchard et al. (2018). The inapplicability criterion was added because it was considered that the presence of an antorbital fenestra implies that the nasal cannot have a wide articulation facet with the maxilla.

35) Modified from Dilkes (1998) ch. 15. *Lacrimal, contacts nasal and reaches external naris (0); contacts nasal but does not reach naris (1); or does not contact nasal or reach naris (2), ORDERED. This character is inapplicable in taxa in which the premaxilla contacts the prefrontal.*

This character was ordered because it is considered to represent a transformational series and state 1 represents an intermediate between states 0 and 2. Furthermore, the inapplicability criterion was included, because a contact between the premaxilla and prefrontal precludes a contact between the lacrimal and nasal.

36) Ezcurra (2016) ch. 90. *Lacrimal, naso-lacrimal duct position: opens on the posterolateral edge of the lacrimal (0); opens on the posterior surface of the lacrimal (1). This character is inapplicable if the prefrontal encloses part of the naso-lacrimal duct (Ezcurra 2016: Fig. 19).*

37) Ezcurra (2016) ch. 95. *Jugal, anterior extension of the anterior process: anterior to the level of mid-length of the orbit (0); up to or posterior to the level of mid-length of the orbit (1).*

38) New, similar to Ezcurra (2016) ch. 92. *Jugal, anterior process is dorsoventrally expanded anteriorly: absent, the anterior process tapers anteriorly and articulates with the dorsal surface of the posterior process of the maxilla (0); present, the anterior process of the jugal is expanded and partially covers the lateral surface of the posterior process of the maxilla (1)* (*Fig. 8*).

In the majority of the taxa sampled here, the anterior process of the jugal fits into a groove or slot on the dorsal surface of the posterior process of the maxilla and is in some cases partially covered by the maxilla in lateral view. In the archosauriforms *Euparkeria capensis* (SAM-PK-5867) and *Erythrosuchus africanus* (BP/I/5207) the jugal is distinctly dorsoventrally taller and partially overlaps the maxilla in lateral view.

39) Modified from Sookias (2016) ch. 81. *Jugal, bulges ventrolaterally at the point where its three processes meet: absent (0); present (1). This character is scored as inapplicable in taxa that lack a posterior process of the jugal* (*Fig. 8*).

This character describes the condition in the archosauriforms *Proterosuchus fergusi* (SAM-PK-11208), *Erythrosuchus africanus* (BP/I/5207), and *Teyujagua paradoxa* (Pinheiro et al. 2019). In these taxa the posterior process of the jugal is located further laterally than their anterior processes. This is caused by a lateral bulging of the jugal at the point where the anterior, posterior, and ascending/dorsal processes of the bone meet. This morphology is clearly distinct from the anteromedially to posterolaterally directed crest described as the anguli oris crest and therefore coded as a separate character.

40) Ezcurra (2016) ch. 98. *Jugal, multiple pits on the lateral surface of the main body: absent (0); present (1) (Ezcurra 2016: Fig. 17).*

41) Ezcurra (2016) ch. 99 *Jugal, ascending process forming the entire anterior border of the infratemporal fenestra: absent (0); present, postorbital excluded from the anterior border of the infratemporal fenestra (1). This character is inapplicable in taxa in which the anterior process of the squamosal possesses an extensive contact with the postorbital and contacts the jugal, or lacks an infratemporal fenestra or an ascending process on the jugal. (Ezcurra 2016: Fig. 17).*

42) New *Jugal, posterior process: present (0); absent (1)* (*Fig. 9*).

A posterior process, typically present in archosauromorphs, is completely absent in *Claudiosaurus germaini* (Carroll 1981), *Pectodens zhenyuensis* (IVPP V18578), *Dinocephalosaurus orientalis* (IVPP V13767), and *Trilophosaurus buettneri* (Spielmann et al. 2008).

43) Modified from Ezcurra (2016) ch. 100. *Jugal, length of the posterior process versus the height of its base: 0.49-1.27 (0); 1.59-3.77 (1); 4.07-5.90 (2), ORDERED RATIO. This character is inapplicable in taxa that lack a posterior process of the jugal (Ezcurra 2016: Figs. 17 and 19).*

The upper margin of state 2 was increased, but otherwise the ratios distribution of Ezcurra (2016) was maintained because these states formed clear demarcations between distinct morphologies as measured in the sampled taxa. The presence of a posterior process and the relative length of the posterior process were considered here as separate characters, since in multiple taxa the presence of the process could be established, but its relative length could not, due to the process not being fully preserved.

44) Modified from Ezcurra (2016) ch. 5. *Skull, dermal sculpturing on the dorsal surface of the frontals, parietals, and nasals: absent (0); shallow or deep pits scattered across surface and/or low ridges (1) (Ezcurra 2016: Fig. 16).*

State 2 of character 5 in Ezcurra (2016) was not included here, because it was not applicable to the taxa sampled here.

45) Ezcurra (2016) ch. 109. *Prefrontal, subtriangular medial process: absent, nasal-frontal suture transversely broad (0); present, nasal-frontal suture strongly transversely reduced (1) (Ezcurra 2016: Fig. 7).*

46) Ezcurra (2016) ch. 111 and Nesbitt et al. (2015) ch. 237. *Prefrontal, lateral surface of the orbital margin: smooth or slight grooves present (0); rugose sculpturing present (1) (Ezcurra 2016: Fig. 17).*

47) Modified from Ezcurra (2016) ch. 16. *Orbit, shape: subcircular (0); distinctly dorsoventrally taller than long (1).*

States 0 and 1 of character 16 in Ezcurra (2016) represent a relatively minor morphological difference of which the accurate observation is easily hampered by compression of specimens. Therefore this character was modified to distinguish between the roughly subcircular orbits present in most of the sampled taxa, and the very dorsoventrally tall orbits of *Proterosuchus fergusi* (SAM-PK-11208), *Proterosuchus alexanderi* (NM QR 1484), and *Erythrosuchus africanus* (BP/1/5207).

48) Modified from Ezcurra (2016) ch. 17. *Orbit, elevated rim: absent or incipient (0); present, orbital margin of the jugal and/or postorbital slightly elevated to form a rim (1) (Ezcurra 2016: Figs. 16 and 17).*

State 2 of character 17 in Ezcurra (2016) was excluded because it was not applicable to the sampled taxa.

49) Modified from Ezcurra (2016) ch. 113. *Frontal, suture with the nasal: transverse (0); oblique, forming an angle of at least 60 degrees with long axis of the skull and frontals entering between both nasals (1); oblique and nasals entering considerably between frontals in a non-interdigitate suture (2); frontals enter nasals medially and nasals enter frontals laterally creating a W-shaped suture (3); frontals possesses a three-pronged anterior process that articulates with the nasals (4). This character is inapplicable if the nasal is received by a slot in the frontal or the nasal does not contact the frontal (Ezcurra 2016: Fig. 23 and Nesbitt 2011: Fig. 18).*

Character states 3 and 4 are new. State 3 is exhibited by *Youngina capensis* (BP/1/3859) and *Tanystropheus hydroides* (PIMUZ T 2790) and state 4 by *Tanystropheus longobardicus* (PIMUZ T 2484).

50) Ezcurra (2016) ch. 114. (character formulation slightly modified) *Frontal, orbital border in skeletally mature individuals: absent or anteroposteriorly short and forms less than half of the dorsal*

edge of the orbit (0); anteroposteriorly long and forms at least more than half of the dorsal edge of the orbit (1) (Ezcurra 2016: Fig. 23).

51) Ezcurra (2016) ch. 118. *Frontal, dorsal surface adjacent to sutures with the postfrontal (if present) and parietal: flat to slightly concave (0); possesses a longitudinal and deep depression (1) (Ezcurra 2016: Fig. 16).*

52) Ezcurra (2016) ch. 119. (inapplicability criterion slightly modified) *Frontal, longitudinal groove: longitudinally extended along most of the surface of the frontal (0); anterolaterally-to-posteromedially extended along the posterior half of the frontal (1). This character is inapplicable in taxa that lack a longitudinal depression on the frontal (Ezcurra 2016: Fig. 16).*

53) Ezcurra (2016) ch. 121. *Frontal, olfactory tract on the ventral surface of the frontal: maximum transverse constriction point well posterior to the moulds of the olfactory bulbs and posterolateral margin of the bulbs delimited by a low ridge (0); maximum transverse constriction of the olfactory tract immediately posterior to the moulds of the olfactory bulbs and posterolateral margin of the bulbs well-delimited by a thick, tall ridge (1). This character is inapplicable in taxa that lack olfactory bulb moulds and constriction of the olfactory tract canal (Ezcurra 2016: Fig. 23).*

54) Ezcurra (2016) 112 and Pritchard et al. (2015) ch. 14. *Frontal, frontals fused to one another: absent (0); present (1) (Ezcurra 2016: Fig. 23).*

This character should only be scored in adult specimens, with the exception of juvenile specimens in which the frontals have already fused.

55) New *Frontal, elongate (0); very wide and plate-like, a single frontal (or half of a fused frontal) being almost as wide as long (1)* (*Fig. 10*).

This character describes the very wide frontals seen in *Tanystropheus hydroides* (PIMUZ T 2790) and *Tanystropheus longobardicus* (MSNM BES SC 1018).

56) Pritchard et al. (2015) ch. 16. *Frontal, shape of contact with parietal in dorsal view: roughly transverse in orientation (0); frontal exhibits posterolateral processes, forming anteriorly curved U-shaped contact (1) (Ezcurra 2016: Figs. 8 and 23).*

This character is similar to character 116 in Ezcurra (2016). However, the version of this character in Pritchard et al. (2015) is preferred because it is more specific to the taxon sample studied here.

57) New, combining information from ch. 122 in Ezcurra (2016), ch. 15 in Pritchard et al. (2015), and ch. 313 in Pritchard et al. (2018). *Postfrontal, suture with the frontal: anteroposteriorly or sagitally orientated (0); distinctly posteromedially inclined by a medial process of the postfrontal, resulting in posteriorly strongly narrowed frontal (1); distinctly posterolaterally inclined, resulting in a posteriorly expanded frontal and reduced postfrontal (2)* (*Fig. 11*).

This character, describing the contact between the frontal and postfrontal, combines the description of several characters of previous analyses. In all non-archosauromorph diapsids included here, as well as in most non-archosauriform archosauromorphs (tanystropheids, *Prolacerta broomi*, *Czatkowiella harae*, and *Protorosaurus speneri*), the articulation between the postfrontal and frontal is sagitally orientated. However, in the rhynchosaurs *Howesia browni* and *Mesosuchus browni*, as well as the allokotosaurs *Trilophosaurus buettneri* and *Azendohsaurus madagaskarensis*, the postfrontal bears a distinct medial process, resulting in a posteriorly narrow frontal and a posteromedially orientated suture between the postfrontal and frontal. This morphology was described by character 313 of Pritchard et al. (2018). However, in the archosauriforms, a posteriorly wider frontal reduces the size of the postfrontal, as seen in the archosauriforms *Proterosuchus fergusi*, *Proterosuchus alexanderi*, and *Erythrosuchus africanus* included here. This morphology was described by character 122 of Ezcurra (2016) as well as character 15 of Pritchard et al. (2015). In most archosaur groups, as well as Proterochampsia, the postfrontal has been lost completely (see character 44 of Nesbitt 2011). However, since no taxa belonging to these clades are included here, a separate character state referring to this has not been included.

58) New, combination of ch. 18 of Pritchard et al. (2015) and ch. 123 of Ezcurra (2016) (=ch. 27 of Pritchard et al. 2015). *Postfrontal, lacks a posterior process and does not participate in the border of the supratemporal fenestra (0); has a posterior process and participates in the border of the supratemporal fenestra (1) (Ezcurra 2016: Fig. 16).*

In all scored taxa, the presence of a posterior process of the postfrontal, or a roughly T-shaped postfrontal, implies that the postfrontal contributes to the margin of the supratemporal fenestra, and thereby prevents a contact between the postorbital and parietal (*Youngina capensis*, *Gephyrosaurus bridensis*, and *Planocephalosaurus robinsonae*). Therefore we consider the contribution of the postfrontal to the supratemporal fenestra dependent on the presence of a T-shape ~~of the~~ postfrontal, and therefore combined the characters describing this morphology.

59) Ezcurra (2016) ch. 124. *Postfrontal, shape of dorsal surface: flat or slightly concave towards raised orbital rim (0); depression with deep pits (1). Scored as inapplicable in taxa that lack a postfrontal (Ezcurra 2016: Fig. 16).*

60) Ezcurra (2016) ch. 130. *Postorbital, posterior process extends close to or beyond the level of the posterior margin of the supratemporal fenestrae: absent (0); present (1) (Ezcurra 2016: Fig. 17).*

Character 137 of Ezcurra (2016), the contribution of the squamosal to the intertemporal bar, is considered to be interdependent with the posterior extension of the posterior process of the postorbital. Therefore, this character was not included here.

61) Ezcurra (2016) ch. 131. *Postorbital, extension of the ventral process: ends much higher than the ventral border of the orbit (0); ends close to or at the ventral border of the orbit (1) (Ezcurra 2016: Fig. 17).*

62) Modified from Dilkes (1998) ch. 23. *Postorbital, length of the ventral process versus the length of the posterior process of the postorbital: 0.40-1.20 (0); 1.30-2.50 (1) RATIO.*

The ratios were modified and the identification of the processes was slightly modified in order for them to be congruent with other character descriptions here.

63) Modified from Ezcurra (2016) ch. 126. *Postorbital-squamosal, upper temporal bar: located approximately at level of mid-height of the orbit (0); located approximately aligned to the dorsal border of the orbit (1) (Ezcurra 2016: Figs. 17 and 19). Scored as inapplicable in taxa without an infratemporal fenestra and in taxa in which the upper temporal bar is very tall, reaching from the dorsal margin of the orbit to or beyond mid-height of the orbit.*

An inapplicability criterion was added to this character, because in *Trilophosaurus buettneri* (Spielmann et al. 2008) the infratemporal fenestra is absent, and therefore an upper temporal bar is not present, and because in *Tanystropheus hydroides* (PIMUZ T 2790) the upper temporal bar is dorsoventrally tall and therefore covers the lateral side of the skull from the dorsal border of the orbit to about mid-height of the orbit.

64) Modified from Ezcurra (2016) ch. 127. *Postorbital-squamosal, contact: restricted to the dorsal margin of the elements (0); the anterior process of the squamosal continues along the posterior margin of the ventral process of the postorbital and contacts the jugal (1) (Nesbitt 2011: Figs. 17 and 19). This character is scored as inapplicable in taxa that lack an infratemporal fenestra.*

State 1 of character 127 in Ezcurra (2016) was not included here, because it is not applicable to any of the included taxa. An inapplicability criterion was included because it was considered that the morphology of *Trilophosaurus buettneri* (Spielmann et al. 2008), in which an infratemporal fenestra is absent, represents a non-homologous morphology from state 0, even though the squamosal and jugal likely did not meet in this taxon.

65) Ezcurra (2016) ch. 18. *Infratemporal fenestra: present (0); absent (1).*

66) Ezcurra (2016) ch. 137. *Squamosal, anterior process forms more than half of the lateral border of the supratemporal fenestra: absent (0); present (1) (Ezcurra 2016: Fig. 16). This character is inapplicable in taxa lacking a supratemporal fenestra.*

67) Modified from Ezcurra (2016) ch. 143 and Pritchard et al. (2015) ch. 33. *Squamosal, ventral process: present (0); absent or completely confluent with anterior process (1)* (*Fig. 12*).

This character was modified based on the observed morphologies in the sampled taxa. In *Tanystropheus hydroides* (PIMUZ T 2790) no clear ventral process can be distinguished, but instead the anterior process of the squamosal is dorsoventrally tall and plate-like. It is unclear whether this is the result of a confluence of the anterior and ventral processes. In *Trilophosaurus buettneri* (Spielmann et al. 2008) the ventral process is also absent.

68) Ezcurra (2016) ch. 139 (slightly reformulated). *Squamosal, ventral process: angle between the ventral and anterior processes of the squamosal 90 degrees or less, forming a roughly square outline (0); angle between the ventral and anterior processes of the squamosal more than 90 degrees, forming a gentle, widely rounded posterodorsal border of the infratemporal fenestra (1) (Ezcurra 2016: Figs. 8, 17, 18 and 24). This character is scored as inapplicable in taxa that lack a ventral process of the squamosal.*

69) Modified from Pritchard et al. (2015) ch. 34. *Squamosal, ventral process: forming a massive flange that covers the quadrate entirely in lateral view (0); anteroposteriorly slender (1).* This character is scored as inapplicable in taxa that lack a ventral process on the squamosal.

See character description of character 135 of Ezcurra (2016), which covers the same distinction. The character description of Pritchard et al. (2015) was preferred here, because it is more informative. The inapplicability criterion is added to prevent overscoring for the absence of a ventral process of the squamosal.

70) Modified from Ezcurra (2016) ch. 140. *Squamosal medial process: short, forming up to half or less of the posterior border of the supratemporal fenestra (0); long, forming entirely or almost entirely the posterior border of the supratemporal fenestra (1) (Ezcurra 2016: Fig. 16). This character is scored as inapplicable in taxa that lack a medial process of the squamosal.*

The inapplicability criterion was added.

71) New, similar to Ezcurra (2016) ch. 149. *Squamosal medial process, dorsoventrally short (0); dorsoventrally tall and plate-like, forming a tall surface of the posterior margin of the supratemporal fenestra (1). This character is scored as inapplicable in taxa that lack a medial process of the squamosal* (*Fig. 12*).

72) Modified from Ezcurra (2016) ch. 141. *Squamosal, posterior process is distinct and extends posterior to the dorsal head of the quadrate absent (0); present (1) (Ezcurra 2016: Fig. 18, 19, and 24). This character is inapplicable in taxa where the quadrate is completely covered by the squamosal in lateral view.*

The description of this character was modified to more clearly describe the morphology observed in the taxon sample studied here.

73) Ezcurra (2016) ch. 157. *Supratemporal: broad element (0); slender, in parietal and squamosal trough (1); absent (2) ORDERED (Ezcurra 2016: Fig. 17).*

The definitive absence of the supratemporal is hard to establish because it is often a small element that is easily obscured by specimen disarticulation or compression. Therefore, this bone is only scored as absent when it can be confidently established as such from well-preserved specimens.

74) Ezcurra (2016) ch. 159 and Pritchard et al. (2015) ch. 19. *Parietal, median contact between both parietals: suture present (0); fused with loss of suture (1) (Ezcurra 2016: Fig. 16).*

State 0 can only be scored based on skeletally mature specimens.

75) Ezcurra (2016) ch. 160. *Parietal, extension over interorbital region: absent or slight (0); present (1) (Ezcurra 2016: Figs. 6 and 23).*

76) Ezcurra (2016) ch. 162. *Parietal, pineal fossa on the median line of the dorsal surface: absent (0); present (1). This character should not be scored for early juveniles (Ezcurra 2016: Fig. 8)* (*Fig. 13*).

This character was considered to be present in *Kadimakara australiensis* and several archosauriforms (see scorings of Ezcurra 2016, character 162). However, we consider a similar fossa, as present in these taxa, can also be identified in *Azendohsaurus madagaskarensis* (Flynn et al. 2010), *Trilophosaurus buettneri* (Spielmann et al. 2008), and *Dinocephalosaurus orientalis* (IVPP V13767).

77) Modified from Ezcurra (2016) ch. 164. *Parietal, pineal foramen in dorsal view: large (0); reduced to a small, circular pit or concavity (1); absent (2) (Ezcurra 2016: Figs. 6 and 8), ORDERED.*

The character was ordered, since it is considered a transformational series in which state 1 represents a clear intermediate between states 0 and 2. Furthermore the concavity statement was added to state 1, because in some taxa this depression is not pit-like.

78) Modified from Ezcurra (2016) ch. 165. *Parietal, position of the pineal foramen in dorsal view: enclosed by parietals and clearly on the posterior part of the bones (0); enclosed by parietals at roughly mid-length of the bones (1); enclosed by parietals on the anterior part of the bones close to the frontals (2); enclosed by both frontals and parietals (3), ORDERED (Ezcurra 2016: Figs. 6 and 8). This character is scored as inapplicable in taxa that lack a pineal foramen.*

The pineal foramen is displaced distinctly posteriorly on the parietals in the non-saurian diapsids *Planocephalosaurus robinsonae* (Fraser 1982), *Orovenator mayorum* (Ford & Benson 2018), and *Youngina capensis* (AMNH FARB 5561), and this was therefore considered as a separate character state. This morphology was extensively discussed in Ford and Benson (2018).

79) Modified from Pritchard et al. (2015) ch. 21. *Parietal, orientation of posterolateral process: roughly transverse (0); strongly angled posterolaterally (1)* (*Fig. 13*).

In the majority of the sampled taxa, the posterolateral processes have a posterolateral orientation. However, in *Tanystropheus hydroides* (PIMUZ T 2819), *Tanystropheus longobardicus* (PIMUZ T 2484), *Dinocephalosaurus orientalis* (IVPP V13767), *Protorosaurus speneri* (NMK S 180), and *Azendohsaurus madagaskarensis* (Flynn et al. 2011), the posterolateral process is a completely transverse or lateral orientation. In *Jesairosaurus lehmani*, this character varies somewhat depending on the specimen.

80) Ezcurra (2016) ch 168. *Parietal, posterolateral process height: dorsoventrally low, usually considerably lower than the supraoccipital (0); dorsoventrally deep, being plate-like in occipital view and subequal to the height of the supraoccipital (1) (Ezcurra 2016: Fig. 27).*

81) Ne *Parietal, supratemporal fossa medial to the supratemporal fenestra: absent (0); present (1)* (*Fig. 13*).

82) Ezcurra (2016) ch. 161. (inapplicability criterion slightly reformulated). *Parietal, supratemporal fossa medial to the supratemporal fenestra: well-exposed in dorsal view and mainly dorsally or dorsolaterally facing (0); poorly exposed in dorsal view and mainly laterally facing (1) (Ezcurra 2016: Fig. 16). This character is scored as inapplicable in taxa that lack a supratemporal fossa on the parietal.*

83) Modified from Pritchard et al. (2015) ch. 20 and Ezcurra (2016) ch. 8. *Parietal, medial extent of the supratemporal fossa: restricted to the lateral edge of the parietal, resulting in a broad flat parietal table (0); expanded distinctly medially, resulting in a mediolaterally narrow parietal table (1); supratemporal fossae strongly expanded medially and only separated by a ridge running along the midline of the parietal, the sagittal crest (2), ORDERED. This character is scored as inapplicable in taxa that lack a supratemporal fossa on the parietal* (*Fig. 13*).

This character was modified to clarify the distinction between the different states. The supratemporal fossa can either be restricted to the lateral portion of the parietal, expressed more widely on the parietal, or cover most of the dorsal surface of the parietal between the supratemporal fenestrae, only leaving a thin sagittal crest between the two fossae. This character is very variable in *Prolacerta broomi* with all three states observed in different specimens (state 0: BP/1/471, state 1: BP/1/5375 and UCMP 37151, state 2: BP/1/5066 and BP/1/5880).

84) Ezcurra (2016) ch. 171. *Postparietal, size (pair of postparietals if they are not fused to each other): sheet-like, not much narrower than the supraoccipital (0); small, splint-like (1); absent as a separate ossification (2) ORDERED (Ezcurra 2016: Fig. 23).*

85) Ezcurra (2016) ch. 172 and Pritchard et al. (2015) ch. 25. *Postparietal, fusion between counterparts: absent (0); present, forming an interparietal (1). This character is inapplicable in taxa that lack postparietals.*

86) Ezcurra (2016) ch. 173 and Pritchard et al. (2015) ch. 37. *Tabular: present (0); absent (1).*

87) Ezcurra (2016) ch. 150 and Pritchard et al. (2015) ch. 38. *Quadratojugal: absent or fused to the quadrate (0); present (1) (Ezcurra 2016: Fig. 24).*

88) Modfied from Ezcurra (2016) ch. 153. *Quadratojugal, anterior process: absent, anteroventral margin of the bone rounded and the quadratojugal and jugal do not connect and therefore the lower*

temporal bar is incomplete (0); incipient, short anterior prong on the anteroventral margin of the bone and the quadratojugal and jugal connect and therefore the lower temporal bar is complete (1); distinctly present, in which the lower temporal bar is complete, but process terminates well posterior to the base of the posterior process of the jugal (2); distinctly present, in which the lower temporal bar is complete and participates in the posteroventral border of the infratemporal fenestra, and process terminates close to the base of the posterior process of the jugal (3), ORDERED. This character is inapplicable in taxa that lack an infratemporal fenestra or quadratojugal (Ezcurra 2016: Figs. 17 and 19).

The description of this character was modified to more clearly describe the morphology observed in the taxon sample studied here.

89) Ezcurra (2016) ch. 156. *Quadratojugal, posterior extension of the ventral end: absent, without a posteriorly arched quadratojugal (0); limited, ventral condyles of the quadrate broadly visible in lateral view (1); strongly developed, overlapping completely or almost completely the ventral condyles of the quadrate in lateral view (2), ORDERED (Ezcurra 2016: Fig. 18). This character is inapplicable in taxa lacking a quadratojugal.*

90) New, combination of ch. 176 and ch. 182 in Ezcurra (2016). *Quadrate, posterior margin in lateral view: straight along entire shaft (0); continuously concave (1); sigmoidal, with a concave dorsal portion and convex ventral portion (2) (Ezcurra 2016: Fig. 24).*

These characters were combined because they both relate to the shape of the quadrate shaft. The presence of a quadrate conch is omitted because its presence is likely closely related to a fusion of the quadratojugal to the quadrate in lepidosauromorphs. This fusion is already coded for by character 87 and its inclusion here would result in the overscoring of this morphology.

91) Ezcurra (2016) ch. 180 and Nesbitt et al. (2015) ch. 207. *Quadrate, dorsal end hooked posteriorly in lateral view: absent (0); present (1) (Ezcurra 2016: Figs. 17 and 24).*

92) New *Quadrate, ventral condyles: lateral and medial condyles not distinctly separated and therefore the ventral surface of the quadrate is rounded, flat, or slightly concave (0); condyles separated by a deep concavity on the ventral surface of the quadrate (1)* (*Fig. 14*).

93) Ezcurra (2016) ch. 183. *Quadrate, ventral condyles: subequally distally extended (0); medial condyle distinctly more distally projected than the lateral one (1)* (*Fig. 14*).

94) New *Quadrate, pterygoid flange: anteriormost extension at about mid-height of the midshaft (0); dorsally located, the anteriormost extension of the flange is at close to the dorsoventral level of the dorsal head of the quadrate (1)* (*Fig. 14*).

This character describes the difference seen in the morphology of the pterygoid flange, as can be clearly observed between for instance *Tanystropheus hydroides* (PIMUZ T 2790) and *Macrocnemus bassanii* (PIMUZ T 2477).

95) Pritchard et al. (2015) ch. 45. *Vomer, teeth: absent (0); present (1).*

96) Modified from Ezcurra (2016) ch. 187. *Vomer, teeth distribution: shagreen tooth distribution with no clear rows distinguishable (0); teeth distributed in multiple clearly defined rows (1); teeth distributed mainly in a single row, but multiple teeth present immediately anterior to the contact with the pterygoid (2); teeth distributed in a single row along entire extension (3). This character is inapplicable in taxa that lack vomerine teeth.*

The presence of vomerine teeth and their distribution were considered in one ordered character in character 187 in Ezcurra (2016). However, we do not consider any of the various tooth distributions to represent an intermediate stage between any of the others. Therefore, we considered the presence of vomerine teeth as a separate character, and the distribution of these teeth, if they are present, as a separate, unordered character.

97) New, related to ch. 189 of Ezcurra (2016). *Palatal dentition, size (height and diameter) of teeth on the vomer: small, considerably smaller than those of the marginal dentition (0); relatively large, similar to those of the marginal dentition (1). This character is inapplicable in taxa lacking vomerine teeth* (*Fig. 15*).

Character 189 in Ezcurra (2016) describes the relative size of the teeth on the palatine and pterygoid. However, in our sampled taxa, a distinct difference in the size of the dentition could also be observed in the vomer, and this was therefore formulated into a separate character, since the size of the vomerine teeth does not appear to be dependent on the size of the palatine or pterygoid teeth in the sampled taxa.

98) Ezcurra (2016) ch. 190 (description of state 1 slightly reformulated). *Palatine, transverse extension: narrow, subequal contribution of the palatine and pterygoid to or pterygoid main component*

of the palate posteriorly to the choanae (0); broad, the palatine is the main component of the palate posteriorly to the choanae (1) (Ezcurra 2016: Fig. 26).

99) Modified from Ezcurra (2016) ch. 191. *Palatine, anterior processes forming the posterior border of the choana: subequal in anterior extension or anterolateral process longer (0); anteromedial process longer (1) (Ezcurra 2016: Fig. 26).*

Character state 2 of character 191 in Ezcurra (2016) was not included here, because it is not applicable to any of the sampled taxa.

100) Ezcurra (2016) ch. 188. *Palatine-pterygoid, teeth on the palatine and ventral surface of the anterior ramus of the pterygoid: present (0); absent (1) (Ezcurra 2016: Figs. 13, 24 and 26).*

101) Part of Ezcurra (2016) ch. 189. *Palatal dentition, size (height and diameter) of teeth on the palatine: small, considerably smaller than those of the marginal dentition (0); relatively large, similar to those of the marginal dentition (1). This character is inapplicable in taxa lacking palatine teeth (Ezcurra 2016: Figs. 25 and 26)* (*Fig. 15*).

Character 189 in Ezcurra (2016) treats the size of the dentition on the palatine and pterygoid as a single character. Because the relative size of the teeth on the palatine and pterygoid differs in *Tanystropheus longobardicus* (PIMUZ T 2484) it was decided here to treat the size of the teeth on both elements as separate characters.

102) Ezcurra (2016) ch. 195. *Pterygoid, teeth on the ventral surface of the anterior ramus (=palatal process), excluding tiny palatal teeth if present: present in two distinct fields (=T2 and T3 of Welman 1998) (0); present in three distinct fields (=T2, T3a and T3b) (1); present in three distinct fields (=T2a, T2b and T3) (2); present in one field that occupies most of the transverse width of the ramus (=T2 + T3) (3); present in only one posteromedially-to-anterolaterally orientated field (=T2) (4); present in only one field adjacent to the medial margin of the ramus (=T3) (5); present in no definable fields but the entire pterygoid is covered by a shagreen of teeth (6). This character is inapplicable in taxa that lack teeth in the palatine and the ventral surface of the anterior ramus of the pterygoid (Ezcurra 2016: Figs. 25 and 26).*

103) Ezcurra (2016) ch. 196. *Pterygoid, number of rows on palatal tooth field T2: more than two or do not dispose on distinct rows (0); two rows parallel to each other (1); single row (2). This character is inapplicable if the tooth field T2 is subdivided in T2a and T2b or is absent (Ezcurra 2016: Figs. 25 and 26).*

104) Ezcurra (2016) ch. 197. *Pterygoid, number of rows on palatal tooth field T3: more than two or not disposed in distinct rows (0); two parallel rows (1); single row (2). This character is inapplicable if the tooth field T3 is subdivided into T3a and T3b or is absent (Ezcurra 2016: Figs. 25 and 26).*

Character 199 in Ezcurra (2016) treats a row of teeth sticking out on the medial side of the anterior ramus of the pterygoid (=T4 of Welman 1998) as a separate character. It is found here, based on observations on *Macrocnemus bassanii* (PIMUZ T 1559) and *Prolacerta broomi* (CT-scan of BP/1/5066) that tooth field T3 in these taxa bears more than two distinct rows. Furthermore, the medial margin of the anterior ramus of the pterygoid is curved, resulting in a number of these teeth facing lateroventrally, whilst others face mediolaterally. Therefore, we conclude that tooth field T4 actually represents the mediolaterally facing teeth of tooth field T3. Therefore character 199 in Ezcurra (2016) has not been included here.

105) Part of Ezcurra (2016) ch. 189. *Palatal dentition, size (height and diameter) of teeth on the ventral surface of the anterior ramus of the pterygoid: small, considerably smaller than those of the marginal dentition (0); relatively large, similar to those of the marginal dentition (1). This character is inapplicable in taxa lacking teeth on the anterior ramus of the pterygoid (Ezcurra 2016: Figs. 25 and 26)* (*Fig. 15*).

See description of character 101.

106) Part of Ezcurra (2016) ch. 202. *Pterygoid, teeth on the lateral ramus (=transverse flange): absent (0); present (1) (Ezcurra 2016: Figs. 13, 25 and 26). This character is inapplicable in taxa that bear shagreen teeth on the pterygoid.*

The inapplicability criterion was added because this tooth row cannot be distinguished from other pterygoid teeth when the pterygoid is covered by shagreen teeth. We separated this character from character 107 because we consider the presence of teeth on the lateral ramus of the pterygoid to represent a separate criterion from the number of tooth rows if such teeth are present. Therefore, we do not consider the presence of a single row of teeth to represent an intermediate step in a transformational series between no teeth present and two rows present.

107) Part of Ezcurra (2016) ch. 202. *Pterygoid, distribution of teeth on the lateral ramus (=transverse flange): teeth distributed in a single row on the posterior edge (=T1 of Welman 1998) (0); teeth distributed in multiple rows (1) (Ezcurra 2016: Figs. 13, 25 and 26). This character is inapplicable in taxa that lack teeth on the lateral ramus of the pterygoid or have shagreen teeth covering the pterygoid.*

See description of character 107.

108) New *Pterygoid, anterior end of the anterior ramus: tapers to an end (0); rounded (1)* (*Fig. 15*).

In most of the sampled taxa, the anterior ramus of the pterygoid gradually tapers anteriorly and thus has an anteriorly pointed end. In contrast, in *Tanystropheus hydroides* (PIMUZ T 2787) and *Dincephalosaurus orientalis* (Rieppel et al. 2008) the anterior ramus of the pterygoid is much wider anteriorly and has a rounded anterior margin.

109) New *Pterygoid, lateral/distal end of the posterior margin of the lateral ramus (=transverse flange) curved posteriorly: absent (0); present (1). This character is scored as inapplicable in taxa with a strongly posterolaterally orientated lateral ramus of the pterygoid* (*Fig. 16*).

This character is closely related to character 201 in Ezcurra (2016). However, because this new character distinguishes within Tanystropheidae, it is considered to be more informative and therefore preferred. Character 201 of Ezcurra (2016) was not included in order to prevent overscoring of this morphology.

110) Modified from Ezcurra (2016) ch. 207. *Ectopterygoid, lateral process is not curved posteriorly (0); is curved posteriorly but not expanded (1); is both curved and expanded posteriorly, giving the ectopterygoid a hook-shape in dorsal or ventral view (2) (Ezcurra 2016: Figs. 7 and 26)* (*Fig. 15*), *ORDERED.*

The lateral portion of the ectopterygoid can be separated into three different morphologies. In some taxa, it is not curved, nor expanded. In other taxa, the lateral end curves posteriorly but it is not expanded anteroposteriorly. Finally, in certain taxa, the lateral portion of the ectopterygoid is curved posteriorly and is expanded anteroposteriorly. Since state 1 is considered to represent an intermediate state between 0 and 2 in a transformational series, this character was ordered.

111) Ezcurra (2016) ch. 204 (state 0 reformulated). *Ectopterygoid, articulation with pterygoid: ectopterygoid overlaps the pterygoid ventrally (0); interlaced articulation, complex articulation between ectopterygoid and pterygoid (1) (Ezcurra 2016: Fig. 26).*

112) Modified from Ezcurra (2016) ch. 205. *Ectopterygoid, connection with pterygoid: does not reach the posterolateral corner of the lateral ramus (=transverse flange) (0); reaches the posterolateral corner of the lateral ramus (1) (Ezcurra 2016: Fig. 26). This character is scored as inapplicable in taxa in which the ectopterygoid simply overlaps the pterygoid.*

An inapplicability criterion is added because the ectopterygoid only reaches the posterolateral corner of the lateral ramus of the pterygoid when the ectopterygoid forms an interlacing suture with the pterygoid. In taxa with this type of articulation, the ectopterygoid wraps around the posterolateral corner of the transverse flange in some cases.

113) Ezcurra (2016) ch. 244 and Pritchard et al. (2015) ch. 65. *Parasphenoid/parabasisphenoid, dentition on cultriform process: present (0); absent (1).*

114) New *Parasphenoid/parabasisphenoid, length of the cultriform process versus its height at its anteroposterior midpoint: 4.00-7.00 (0); 9.00-18.00 (1) RATIO.*

This character treats the large discrepancy in the relative length of the cultriform process. In most taxa it is a thin elongate element, whereas in allokotosaurs and rhynchosaurs it is much shorter and dorsoventrally taller.

115) New *Parasphenoid/parabasisphenoid, anterior projections of the cristae trabeculares, present (0); absent (1).*

The cristae trabeculars are small bony projections on the anterolateral surface of the cultriform process of the parabasisphenoid, which occur in certain non-saurian diapsids and lepidosaurs. These structures and their occurrence among diapsids were discussed in detail by Ford and Benson (2018, page 18).

116) Ezcurra (2016) ch. 236. *Parasphenoid/parabasisphenoid, posterodorsal portion: incompletely ossified (0); completely ossified (1).*

117) Modified from Ezcurra (2016) ch. 237. *Parasphenoid/parabasisphenoid, intertuberal plate: present (0); absent (1) (Ezcurra 2016: Figs. 10 and 28).*

Character states 1 and 2 of character 237 in Ezcurra (2016) were fused here, because there was no clear distinction between a rounded and a straight posterior edge of the intertuberal plate in the sampled taxa, and this distinction is likely only relevant in more derived archosauriforms.

118) Modified from Ezcurra (2016) ch. 239. *Parasphenoid/parabasisphenoid, recess (=median pharyngeal recess, =hemispherical sulcus, =hemispherical fontanelle): absent, the ventral floor of the parabasisphenoid posterior to the basipterygoid processes (and posterior to a potentially present intertuberal plate) is flat (0); present, the ventral floor forms a shallow depression (1); the ventral floor is deeply excavated (2) (Ezcurra 2016: Fig. 27), ORDERED.*

The pharyngeal recess originally identified in archosauriforms, but has subsequently also been described for certain non-archosauriform archosauromorphs (e.g. *Azendohsaurus madagaskarensis*; Flynn et al. 2010~~, and~~ *Mesosuchus browni*; Sobral & Müller 2019). Observation of this character in the sampled taxa indicates that this character occurs in two states. The pharyngeal recess was first described as a very deep ventral cavity (e.g. the basisphenoid recess of Witmer 1997). This occurs in *Tanystropheus hydroides* (PIMUZ T 2790) and *Erythrosuchus africanus* (BP/1/3893) among the sampled taxa. However, a much shallower excavation of the ventral surface of the parabasisphenoid posterior to the basipterygoid processes occurs in the majority of non-archosauriform archosauromorphs, as well as *Youngina capensis* (Gardner et al. 2010). This shallow excavation was also identified as the pharyngeal recess by Sobral et al. (2016) and Sobral & Müller (2019). We here distinguish the shallow excavation from the deeper excavation as separate character states for the first time, and consider the former to possibly represent an intermediate morphology between the absence of a pharyngeal recess and the deeply excavated pharyngeal recess.

119) Ezcurra (2016) ch. 238. *Parasphenoid/parabasisphenoid, semilunar depression on the posterolateral surface of the bone: absent (0); present (1). This character is inapplicable in taxa that the posterodorsal portion of the parasphenoid/parabasisphenoid is not ossified, resulting in an unossified gap between this element and the prootic (Ezcurra 2016: Fig. 28).*

120) Ezcurra (2016) ch. 235 and Nesbitt et al. (2015) ch. 208 (description of state 1 slightly reformulated). *Basisphenoid/parabasisphenoid, orientation of the body between the posterior end of the bone and the basipterygoid processes: horizontal (0); oblique, main axis posterodorsally-to-anteroventrally orientated (1) (Ezcurra 2016: Figs. 27 and 28).*

121) Ezcurra (2016) ch. 225. *Basioccipital-parasphenoid/parabasisphenoid, contact with each other in skeletally mature individuals: loose, overlapping suture (0); tightly sutured, sometimes by an interdigitated suture, or both bones fused to each other (1) (Ezcurra 2016: Fig. 28).*

122) New *Basioccipital-parasphenoid/parabasisphenoid, two pneumatic foramina ~~in~~ between the basioccipital and parabasisphenoid: absent (0); present (1).*

Pneumatic foramina were described as present in a number of early archosauromorphs by Sobral & Müller (2019). This character is now implemented in a quantitative phylogenetic analysis for non-archosauriform archosauromorphs for the first time. See Figs. 3 and 13 in Sobral & Müller (2019).

123) Ezcurra (2016) ch. 226. *Basioccipital-parasphenoid/parabasisphenoid, basal tubera: absent (0); present (1) (Ezcurra 2016: Fig. 27).*

124) Modified from Ezcurra (2016) ch. 227. *Basioccipital-parasphenoid/parabasisphenoid, low ridge between basal tubera: absent or very strongly reduced (0); present (1). This character is scored as inapplicable in taxa that lack basal tubera (Ezcurra 2016: Fig. 27)* (*Fig. 16*).

Character 227 in Ezcurra (2016) is applicable to a wide range of archosauromorphs. This character was modified to more specifically address the variation observed in the taxa sampled here. A clear but low, transversely orientated ridge is present between the basal tubera of the basioccipital of *Tanystropheus hydroides* (PIMUZ T 2790) and *Tanystropheus longobardicus* (PIMUZ T 2484). Such a ridge cannot be observed in any of the other sampled taxa.

125) Modified from Pritchard et al. (2018) ch. 318. *Basioccipital, ventral margin: prominent embayment or ridge between basal tubera at least as transversely broad as occipital condyle (0); transversely narrow embayment or ridge between basal tubera, narrower than occipital condyle (1). This character is scored as inapplicable in taxa that lack basal tubera.*

The inapplicability criterion was added. See the description of character 318 in Pritchard et al. (2018).

126) Ezcurra (2016) ch. 229. *Basioccipital, articular surface of the occipital condyle: concave (0); hemispherical (1) (Ezcurra 2016: Fig. 28).*

127) Ezcurra (2016) ch. 211 and Pritchard et al. (2015) ch 62. *Otoccipital, fusion between opisthotic and exoccipital: absent or partial (0); present (1) (Ezcurra 2016: Fig. 27).*

128) New, combination of character 209 of Ezcurra (2016) (= character 60 of Pritchard et al. 2015) and character 219 of Ezcurra (2016) (= character 59 of Pritchard et al. 2015). *Exoccipital, morphology of the dorsal end: exoccipital columnar through dorsoventral height, forming transversely narrow dorsal contact with more dorsal occipital elements (0); dorsal portion of exoccipital exhibits dorsomedially inclined process that forms transversely broad contact with more dorsal occipital elements but exoccipitals do not meet on the dorsal margin of the foramen magnum (1); dorsal portion of exoccipital exhibits dorsomedially inclined process that meets the process of the opposite exoccipital on the dorsal margin of the foramen magnum, thus excluding the supraoccipital from contributing to the margin of the foramen magnum (2), ORDERED* (*Fig. 16*). *This character is inapplicable in taxa without a discernable suture between the supraoccipital and the exoccipital or fused opisthotic-exoccipital.*

These two characters were fused because the exclusion of the supraoccipital from the margin of the foramen magnum implies that the exoccipitals connect to each other dorsally, which is caused by an extensive dorsomedial inclination of the dorsal portions of the exoccipitals.

129) Modified from Ezcurra (2016) ch. 221. *Exoccipital, medial margin of their distal ends: no contact with its counterpart (0); contact with its counterpart to partially or fully exclude basioccipital from the floor of the endocranial cavity (1) (Ezcurra 2016: Fig. 27).*

States 1 and 2 of character 221 in Ezcurra (2016) were fused here, because it is very difficult to distinguish between them in the sampled taxa.

130) Ezcurra (2016) ch. 213 (both states slightly reformulated). *Opisthotic, paroccipital processes orientation: extend laterally or slightly posterolaterally (0); deflected strongly posterolaterally at an angle of more than 20 degrees from the transverse plane of the skull (1) (Ezcurra 2016: Fig. 16).*

131) Pritchard et al. (2015) ch. 58. *Opisthotic, paroccipital process: ends freely (0); contacts the suspensorium (1).*

132) Ezcurra (2016) ch. 216. *Opisthotic, fossa immediately lateral to the foramen magnum: absent (0); present (1).*

133) Modified from Ezcurra (2016) ch. 217. *Opisthotic, ventral ramus shape: pyramidal, with a tapering distal end (0); club-shaped with a large bulbous distal head (1); columnar-like shaft of the ramus and an anteroposteriorly expanded but not a bulbous distal head (2); anteroposteriorly flattened shaft of the ramus, forming a blade-like ramus in lateral view and an anteroposteriorly expanded but not a bulbous distal head (3) (Ezcurra 2016: Fig. 28)* (*Fig. 17*).

This character was modified to more precisely fit the morphology of the ventral ramus of the opisthotic as we observed it for the sampled taxa.

134) Ezcurra (2016) ch. 218 (state 1 slightly reformulated). *Opisthotic, ventral ramus: extends further laterally than the lateralmost edge of the exoccipital in posterior view (0); ventral ramus completely or almost completely covered by the lateralmost edge of the exoccipital in posterior view (1) (Ezcurra 2016: Fig. 27).*

135) Ezcurra (2016) ch. 223. *Pseudolagenar recess, opening externally between the ventral surface of the ventral ramus of the opisthotic and the basal tubera: present (0); absent (1) (Ezcurra 2016: Fig. 27).*

136) Modified from Ezcurra (2016) ch. 19. *Posttemporal fenestra, size: large, roughly similar in size to the supraoccipital (0); strongly reduced in size and much smaller than the supraoccipital (1); absent or developed as a foramen or very narrow slit (2) ORDERED (Ezcurra 2016: Fig. 27).*

This character has been modified according to observations on the sampled taxa. In most taxa, the posttemporal fenestra is large with little variation in its construction. However, in *Azendohsaurus madagkarensis* (Flynn et al. 2010), the parietal encloses the fenestra laterally, distinctly reducing it in size. In *Erythrosuchus africanus* (BP/1/4680), *Proterosuchus fergusi* (SAM-PK-K10603), and *Proterosuchus alexanderi* (NM QR 1484), the fenestra is only represented by a very narrow slit or foramen.

137) Ezcurra (2016) ch. 254 (reformulated). *Prootic, a clear crest on the lateral surface that is roughly orientated posterodorsally to anteroventrally (crista prootica sensu Sobral & Müller 2019) is absent (0); crista prootica present (1) (Ezcurra 2016: Fig. 28)* (*Fig. 17*).

138) New *Prootic, a clear crest along the lateral surface that curves dorsally at the anterior margin of the prootic is absent (crista alaris sensu Sobral & Müller 2019) (0); crista alaris is present (1)* (*Fig. 17*).

Although character 254 in Ezcurra (2016) addressed the presence of crista prootica in a phylogenetic context, the presence of another crest on the lateral surface of the prootic, the crista alaris, is also variable for the sampled taxa, which is addressed with this character.

139) Pritchard et al. (2015) ch. 75 (reformulated). *Prootic, paroccipital contribution: does not contribute to anterior surface of paroccipital process (0); contributes laterally tapering lamina to the anterior surface of the paroccipital process (1)* (*Fig. 17*).

140) Modified from Ezcurra (2016) ch. 258 and Pritchard et al. (2015) ch. 72. *Laterosphenoid, ossification: absent (0); present, laterosphenoid is a narrow dorsoventrally orientated bone and lacks an anterior portion (1); present, laterosphenoid with an anterior portion located along the ventral surface of the parietal and frontals (2) (Ezcurra: Fig. 28)* (*Fig. 17*)*, ORDERED.*

The presence of a laterosphenoid was until recently not known for non-archosauriform archosauromorphs. However, a laterosphenoid has now also been identified in *Azendohsaurus madagskarensis* (Flynn et al. 2010) and *Tanystropheus hydroides* (PIMUZ T 2790). In these taxa, the laterosphenoid is small and does not extend far anteriorly as in archosauriforms. This information is added to the character. The small, unexpanded laterosphenoid, is considered to represent an intermediate step between the absence of a laterosphenoid and the larger, further anterior reaching laterosphenoid of archosauriforms.

141) Ezcurra (2016) ch. 296. *Stapes, shape: robust, with thick shaft (0); slender, rod-like shaft (1).*

142) Ezcurra (2016) ch. 297 and Pritchard et al. (2015) ch. 77. *Stapes, stapedial foramen piercing the columellar process: present (0); absent (1).*

143) Simões et al. (2018) ch. 176. *Splenial: present (0); absent (1).*

144) Modified from Ezcurra (2016) ch. 266. *Dentary, height at the third alveolus of the bone (or directly posterior to the tapering anterior end of the dentary in taxa with an anteriorly edentulous dentary) versus length of the alveolar margin (including edentulous anterior end if present): 0.02-0.11 (0); 0.15-0.19 (1); 0.21-0.29 (2); 0.34-0.36 (3) ORDERED RATIO (Ezcurra 2016: Figs. 17 and 18).*

Instead of comparing the length of the alveolar margin of the dentary to the minimum height of the dentary, it was here considered to compare it to the height of the dentary at the third alveolus, as this represents a more consistent measurement across the sampled taxa.

145) Ezcurra (2016) ch. 267 (reformulated). *Dentary, shape of the tooth bearing portion (including edentulous anterior end if present): roughly straight (0); dorsally curved for all or most of its anteroposterior length (1); ventrally curved or deflected at its anterior end (2) (Ezcurra 2016: Figs. 17 and 29).*

146) New *Dentary, distinct dorsoventral expansion forming a keel at the anterior end of the dentary: absent (0); present (1). This character is inapplicable in taxa with an edentulous anterior end of the dentary* (*Fig. 18*).

State 1 represents an autapomorphy for *Tanystropheus hydroides* (PIMUZ T 2790) among the sampled taxa.

147) Ezcurra (2016) ch. 270. *Dentary, position of the Meckelian groove on the anterior half of the bone: dorsoventral centre of the dentary (0); restricted to the ventral border (1) (Nesbitt 2011: Fig. 27).*

148) Ezcurra (2016) ch. 272. *Dentary, posterodorsal process, in which its dorsal margin is confluent with the dorsal margin of the lower jaw: absent (0); present (1) (Ezcurra 2016: Figs. 17 and 29).*

149) Ezcurra (2016) ch. 273. *Dentary, posterocentral process, in which its margins are not confluent with the dorsal or ventral margin of the lower jaw: absent (0); present (1) (Ezcurra 2016: Figs. 17 and 29).*

150) Modified from Ezcurra (2016) ch. 275. *Dentary, posteroventral process, in which its ventral margin is confluent with the ventral margin of the lower jaw: absent (0); present (1) (Ezcurra 2016: Figs. 17 and 29).*

Character state 2 of character 275 in Ezcurra (2016) was omitted here because the majority of the included taxa here do not bear an external mandibular fenestra.

151) Ezcurra (2016) ch. 276. *Dentary, posteroventral process length: extended posteriorly to the level of the posterodorsal and/or posterocentral processes (0); extended posteriorly beyond the level of the posterodorsal and/or posterocentral processes (1). This character is inapplicable in taxa that lack a posteroventral process in the dentary (Ezcurra 2016: Fig. 29).*

152) Ezcurra (2016) ch. 262 and Pritchard et al. (2015) ch. 84. *Lower jaw, external mandibular fenestra: absent (0); present (1) (Ezcurra 2016: Figs. 17 and 29).*

153) New, combination of ch. 261 (partially) of Ezcurra (2016) and character 319 of Pritchard et al. (2018) *Lower jaw, distinct dorsal process behind the alveolar margin: absent, with a slightly convex dorsal margin behind the alveolar portion (0); present but low, not protruding dorsally behind the anterior process of the jugal (1); present and tall, protruding dorsally behind the anterior process of the jugal (2) (Ezcurra 2016: Fig. 29), ORDERED.*

Both characters from the literature were considered to be informative and strongly related and they were therefore combined here. The identification of which bone forms the coronoid process is not considered because this often is hard to establish confidently in the sampled taxa. Furthermore, this information is strongly interdependent with the subsequent character (154).

154) New. *Separate coronoid bone: present (0); absent (1).*

Although it has been previously established that several archosauromorphs lack a separate coronoid bone, this has not been coded as a character in phylogenetic analyses until now.

155) Modified from Ezcurra (2016) ch. 286. *Surangular, lateral shelf: absent (0); present, low ridge near dorsal margin (1); present, laterally or ventrolaterally projecting shelf with a lateral edge (2) (Ezcurra 2016: Figs. 18 and 29).*

States 2 and 3 of character 286 in Ezcurra (2016) were combined here because this distinction was considered to be somewhat subjective and not of relevance for the sampled taxa.

156) Ezcurra (2016) ch. 288 and Pritchard et al. (2015) ch. 80. *Surangular, anterior surangular foramen on the lateral surface of the bone, near surangular-dentary contact: absent (0); present (1) (Ezcurra 2016: Fig. 29).*

157) Ezcurra (2016) ch. 289 and Pritchard et al. (2015) ch. 81. *Surangular, posterior surangular foramen on the lateral surface of the bone, positioned directly anterolateral to the glenoid fossa: absent (0); present (1) (Ezcurra 2016: Fig. 29).*

158) Modified from Ezcurra (2016) ch. 282. *Surangular-angular, suture along the anterior half of the bones in lateral view: anteroposteriorly convex ventrally (0); roughly straight (1); anteroposteriorly concave ventrally (2) (Ezcurra 2016: Fig. 29)* (*Fig. 18*) *ORDERED.*

In *Tanystropheus hydroides* (PIMUZ T 2790), *Trilophosaurus buettneri* (Spielmann et al. 2008), and *Orovenator mayorum* (Ford and Benson 2018) the surangular-angular suture is neither convex nor concave but straight, which was therefore included as a separate character state here. A straight suture is considered an intermediate step in a transformational series from concave to convex and the character has therefore been ordered.

159) Modified from Ezcurra (2016) ch. 290 and Pritchard et al. (2015) ch. 82. *Angular, dorsoventral exposure on the lateral surface of the lower jaw: wide (0); forming about half of the dorsoventral height of the mandible at its greatest width (1); narrow (2) (Ezcurra 2016: Fig. 29)* (*Fig. 18*) *ORDERED.*

In *Tanystropheus hydroides* (PIMUZ T 2790), *Tanystropheus longobardicus* (PIMUZ T 2484), *Azendohsaurus madagaskarensis* (Flynn et al. 2011), *Proterosuchus fergusi* (SAM-PK-11208), and *Proterosuchus alexanderi* (NM QR 1484) covers approximately half of the lateral surface of the mandible posteriorly, which was therefore included as separate character state here. This exposure is considered an intermediate step in a transformational series from a very wide to a very narrow exposure and the character has therefore been ordered.

160) Pritchard et al. (2015) ch. 83 (state 0 reformulated). *Angular, exposure on lateral mandibular surface: terminates significantly anterior to the glenoid (0); extends to the glenoid (1).*

161) Modified from Senter (2004) ch. 16. *Location of glenoid fossa compared to tooth row of the dentary: roughly at the same dorsoventral level as the tooth row (0); considerably ventrally displaced compared to the tooth row (1)* (*Fig. 18*).

In several tanystropheids (*Tanystropheus hydroides*, PIMUZ T 2790; *Tanystropheus longobardicus*, PIMUZ T 2482; *Tanytrachelos ahynis*, YPM 7496a; *Pectodens zhenyuensis*, IVPP V18578; and *Dinocephalosaurus orientalis*, IVPP V13767), and in *Azendohsaurus madagaskarensis* (Flynn et al. 2011) and *Gephyrosaurus bridensis* (Evans 1980), the glenoid fossa is located distinctly ventrally compared to the dentary tooth row. This character was first employed by Senter (2004).

162) Ezcurra (2016) ch. 283. *Articular, retroarticular process: absent (0); anteroposteriorly short, being poorly developed posteriorly to the glenoid fossa (1); anteroposteriorly long, extending considerably posterior to the glenoid fossa (2) ORDERED (Ezcurra 2016: Figs. 17 and 29).*

163) Ezcurra (2016) ch. 284. *Articular, retroarticular process: not upturned (0); upturned (1). This character is scored as inapplicable in taxa that lack a retroarticular process (Ezcurra 2016: Figs. 17 and 29).*

164) Pritchard et al. (2015) ch. 92. *Marginal dentition, arrangement: single row of marginal teeth (0); multiple zahnreihen in maxilla and dentary (1).*

Characters 73 and 279 in Ezcurra (2016) treat the number of tooth rows on the upper and lower jaws separately. We consider these characters to be strongly interdependent for the sampled taxa and therefore prefer to treat both jaws in one character here.

165) New *Marginal dentition, anterior teeth are interlocking fangs forming a fish-trap sensu (Rieppel 2002): absent (0); present (1). This character is inapplicable in taxa with an edentulous premaxilla* (*Fig. 18*).

In *Tanystropheus hydroides* (PIMUZ T 2790), *Tanystropheus longobardicus* (MSNM BES SC 1018), and *Dinocephalosaurus orientalis* (IVPP V13767), the anterior marginal dentition is fang-like and elongate. These teeth interlock to form a ‘fish-trap’ type dentition.

166) Modified from Ezcurra (2016) ch. 280. *Marginal dentition, occlusion of marginal teeth: single-sided overlap (excluding potentially present interlocking fish-trap dentition anteriorly) (0); flat occlusion (1); teeth interlocking tightly (2). This character is inapplicable in taxa in which multiple tooth rows are present on the marginal dentition (Ezcurra 2016: Fig. 14).*

The character states were modified to more specifically address the morphologies observed in the sampled taxa.

167) Ezcurra (2016) ch. 298. *Marginal dentition, posterior extent of mandibular and maxillary tooth rows: subequal (0); maxillary teeth extending further posteriorly (1).*

168) Ezcurra (2016) ch. 277. *Marginal dentition, posteriormost dentary teeth: on the anterior half of lower jaw (0); on the posterior half of lower jaw (1) (Ezcurra 2016: Fig. 17).*

169) Ezcurra (2016) ch 299. *Marginal dentition, tooth implantation: subthecodont (=protothecodont) (0); ankylothecodont (teeth fused to the bone at the base of the crown by bony ridges and the root can be discerned; there is continuous tooth replacement) (1); pleurodont (2); acrodont (teeth fused to the bone in adults so that no root can be discerned) (3); thecodont (4) (Ezcurra 2016: Figs. 12, 14 and 22).*

170) Ezcurra (2016) ch. 308. *Marginal dentition, multiple maxillary and dentary tooth crowns distinctly mesiodistally expanded above the root: absent (0); present (1) (Ezcurra 2016: Fig. 14).*

171) Modified from Ezcurra (2016) ch. 303. *Marginal dentition, maxillary teeth: straight or very slightly recurved (0); distinctly recurved (1) (Ezcurra 2016: Fig. 14). This character is not applicable in taxa with maxillary teeth that expand above the root or that possess multiple tooth rows in the maxilla.*

Certain taxa have very slightly recurved teeth (e.g. *Petrolacosaurus kansensis, Czatkowiella harae*, and *Orovenator mayorum*). However, we choose not to maintain a separate character state for this morphology as in these taxa not all teeth are recurved and many are straight, therefore forming a very minimal distinction from the straight morphology. Only taxa in which the curvature of the teeth is distinct are scored as 1.

172) Ezcurra (2016) ch. 304. *Marginal dentition, serrations on the maxillary/dentary crowns: absent (0); distinctly present on the distal margin and usually apically restricted, low or absent on the mesial margin (1); present and distinct on both margins (2) (Ezcurra 2016: Fig. 14).*

173) Ezcurra (2016) ch. 306. *Marginal dentition, multiple maxillary or dentary tooth crowns with longitudinal labial or lingual striations or grooves: absent (0); present (1) (Ezcurra 2016: Fig. 14).*

174) Modified from Pritchard et al. (2015) ch. 98. *Marginal dentition, tooth shape at crown base: circular or labiolingually compressed (0); labiolingually wider than mesiodistally long (1).*

States 0 and 1 of character 98 of Pritchard et al. (2015) were fused here, because the distinction between labiolingually compressed and circular teeth is very difficult to assess in the sampled taxa, as it represents an often minor distinction and many of the sampled specimens are compressed.

175) Modified from Pritchard et al. (2015) ch. 93. *Marginal dentition, morphology of crown base: all tooth crowns form a single, pointed or rounded crown (0); at least some tooth crowns form a flattened platform with pointed cusps (1); at least some tooth crowns have three, mesiodistally arranged cusps (2).*

The character states were modified to more specifically address the morphologies observed in the sampled taxa.

176) Ezcurra (2016) ch. 310. *Cervical, dorsal, sacral and caudal vertebrae, notochordal canal piercing the centrum: present throughout ontogeny (0); absent in adults (1) (Ezcurra 2016: Fig. 31).*

177) Ezcurra (2016) ch. 313. *Presacral vertebrae, at least one or more cervical or anterior dorsal with parallelogram-shaped centra in lateral view, in which the anterior articular surface is situated higher than the posterior one: absent (0); present (1) (Ezcurra 2016: Figs. 11 and 33).*

178) New. *Cervical vertebrae, maximum height of postaxial anterior or middle cervical neural spines: considerably taller than the posterior articular surface of the centrum (0); approximately equally tall as the posterior articular surface of the centrum (1); considerably shorter than the posterior articular surface of the centrum (2); low neural spines are only present at the anterior and posterior ends of the vertebrae but are completely or virtually lost at their anteroposterior midpoints (3); neural spine is completely reduced or lost (4) (Ezcurra 2016: Fig. 11)* (*Fig. 19*)*, ORDERED.*

Characters 342 and 344 in Ezcurra (2016) addressed the height of the neural spine in the postaxial cervical vertebrae, which is a variable and phylogenetically important trait among tanystropheids. We have combined the information of these two characters, because we considered them to be interdependent, and modified the states distinctly to address the specific morphologies observed in the sampled taxa.

179) New. *Cervical vertebrae, shape of distal margin of anterior and middle cervical postaxial neural spines in lateral view: slightly convex (0); completely straight along anteroposterior length (1); concave (2)* (*Fig. 20*). *This character is inapplicable in taxa that have reduced the neural spine of their anterior and mid cervicals completely or at their anteroposterior midpoint.*

We find that in a number of taxa the distal margin of the neural spine of the anterior to mid cervical vertebrae is completely straight along its entire anteroposterior length (e.g. *Macrocnemus bassanii*, PIMUZ T 4822; and *Pamelaria dolichotrachela*, ISIR 316/1). This straight margin often, but not always, occurs together with a distally expanded neural spine (= spine table). However, due to both structures also occurring without the presence of the other, they were scored here as separate characters. Furthermore, the distal margin of the neural spines of certain taxa are conspicuously concave (particularly in *Dinocephalosaurus orientalis*, Rieppel et al. 2008).

180) New, combination of Ezcurra (2016) ch. 320 and 321. *Cervical vertebrae, distal expansion of the anterior to middle postaxial cervical neural spines (not mammillary process): absent (0); present, gradual transverse expansion of the distal half of the neural spine (1); present, but transverse expansion is restricted to the distal end of the neural spine (= spine table) (2) (Fig. 20). This character is inapplicable in taxa that have reduced the neural spine of their anterior and mid cervicals completely.*

A distal expansion of the postaxial neural spines was previously addressed by character 117 in Pritchard et al. (2015) and characters 320 and 321 in Ezcurra (2016). Here, we combined information of these characters to form a new character that addresses the variation seen in this trait in the sampled taxa. We consider the gradual transverse expansion to represent a separate state from the presence of a spine table, following Ezcurra (2016). However, since a gradual expansion and a distinct spine table both address a widening of the neural spine, which is separate from the presence of mammillary processes, we consider them part of the same morphological character. This character should only be scored in skeletally mature specimens, since a transverse expansion of the neural spine is generally absent in early ontogenetic stages.

181) Modified from Simões et al. (2018) ch. 228. *Presacral vertebrae, type of articular surface: opistocoelous (0); procoelous (1); amphicoelous (2); acoelous (3). This character is inapplicable in taxa that have a notochordal canal running through their centra.*

The articulation surfaces of the centra of presacral vertebrae was previously considered by characters 101 and 102 in Pritchard et al. (2015), which considered the anterior and posterior surfaces separately. We follow Simões et al. (2018) and treat the articulation surfaces of the centra as a single character.

182) Nesbitt (2011) ch. 177. *Presacral vertebrae, postaxial intercentra: present (0); absent (1).*

The presence of intercentra was scored separately for postaxial cervical vertebrae and dorsal vertebra in characters 346 and 366 in Ezcurra (2016). However, we score only the presence or absence of postaxial intercentra since in most cases for the sampled taxa, the presence of intercentra often occurs in both segments of the vertebral column. Thus, separating these segments results in overscoring of the presence of postaxial intercentra.

183) Ezcurra (2016) ch. 326 and Nesbitt et al. (2015) ch. 243. *Cervical vertebrae, centrum of atlas in skeletally mature individuals: separate from axial intercentrum (0); fused to axial intercentrum (1) (Ezcurra 2016: Fig. 30).*

184) New. *Cervical vertebrae, proatlas elements dorsal to atlantal neural arches: present (0); absent or fused with atlantal neural arch (1)* (*Fig. 21*).

No proatlases are present in *Tanystropheus hydroides* (PIMUZ T 2790), in contrast to all other sampled taxa for which this character could be scored.

185) Modified from Ezcurra (2016) ch. 328. *Cervical vertebrae, height of neural spine of the axis: ratio between the maximum height of the neural spine and the posterior articular surface height of the centrum of the axis: 0.40-0.60 (0); 0.75-1.25 (1); 1.45-2.25 (2), ORDERED RATIO (Ezcurra 2016: Fig. 30).*

The distinction between the states of character 328 of Ezcurra (2016) is considered to be ambiguous. Therefore, the states were modified into ratios to make a more discrete distinction between the states.

186) Ezcurra (2016) ch. 329. *Cervical vertebrae, shape of the neural spine of the axis: expanded posterodorsally or the height of the anterior portion is equivalent to the posterior height (0); expanded anterodorsally (1) (Ezcurra 2016: Fig. 30).*

187) Ezcurra (2016) ch. 331. *Cervical vertebrae, lengths of the fourth or fifth cervical centra versus the heights of their anterior articular surfaces: 0.60-2.45 (0); 2.70-5.15 (1); 6.30-8.00 (2); 8.30-11.10 (3); 15.00-21.00 (4) ORDERED RATIO (E: Fig. 15).*

Character states were defined after comparison of all the different measured ratios.

188) Ezcurra (2016) ch. 332 *Cervical vertebrae, diapophysis and parapophysis of anterior to middle cervical postaxial vertebrae: single facet or both situated on the same process (0); situated on different processes and well-separated (1); situated on different processes and nearly touching (2) (Ezcurra 2016: Fig. 30).*

189) New, combination of ch. 334 and 340 of Ezcurra (2016) *Cervical vertebrae, laminae extending posteriorly from the base of the dia –and/or parapophysis in anterior and middle postaxial cervical vertebrae: absent (0); present (1) (Ezcurra 2016: Fig. 30).*

Laminae project from the base of the dia –and/or parapophysis in most of the sampled taxa, except for *Youngina capensis* (BP/1/3859)*, Erythrosuchus africanus* (BP/1/5207)*, Mesosuchus browni* (SAM-PK-5882), and *Planocephalosaurus robinsonae* (Fraser & Walkden 1984). The laminae as described in character 340 in Ezcurra (2016) are considered to represent the same structure as that of character 334 and therefore these characters were fused.

190) Ezcurra (2016) ch. 336. *Cervical vertebrae, epipophysis in postaxial cervicals: absent (0); present in at least the third to fifth cervical vertebrae (1) (Ezcurra 2016: Figs. 30 and 33).*

191) Modified from Pritchard et al. (2018) ch. 271. *Cervical vertebrae, posterior extension of epipophysis: not extended posterior to the postzygapophysis (0); overhanging the postzygapophysis posteriorly (1). This character is inapplicable in taxa that lack epipophyses on their cervical vertebrae* (*Fig. 22*).

In all tanystropheids, with the exception of certain specimens of *Tanystropheus "conspicuus"* (U-MO BT 740), *Sclerostropheus fossai* (MCSNB 4035), *Macrocnemus fuyuanensis* (IVPP V15001), *Langobardisaurus pandolfii* (MCSNB 2883), the epipophyses are well-developed and extend posteriorly beyond the level of the postzygapophyses. In all other sampled taxa that bear epipophyses, they are not extended as far posteriorly. The character was modified from character 271 of Pritchard et al. (2018) because the distinction between states 1 and 2 therein was considered to be difficult to distinguish confidently in the sampled taxa.

192) Modified from Ezcurra (2016) ch. 338 and Nesbitt et al. (2015) ch. 213. *Cervical vertebrae, anterior cervical vertebrae (presacral vertebrae 3-5) postzygapophyses: postzygapophyseal trough (sensu Rieppel 2001) formed by a well-developed posteriorly extending shelf (= transpostzygapophyseal lamina) ~~which~~ in some cases bears a notch on its posterior end: absent (0); present (1)* (*Fig. 23*).

This character was modified based on detailed observations of the vertebrae of *Tanystropheus* spp.

193) Modified from Pritchard et al. (2015) ch. 113. *Cervical vertebrae, neural spine base of anterior postaxial cervical vertebrae: elongate, subequal in length to the neural arch (0); shortened, spine restricted to posterior half of neural arch (1). This character is inapplicable in taxa that have completely reduced the neural spine of their anterior and mid cervicals.*

The inapplicability criterion was added.

194) New, combination of Ezcurra (2016) ch. 343 and Pritchard et al. (2015) ch. 116. *Cervical vertebrae, orientation of the anterior margin of the neural spine of anterior and middle postaxial cervical vertebrae: straight or posterodorsally inclined (0); anterodorsally inclined at an angle of more than 60 degrees from the horizontal plane (1); anterodorsally inclined at an angle of less than 60 degrees from the horizontal plane (2) (Ezcurra 2016: Figs. 30 and 33), ORDERED. This character is inapplicable in taxa that have completely reduced the neural spine of their anterior and mid cervicals.*

The notch referred to by character 115 in Pritchard et al. (2015) was reinterpreted as an anterior overhang or inclination by character 343 in Ezcurra (2016). Here, this inclination is considered to represent a similar morphology as the inclination described by character 116 of Pritchard et al. (2015), and therefore these characters were fused here. The degree of an anterodorsal inclination of the anterior margin of the neural spine in the anterior to middle postaxial cervical vertebrae is strongly variable among the sampled taxa, and therefore we distinguish between two clearly demarcated states. State 1 represents an intermediate morphology between states 0 and 2, and the character was therefore ordered. This character is scored as ? for *Tanystropheus hydroides*, *Tanystropheus longobardicus*, and *Tanystropheus "conspicuus"*. In these taxa the anterior margin of the neural spine is complex as it is bifurcated and therefore does not alow for a confident scoring of this character (see fig. 57 of Nosotti 2007).

195) Modified from Ezcurra (2016) ch. 324. *Cervical vertebrae, total number: six or fewer (0); between seven and 10 (1); between 11 and 13 (2); more than 13 (3), ORDERED.*

The states were modified based on the distribution of the number of cervical vertebrae in the sampled taxa.

196) New. *Cervical vertebrae, presence of a foramen on the ventral surface of the centrum around the anteroposterior midpoint: absent (0); present (1)* (*Fig. 24*).

A conspicuous nutrient foramen (foramina venae vertebralis sensu Wild 1973) is present on the ventral surface of several cervical vertebrae of *Tanystropheus "conspicuus"* (e.g. U-MO BT 740) and *Gephyrosaurus bridensis* (Evans 1981). This foramen is absent in other taxa for which this character could be assessed.

197) Pritchard et al. (2015) ch. 109 (reforumulated). *Cervical vertebrae, anterior to mid postaxial cervical vertebrae, shape of ventral surface in the coronal plane excluding keel: rounded or curved (0); ventral face flattened (1).*

198) New. *Cervical vertebrae, neural canal of anterior to mid cervical vertebrae separated from vertebral centrum (0); neural canal enters into a cavity of the vertebral centrum (1) (Spiekman et al. subm.: Fig. 29).*

In the tanystropheids *Macrocnemus bassanii*, *Tanytrachelos ahynis*, and *Tanystropheus* spp. the neural canal of the anterior to mid cervical vertebrae enters the vertebral centrum. This morphology was first described for *Tanystropheus "conspicuus"* by Edinger (1924) and has recently been identified for several other tanystropheids through micro computed tomography. Although this character has so far not be examined for most taxa, it might represent a widespread feature among tanystropheids.

199) Ezcurra (2016) ch. 349 (state 2 reformulated). *Cervical ribs, shape: short, being less than two times the length of its respective vertebra, and tapering at a high angle to the neck (0); short, being less than two times the length of its respective vertebra, and shaft parallel to the neck (1); very long, at least some ribs being more than two times the length of its respective vertebra, and parallel to the neck (2) (Nesbitt 2011: Figs. 28 and 30)* (*Fig. 25*).

200) Modified from Ezcurra (2016) ch. 350 and Pritchard et al. (2015) ch. 105. *Cervical ribs, anterior free-ending process (=accessory process) on anterior surface of anterior cervical ribs: absent (0); present and short, not reaching anterior to the prezygapophyses of the corresponding vertebra when in articulation (1); present and long, extending anterior to the prezygapophyses of the corresponding vertebra when in articulation (2) (Ezcurra 2016: Fig. 30)* (*Fig. 25*)*, ORDERED.*

The anterior free-ending process of the cervical ribs in certain tanystropheids (*Sclerostropheus fossai*, MCSNB 4035; *Tanytrachelos ahynis*, VMNH 120346a; *Pectodens zhenyuensis*, IVPP V18578; *Dinocephalosaurus orientalis*, Rieppel et al. 2008) and *Czatkowiella harae* (ZPAL RV/937) is particularly elongate and extends distinctly anterior to the corresponding vertebra. This represents a clearly separate morphology from the shorter processes seen in most archosauromorphs, and therefore treated as a new, separate character state. The short processes are considered an intermediate morphology in a transformational series between the absence of the process and the elongate processes, and therefore the character is ordered.

201) Modified from Ezcurra (2016) ch. 320. *Presacral vertebrae, mammillary processes (sensu Ezcurra & Butler 2015b) occurring in the posterior cervical to mid-dorsal vertebrae: absent (0); present (1) (Ezcurra 2016: Figs. 31, 32 and 34).*

We follow the description of Ezcurra & Butler (2015b) for our identification of mammillary processes. Therefore we differentiate mammillary processes from a transverse expansion of the neural spine (=spine table) by the presence of a longitudinal cleft between the process and the spine in the former, which results in a neural spine with three separate projections on its distal end rather than a single flattened surface, as in the latter. The presence of mammillary processes are considered to preclude the possibility of a distally expanded neural spine in the anterior to mid-dorsal vertebrae, since an expansion is already formed by the mammillary processes. This character should only be scored in skeletally mature specimens, since mammillary processes are generally not yet developed in early ontogenetic stages.

202) New. *Dorsal vertebrae, shape of distal margin of anterior to middle dorsal neural spines in lateral view: slightly convex in lateral view (0); completely straight along anteroposterior length in lateral view (1). This character is inapplicable in taxa that possess mammillary processes* (*Fig. 26*).

As in the cervical vertebrae, the anterior to mid dorsal vertebrae of certain taxa bears a straight dorsal margin of the neural spine. This character is scored separately from character 179 because several of the sampled taxa exhibit clear variation in the presence of the dorsal expansion of the neural spine between the dorsal and cervical vertebrae.

203) New, combining Ezcurra (2016) ch. 320 and 321, and Pritchard et al. (2015) ch. 125. *Dorsal vertebrae, distal expansion of the dorsal neural spines (not mammillary process) of the anterior to mid dorsal vertebrae: absent (0); present, gradual transverse expansion of the distal half of the neural spine (1); present, but transverse expansion is restricted to the distal end of the neural spine (= spine table) (2) (Fig. 26). This character is inapplicable in taxa that bear mammillary processes on their dorsal vertebrae.*

This character describes the same morphology as is described for the cervical vertebrae in character 180. The occurrence of the expansion in the cervical and dorsal vertebrae is split into two different characters for the same arguments as character 202. This character should only be scored in skeletally mature specimens, since a transverse expansion of the neural spine is generally absent in early ontogenetic stages.

204) Modified from Senter (2004), ch. 42. *Dorsal vertebrae, total number of dorsal vertebrae: ≤24 (0); ≥25 (1).*

The states of this character were modified to distinguish between the very high number of dorsal vertebrae seen in *Dinocephalosaurus orientalis* (Rieppel et al. 2008) and the 13 to 20 dorsal vertebrae seen in other taxa. No other states are incorporated because the exact number of dorsal vertebrae is hard to establish in many of the sampled taxa.

205) Modified from Ezcurra (2016) ch. 352. *Dorsal vertebrae, length versus height of the centrum (excluding neural arch and spine) at mid-length in posterior dorsals: 0.66-1.39 (0); 1.48-1.86 (1); 1.95-2.17 (2); 2.35-3.30 (3), ORDERED RATIO.*

The formulation of the character and the ratios were slightly modified.

206) Modified from Ezcurra (2016), ch. 354. *Dorsal vertebrae, lateral fossa on the centrum below the neurocentral suture: absent (0); present (1) (Ezcurra 2016: Figs. 31 and 34).*

States 1 and 2 of character 254 in Ezcurra (2016) were combined because this distinction was somewhat ambiguous and uninformative for the sampled taxa.

207) Modified from Nesbitt (2011) ch. 199. *Dorsal vertebrae, development of the transverse process in middle dorsals: short, projecting only slightly beyond the lateral surface of the neural arch (0); long (1) (Ezcurra 2016: Fig. 32).*

This character was modified based on the observed morphologies in the sampled taxa.

208) Ezcurra (2016), ch. 359. *Dorsal vertebrae, hyposphene-hypantrum accessory intervertebral articulation in middle-posterior dorsals: absent (0); present (1) (Ezcurra 2016: Figs. 31 and 32).*

209) Ezcurra (2016) ch. 361. *Dorsal vertebrae, dorsally opening pit lateral to the base of the neural spine: absent (0); shallow (fossa) (1); developed as a deep pit (2) ORDERED (Ezcurra 2016: Fig. 34).*

210) Ezcurra (2016) ch. 363. *Dorsal vertebrae, fan-shaped neural spine in lateral view: absent (0); present (1).*

211) Modified from Pritchard et al. (2015) ch. 129. *Dorsal vertebrae, height of neural spines in mid-dorsals: tall, greater in dorsoventral height than anteroposterior length (0); long and low, approximately similar in dorsoventral height and anteroposterior length or less in height than in length (1).*

We modified the character so that it only applies to mid-dorsal vertebrae, because anterior dorsal vertebrae often have a different morphology from more posterior vertebrae, and their inclusion therefore might result in inconsistent character scoring.

212) Pritchard et al. (2015) ch. 121. *Dorsal vertebrae, position of parapophysis (or ventral margin of dorsal synapophysis) in posterior dorsals: positioned partially on lateral margin of centrum (0); positioned entirely on neural arch (1).*

213) Pritchard et al. (2015) ch. 122 (reformulated). *Dorsal ribs, proximal end of anterior dorsal ribs: holocephalous (one facet) (0); dichocephalous (two facets) (1); tricephalous (three facets) (2).*

214) Modified from Ezcurra (2016) ch. 368. *Dorsal ribs, proximal end of middle dorsal ribs: dichocephalous (0); holocephalous (1). This character is inapplicable in taxa that have holocephalous anterior dorsal ribs, since these imply the presence of holocephalous middle dorsal ribs.*

The inapplicability criterion has been added.

215) Ezcurra (2016) ch. 372 and Nesbitt et al. (2015) ch. 216. *Sacral ribs, anteroposterior length of the first primordial sacral rib versus the second primordial sacral rib in dorsal view: primordial sacral rib one is longer anteroposteriorly than primordial sacral rib two (0); primordial sacral rib two is about the same length or longer anteroposteriorly than primordial sacral rib one (1).*

216) Ezcurra (2016) ch. 373 and Pritchard et al. (2015) ch. 131. *Sacral ribs, second rib shape: single unit (0); bifurcates distally into anterior and posterior processes (1) (Ezcurra 2016: Fig. 35).*

217) Ezcurra (2016) ch. 374 and Pritchard et al. (2015) ch. 132. *Sacral ribs, morphology of posterior process: pointed bluntly (0); pointed sharply (1). This character is inapplicable in taxa without a bifurcated second sacral rib (Ezcurra 2016: Fig. 35). This character is inapplicable in taxa without bifurcating sacral ribs.*

218) Ezcurra (2016) ch. 375 (reformulated). *Sacral and caudal vertebrae, transverse processes/ribs of sacral and anterior caudal vertebrae in skeletally mature individuals: rib/transverse process and vertebra unfused (0); rib/transverse process and vertebra fused to each other (1) (Ezcurra 2016: Fig. 35).*

219) Modified from Ezcurra (2016) ch. 377. *Caudal vertebrae, length of the transverse process + rib versus length across zygapophyses in anterior caudal vertebrae (third to fifth caudal): 0.62-1.30 (0); 1.60-2.00 (1); 2.20-2.72 (2) ORDERED RATIO (Ezcurra 2016: Fig. 35).*

We specified on which caudal vertebrae this character should be scored and modified the ratios based on the findings in the sampled taxa.

220) Modified from Dilkes (1998) ch. 88. *Caudal vertebrae, height versus maximum anteroposterior length of proximal caudal neural spine (measured in one of the first five caudals): 0.50-0.83 (0); 0.90-1.05 (1); 1.12-1.70 (2); 2.00-2.50 (3), ORDERED RATIO.*

Character states were defined after comparison of all the different measured ratios.

221) Modified from Pritchard et al. (2015) ch. 134. *Caudal vertebrae, orientation of transverse processes: base of process perpendicular to the long axis of the vertebra or slightly posterolaterally angled (0); processes distinctly angled posterolaterally from base (1).*

The states were modified to represent a clearer morphological distinction between them based on the sampled taxa.

222) Modified from Dilkes (1998) ch. 141. *Chevrons, curvature of haemal spines in mid-caudal vertebrae. No curvature or posterior curvature (0); anterior curvature present (1).*

The states were modified to represent a clearer morphological distinction between them based on the sampled taxa.

223) Modified from Pritchard et al. (2015) ch. 136. *Chevrons, shape of haemal spine: tapers along its anteroposterior length (0); maintains breadth along its length (1); gradually broadens distally (2); broadens abruptly distally, forming an inverted T shape (3).*

This character was modified based on the observed morphologies in the sampled taxa.

224) New. *Chevrons, anteroposterior length of vertebral centrum versus proximodistal length of corresponding haemal spine in anterior caudals (third to fifth caudal): 0.30-0.55 (0); 0.65-1.10 (1)* (*Fig. 27*).

The relative length of the chevrons in the anterior caudal vertebrae differs among the sampled taxa and is possibly phylogenetically informative and it was therefore included as a character here.

225) Pritchard et al. (2015) ch. 200. *Heterotopic ossifications: absent in a minimum of 5 individuals (0); present (1) (Fig. 28).*

See the character description of character 200 in Pritchard et al. (2015).

226) Ezcurra (2016) ch. 384. *Scapulocoracoid, both bones fuse with each other in skeletally mature individuals: present (0); absent (1) (Ezcurra 2016: Fig. 36).*

227) New, combination of ch. 385 and 388 of Ezcurra (2016) *Scapulocoracoid, the anterior margin at the level of the suture between both bones: roughly continuous margin (0); distinct notch present (1); large fenestra between scapula and coracoid (scapulocoracoidal fenestra) present (2) (Ezcurra 2016: Fig. 36) (Fig. 29).*

Characters 385 and 388 in Ezcurra (2016) are fused because both refer to the anterior margin of the scapulocoracoid and the presence of state 1 precludes the possibility of state 2, and vice versa. However, because it is not clear whether the notch and the fenestra represent transitional morphologies of the same structure, the character is not ordered.

228) Modified from Pritchard et al. (2015) ch. 145 and Ezcurra (2016) ch. 389. *Scapula, scapular blade, dorsally or posterodorsally orientated blade with a rectangular outline (0); blade is largely posteriorly directed and semi-circular in outline with a continuously curved anterior/dorsal margin (1) (Fig. 29)***.**

The semi-circular or semi-lunar shape of the scapula in tanystropheids represents a unique morphology among archosauromorphs and has been previously incorporated in phylogenetic analyses. We have redescribed this character to more specifically address this morphology as it is observed in a wide sample of tanystropheids.

229) Modified from Ezcurra (2016) ch. 390 and Nesbitt et al. (2015) ch. 219. *Scapula, anterior margin of the scapular blade in lateral view, excluding the margin of a potentially present scapulocoracoidal fenestra: straight or convex along entire length (0); distinctly concave (1) (Ezcurra 2016: Fig. 36). This character is inapplicable in taxa that have a semicircular scapular blade.*

This character was modified to prevent it from being interdependent with characters 227 and 228.

230) Modified from Ezcurra (2016) ch. 391 and Nesbitt et al. (2015) ch. 220 *Scapula, constriction distal to the glenoid: minimum anteroposterior length greater than half the proximodistal length of the scapula (0); minimum anteroposterior length less than half but more than a quarter of the proximodistal*

length of the scapula (1); minimum anteroposterior length less than a quarter of the proximodistal length of the scapula (2) (Ezcurra 2016: Figs. 36 and 37), ORDERED. This character is inapplicable in taxa that have a semi-circular scapular blade.

This character was modified based on the observed morphologies in the sampled taxa. The inapplicability criterion was added because a semi-circular shape of the scapular blade implies that it is comparatively much wider than the other morphologies. Thus, scoring those scapulae for this character would always result in state 0, thus representing an overscoring of the semi-circular shaped scapular blade.

231) Ezcurra (2016) ch. 392. *Scapula, supraglenoid foramen: absent (0); present (1).*

232) Ezcurra (2016) ch. 398 (state 2 reformulated). *Coracoid, posterior border in lateral view: unexpanded posteriorly (0); moderately expanded posteriorly (1); strongly expanded posteriorly - the entire border, not only the posteroventral region as is the case in the postglenoid process - and, as a result, the articulated scapula and coracoid are L-shaped in lateral view (in taxa in which the scapular blade is not semi-circular in shape) (2) ORDERED (Ezcurra 2016: Fig. 37).*

233) Ezcurra (2016) ch. 404 and Pritchard et al. (2015) ch. 140. *Cleithrum: present (0); absent (1).*

234) Ezcurra (2016) ch. 405. *Interclavicle: present (0); absent (1) (Ezcurra 2016: Fig. 15).*

235) Modified from Ezcurra (2016) ch. 406. *Interclavicle, long anterior process, resulting in a cross-shaped interclavicle in ventral or dorsal view: present (0); absent (1) (Ezcurra 2016: Fig. 38). This character is inapplicable in taxa that lack an ossified interclavicle.*

An inapplicability criterion was added.

236) Modified from Ezcurra (2016) ch. 407 and Pritchard et al. (2015) ch. 143. *Interclavicle, anterior margin with a median notch: absent (0); present (1) (Ezcurra 2016: Fig. 38). This character is inapplicable in taxa that lack an ossified interclavicle.*

An inapplicability criterion was added.

237) Modified from Ezcurra (2016) ch. 409 *Interclavicle, webbed between lateral and posterior processes: present, proximal half of the bone subtriangular or diamond-shaped (0); absent, sharp angles between processes (1) (Ezcurra 2016: Fig. 38). This character is inapplicable in taxa that lack an ossified interclavicle.*

An inapplicability criterion was added.

238) Modified from Ezcurra (2016) ch. 411 and Pritchard et al. (2015) ch. 144. *Interclavicle, posterior ramus: little change in width along entire length (0); gradual transverse expansion present (1) (Ezcurra 2016: Fig. 38). This character is inapplicable in taxa that lack an ossified interclavicle.*

An inapplicability criterion was added.

239) New. *Limbs, flipper-like, indicated by the presence of ~~a~~ rod-like ~~shape of the~~ stylopodial and zygapodial elements, ~~a~~ simple disc-like ~~shape of the~~ tarsal and carpal bones, and hyperphalangy: absent (0); present (1).*

In *Dinocephalosaurus orientalis* (Rieppel et al. 2008) the limbs have been modified to function as flippers for aquatic propulsion. The presence of at least one more *Dinocephalosaurus*-like taxon indicates that more non-archosauriform archosauromorphs might have had flippers (Li et al. 2017b).

240) New. *Long bone histology, fibrolamellar bone tissue in the cortex: absent (0); present (1).*

Early archosauromorphs exhibit considerable variation in their bone tissue (e.g. Botha-Brink & Smith 2011; Cubo & Jalil 2019; Jaquier & Scheyer 2017; Werning & Irmis 2010). The presence of fibrolamellar bone tissue can contain a strong phylogenetic signal, as it has important implications for growth rates and metabolism. Therefore, this character has been included in a phylogenetic context here for the first time.

241) Ezcurra (2016) ch. 415. *Humerus, torsion between proximal and distal ends: approximately 45 degrees or more (0); 35 degrees or less (1) (Ezcurra 2016: Fig. 39).*

242) Modified from Ezcurra (2016) ch. 416. *Humerus, transverse width of the proximal end versus total length of the bone in skeletally mature individuals: 0.10-0.41 (0); 0.44-0.70 (1) (Ezcurra 2016: Fig. 39).*

State 0 was slightly modified to fit the observed morphologies in the sampled taxa.

243) Ezcurra (2016) ch. 420. *Humerus, conical process on the proximal surface, placed immediately adjacent to the base of the deltopectoral crest: absent (0); present (1) (Ezcurra 2016: Fig. 39).*

244) Ezcurra (2016) ch. 423. *Humerus, ventral margin of the deltopectoral crest developed as a thick subcilindrical tuberosity that is well-differentiated from the thinner dorsal margin: present (0); absent (1) (Ezcurra 2016: Fig. 39).*

245) Ezcurra (2016) ch. 425. *Humerus, entepicondyle size in skeletally mature individuals: moderately large (0); strongly developed (1) (Ezcurra 2016: Fig. 39).*

246) Ezcurra (2016) ch. 426 and Pritchard et al. (2015) ch. 153. *Humerus, entepicondylar foramen: present (0); absent (1) (Ezcurra 2016: Fig. 39).*

247) Ezcurra (2016) ch. 427. *Humerus, ectepicondylar region: foramen present (0); foramen absent, supinator process and groove present (1); supinator process, groove or foramen absent (2) (Ezcurra 2016: Fig. 39).*

248) Modified from Ezcurra (2016) ch. 414. *Humerus, total length of the humerus versus the total length of the femur: 0.65-0.85 (0); 0.90-1.05 (1), RATIO.*

This character is modified to compare the total length of the humerus to the femur rather than the entire forelimb to the entire hindlimb.

249) Pritchard et al. (2015) ch. 157 and Ezcurra (2016) ch. 430 (reformulated). *Ulna, olecranon process: absent, not ossified or very low in skeletally mature individuals (0); present (1) (Ezcurra 2016: Fig. 40).*

250) Ezcurra (2016) ch. 433. *Ulna, lateral tuber (=radius tuber) on the proximal portion: absent in skeletally mature individuals (0); present (1) (Nesbitt 2011: Figs. 40 and 31).*

251) Modified from Ezcurra (2016) ch. 435. *Radius, total length versus total length of the humerus: 0.50-0.72 (0); 0.81-0.92 (1); 1.00-1.10 (2), ORDERED RATIO (Ezcurra 2016: Fig. 15).*

Character states were defined after comparison of all the different measured ratios.

252) Ezcurra (2016) ch. 440 and Pritchard et al. (2015) ch. 161. *Carpals, perforating foramen between intermedium and ulnare: present (0); absent in skeletally mature individuals (1). This character is inapplicable in taxa that lack an intermedium.*

253) New, combination of ch. 441 and 442 of Ezcurra (2016). *Centrale of the manus of skeletally mature individuals: both the lateral and medial centrale are present (0); only the lateral centrale is present (1); only the medial centrale is present (2); both are absent (3).*

254) Ezcurra (2016) ch. 443. *Carpals, pisiform: present (0); absent in skeletally mature individuals (1) (Ezcurra 2016: Fig. 40).*

255) Benton & Allen (1997) ch. 31 and Jalil (1997) ch. 46 *First distal carpal: present (0); absent in skeletally mature individuals (1).*

256) Ezcurra (2016) ch. 444 and Pritchard et al. (2015) ch 159. *Carpals, distal carpal five: absent in skeletally mature individuals (0); present (1) (Ezcurra 2016: Fig. 40).*

257) Ezcurra (2016) ch 445. *Manus, longest metacarpal + digit: longer than humeral length (0); subequal to shorter than humeral length (1).*

258) Modified from Ezcurra (2016) ch. 446 *Metacarpus, length of the longest metacarpal versus length of the longest metatarsal: 0.30-0.41 (0); 0.46-0.65 (1), RATIO.*

Character states were defined after comparison of all the different measured ratios.

259) Modified from Ezcurra (2016) ch. 448. *Metacarpus, width of the distal end of the metacarpal I versus its total length: 0.25-0.33 (0); 0.38-0.50 (1); 0.56-0.67 (2), ORDERED RATIO (Ezcurra 2016: Fig. 40).*

Character states were defined after comparison of all the different measured ratios.

260) Ezcurra (2016) ch. 450. *Metacarpus, metacarpal IV: longer than metacarpal III (0); equal or shorter than metacarpal III (1) (Ezcurra 2016: Fig. 40).*

261) Ezcurra (2016) ch. 453 *Manual digits, second phalanx of manual digit II: shorter than the first phalanx of manual digit II (0); longer than the first phalanx of manual digit II (1) (Nesbitt 2011: Fig. 32).*

262) Modified from Ezcurra (2016) ch. 451 and Nesbitt et al. (2015) ch. 222. *Manual digits, unguals length: about the same length or shorter than the last non-ungual phalanx of the same digit (0); distinctly longer than the last non-ungual phalanx of the same digit (1). This character is inapplicable in taxa in which the terminal phalanx of each digit does not form an ungual.*

An inapplicability criterion was added because in the aquatic *Dinocephalosaurus orientalis* no ungual is formed by the terminal phalanges.

263) Modified from Ezcurra (2016) ch. 454. *Manual digits, number of phalanges in digit IV: five (0); four (1) (Nesbitt 2011: Fig. 32).*

State 2 of character 454 in Ezcurra (2016) was removed because it was irrelevant for the sampled taxa.

264) Modified from Ezcurra (2016) ch 460. *Ilium, preacetabular process: absent or incipient (0); present, being considerably anteroposteriorly shorter than its dorsoventral height (1); present, being longer than two thirds of its height (2), ORDERED.*

States 2 and 3 of character 460 in Ezcurra (2016) were fused and redescribed to address the specific morphology observed in the sampled taxa.

265) Modified from Sookias (2016) ch. 268. *Ilium, shape of preacetabular process: rounded (0); approximately straight-sided with a distinct angle between the anterior and dorsal margins (1). This character is inapplicable in taxa that lack a preacetabular process on the ilium.*

States 1 and 2 were fused and state 3 was removed of the original character of Sookias (2016) to specifically address the observed morphologies in the sampled taxa.

266) Modified from Pritchard et al. (2015) ch. 170 and Ezcurra (2016) ch. 461. *Ilium, anterior process/tuber on the anterior margin of the ilium: anterior process/tuber absent or incipient (0); clearly defined anteriorly projecting tuber on the anterior margin of the preacetabular process (1). This character is inapplicable in taxa that lack a preacetabular process on the ilium (Fig. 30).*

Pritchard et al. (2015) indicated the presence of a small tuber on the anterior margin of the iliac blade in certain tanystropheids to represent the same structure as the preacetabular process, which was incorporated into their character 170. This character interpreted the presence of an anteriorly expanded preacetabular process to represent a more strongly exhibited version of this tuber. However, we consider this tuber to represent a separate structure on the preacetabular process, since this tuber occurs in certain taxa that also have a smooth, anterodorsally curved preacetabular process. The presence of a small finger-like tuber on the anterior margin of the preacetabular process is subject to intraspecific variation and occurs in *Tanystropheus longobardicus* (PIMUZ T 1277), a juvenile specimen of *Macrocnemus bassanii* (MSNM BES SC 111), and *Fuyuansaurus acutirostris* (IVPP V17983) among the sampled taxa and it is considered to represent an informative character independent of the size of the preacetabular process. This tuber is very similar to that seen in “*Exilisuchus tubercularis*” (Ochev 1979; Fig. 9 of Ezcurra 2016).

267) Modified from Ezcurra (2016) ch. 463. *Ilium, length of the postacetabular process measured from the most proximal point on the posterior/ventral margin of the process versus anteroposterior length of the acetabulum: 0.40-0.71 (0); 0.88-1.32 (1); 1.43-1.80 (2), ORDERED RATIO (Ezcurra 2016: Fig. 41).*

The measurement of the length of the postacetabular process was specified and character states were defined after comparison of all the different measured ratios.

268) Ezcurra (2016) ch. 464 and Pritchard et al. (2015) ch. 164. *Ilium, main axis of the postacetabular process in lateral or medial view: posterodorsally orientated (0); mainly posteriorly orientated (1) (Ezcurra 2016: Figs. 9 and 41).*

269) Modified from Ezcurra (2016) ch. 465. *Ilium, caudifemoralis brevis muscle origin on the lateroventral surface of the postacetabular process: not dorsally or laterally rimed by a brevis shelf (0); dorsally rimed by a low brevis shelf (1) (Ezcurra 2016: Fig. 9).*

State 0 of character 465 in Ezcurra (2016) has been removed because it is irrelevant to the sampled taxa.

270) Pritchard et al. (2015) ch. 166. *Ilium, supra-acetabular crest: crest absent, anterodorsal margin of acetabulum similar in development to posterodorsal margin (0); prominent anterodorsal lamina frames the anterodorsal margin of the acetabulum (1).*

271) Pritchard et al. (2015) ch. 167 *Ilium, shape of supra-acetabular margin: dorsalmost margin of acetabulum is unsculptured (0); prominent, bulbous rugosity superior to acetabulum (1). This character is inapplicable in taxa that lack a distinct supra-acetabular crest.*

272) Pritchard et al. (2015) ch. 165 *Ilium, anteroventral process extending from anterior margin of pubic peduncle: absent (0); present, process draping across anterior surface of pubis (1).*

273) Ezcurra (2016) ch. 471 and Pritchard et al. (2015) ch. 163. *Pubis-ischium, thyroid fenestra: absent (0); present (1) (Ezcurra 2016: Fig. 41).*

274) Pritchard et al. (2015) ch. 175 *Pubis, lateral surface, development of a lateral tubercle (sensu Vaughn 1955): present (0); absent (1).*

275) Ezcurra (2016) ch. 477. *Pubis, pubic apron: absent, symphysis extended along the ventral margin of the pelvic girdle and visible in lateral view (0); present, symphysis restricted anteriorly and obscured by the pubic shaft in lateral view (1) (Ezcurra 2016: Fig. 41).*

This character is discussed on page 61 and figured in Fig. 58 of Nesbitt et al. (2015).

276) Modified from Ezcurra (2016) ch. 482 and Nesbitt et al. (2015) ch. 225. *Ischium, maximal length versus anteroposterior length of the acetabulum: 1.47-2.23 (0); 2.51-2.90 (1). RATIO*

Character states were defined after comparison of all the different measured ratios.

277) Ezcurra (2016) ch. 486. *Ischium, symphysis raised on a distinct low peduncle: absent (0); present (1) (Ezcurra 2016: Fig. 41).*

This character is discussed on page 62 Nesbitt et al. (2015).

278) Modified from Pritchard et al. (2015) ch. 176 and Ezcurra (2016) ch. 488. *Ischium, distinct concavity or constriction on the posterior half of the ventral margin of the ischium, thus separating a distinct posterior process from the rest of the ischium: absent (0); present (1) (Ezcurra 2016: Fig. 41) (Fig. 30).*

This character was discussed by Pritchard et al. (2015)~~, in which this character~~ was considered homologous to the spina ischia described by El-Toubi (1949). We reformulate the character based on our observations of the ischia in the sampled taxa. A posterior process of the ischium is formed by a distinct concavity or constriction of the ventral margin of the ischium in *Planocephalosaurus robinsonae*, *Pectodens zhenyuensis*, and *Langobardisaurus pandolfii*. Furthermore, this trait is also present in some, but not all, specimens of *Macrocnemus bassani*, *Macrocnemus fuyuanensis*, *Tanystropheus longobardicus*, and *Amotosaurus rotfeldensis*. Therefore, this character clearly shows a large amount of intraspecific variability.

279) Ezcurra (2016) ch. 491. *Femur, proximal articular surface in skeletally mature individuals: well-ossified, being flat or convex (0); partially ossified, being concave and sometimes with a circular pit (1) (Ezcurra 2016: Fig. 42).*

280) Modified from Ezcurra (2016) ch. 504. *Femur, attachment of the caudifemoralis musculature on the posterior surface of the bone: crest-like and with intertrochanteric fossa (=internal trochanter), and convergent with proximal end (0); crest-like and with intertrochanteric fossa (=internal trochanter), and not convergent with proximal end (1); crest-like and without intertrochanteric fossa (=fourth trochanter), and not convergent with proximal end (2) (Ezcurra 2016: Figs. 42 and 43). This character is inapplicable to taxa without a distinct process for the attachment of the caudifemoralis musculature on the femur.*

Character 504 in Ezcurra (2016) is ordered. We decided not to order this character here because we do not consider it clear that the states represent intermediate steps in a transformational series.

281) Ezcurra (2016) ch. 511. *Femur, distal condyles: prominent, strong dorsoventral expansion (in sprawling orientation) restricted to the distal end (0); not projecting markedly beyond shaft and expand gradually if there is any expansion (1) (Ezcurra 2016: Fig. 43).*

See description of character 318 in Nesbitt (2011).

282) Ezcurra (2016) ch. 512. *Femur, distal articular surface: uneven, lateral (=fibular) condyle projecting distally distinctly beyond medial (=tibial) condyle (0); both condyles prominent distally and approximately at same level (1); both condyles do not project distally (distal articular surface concave or almost flat) (2) (Ezcurra 2016: Figs. 42 and 43).*

283) Ezcurra (2016) ch. 513. *Femur, anterior extensor groove: absent, anterior margin of the bone straight or convex in distal view (0); present, anterior margin of the bone concave in distal view (1) (Ezcurra 2016: Fig. 42).*

284) Ezcurra (2016) ch. 515. *Femur, shape of lateral (=fibular) condyle in distal view: lateral surface is rounded and mound-like (0); lateral surface is triangular and sharply pointed (1) (Ezcurra 2016: Fig. 42).*

285) Benton & Allen (1997) ch. 39. *Femur, length of tibia relative to length of femur: tibia shorter than, or subequal to, femur in length (0); tibia longer than femur (1).*

286) Pritchard et al. (2015) ch. 177. *Femur, shape in lateral view: femoral shaft exhibits sigmoidal curvature (0); femoral shaft linear with slight ventrodistal curvature (1).*

287) Ezcurra (2016) ch. 528 *Fibula, transverse width at mid-length: subequal to transverse width of the tibia (0); distinctly narrower than transverse width of the tibia (1) (Ezcurra 2016: Fig. 15).*

288) Ezcurra (2016) ch. 531 *Fibula, distal end in lateral view: angled anterodorsally (asymmetrical) (0); rounded or flat (symmetrical) (1) (Ezcurra 2016: Fig. 44, Nesbitt 2011: Fig. 41)*.

289) Modified from Ezcurra (2016) ch. 532. *Proximal tarsals, articulation between astragalus and calcaneum: roughly flat (0); concavoconvex with concavity on the astragalus (1); fused (2) (Ezcurra 2016: Fig. 45).*

State 1 of character 532 of Ezcurra (2016) is excluded because it does not apply to the sampled taxa. This character can best be observed in plantar view. For a detailed description of the articulation between the astragalus and calcaneum, see the extensive discussion in Sereno (1991), in particular Figs. 3-4, 8 therein, and Cruickshank (1979).

290) Ezcurra (2016) ch. 539. *Astragalus, posterior groove: present (0); absent (1) (Nesbitt 2011: Fig. 46).*

This character is extensively discussed in page. 353 of Gower (1996). Due to the three-dimensional structure of the astragalus and the variation observed in its morphology in the sampled taxa, it is hard to distinguish the groove from other curves and concavities in the bone in certain taxa, since this character was originally formed to describe the astragalus of archosauriforms. Taxa are scored as 0 when a clear concavity is present on the ventral/plantar surface of the astragalus, often connecting to the perforating foramen between the astragalus and calcaneum.

291) Pritchard et al. (2015) ch. 184 (reformulated) and part of Ezcurra (2016) ch. 557. *Distal tarsals, pedal centrale: present (0); absent as a separate ~~ossification, being either unossified or fused to the astragulus in skeletally mature individuals~~ (1) (Ezcurra 2016: Figs. 45 and 46).*

292) New, combination of Ezcurra (2016) ch. 558, same as Pritchard et al. (2015) ch. 193, and Ezcurra (2016) ch. 559, same as Pritchard et al. (2015) ch. 194. *Distal tarsals of skeletally mature individuals, distal tarsal 1 and 2: both present (0); only one of the two elements is present (1); both absent (2), ORDERED.*

Characters 558 and 559 in Ezcurra (2016) were fused here, because in certain taxa (*Macrocnemus bassanii*, PIMUZ T 4822; *Macrocnemus fuyuanensis*, IVPP V15001; and *Amotosaurus rotfeldensis*, SMNS 54783a/b) one of the distal tarsals is present, but it cannot be established confidently whether this represents distal tarsal 1 or 2. We consider this of secondary importance, as this character treats the degree of ossification in the tarsus, and both distal tarsals ossify at roughly the same developmental stage (Rieppel 1989).

293) Ezcurra (2016) ch. 563 and Pritchard et al. (2015) ch. 195. *Distal tarsals, distal tarsal 5: present (0); absent in skeletally mature individuals (1).*

294) Modified from Ezcurra (2016) ch. 564. *Pes, foot length (articulated fourth metatarsal and digit) versus tibia-fibula length: 0.60-1.00 (0); 1.02-1.60 (1); 2.00-2.50 (2) (Ezcurra 2016: Fig. 15), ORDERED RATIO.*

Character states were defined after comparison of all the different measured ratios.

295) Ezcurra (2016) ch. 533 and Pritchard et al. (2015) ch. 186. *Proximal tarsals, foramen for the passage of the perforating artery between the astragalus and calcaneum (=perforating foramen): present (0); absent in skeletally mature individuals (1) (Ezcurra 2016: Fig. 45).*

296) Ezcurra (2016) ch. 565. *Metatarsus, configuration: metatarsals diverging from ankle (0); compact, metatarsals I-IV tightly bunched (1) (Ezcurra 2016: Fig. 46).*

297) Modified from Ezcurra (2016) ch. 569. *Metatarsus, length of metatarsal I versus metatarsal III: 0.30-0.36 (0); 0.42-0.51 (1); 0.54-0.83 (2), ORDERED RATIO (Ezcurra 2016: Fig. 46).*

Character states were defined after comparison of all the different measured ratios.

298) Modified from Ezcurra (2016) ch. 571. *Metatarsus, length of the metatarsal II versus length of the metatarsal IV: 0.52-0.67 (0); 0.70-0.91 (1); 0.94-1.07 (2), ORDERED RATIO (Ezcurra 2016: Fig. 46).*

Character states were defined after comparison of all the different measured ratios.

299) Modified from Ezcurra (2016) ch. 574. *Metatarsus, length of metatarsal IV versus length of metatarsal III: 0.85-1.00 (0); 1.04-1.08 (1); 1.11-1.28 (2) ORDERED RATIO (Ezcurra 2016: Fig. 46).*

Character 581 in Ezcurra (2016) is not included in our analysis, because the length of the entire digit is strongly dependent on the length of the metatarsal, and these characters are therefore interdependent. It was preferred to compare the relative lengths of the metatarsals over the lengths of the entire digits because this can be scored in a wider range of the sampled taxa. Character states were defined after comparison of all the different measured ratios.

300) Modified from Ezcurra (2016) ch. 577 (reformulated). *Metatarsus, metatarsal V with a hook-shaped proximal end: absent (0); present, with a gradually medially curved proximal process (1); present, with an abruptly medially flexed proximal process and, as a result, the metatarsal acquires a L-shape in dorsal or ventral view (2) (Ezcurra 2016: Fig. 46).*

301) Ezcurra (2016) ch. 576 (reformulated). *Metatarsus, dorsal prominence separated from the proximo-medial surface by a concave gap in metatarsal V: absent (0); present (1) (Ezcurra 2016: Fig. 46, Nesbitt 2011: Fig. 47). This character is inapplicable in taxa that lack a hook-shaped metatarsal V.*

302) Ezcurra (2016) ch. 578 and Pritchard et al. (2015) ch. 196 *Metatarsus, metatarsal V outer process on the proximal lateral margin: absent, smooth curved margin (0); present, prominent pointed process (1).*

303) Ezcurra (2016) ch. 579. *Metatarsus, metatarsal V lateral plantar tubercle: absent (0); present (1) (Ezcurra 2016: Fig. 46).*

304) Ezcurra (2016) ch. 580. *Metatarsus, metatarsal V medial plantar tubercle: absent (0); present (1) (Ezcurra 2016: Fig. 46).*

305) Modified from Benton & Allen (1997) ch. 45. *Metatarsus, length of metatarsal IV versus the proximodistal length of metatarsal V: 1.25-1.65 (0); 1.90-2.85 (1); 3.16-3.65 (2); 4.00-5.15 (3), ORDERED RATIO.*

Character states were defined after comparison of all the different measured ratios.

306) Ezcurra (2016) ch. 584 and Pritchard et al. (2015) ch. 199. *Pedal digits, phalanx V-1: subequal to or shorter than other non-ungual phalanges (0); metatarsal-like, considerably longer than other non-ungual phalanges (1).*

307) Ezcurra (2016) ch 587 and Nesbitt et al. (2015) ch. 233 *Pedal digits, ventral tubercle in unguals: absent or small (0); well-developed and extended ventral to the articular portion of the ungual (1).*

Results

As mentioned above, the taxonomic status of "*Tanystropheus antiquus*" is currently uncertain and under revision (Spiekman et al. 2019; Spiekman & Scheyer 2019; Szczygielski, personal commun. 2019). Due to the taxonomic uncertainty regarding this OTU, analyses 1 and 2 were performed once with the complete sample of taxa (iteration A) and once with the complete sample of taxa except for "*Tanystropheus antiquus*" (iteration B). In analysis 1 the characters indicated as ordered were treated as such (*Fig. 31*), whereas analysis 2 treated all characters as unordered, and excluded all 23 ratio characters (*Fig. 32*). Analysis 1A found 1132 most parsimonious trees (MPTs) of 1177 steps with a consistency index (CI) of 0.352 and a retention index (RI) of 0.575 (*Fig. 31a*), and analysis 1B found 587 MPTs of 1173 steps with a CI of 0.352 and RI of 0.575 (*Fig. 31b*). The second analysis found 1646 MPTs of 974 steps with a CI of 0.375 and RI of 0.581 for analysis 2A (*Fig. 32a*), and 1996 MPTs of 971 steps with a CI of 0.376 and RI of 0.583 for analysis 2B (*Fig. 32b*). Analyses 3 and 4 are the pruned analyses, with analysis 3 including ordered characters and analysis 4 excluding ratio characters and treating all remaining characters as unordered. Analysis 3 found 11 MPTs of 1130 steps with a CI of 0.366 and RI of 0.604 (*Fig. 33*). Analysis 4 found a single MPT of 934 steps with a CI of 0.391 and RI of 0.611 (*Fig. 34*). Support values for the trees can be found in the figure captions.

Comparison of analyses 1 and 2

The base of the tree of analysis 1 is poorly resolved with a large polytomy that is formed by ~~the~~ non-saurian diapsids, excluding the outgroup *Petrolacosaurus kansensis*, and the monophyletic Archosauromorpha and Lepidosauromorpha ~~clades~~ (*Fig. 31*). Analysis 2 shows a slightly higher resolution and a polytomy is formed at the base of the tree by *Claudiosaurus germaini*, *Acerosodontosaurus piveteaui*, *Youngina capensis*, and Sauria (*Fig. 32*). *Orovenator mayorum* is the sister taxon to this polytomy. Although it is generally considered that *Orovenator mayorum* is most distantly related to Sauria of all the taxa included here except for the outgroup *Petrolacosaurus kansensis* (Ford & Benson 2020; Reisz et al. 2011a), there is no clear consensus in the relationships between *Youngina capensis*, *Claudiosaurus germaini*, and *Acerosodontosaurus piveteaui* (Bickelmann et al. 2009). Since the focus of this study is not to resolve early diapsid phylogeny, only these taxa, which are among the morphologically best-known early diapsids, were included, and the lack of resolution can possibly be attributed to the low taxonomic sample for this part of the tree. Both analyses recover a monophyletic Archosauromorpha ~~and~~ Lepidosauromorpha, ~~and the monophyletic clades~~ Rhynchosauria, Allokotosauria, and Archosauriformes ~~within Archosauromorpha~~. In both analyses 1A and 2A a huge polytomy is formed by most non-archosauriform archosauromorphs (*Figs. 31a and 32a*). In analysis 1, *Czatkowiella harae* is recovered as the sister taxon to all other archosauromorphs and *Protorosaurus speneri* as the sister taxon to all archosauromorphs except for *Czatkowiella harae* (*Fig. 31*). Both taxa are part of the large polytomy in analysis 2A (*Fig. 32a*). In analysis 1A, two clades are recovered among the OTUs generally considered to be tanystropheid. One clade comprising all three *Macrocnemus* species, which together form a polytomy, and the second clade is ~~made up~~ of **AMNH FARB 7206**, *Tanytrachelos ahynis*, and *Langobardisaurus pandolfii* as successive sister taxa. These OTUs are part of the large unresolved polytomy in analysis 2A. When "*Tanystropheus antiquus*" is excluded, the tree resolution improves distinctly, particularly in analysis 1B (*Fig. 31b*). This analysis recovers a monophyletic Tanystropheidae. The unresolved clade of the three *Macrocnemus* species forms the sister group to all other tanystropheids and the clade containing **AMNH FARB 7206**, *Tanytrachelos ahynis*, and *Langobardisaurus pandolfii* forms the sister group to a large, unresolved clade that includes the remaining tanystropheids. Analysis 2B does not recover a monophyletic Tanystropheidae, but the exclusion of "*Tanystropheus antiquus*" does result in the recovery of several additional clades (*Fig. 32b*). As in both iterations of analysis 1 **AMNH FARB 7206**, *Tanytrachelos ahynis*, and *Langobardisaurus pandolfii* form a clade, with *Langobardisaurus pandolfii* and *Tanytrachelos ahynis* as direct sister taxa. *Macrocnemus bassanii* and *Macrocnemus fuyuanensis* form a clade and an unresolved clade is formed by the four *Tanystropheus* OTUs and *Raibliania calligarisi*. In both iterations of analysis 2 and in iteration B of analysis 1, *Prolacerta broomi* is found as the sister taxon to all other crocopods within a monophyletic Crocopoda (*Figs. 31b and 32*), but in iteration A of analysis 1 *Prolacerta broomi* is found outside this clade within the larger polytomy that also includes most tanystropheids (*Fig. 31a*). This differs from other recent analyses in which *Prolacerta broomi* was found to be more closely related to Archosauriformes than both rhynchosaurs and allokotosaurs (e.g. Ezcurra 2016; Nesbitt et al. 2015; Pinheiro et al. 2019; Pritchard et al. 2018; Pritchard & Sues 2019; Pritchard et al. 2015; Spiekman 2018). Both in analyses 1 and 2, the interrelationships between the monophyletic clades Allokotosauria, Rhynchosauria, and *Teyujagua paradoxa* + Archosauriformes are unresolved. In iteration A of analysis 2 Rhynchosauria is unresolved, whereas in analysis 1 and iteration B of analysis 2 *Eohyosaurus wolvaardti* and *Howesia browni* are more closely related to each other than to *Mesosuchus browni*.

Comparison of analyses 3 and 4

The strict consensus tree of analysis 3 is largely resolved, whereas that of analysis 4 is completely resolved. Both trees are largely in agreement with each other, and recover a monophyletic Sauria, Lepidosauromorpha, Archosauromorpha, Rhynchosauria, Allokotosauria, and Archosauriformes. Nevertheless, the trees differ in several important aspects. In analysis 3 *Claudiosaurus germaini* is found as sister taxon to all other included taxa apart from *Petrolacosaurus kansensis*, and the other non-saurian diapsids form a polytomic sister clade to Sauria (*Fig. 33*). In analysis 4 *Orovenator mayorum*, *Claudiosaurus germaini*, and a clade of *Acerosodontosaurus piveteaui* and *Youngina capensis* form successive sister groups to Sauria (*Fig. 34*). In this regard, analysis 4 is in congruence with other analyses on early amniote relationships, whereas analysis 3 differs with the regards to the position of *Orovenator mayorum* (Bickelmann et al. 2009; Ford & Benson 2018; Reisz et al. 2011a). Both analyses find *Protorosaurus speneri* to be the sister taxon to all other archosauromorphs. Analysis 4 finds a monophyletic Tanystropheidae. In contrast, Analysis 3 finds two separate clades comprised of taxa that have previously been considered as tanystropheids or putative tanystropheids. One clade consists of *Jesairosaurus lehmani*, *Dinocephalosaurus orientalis*, and *Pectodens zhenyuensis* as successive sister taxa. All these taxa have previously been considered as putative tanystropheids or closely allied to the tanystropheid clade as “protorosaurs” (Ezcurra 2016; Jalil 1997; Li et al. 2017a; Rieppel et al. 2008). The second clade comprises taxa that have broadly been interpreted as tanystropheids, and additionally includes the putative tanystropheids *Fuyuansaurus acutirostris* and *Ozimek volans*. The clade comprising *Macrocnemus bassanii* and *Macrocnemus fuyuanensis* forms the sister group to the other members of this tanystropheid clade, which together form a polytomy consisting of *Fuyuansaurus acutirostris*, *Tanytrachelos ahynis*, *Langobardisaurus pandolfii*, a clade consisting of *Ozimek volans* and *Amotosaurus rotfeldensis*, and a clade consisting of *Tanystropheus longobardicus* and *Tanystropheus hydroides*. In analysis 4 the tanystropheid clade is completely resolved and formed by the following successive sister groups: *Jesairosaurus lehmani*, a clade comprising of *Dinocephalosaurus orientalis* and *Pectodens zhenyuensis*, *Fuyuansaurus acutirostris*, a clade consisting of *Macrocnemus bassanii* and *Macrocnemus fuyuanensis*, a clade consisting of *Tanytrachelos ahynis* and *Langobardisaurus rotfeldensis*, and two clades, one consisting of *Ozimek volans* and *Amotosaurus rotfeldensis*, and the other of *Tanystropheus longobardicus* and *Tanystropheus hydroides*. The topology of Crocopoda, the clade consisting of *Prolacerta broomi*, *Teyujagua paradoxa*, Allokotosauria, Rhynchosauria, and Archosauriformes is largely congruent between the two analyses. The topology of Allokotosauria, Rhynchosauria, and Archosauriformes is the same between the two analyses and in both cases *Prolacerta broomi* represents the sister taxon to all other crocopods and *Teyujagua paradoxa* is the sister taxon to Archosauriformes. The only difference is in the relative positions of Rhynchosauria and Allokotosauria. In analysis 3 Rhynchosauria is the sister group to *Teyujagua paradoxa* and Archosauriformes, whereas in analysis 4 Allokotosauria occupies this position.

Clade definitions and synapomorphies

Based on the results of analysis 4 (*Fig. 34*), which represents the most stable analysis and makes the least assumptions about character transformations (i.e. it does not order characters and excludes artificially defined ratios), the included clades can be defined as follow~~ed~~.

Unnamed clade (*Orovenator mayorum* + *Claudiosaurus germaini* + *Acerosodontosaurus piveteaui* + *Youngina capenis* + Sauria)

Unambiguous synapomorphies. There are no synapomorphies for this clade in the present analysis.

Unnamed clade (*Claudiosaurus germaini* + *Acerosodontosaurus piveteaui* + *Youngina capenis* + Sauria)

Unambiguous synapomorphies. Lacrimal contacts nasal but does not reach external naris (35-1); postfrontal with a posterior process and participates in the border of the supratemporal fenestra (58-1); parietal with a supratemporal fossa medial to the supratemporal fenestra (81-1); palatine with the anteromedial process being longer than the anterolateral process (99-1); parabasisphenoid recess ~~with~~ the ventral floor forming a shallow depression (118-1).

Unnamed clade (*Acerosodontosaurus piveteaui* + *Youngina capenis* + Sauria)

Unambiguous synapomorphies. Scapula with a distinctly concave anterior margin of the scapular blade in lateral view (229-1); minimum anteroposterior length of the scapula less than half but more than a quarter of the proximodistal length of the scapula (230-1); femur with distal condyles not projecting markedly beyond shaft (281-1); metatarsus compact, metatarsals I-IV tightly bunched (296-1).

Unnamed clade (*Acerosodontosaurus piveteaui* + *Youngina capenis*)

Unambiguous synapomorphies. Postorbital with a posterior process extending close to or beyond the level of the posterior margin of the supratemporal fenestrae (60-1); dorsal vertebrae with parapophyses positioned entirely on neural arch (212-1).

Sauria Gauthier 1984

Unambiguous synapomorphies. Postparietal absent as a separate ossification (84-2); tabular absent (86-1); quadrate, posterior margin in lateral view continuously concave (90-1); pterygoid without teeth on the lateral ramus (106-0); parabasisphenoid without an intertuberal plate (117-1); anterior surangular foramen on the lateral surface of the surangular, near surangular-dentary contact (156-1); chevrons gradually broaden distally (223-2); hook-shaped metatarsal V with a gradually medially curved proximal process (300-1).

Lepidosauromorpha Gauthier 1984

Unambiguous synapomorphies. Jugal, anterior extension of the anterior process up to or posterior to the level of mid-length of the orbit (37-1); frontals fused to one another (54-1); postorbital-squamosal contact, the anterior process of the squamosal continues along the posterior margin of the ventral process of the postorbital and contacts the jugal (64-1); supratemporal absent (73-2); quadratojugal absent or fused to the quadrate (87-0); broad palatine is the main component of the palate posteriorly to the choanae (98-1); palatine dentition relatively large, similar to those of the marginal dentition (101-1); pterygoid, teeth on the ventral surface of the anterior ramus present in three distinct fields (=T2, T3a and T3b) (102-1); parabasisphenoid recess absent (118-0); splenial absent (143-1); dentary without posterodorsal process (148-0); dentary with posterocentral process (149-1); cervical vertebrae, centrum of atlas fused to axial intercentrum (183-1); height of neural spines in mid-dorsals long and low, approximately similar in dorsoventral height and anteroposterior length or less in height than in length (211-1); primordial sacral rib two is about the same length or longer anteroposteriorly than primordial sacral rib one (215-1); caudal vertebrae, transverse processes distinctly angled posterolaterally from base (221-1); anterior curvature of haemal spines in mid-caudal vertebrae (222-1); humerus, ectepicondylar region with foramen (247-0); ilium with anteroventral process extending from anterior margin (272-1); pubis-ischium, thyroid fenestra present (273-1); proximal tarsals, astragalus and calcaneum fused (289-2); metatarsal V with a medial plantar tubercle (304-1).

Archosauromorpha Huene 1946

Unambiguous synapomorphies. Maxilla, alveolar margin in lateral view concave (25-1); postfrontal without a posterior process and postfrontal does not participate in the border of the supratemporal fenestra (58-0); parietal, supratemporal fossae strongly expanded medially and only separated by a ridge running along the midline of the parietal, the sagittal crest (83-2); suture between the surangular and angular anteroposteriorly convex ventrally along the anterior half of the bones in lateral view (158-0); articular, retroarticular process upturned (163-1); diapophysis and parapophysis of anterior to middle cervical postaxial vertebrae situated on different processes and nearly touching (188-2); long transverse processes in middle ~~dorsals~~ (207-1); coracoid, posterior border in lateral view moderately expanded posteriorly (232-1); interclavicle webbed between lateral and posterior processes (237-0); humerus, torsion between proximal and distal ends 35 degrees or less (241-1); humerus with entepicondylar foramen (246-0).

Unnamed clade (*Jesairosaurus* + Dinocephalosauridae + Tanystropheidae + Crocopoda)

Unambiguous synapomorphies. Premaxilla, acute or right angle between the alveolar margin and the anterior margin of the premaxillary body in lateral view (6-0); postnarial process of premaxilla well-developed and forms most of the ventral border of the external naris but process does not contact prefrontal (9-2); subnarial foramen present between premaxilla and maxilla (16-1); the dorsal apex of the maxilla ends abruptly and its posterior margin is concave (20-1); ribs of second sacral vertebra bifurcate distally into anterior and posterior processes (216-1); scapula without supraglenoid foramen (231-0); anterior margin of interclavicle with a median notch (236-1); metatarsal V without outer process on the proximal lateral margin (302-0).

Unnamed clade (*Jesairosaurus lehmani* + Dinocephalosauridae +Tanystropheidae)

Definition. All taxa more closely related to *Tanystropheus longobardicus* Bassani 1886 and *Dinocephalosaurus orientalis* Li 2003 than to *Protorosaurus speneri* Meyer 1832, *Mesosuchus browni* Watson 1912, or *Pamelaria dolichotrachela* Sen 2003.

Temporal range. Early Triassic (latest Olenekian, *Augustaburiania vatagini*, but likely Induan to early Olenekian; De Oliveira et al. 2018) to late Late Triassic (late Norian, *Sclerostropheus fossai*).

Unambiguous synapomorphies. Pterygoid, lateral/distal end of the posterior margin of the lateral ramus curved posteriorly (109-1); height of neural spines in mid-dorsals tall, greater in dorsoventral height than anteroposterior length (211-1); parapophysis (or ventral margin of dorsal synapophysis) in posterior ~~dorsals~~ positioned entirely on neural arch (212-1); primordial sacral rib two is about the same length or longer anteroposteriorly than primordial sacral rib one (215-1); ilium, preacetabular process approximately straight-sided with a distinct angle between the anterior and dorsal margins (268-1).

Unnamed clade (Dinocephalosauridae + Tanystropheidae)

Unambiguous synapomorphies. Premaxilla without plate-like palatal shelf or process on the medial surface (11-0); maximum height of postaxial anterior or middle cervical neural spines considerably shorter than the posterior articular surface of the centrum (178-2); postaxial cervicals with epipophyses (190-1); between 11 and 13 cervical vertebrae (195-2); scapular blade is largely posteriorly directed and semi-circular in outline with a continuously curved anterior/dorsal margin (228-1); distinct concavity or constriction on the posterior half of the ventral margin of the ischium, thus separating a distinct posterior process from the rest of the ischium (278-1).

Dinocephalosauridae new clade

Definition. All taxa more closely related to *Dinocephalosaurus orientalis* Li 2003 and *Pectodens zhenyuensis* Li, Fraser, Rieppel, Zhao & Wang 2017 than to *Macrocnemus bassanii* Nopsca 1930 or *Tanystropheus longobardicus* Bassani 1886.

Temporal range. Anisian (Middle Triassic)

Unambiguous synapomorphies. Jugal without a posterior process (42-1); glenoid fossa of the articular considerably ventrally displaced compared to the tooth row (161-1); anterior free-ending process on anterior surface of anterior cervical ribs long, extending anterior to the prezygapophyses of the corresponding vertebra when in articulation (200-2); metatarsal V without a hook-shaped proximal end (300-0).

Tanystropheidae Camp 1945

Definition. All taxa more closely related to *Macrocnemus bassanii* Nopsca 1930 and *Tanystropheus longobardicus* Bassani 1886 than to *Dinocephalosaurus orientalis* Li 2003 or *Pectodens zhenyuensis* Li, Fraser, Rieppel, Zhao & Wang 2017.

Temporal range. Early Triassic (latest Olenekian, *Augustaburiania vatagini*, but possibly Induan to early Olenekian; De Oliveira et al. 2018) to late Late Triassic (late Norian, *Sclerostropheus fossai*).

Unambiguous synapomorphies. ~~d~~istal margin of anterior and middle cervical postaxial neural spines completely straight along anteroposterior length in lateral view (179-1); dichocephalous anterior dorsal ribs (213-1); ilium dorsally rimed by a low brevis shelf (269-1).

Unnamed clade (*Macrocnemus* spp. + *Tanytrachelos ahynis* + *Langobardisaurus pandolfii* + *Ozimek volans* + *Amotosaurus rotfeldensis* + *Tanystropheus* spp.)

Unambiguous synapomorphies. Squamosal medial process long, forming entirely or almost entirely the posterior border of the supratemporal fenestra (70-1); supra-acetabular margin of ilium with a prominent, bulbous rugosity superior to acetabulum (271-1); pubis-ischium, thyroid fenestra present (273-1).

***Macrocnemus* spp.**

Unambiguous synapomorphies. Parietal without a pineal foramen (77-2); pterygoid with teeth on the lateral ramus (106-1), pterygoid, lateral/distal end of the posterior margin of the lateral ramus not curved posteriorly (109-0); thecodont marginal teeth implantation (169-4); maxillary teeth distinctly recurved (171-1); maximum height of postaxial anterior or middle cervical neural spines approximately equally tall as the posterior articular surface of the centrum (178-1); between seven and 10 cervical vertebrae (195-1); only one of the two ~~elements~~ distal tarsals 1 and 2 is present (292-1); metatarsal V with medial plantar tubercle (304-1).

Unnamed clade (*Tanytrachelos ahynis* + *Langobardisaurus pandolfii* + *Ozimek volans* + *Amotosaurus rotfeldensis* + *Tanystropheus* spp.)

Unambiguous synapomorphies. Frontal contribution to the orbital border anteroposteriorly long and forms at least more than half of the dorsal edge of the orbit (50-1); tooth bearing portion of the dentary ventrally curved or deflected at its anterior end (145-2); anterior to mid postaxial cervical vertebrae with ventral face flattened (197-1); presence of heterotopic ossifications (225-1); pedal phalanx V-1 metatarsal-like, considerably longer than other non-ungual phalanges (306-1).

Unnamed clade (*Tanytrachelos ahynis* + *Langobardisaurus pandolfii*)

Unambiguous synapomorphies. Procoelous presacral vertebrae (181-1); short cervical ribs, being less than two times the length of its respective vertebra, and shaft parallel to the neck (199-1); preacetabular process of the ilium longer than two thirds of its height (264-2); femoral shaft linear with slight ventrodistal curvature in lateral view (286-1).

Unnamed clade (*Ozimek volans* + *Amotosaurus rotfeldensis* + *Tanystropheus* spp.)

Unambiguous synapomorphies. Postorbital, posterior process extends close to or beyond the level of the posterior margin of the supratemporal fenestrae (60-1); retroarticular process not upturned (163-0); epipophyses of cervical vertebrae overhanging the postzygapophyses posteriorly (191-1); interclavicle absent (234-1).

Unnamed clade (*Ozimek volans* + *Amotosaurus rotfeldensis*)

Unambiguous synapomorphies. Tibia longer than femur (285-1).

Tanystropheus spp.

Unambiguous synapomorphies. Eleven to 17 maxillary tooth positions (26-0); frontals very wide and plate-like, a single frontal (or half of a fused frontal) being almost as wide as long (55-1); posterolateral processes of the parietal orientated roughly transverse (79-0); dorsal end of the quadrate hooked posteriorly in lateral view (91-1); glenoid fossa of the articular considerably ventrally displaced compared to the tooth row (161-1); anterior marginal dentition are interlocking fangs forming a fish-trap (165-1); second sacral rib is a single unit, i.e. not bifurcated (216-0); transverse width of the fibula subequal to that of the tibia (287-0).

Crocopoda Ezcurra 2016

Unambiguous synapomorphies. Premaxilla slightly downturned, in which the alveolar margin is angled at approximately 20 degrees to the alveolar margin of the maxilla (5-1); premaxilla-maxilla suture notched along the ventral margin (15-1); prootic with crista prootica (137-1); surangular ~~shelf~~ with low ridge near dorsal margin (155-1); posteriormost dentary teeth on the anterior half of lower jaw (168-0); ankylothecodont marginal teeth implantation (169-1); cervical ribs short, being less than two times the length of its respective vertebra, and shaft parallel to the neck (199-1); dichocephalous anterior dorsal ribs (213-1); fibrolamellar bone tissue in the cortex of long bones (240-1); supra-acetabular margin of ilium with a prominent, bulbous rugosity superior to acetabulum (271-1); distal condyles of the femur with a prominent, strong dorsoventral expansion restricted to the distal end (281-0); articulation between astragalus and calcaneum concavoconvex with concavity on the astragalus (289-1).

Unnamed clade (Allokotosauria + Rhynchosauria + *Teyujagua paradoxa* + Archosauriformes)

Unambiguous synapomorphies. ~~p~~ostnarial process of premaxilla wide and plate-like (10-0); maxilla, alveolar margin in lateral view straight or convex (25-0/2); external nares confluent (29-1); orbit with an elevated rim (48-1); frontal-parietal contact roughly transverse in dorsal view (56-0); posterolateral processes of parietal dorsoventrally deep, being plate-like in occipital view and subequal to the height of the supraoccipital (80-1); posterodorsal portion of the parabasisphenoid completely ossified (116-1); orientation of the parabasisphenoid oblique, main axis posterodorsally-to-anteroventrally oriented (120-1); basioccipital-parabasisphenoid tightly sutured, sometimes by an interdigitated suture, or both bones fused to each other (121-1); basioccipital-parabasisphenoid with two pneumatic foramina between them (122-1); prootic contributes laterally ~~tapering lamina~~ to the anterior surface of the paroccipital process (139-1).

Rhynchosauria Osborn 1903

Unambiguous synapomorphies. Lateral surface of the nasal meets entire dorsoventral height of medial surface of supra-alveolar portion of maxilla (34-1); shallow or deep pits scattered across surface of the skull and/or low ridges (44-1); dorsal surface of the frontal adjacent to sutures with the postfrontal possesses a longitudinal and deep depression (51-1); dorsal surface of postfrontal depressed with deep pits (59-1); supratemporal is present and broad (73-0); opisthotic with fossa immediately lateral to the foramen magnum (132-1); multiple zahnreihen in maxilla and dentary (164-1).

Unnamed clade (*Howesia browni* + *Eohyosaurus wolvaardti*)

Unambiguous synapomorphies. Maxilla-jugal with anguli oris crest (27-1); supratemporal fossa medial to the supratemporal fenestra on the parietal well-exposed in dorsal view and mainly dorsally or dorsolaterally facing (82-0).

Unnamed clade (Allokotosauria + *Teyujagua paradoxa* + Archosauriformes)

Unambiguous synapomorphies. Posterior margin of quadrate in lateral view sigmoidal, with a concave dorsal portion and convex ventral portion (90-2); basioccipital with a transversely narrow embayment or ridge between basal tubera (125-1); scapulacoracoid not fused (226-1); interclavicle not webbed between lateral and posterior processes (237-1); postacetabular process of the ilium mainly posteriorly oriented (268-1); distal end of fibula angled anterodorsally in lateral view (288-0).

Allokotosauria Nesbitt, Flynn, Pritchard, Parrish, Ranivoharimanana & Wyss 2015

Unambiguous synapomorphies. Medial process of squamosal long, forming entirely or almost entirely the posterior border of the supratemporal fenestra (70-1); supratemporal absent (73-2); dorsal end of quadrate hooked posteriorly in lateral view (91-1); vomerine dentition relatively large, similar to those of the marginal dentition (97-1); palatine dentition relatively large, similar to those of the marginal dentition (101-1); dentition on the anterior ramus of the pterygoid relatively large, similar to those of the marginal dentition ([illegible]05-1); pterygoid, lateral/distal end of the posterior margin of the lateral ramus curved posteriorly (109-1); tooth bearing portion of the dentary ventrally curved or deflected at its anterior end (145-2); articular, retroarticular process anteroposteriorly short, being poorly developed posteriorly to the glenoid fossa (162-1); distal condyles of the femur uneven with the lateral condyle projecting distally distinctly beyond the medial condyle (282-0); ventral tubercle of the pedal unguals well-developed and extended ventral to the articular portion of the ungual (307-1).

Unnamed clade (*Trilophosaurus buettneri* + *Azendohsaurus madagaskarensis*)

Unambiguous synapomorphies. Posterior end of the horizontal process of the maxilla distinctly ventrally deflected from the main axis of the alveolar margin (24-1); postfrontal-frontal suture distinctly posteromedially inclined (57-1); opisthotic and exoccipital fused (127-1); paroccipital processes of the opisthotics extend laterally or slightly posterolaterally (130-0); posteriormost dentary teeth on the posterior half of lower jaw (168-1); multiple maxillary and dentary tooth crowns distinctly mesiodistally expanded above the root (170-1); postaxial cervicals with epipophyses (190-1); second sacral rib is a single unit, i.e. not bifurcated (216-0); ulna with olecranon process (249-1); ulna with lateral tuber on the proximal portion (250-1); proximal articular surface of the femur well-ossified, being flat or convex (279-0); attachment of the caudifemoralis musculature on the posterior surface of the femur crest-like and with intertrochanteric fossa, and not convergent with proximal end (280-1).

Unnamed clade (*Teyujagua paradoxa* + Archosauriformes)

Unambiguous synapomorphies. Jugal bulges ventrolaterally at the point where its three processes meet (39-1); extension of the ventral process of the postorbital ends much higher than the ventral border of the orbit (61-0); medial extent of the supratemporal fossa of the parietal restricted to the lateral edge of the parietal (83-0); posttemporal fenestra absent or developed as a foramen or very narrow slit (136-2);

lower jaw with an external mandibular fenestra (152-1); serrations on the distal margin of the maxillary/dentary crowns usually apically restricted and low or absent on the mesial margin (172-1).

Archosauriformes Gauthier, Kluge & Rowe 1988

Unambiguous synapomorphies. ~~Snout~~ at the level of the anterior border of the orbit dorsoventrally taller than transversely broad (3-1), antorbital fenestra present (22-1); external nares not confluent (29-0); postparietal sheet-like, not much narrower than the supraoccipital (84-0); shape of the tooth bearing portion of the dentary dorsally curved for all or most of its anteroposterior length (145-1); dentary with posterocentral process (149-1); diapophysis and parapophysis of anterior to middle cervical postaxial vertebrae situated on different processes and well-separated (188-1).

Proterosuchidae Huene 1908

Unambiguous synapomorphies. Premaxilla strongly downturned, prenarial process obscured by the postnarial process in lateral view (5-2); postorbital, posterior process extends close to or beyond the level of the posterior margin of the supratemporal fenestrae (60-1); pterygoid with teeth on the lateral ramus (106-1); orientation of the parabasisphenoid horizontal (120-0); basioccipital-parabasisphenoid with a loose, overlapping suture (121-0); angular forming about half of the dorsoventral height of the mandible at its greatest width (159-1).

Unnamed clade (*Erythrosuchus africanus* + *Euparkeria capensis*)

Unambiguous synapomorphies. ~~s~~imple continuous contact between premaxilla and maxilla (15-0); anterior process of the jugal is dorsoventrally expanded anteriorly (38-1); supratemporal absent (73-2); anterior process of the quadratojugal is distinctly present and the lower temporal bar is complete, but the process terminates well posterior to the base of the posterior process of the jugal (88-2); quadrate, posterior margin in lateral view continuously concave (90-1); paroccipital processes of the opisthotics extend laterally or slightly posterolaterally (130-0); surangular with a laterally or ventrolaterally projecting shelf with a lateral edge (155-2); serrations on the distal margin of the maxillary/dentary crowns and on both margins (172-2); dichocephalous proximal end of middle dorsal ribs (214-0); second sacral rib is a single unit, i.e. not bifurcated (216-0); coracoid, posterior border unexpanded posteriorly (232-0); shape of the preacetabular process of the ilium approximately straight-sided with a distinct angle between the anterior and dorsal margins (265-1); dorsalmost margin of acetabulum is unsculptured (271-0); pubic symphysis restricted anteriorly and obscured by the pubic shaft in lateral view (275-1); pedal centrale absent as a separate ossification (291-1); both distal tarsal 1 and 2 are absent (292-2); perforating foramen between astragalus and calcaneum absent (295-1); no concave gap on the proximal surface of metatarsal V (301-0).

Discussion

The resolution of the tree topology is distinctly higher in the pruned analyses for both ~~the~~ analyses (*Figs. 33-34*). Our findings indicate that the taxa previously considered as “protorosaurs” (*Czatkowiella harae*, *Protorosaurus speneri*, *Jesairosaurus lehmani*, Tanystropheidae, Dinocephalosauridae, and *Prolacerta broomi*) do not form a monophyletic grouping (*Figs. 31-34*), corroborating the findings of various previous analyses (e.g. Dilkes 1998; Ezcurra 2016; Pritchard et al. 2015; Rieppel et al. 2003). We recovered *Protorosaurus speneri* as the sister taxon to all other Archosauromorpha in analyses 3 and 4, and as the sister taxon of all Archosauromorpha except for *Czatkowiella harae* in analysis 1. This result is also consistent with recent analyses (e.g. Ezcurra 2016; Pritchard et al. 2015), and we therefore suggest abandoning the term “protorosaur” for taxa that are less closely related to *Protorosaurus speneri* than to tanystropheids, *Prolacerta broomi*, rhynchosaurs, allokotosaurs, or archosauriforms, given the current framework of early archosauromorph relationships.

The phylogenetic position of Jesairosaurus lehmani

Jesairosaurus lehmani was originally considered as a “protorosaur” ~~that is~~ closely related to Tanystropheidae (Jalil 1997). More recently, Ezcurra (2016) recovered *Jesairosaurus lehmani* as the sister taxon to Tanystropheidae. The position of *Jesairosaurus lehmani* is not stable in our analyses. In analysis 4 it is recovered as the sister taxon of Tanystropheidae, *Fuyuansaurus acutirostris*, and Dinocephalosauridae (*Fig. 34*). This position is reasonably well-supported by a Bremer support of 3. However, in analysis 1B and analysis 3, *Jesairosaurus lehmani* is also recovered as the sister taxon to Dinocephalosauridae, but it is equally closely related to both Tanystropheidae and Crocopoda (*Fig. 31b, 33*). In analysis 1A and analysis 2A and 2B it is part of the large polytomy that includes most non-archosauriform archosauromorphs (*Figs. 31a, 32*). With the currently available morphological information for *Jesairosaurus lehmani*, its position as a non-crocopod archosauromorph is well-supported, but its exact relationships within this group remains contentious.

Dinocephalosauridae

Dinocephalosaurus orientalis has been included in three previous phylogenetic analyses. In the analysis of Rieppel et al. (2008), it formed a polytomy with drepanosaurs, tanystropheids, and *Jesairosaurus lehmani*. In the analysis of Liu et al. (2017), which is derived from the same character matrices employed by Rieppel et al. (2008), *Dinocephalosaurus orientalis* was recovered within Tanystropheidae as the sister taxon to all other included tanystropheids. Finally, *Dinocephalosaurus orientalis* was also included in the phylogenetic analysis of De Oliveira et al. (2020), in which it was recovered in a clade with *Jesairosaurus lehmani* that represented the sister clade to all other archosauromorphs. However, the overall resolution of this analysis was poor and both *Dinocephalosaurus orientalis* and *Jesairosaurus lehmani* were pruned for the final analysis presented ~~in~~ De Oliveira et al. (2020). In analysis 1B and analyses 3 and 4 *Dinocephalosaurus orientalis* is found in a clade with *Pectodens zhenyuensis*, a taxon which has previously not been considered in a quantitative phylogenetic analysis (*Figs. 31b, 33-34*). For analysis 1B this clade has a Bremer support of 1, whereas for analyses 3 and 4 these supports are 4 and 2, respectively. In analysis 1A and analysis 2A-B this clade is not recovered, and both *Dinocephalosaurus orientalis* and *Pectodens zhenyuensis* are part of the large polytomy that includes most non-archosauriform archosauromorphs (*Fig. 31a, 32*). The presence of more *Dinocephalosaurus*-like taxa has also been alluded to through the description of IVPP V22788, an embryonic specimen that is very similar to *Dinocephalosaurus orientalis* but differs in several aspects, most notably a lower number of cervical vertebrae (Li et al. 2017b). Due to the very early ontogenetic stage of this specimen, it has not been referred to a separate taxon and it has also not been included here, since very early ontogenetic features would have likely introduced bias into the analyses. Nevertheless, the clade formed by *Dinocephalosaurus orientalis* and *Pectodens zhenyuensis* that is found in analysis 1B and our pruned analyses, combined with the existence of at least one more *Dinocephalosaurus*-like taxon, merits the erection of a new higher-level taxon to describe this clade. Dinocephalosauridae is therefore erected. ~~It can be distinguished from other archosauromorph clades through the combination of the following characters: absence of a posterior process of the jugal, ventrally displaced glenoid fossa of the mandible, an elongated free-ending anterior process of the cervical ribs, and a straight metatarsal V.~~ In analysis 4 Dinocephalosauridae forms a monophyletic clade together with Tanystropheidae (*Fig. 34*), whereas in analyses 1B and 3 it forms a distinct lineage within non-archosauriform archosauromorphs (*Figs. 31, 33*).

The monophyly of Tanystropheidae

A monophyletic Tanystropheidae is recovered in analyses 1B, 3, and 4 (*Figs. 31B, 33-34*), which agrees with most previous analyses (e.g. Benton & Allen 1997; Dilkes 1998; Ezcurra 2016; Jalil 1997; Pritchard et al. 2015). In analyses 1A and 2A-B a monophyletic Tanystropheidae is not recovered (*Figs. 31A, 32*). Analyses 1 and 2 include all relevant “protorosaur” OTUs, regardless of completeness, and therefore also include taxa that are solely known from a few isolated remains (*Tanystropheus* *"conspicuus"*, *Augustaburiania vatagini*) or a single, partial postcranial specimen (*Sclerostropheus fossai*, *Elessaurus gondwanoccidens*, *Raibliania calligarisi*). Therefore, it is unsurprising that these analyses are poorly resolved in this part of the tree and that the resolution is dramatically increased after pruning these and other OTUs for which less than 25% of characters could be scored. Nevertheless, analysis 1B, which is comparatively well-resolved and includes all tanystropheids except for "*Tanystropheus antiquus*", corroborates the assignment of the poorly known taxa *Raibliania calligarisi*, *Sclerostropheus fossai*, and *Augustaburiania vatagini* to Tanystropheidae, as had previously been suggested but not tested cladistically (*Fig. 31b*). Furthermore, *Elessaurus gondwanoccidens* is also recovered within Tanystropheidae, corroborating the result of De Oliveira et al. (2020). However, whereas *Elessaurus gondwanoccidens* was recovered as the sister taxon to ~~all other tanystropheids~~ in De Oliveira et al. (2020), it is found in a large polytomy in analysis 1B that is deeply nested within Tanystropheidae.

It is important to note that the cranial morphology of the two best-known tanystropheid species, *Tanystropheus hydroides* and *Macrocnemus bassanii*, was recently revised, revealing a large cranial disparity between the two (Miedema et al. 2020; Spiekman et al. 2020). The analyses presented here are the first to incorporate this new information, yet still confirm the monophyly of the Tanystropheidae. Analyses 1A, 1B, and 2B indicate that **AMNH FARB 7206** is closely related to *Tanytrachelos ahynis* (*Figs. 31*, *32b*), but do not support its referral to this taxon as has previously been proposed (Pritchard et al. 2015), since *Langobardisaurus pandolfii* represents the closest related OTU to *Tanytrachelos ahynis*. A detailed study of **AMNH FARB 7206** and other specimens from the Lockatong Formation are required to assess whether this material can be assigned to a separate taxon.

Fuyuansaurus acutirostris is recovered within Tanystropheidae or among tanystropheid taxa (*Figs. 31-34*). However, its position within the group is unstable. In analysis 4 it is recovered as the sister taxon to all other Tanystropheidae, whereas in analyses 1B and 3 it is found deeply nested within Tanystropheidae. *Fuyuansaurus acutirostris* had previously not been included in any phylogenetic analysis, and its phylogenetic placement was deemed uncertain in its initial description, since it shared several characters with known tanystropheid taxa (e.g. the presence of 12 to 13 cervical vertebrae, elongate cervical vertebrae with low neural spines, cervical ribs with an anterior process), but also deviated from them in several traits such as the absence of a thyroid fenestra and elongation of the snout (Fraser et al. 2013). These considerations are also reflected in analysis 4, in which *Fuyuansaurus acutirostris* is found within Tanystropheidae, but not deeply nested within the clade (*Fig. 34*).

Ozimek volans is another taxon that has been tentatively referred to Tanystropheidae. It differs clearly from other tanystropheids in its extremely gracile and elongate appendicular elements and the morphology of its pectoral girdle (Dzik & Sulej 2016). *Ozimek volans* is considered to be most closely related to *Sharovipteryx mirabilis*, although this has not been investigated quantitatively so far. *Sharovipteryx mirabilis* was not included here, since it is generally not considered within Archosauromorpha and is only known from poorly preserved remains. *Sharovipteryx mirabilis* has been interpreted as a gliding reptile (Gans et al. 1987), and due to the highly derived, gracile morphology of *Ozimek volans*, a similar lifestyle was also tentatively proposed for this taxon (Dzik & Sulej 2016). The phylogenetic placement of *Ozimek volans* was recently tested and it was found well-nested within Tanystropheidae as the sister taxon to a *Langobardisaurus pandolfii* - *Tanytrachelos ahynis* clade (Pritchard & Sues 2019). The presence of a possible gliding reptile would represent a remarkable ecomorphological divergence within the tanystropheid clade. Our results corroborate the placement of *Ozimek volans* within Tanystropheidae. Both analyses 3 and 4 recover *Ozimek volans* as the sister taxon to *Amotosaurus rotfeldensis*, whereas analyses 1A and 2 find it in the large polytomy that also includes all other tanystropheids. In analysis 1B, *Ozimek volans* is part of a large polytomy that includes all tanystropheids except *Macrocnemus* spp., **AMNH FARB 7206**, *Langobardisaurus pandolfii*, and *Tanytrachelos ahynis* (*Figs. 31-34*). *Ozimek volans* was scored here based on its original description (Dzik & Sulej 2016), which largely employs reconstruction drawings for clarification of morphological details. A personal observation of all the referred specimens, possibly in combination with additional aid of µCT methodologies, would have to confirm the presence of tanystropheid synapomorphies, such as the configuration of the skull and the cervical vertebrae and accompanying ribs, within this taxon.

The *Macrocnemus* taxa form a generic clade in analyses 1, 3, and 4 that is either the sister group to all other Tanystropheidae (*Figs. 31B, 33*) or to all other Tanystropheidae excluding *Fuyuansaurus acutirostris* (*Fig. 34*). This can likely be attributed to the many plesiomorphic cranial characters this genus exhibits in comparison to *Tanystropheus* spp. (Jaquier et al. 2017; Miedema et al. 2020). The *Tanystropheus* taxa are recovered within a clade that also includes *Raibliania calligarisi* in analysis 2B, highlighting the close affinity of the former to the *Tanystropheus* genus (*Fig. 32b*). *Tanystropheus longobardicus* and *Tanystropheus hydroides* are also recovered in a generic clade that is deeply nested within Tanystropheidae in the pruned analyses (*Figs. 33-34*). Although the topology of Tanystropheidae is fully resolved in analysis 4, it is poorly supported (*Fig. 34*). The Bremer support for all ~~nodes~~ within Tanystropheidae is 1, except for the generic nodes of *Macrocnemus* and *Tanystropheus*, which both have a Bremer support of 4. This is also reflected in the topologies of the other analyses, in which many nodes within Tanystropheidae are collapsed. The lack of resolution within tanystropheids, even when excluding the least informative OTUs, is attributable to the poorly known cranial morphology of most tanystropheid taxa except for *Macrocnemus* spp. and *Tanystropheus* spp. Complete skulls are known for both *Tanytrachelos ahynis* and *Langobardisaurus pandolfii*, but their cranial morphology is exceedingly hard to infer due to the poor preservation of available specimens, which is related to diagenetic factors (Olsen 1979; Renesto & Dalla Vecchia 2000). Additional specimens or studies employing high-resolution tomographic technologies will hopefully contribute to our future understanding of the considerable cranial disparity present within Tanystropheidae, and aid in resolving intra-tanystropheid relationships.

The monophyly of Crocopoda

Crocopoda is a recently erected clade that includes all archosauromorph taxa that are more closely related to *Trilophosaurus buettneri*, *Azendohsaurus madagaskarensis*, *Rhynchosaurus articeps*, and *Proterosuchus fergusi* than to *Protorosaurus speneri* and *Tanystropheus longobardicus* (Ezcurra 2016, but see Pritchard & Sues 2019, Simões et al. 2018, and Spiekman et al. 2020, which found Crocopoda to be polyphyletic). The monophyly of this clade is recovered here in analyses 2, 3, and 4 (*Figs. 31-34*) and is well-supported (Bremer support of 7 in analysis 4). All analyses recovered a monophyletic Allokotosauria and Rhynchosauria, which is in correspondence with other recent analyses (Ezcurra 2016, Nesbitt et al. 2015 and subsequent modifications of these matrices). In these analyses *Prolacerta broomi* was more closely related to Archosauriformes than both allokotosaurs and rhynchosaurs. In analyses 2, 3, and 4 *Prolacerta broomi* is recovered within Crocopoda as the sister taxon to all other members of this clade, and it is found outside Crocopoda in analysis 1 (*Figs. 31-34*). *Prolacerta broomi* is found to be more distantly related to Archosauriformes than both rhynchosaurs and allokotosaurs ~~are through~~ the combination of the following traits, which are absent in either all or most other crocopods included in the analysis: a thin postnarial process of the premaxilla (also present in *Teyujagua paradoxa*), a concave alveolar margin of the maxilla in lateral view, absence of an anguli-ori crest (also absent in *Trilophosaurus buettneri* and Archosauriformes), absence of an elevated orbital rim (also absent in *Trilophosaurus buetteri* and *Euparkeria capensis*), a U-shaped frontoparietal suture (also present in *Euparkeria capensis*), dorsoventrally low posterolateral processes of the parietal in occipital view, a posterodorsally incompletely ossified parabasisphenoid, a horizontally oriented parabasisphenoid (also present in *Trilophosaurus buettneri* and *Proterosuchus* spp.), a loose attachment between the parabasisphenoid and basioccipital (also present in *Proterosuchus* spp.), the absence of pneumatic foramina between the parabasisphenoid and basioccipital (also absent in *Trilophosaurus buettneri* and *Euparkeria capensis*), and no paroccipital contribution of the prootic. This has important macroevolutionary implications, since *Prolacerta broomi* was previously considered to be very closely related to Archosauriformes and has been treated as such in discussions on character trait evolution (e.g. Ezcurra & Butler 2015a; Pinheiro et al. 2016; Pritchard & Sues 2019).

Teyujagua paradoxa is consistently recovered as the sister taxon to Archosauriformes (*Figs. 31-34*). ~~However,~~ in analysis 4 Allokotosauria is recovered as the sister clade to *Teyujagua* and Archosauriformes (Bremer support of 2), whereas analysis 3 finds Rhynchosauria to be the sister clade to this node (Bremer support of 1) and analyses 1 and 2 resulted in a polytomy between Allokotosauria, Rhynchosauria, and the clade encompassing *Teyujagua paradoxa* and Archosauriformes. Therefore, our results are inconclusive regarding the relative position of Allokotosauria and Rhynchosauria among non-archosauriform Crocopoda.

Conclusion

Our results corroborate the polyphyly of "Protorosauria" as established by previous studies (e.g. Dilkes 1998; Ezcurra 2016; Pritchard et al. 2015). Consequently, the usage of a historical "protorosaur" clade that includes tanystropheids, dinocephalosaurids, and *Prolacerta broomi* should be abandoned. The Chinese taxa *Pectodens zhenyuensis* and *Dinocephalosaurus orientalis* form a newly erected clade, Dinocephalosauridae. *Fuyuansaurus acutirostris* is recovered within Tanystropheidae despite the presence of several plesiomorphic characters. *Jesairosaurus lehmani* is a non-crocopodan archosauromorph that is closely related to tanystropheids and dinocephalosaurids. The interrelationships within Tanystropheidae are poorly resolved, which can be attributed to the poorly known cranial morphology of most tanystropheid taxa. *Prolacerta broomi* is recovered as the sister taxon to all other Crocopoda and is thus more distantly related to Archosauriformes than previously considered.

Institutional abbreviations

AMNH – American Museum of Natural History, New York, New York, USA

AUP – University of Aberdeen, Palaeontology collection, Aberdeen, Scotland

BP – Evolutionary Studies Institute, University of Witwatersrand, Johannesburg, South Africa

BSPG - Bayerische Staatssammlung für Paläontologie und Geologie, Munich, Germany

FMNH - Field Museum of Natural History, Chicago, Illinois, USA

GMPKU - Geological Museum of Peking University, Beijing, China

IGWuG - Institut für Geologische Wissenschaften und Geiseltalmuseum, Martin-Luther-Universität Halle-Wittenberg, Halle, Germany

IVPP - Institute of Vertebrate Paleontology and Paleoanthropology, Beijing, China

KUVP - Kansas University Museum of Natural History, Lawrence, Kansas, USA

LPV – Chengdu Center of the China Geological Survey, Chengdu, Sichuan, China

MCSN - Museo Cantonale di Scienze Naturali di Lugano, Lugano, Switzerland

MCSNB - Museo Civico di Scienze Naturali "E. Caffi" Bergamo, Bergamo, Italy

MFSN - Museo Friulano di Scienze Naturali, Udine, Italy

MGUWr - Geological Museum, Institute of Geological Sciences, University of Wrocław, Wrocław, Poland

MSNM - Museo di Storia Naturale, Milan, Italy

NMS – National Museums Scotland, Edinburgh, UK

NHMW – Naturhistorisches Museum Wien, Vienna, Austria

NMK – Naturkundemuseum im Ottoneum, Kassel, Germany

OMNH – Sam Noble Oklahoma Museum of Natural History, Norman, Oklahoma, USA

P – Palaeontological Collection of the Department of Geology and Palaeontology, University of Innsbruck, Innsbruck, Austria

PIMUZ - Paläontologisches Institut und Museum der Universität Zürich, Zurich, Switzerland

PIN - Paleontological Institute of the Russian Academy of Sciences, Moscow, Russia

RC – Rubidge Collection, Wellwood, Graaff-Reinet, South Africa

RCSHC –Royal College of Surgeons Hunterian Collection, London, England

SAM-PK - Iziko South African Museum, Cape Town, South Africa

SMNS – Staatliches Museum für Naturkunde, Stuttgart, Germany

SMNK - Staatliches Museum für Naturkunde Karlsruhe, Germany

TMM – Texas Memorial Museum, Austin, Texas, USA

TWCMS - Sunderland Museum and Winter Gardens, Tyne & Wear Archives & Museums, Sunderland, England

UA – University of Antananarivo, Antananarivo, Madagascar

UCMP – University of California Museum of Paleontology, Berkeley, California, USA

UFSM – Universidade Federal de Santa Maria, Santa Maria, Brazil

UMMP – University of Michigan Museum of Paleontology, Ann Arbor, Michigan, USA

UMZC – University Museum of Zoology, Cambridge, England

UNIPAMPA – Universidade Federal do Pampa, São Gabriel, Brazil

UWBM – Burke Museum of Natural History and Culture, University of Washington, Seattle, Washington, USA

VMNH – Virginia Museum of Natural History, Martinsville, Virginia, USA

WMsN - LWL-Museum für Naturkunde, Westfälisches Landesmuseum mit Planetarium, Münster, Germany

YPM - Yale Peabody Museum, New Haven, Connecticut, USA

ZAR – Zarzaitine Collection, Muséum National d'Histoire Naturelle, Paris, France

ZMNH - Zhejiang Museum of Natural History, Hangzhou, China

ZPAL - Institute of Paleobiology, Polish Academy of Sciences, Warsaw, Poland

Acknowledgements

We kindly thank Mark Norell and Carl Mehling (AMNH), Kevin Padian and Pat Holroyd (UCMP), Christian Sidor and Meredith Rivin (UWBM), Claire Browning and Roger Smith (SAM-PK), Anna Paganoni (MCSNB), Bernhard Zipfel, Sifelani Jirah, and Jonah Choiniere (BP), Rudolf Stockar (MCSN), Cristiano Dal Sasso and Stefania Nosotti (MSNM), Cristina Lombardo (MPUM), Nour-Eddine Jalil (ZAR), Christian Klug and Beat Scheffold (PIMUZ), Alexander Hastings and Christina Byrd (VMNH), Rainer Schoch (SMNS), Eberhard “Dino” Frey (SMNK), Lothar Schöllmann (WMsN), Cornelia Kurz (NMK), Giuseppe Muscio, Luca Simonetto, and Fabia Dalla Vecchia (MFSN), Li Chun (IVPP), Da-Yong Jiang (GMPKU), and Olivier Rieppel and William

Simpson (FMNH), for access to specimens under their care. Thodoris Argyriou, Gabriel Aguirre Fernandez, Dylan Bastiaans, Feiko Miedema, and Olivier Rieppel are thanked for discussions. Martín Ezcurra and Sterling Nesbitt kindly provided photographs of several specimens of *Azendohsaurus madagaskarensis*, *Pamelaria dolichotrachela*, and *Proterosuchus alexanderi*.

References

Abdala F, Hancox PJ, and Neveling J. 2005. Cynodonts from the uppermost Burgersdorp Formation, South Africa, and their bearing on the biostratigraphy and correlation of the Triassic *Cynognathus* Assemblage Zone. *Journal of Vertebrate Paleontology* 25:192-199. 10.1671/0272-4634(2005)025[0192:CFTUBF]2.0.CO;2

Arthaber Gv. 1922. Über Entwicklung, Ausbildung und Absterben der Flugsaurier. *Paläontologische Zeitschrift* 4:1-47.

Bartholomai A. 1979. New lizard-like reptiles from the Early Triassic of Queensland. *Alcheringa* 3:225-234.

Bassani F. 1886. Sui fossili e sull'eta degli schisti bituminosi triasici di Besano in Lombardia. *Atti Società Italiana di scienze naturali* 29:15-72.

Bennett SC. 1996. The phylogenetic position of the Pterosauria within the Archosauromorpha. *Zoological Journal of the Linnean Society* 118:261-308.

Benton MJ. 1983. The Triassic reptile *Hyperodapedon* from Elgin: functional morphology and relationships. *Philosophical Transactions of the Royal Society of London B, Biological Sciences* 302:605-718.

Benton MJ. 1984. The relationships and early evolution of the Diapsida. *In: Ferguson MWJ, ed The structure, evolution, and development of reptiles London: Symposia of the Zoological Society of London* 52:575-596.

Benton MJ. 1985. Classification and phylogeny of the diapsid reptiles. *Zoological Journal of the Linnean Society* 84:97-164.

Benton MJ. 2005. Vertebrate Palaeontology. *Wiley-Blackwell* 3rd Edition:472 pages.

Benton MJ, and Allen JL. 1997. *Boreopricea* from the Lower Triassic of Russia, and the relationships of the prolacertiform reptiles. *Palaeontology* 40:931-953.

Benton MJ, and Walker AD. 1996. *Rhombopholis*, a prolacertiform reptile from the Middle Triassic of England. *Palaeontology* 39:763-782.

Bickelmann C, Müller J, and Reisz RR. 2009. The enigmatic diapsid *Acerosodontosaurus piveteaui* (Reptilia: Neodiapsida) from the Upper Permian of Madagascar and the paraphyly of "younginiform" reptiles. *Canadian Journal of Earth Sciences* 46:651-661. 10.1139/E09-038

Bizzarini F, and Muscio G. 1995. Un nuovo rettile (Reptilia, Prolacertiformes) dal Norico di Preone (Udine, Italia Nordorientale). Nota preliminare. *Gortania - Atti del Museo Friulano di Storia Naturale* 16:67-76.

Borsuk-Bialynicka M, and Evans SE. 2003. A basal archosauriform from the Early Triassic of Poland. *Acta Palaeontologica Polonica* 48.

Borsuk-Białynicka M, and Evans SE. 2009a. Cranial and mandibular osteology of the Early Triassic archosauriform *Osmolskina czatkowicensis* from Poland. *Palaeontologia Polonica* 65:235–281.

Borsuk-Białynicka M, and Evans SE. 2009b. A long-necked archosauromorph from the Early Triassic of Poland. *Palaeontologia Polonica* 65:203-234.

Borsuk-Białynicka M, and Lubka M. 2009. Procolophonids from the Early Triassic of Poland. *Palaeontologia Polonica* 65:107-144.

Borsuk-Białynicka M, and Sennikov AG. 2009. Archosauriform postcranial remains from the Early Triassic karst deposits of southern Poland. *Palaontol Pol* 65:283-328.

Botha-Brink J, and Smith RMH. 2011. Osteohistology of the Triassic Archosauromorphs *Prolacerta*, *Proterosuchus*, *Euparkeria*, and *Erythrosuchus* from the Karoo Basin of South Africa. *Journal of Vertebrate Paleontology* 31:1238-1254.

Brazeau MD. 2011. Problematic character coding methods in morphology and their effects. *Biological Journal of the Linnean Society* 104:489-498.

Broili F, and Fischer E. 1918. *Trachelosaurus fischeri* nov. gen. nov. sp. Ein neuer Saurier aus dem Buntsandstein von Bernburg. *Jahrbuch der Königlich Preussischen Geologischen Landesanstalt zu Berlin* 37:359-414.

Broom R. 1905a. Preliminary notice of some new fossil reptiles collected by Mr. Alfred Brown at Aliwal North, South Africa. *Rec Albany Mus* 1:269-275.

Broom R. 1905b. Notice of some new fossil reptiles from the Karroo beds of South Africa. *Records of the Albany Museum* 1:331-337.

Broom R. 1913a. Note on Mesosuchus browni, Watson, and on a new South African Triassic pseudosuchian (Euparkeria capensis). *Records of the Albany Museum* 2:394-396.

Broom R. 1913b. On the South-African Pseudosuchian *Euparkeria* and Allied Genera. Proceedings of the Zoological Society of London: Wiley Online Library. p 619-633.

Broom R. 1914. A new Thecodont Reptile. *Proceedings of the Zoological Society of London*:1072-1077.

Broom R. 1922. An imperfect skeleton of *Youngina Capensis*, Broom, in the collection of the Transvaal Museum. *Annals of the Transvaal Museum* 8:273-276.

Broom R. 1925. On the origin of lizards. Proceedings of the Zoological Society of London: Wiley Online Library. p 1-16.

Broom R. 1937. A further contribution to our knowledge of the fossil reptiles of the Karroo. *Journal of Zoology* 107:299-318.

Broom R, and Robinson JT. 1948. Some New Fossil Reptiles from the Karoo Beds of South Africa. *Journal of Zoology* 118:392-407.

Butler RJ, Ezcurra MD, Liu J, Sookias RB, and Sullivan C. 2019. The anatomy and phylogenetic position of the erythrosuchid archosauriform *Guchengosuchus shiguaiensis* from the earliest Middle Triassic of China. *PeerJ* 7:e6435. 10.7717/peerj.6435

Butler RJ, Ezcurra MD, Montefeltro FC, Samathi A, and Sobral G. 2015. A new species of basal rhynchosaur (Diapsida: Archosauromorpha) from the early Middle Triassic of South Africa, and the early evolution of Rhynchosauria. *Zoological Journal of the Linnean Society* 174:571-588.

Caldwell MW. 1995. Developmental constraints and limb evolution in Permian and extant lepidosauromorph diapsids. *Journal of Vertebrate Paleontology* 14:459-471. 10.1080/02724634.1995.10011572

Calzavara M, Muscio G, and Wild R. 1980. *Megalancosaurus preonensis* n.g., n.sp., a new reptile from the Norian of Friuli, Italy. *Gortania - Atti del Museo Friulano di Storia Naturale* 2:59-64.

Camp CL. 1945. *Prolacerta* and the protorosaurian reptiles. Part I and Part II. *American Journal of Science* 243:17-32, 84-101.

Carroll RL. 1981. Plesiosaur ancestors from the Upper Permian of Madagascar. *Philosophical Transactions of the Royal Society of London B, Biological Sciences* 293:315-383. 10.1098/rstb.1981.0079

Case EC. 1928. A cotylosaur from the Upper Triassic of western Texas. *Journal of the Washington Academy of Sciences* 18:177-178.

Casey MM, Fraser NC, and Kowalewski M. 2007. Quantative Taphnomy of a Triassic Reptile *Tanytrachelos ahynis* from the Cow Branch Formation, Dan River Basin, Solite Quarry, Virginia. *PALAIOS* 22:598-611.

Castiello M, Renesto S, and Bennett SC. 2016. The role of the forelimb in prey capture in the Late Triassic reptile *Megalancosaurus* (Diapsida, Drepanosauromorpha). *Historical Biology* 28:1090-1100.

Chatterjee S. 1980. *Malerisaurus*, A New Eosuchian Reptile from the Late Triassic of India. *Philosophical Transactions of the Royal Society of London B: Biological Sciences* 291:163-200.

Chatterjee S. 1986. *Malerisaurus langstoni*, a new diapsid reptile from the Triassic of Texas. *Journal of Vertebrate Paleontology* 6:297-312.

Cohen K, Finney S, Gibbard P, and Fan J-X. 2013. The ICS international chronostratigraphic chart. *Episodes* 36:199-204.

Colbert EH. 1945. The Dinosaur Book: The Ruling Reptiles and their Relatives. *Man and Nature Publications Handbook*.

Colbert EH. 1965. The Age of Reptiles. *Norton, New York*:262 p.

Colbert EH. 1987. The Triassic Reptile *Prolacerta* in Antartica. *American Museum Novitates*:1-19.

Colbert EH, and Olsen PE. 2001. A new and unusual aquatic reptile from the Lockatong Formation of New Jersey (Late Triassic, Newark Supergroup). *American Museum Novitates* 2001:1-24. 10.1206/0003-0082(2001)334<0001:ANAUAR>2.0.CO;2

Conrad J. 2008. Phylogeny and systematics of Squamata (Reptilia) based on morphology. *Bulletin of the American Museum of Natural History* 310.

Cope ED. 1900. The Crocodilians, lizards and snakes of North America. *Washington: Government Printing Office*.

Cowen R. 1981. Homonyms of *Podopteryx*. *Journal of Paleontology* 55:483.

Cubo J, and Jalil N-E. 2019. Bone histology of *Azendohsaurus laaroussii*: Implications for the evolution of thermometabolism in Archosauromorpha. *Paleobiology* 45:317-330.

Currie PJ. 1980. A new younginid (Reptilia: Eosuchia) from the Upper Permian of Madagascar. *Canadian Journal of Earth Sciences* 17:500-511. 10.1139/e80-046

Currie PJ. 1981. The vertebrae of *Youngina* (Reptilia: Eosuchia). *Canadian Journal of Earth Sciences* 18:815-818.

Dalla Vecchia FM. 2020. *Raibliania calligarisi* gen. n., sp. n., a new tanystropheid (Diapsida, Tanystropheidae) from the Upper Triassic (Carnian) of northeastern Italy. *Rivista Italiana di Paleontologia e Stratigrafia* 126:197-222. 10.13130/2039-4942/13041

De Oliveira TM, Oliveira D, Schultz CL, Kerber L, and Pinheiro FL. 2018. Tanystropheid archosauromorphs in the Lower Triassic of Gondwana. *Acta Palaeontologica Polonica*. 10.4202/app.00489.2018

De Oliveira TM, Pinheiro FL, Stock Da Rosa ÁA, Dias Da Silva S, and Kerber L. 2020. A new archosauromorph from South America provides insights on the early diversification of tanystropheids. *PLoS ONE* 15:e0230890. 10.1371/journal.pone.0230890

DeBraga M, and Reisz RR. 1995. A new diapsid reptile from the uppermost Carboniferous (Stephanian) of Kansas. *Palaeontology* 38:199-212.

DeBraga M, and Rieppel O. 1997. Reptile phylogeny and the interrelationships of turtles. *Zoological Journal of the Linnean Society* 120:281-354.

Demes B, and Krause DW. 2005. Suction feeding in a Triassic protorosaur? *Science* 308:1112-1113.

Desojo JB, Ezcurra MD, and Schultz CL. 2011. An unusual new archosauriform from the Middle–Late Triassic of southern Brazil and the monophyly of Doswelliidae. *Zoological Journal of the Linnean Society* 161:839-871.

Dias-da-Silva S, Pinheiro FL, Da-Rosa ÁAS, Martinelli AG, Schultz CL, Silva-Neves E, and Modesto SP. 2017. Biostratigraphic reappraisal of the Lower Triassic Sanga do Cabral Supersequence from South America, with a description of new material attributable to the parareptile genus *Procolophon*. *Journal of South American Earth Sciences* 79:281-296. 10.1016/j.jsames.2017.07.012

Dilkes DW. 1995. The rhynchosaur *Howesia browni* from the Lower Triassic of South Africa. *Palaeontology* 38:665-686.

Dilkes DW. 1998. The Early Triassic rhynchosaur *Mesosuchus browni* and the interrelationships of basal archosauromorph reptiles. *Philosophical Transactions of the Royal Society of London B: Biological Sciences* 353:501-541. 10.1098/rstb.1998.0225

Dilkes DW, and Arcucci AB. 2012. *Proterochampsa barrionuevoi* (Archosauriformes: Proterochampsia) from the Late Triassic (Carnian) of Argentina and a phylogenetic analysis of Proterochampsia. *Palaeontology* 55:853-885.

Dilkes DW, and Sues H-D. 2009. Redescription and phylogenetic relationships of *Doswellia kaltenbachi* (Diapsida: Archosauriformes) from the Upper Triassic of Virginia. *Journal of Vertebrate Paleontology* 29:58-79.

Dong W, Lin S, and Chen Y. 1997. Stratigraphy (Lithostratic) of Guizhou Province. *China University of Geosciences Press, Beijing*.

Dutuit J. 1972. Découverte d'un dinosaure ornithischien dans le Trias supérieur de l'Atlas occidental marocain. *Comptes Rendus de l'Académie des Sciences* 275:2841–2844.

Dzik J, and Sulej T. 2007. A review of the early Late Triassic Krasiejów biota from Silesia, Poland. *Palaeontologia Polonica*:3-27.

Dzik J, and Sulej T. 2016. An early Late Triassic long-necked reptile with a bony pectoral shield and gracile appendages. *Acta Palaeontologica Polonica* 61:805-823.

Edinger T. 1924. Rückenmark im Wirbelkörper! *Anatomischer Anzeiger* 57:515-519.

El-Toubi MR. 1949. The post-cranial osteology of the lizard, *Uromastyx aegyptia* (Forskål). *Journal of Morphology* 84:281-292.

Ellenberger P. 1977. Quelques précisions sur l'anatomie et la place systématique trés spéciale de Cosesaurus Aviceps.(Ladinien Su périeur de Montral, Catalogne). *Cuadernos de geología ibérica= Journal of iberian geology: an international publication of earth sciences*:169-188.

Ellenberger P. 1978. L'origine des oiseaux. Historique et méthodes nouvelles. Les problèmes des Archaeornithes. La venue au jour de *Cosesaurus aviceps*. *Mémoires Travaux EPHE, Institut Montpellier* 4:91-117.

Ellenberger P, and De Villalta JF. 1974. Sur la présence d'un ancêtre probable des oiseaux dans le Muschelkalk supérieur de Catalogne (Espagne). Note préliminaire. *Acta geológica hispánica* 9:162-168.

Evans SE. 1980. The skull of a new eosuchian reptile from the Lower Jurassic of South Wales. *Zoological Journal of the Linnean Society* 70:203-264. 10.1111/j.1096-3642.1980.tb00852.x

Evans SE. 1981. The postcranial skeleton of the Lower Jurassic eosuchian *Gephyrosaurus bridensis*. *Zoological Journal of the Linnean Society* 73:81-116. 10.1111/j.1096-3642.1981.tb01580.x

Evans SE. 1986. The braincase of *Prolacerta broomi* (Reptilia, Triassic). *Neues Jahrbuch für Geologie und Paläontologie Abhandlungen* 173:181-200.

Evans SE. 1987. The braincase of *Youngina capensis* (Reptilia: Diapsida; Permian). *Neues Jahrbuch für Geologie und Paläontologie Monatshefte* 1987:193-203.

Evans SE. 1988. The early history and relationships of the Diapsida. *In The Phylogeny and Classification of the Tetrapods, Volume 1: Amphibians, Reptiles, Birds, by Benton, M J, Clarendon Press, Oxford* Systematics Association Special Volume No. 35A:221-260.

Evans SE. 2009. An early kuehneosaurid reptile from the Early Triassic of Poland. *Palaeontologia Polonica* 65:145-178.

Evans SE, and Borsuk-Białynicka M. 2009. A small lepidosauromorph reptile from the Early Triassic of Poland. *Palaeontologia Polonica* 65:179-202.

Evans SE, and Jones MEH. 2010. The origin, early history and diversification of lepidosauromorph reptiles. *New aspects of Mesozoic biodiversity*: Springer, 27-44.

Evans SE, and Kermack K. 1994. Assemblages of small tetrapods from the Early Jurassic of Britain. In: Fraser NC, and Sues H-D, eds. *In the shadow of the dinosaurs: Early Mesozoic tetrapods*: Cambridge University Press, 271-283.

Evans SE, and King MS. 1993. A new specimen of *Protorosaurus* (Reptilia: Diapsida) from the Marl Slate (late Permian) of Britain. *Proceedings of the Yorkshire Geological Society* 49:229-234.

Evans SE, and Van Den Heever JA. 1987. A new reptile (Reptilia: Diapsida) from the Upper Permian *Daptocephalus* zone of South Africa. *South African Journal of Science* 83:724-730.

Ewer RF. 1965. The anatomy of the thecodont reptile *Euparkeria capensis* Broom. *Philosophical Transactions of the Royal Society B* 248:379-435.

Ezcurra MD. 2016. The phylogenetic relationships of basal archosauromorphs, with an emphasis on the systematics of proterosuchian archosauriforms. *PeerJ* 4:e1778. 10.7717/peerj.1778

Ezcurra MD, and Butler RJ. 2015a. Post-hatchling cranial ontogeny in the Early Triassic diapsid reptile *Proterosuchus fergusi*. *Journal of Anatomy* 226:387-402.

Ezcurra MD, and Butler RJ. 2015b. Taxonomy of the proterosuchid archosauriforms (Diapsida: Archosauromorpha) from the earliest Triassic of South Africa, and implications for the early archosauriform radiation. *Journal of Anatomy* 58:141–170.

Ezcurra MD, and Butler RJ. 2018. The rise of the ruling reptiles and ecosystem recovery from the Permo-Triassic mass extinction. *Proceedings of the Royal Society B: Biological Sciences* 285. 10.1098/rspb.2018.0361

Ezcurra MD, Desojo JB, and Rauhut OWM. 2015. Redescription and phylogenetic relationships of the proterochampsid *Rhadinosuchus gracilis* (Diapsida: Archosauriformes) from the early Late Triassic of southern Brazil. *Ameghiniana* 52:391-417.

Ezcurra MD, Fiorelli LE, Martinelli AG, Rocher S, von Baczko MB, Ezpeleta M, Taborda JR, Hechenleitner EM, Trotteyn MJ, and Desojo JB. 2017. Deep faunistic turnovers preceded the rise of dinosaurs in southwestern Pangaea. *Nature ecology & evolution* 1:1477-1483. 10.1038/s41559-017-0305-5

Ezcurra MD, Gower DJ, Sennikov AG, and Butler RJ. 2019. The osteology of the holotype of the early erythrosuchid *Garjainia prima* (Diapsida: Archosauromorpha) from the upper Lower Triassic of European Russia. *Zoological Journal of the Linnean Society* 185:717-783.

Ezcurra MD, Lecuona A, and Martinelli A. 2010. A new basal archosauriform diapsid from the Lower Triassic of Argentina. *Journal of Vertebrate Paleontology* 30:1433-1450.

Ezcurra MD, Montefeltro F, and Butler RJ. 2016. The early evolution of rhynchosaurs. *Frontiers in Ecology and Evolution* 3:142. 10.3389/fevo.2015.00142

Ezcurra MD, Scheyer TM, and Butler RJ. 2014. The origin and early evolution of Sauria: reassessing the Permian saurian fossil record and the timing of the crocodile-lizard divergence. *PLoS ONE* 9:e89165.

Feduccia A. 1996. The origin and evolution of Birds. *Yale University Press New Haven and London*.

Feduccia A, and Wild R. 1993. Birdlike Characters in the Triassic Archosaur *Megalancosaurus*. *Naturwissenschaften* 80:564-566.

Feist-Burkhardt S, Götz AE, Szulc J, Borkhataria R, Geluk M, Haas J, Hornung J, Jordan P, Kempf O, and Michalík J. 2008. Triassic. *The geology of central Europe* 2:749-821.

Fichter J. 1995. Katalog des publizierten Materials aus der palaontologischen Sammlung des Naturkundemuseums der Stadt Kassel. *Philippia* 7:129-157.

Flynn JJ, Nesbitt SJ, Michael Parrish J, Ranivoharimanana L, and Wyss AR. 2010. A new species of *Azendohsaurus* (Diapsida: Archosauromorpha) from the Triassic Isalo Group of southwestern Madagascar: cranium and mandible. *Palaeontology* 53:669-688.

Ford DP, and Benson RB. 2018. A redescription of *Orovenator mayorum* (Sauropsida, Diapsida) using high-resolution μ CT, and the consequences for early amniote phylogeny. *Papers in Palaeontology*.

Ford DP, and Benson RB. 2020. The phylogeny of early amniotes and the affinities of Parareptilia and Varanopidae. *Nature ecology & evolution* 4:57-65. 10.1038/s41559-019-1047-3

Formoso KK, Nesbitt SJ, Pritchard AC, Stocker MR, and Parker WG. 2019. A long-necked tanystropheid from the Middle Triassic Moenkopi Formation (Anisian) provides insights into the ecology and biogeography of tanystropheids. *Palaeontologia Electronica* 22:1-15. 10.26879/988

Fraser N. 1982. A new rhynchocephalian from the British Upper Trias. *Palaeontology* 25:709-725.

Fraser N, and Walkden G. 1984. The postcranial skeleton of the Upper Triassic sphenodontid *Planocephalosaurus robinsonae*. *Palaeontology* 27:575-595.

Fraser NC, and Furrer H. 2013. A new species of *Macrocnemus* from the Middle Triassic of the eastern Swiss Alps. *Swiss Journal of Geosciences* 106:199-206. 10.1007/s00015-013-0137-5

Fraser NC, Grimaldi DA, Olsen PE, and Axsmith B. 1996. A Triassic Lagerstätte from eastern North America. *Nature* 380:615-619. 10.1038/380615a0

Fraser NC, and Rieppel O. 2006. A New Protorosaur (Diapsida) from the Upper Buntsandstein of the Black Forest, Germany. *Journal of Vertebrate Paleontology* 26:866-871. 10.1671/0272-4634(2006)26[866:anpdft]2.0.co;2

Fraser NC, Rieppel O, and Li C. 2013. A long-snouted protorosaur from the Middle Triassic of southern China. *Journal of Vertebrate Paleontology* 33:1120-1126. 10.1080/02724634.2013.764310

Fröbisch J, Schoch RR, Müller J, Schindler T, and Schweiss D. 2011. A new basal sphenacodontid synapsid from the Late Carboniferous of the Saar−Nahe Basin, Germany. *Acta Palaeontologica Polonica* 56:113-120.

Gans C, Darevski I, and Tatarinov LP. 1987. *Sharovipteryx*, a reptilian glider? *Palaeobiology* 13:415-426.

Gardner NM, Holiday CM, and O'Keefe FR. 2010. The Braincase of *Youngina capensis* (Reptilia, Dipsida): New Insights from High-Resolution CT Scanning of the Holotype. *Palaeontologica Electronica* 13.

Gauffre F-X. 1993. The prosauropod dinosaur *Azendohsaurus laaroussii* the upper Triassic of Morocco. *Palaeontology* 36:897-908.

Gauthier JA. 1984. A Cladistic Analysis of the Higher Categories of the Diapsida. *PhD thesis, University of California, Berkeley*:564 p.

Gauthier JA. 1994. The diversification of the amniotes. *In Spencer RS ed Major features of vertebrate evolution Knoxville: The University of Tennessee*:129-159.

Gauthier JA, Estes R, and De Queiroz K. 1988a. A phylogenetic analysis of Lepidosauromorpha. *In The Phylogenetic Relationships of the Lizard Families, by Estes, R, ed Stanford University Press, Palo Alto, California*:15-98.

Gauthier JA, Kluge AG, and Rowe T. 1988b. Amniote Phylogeny and the Importance of Fossils. *Cladistics* 4:105-209.

Goloboff PA, and Catalano SA. 2016. TNT version 1.5, including a full implementation of phylogenetic morphometrics. *Cladistics* 32:221-238. 10.1111/cla.12160

Goodrich E. 1942. The hind foot of *Youngina* and fifth metatarsal in Reptilia. *Journal of Anatomy* 76:308.

Gottmann-Quesada A, and Sander PM. 2009. A redescription of the early archosauromorph *Protorosaurus speneri* Meyer, 1832, and its phylogenetic relationships. *Palaeontographica Abteilung A*:123-220.

Gow CE. 1975. The morphology and relationships of *Youngina capensis* Broom and *Prolacerta broomi* Parrington. *Palaeontologica Africana* 18:89-131.

Gower D. 2003. Osteology of the early archosaurian reptile *Erythrosuchus africanus*, Broom. *Annals of the South African Museum* 110:1-88.

Gower DJ. 1996. The tarsus of erythrosuchid archosaurs, and implications for early diapsid phylogeny. *Zoological Journal of the Linnean Society* 116:347-375.

Gower DJ. 1997. The braincase of the early archosaurian reptile *Erythrosuchus africanus*. *Journal of Zoology* 242:557-576.

Gower DJ, and Sennikov AG. 1996. Morphology and phylogenetic informativeness of early archosaur braincases. *Palaeontology* 39:883-906.

Gower DJ, and Sennikov AG. 1997. *Sarmatosuchus* and the early history of the Archosauria. *Journal of Vertebrate Paleontology* 17:60-73.

Grand A, Corvez A, Duque Velez LM, and Laurin M. 2013. Phylogenetic inference using discrete characters: performance of ordered and unordered parsimony and of three-item statements. *Biological Journal of the Linnean Society* 110:914-930. 10.1111/bij.12159

Gregory J. 1945. Osteology and relationships of *Trilophosaurus*. *University of Texas Publication* 4401:273-359.

Groenewald GH, and Kitching JW. 1995. Biostratigraphy of the *Lystrosaurus* assemblage zone. *In Biostratigraphy of the Beaufort Group (Karoo Supergroup), by Rubidge BS, eds Pretoria: Council for Geosciences* 1.

Hancox P. 2000. The continental Triassic of South Africa. *Zentralblatt für Geologie und Paläontologie Teil I* 1998:1285-1324.

Haubold HA, and Schaumberg G. 1985. Die Fossilien des Kupferschiefers: Pflanzen-und Tierwelt zu Beginn des Zechsteins; eine Erzlagerstätte und ihre Paläontologie. *Ziemsen*.

Haughton S. 1922. On the reptilian genera *Euparkeria* Broom, and *Mesosuchus* Watson. *Transactions of the Royal Society of South Africa* 10:81-88.

Haughton S. 1924a. On a skull and partial skeleton of *Mesosuchus browni* Watson. *Transactions of the Royal Society of South Africa* 12:17-26.

Heckert AB. 2004. *Late Triassic microvertebrates from the lower Chinle Group (Otischalkian-Adamanian: Carnian), southwestern USA*: New Mexico Museum of Natural History and Science.

Hone DW, and Benton MJ. 2007. An evaluation of the phylogenetic relationships of the pterosaurs among archosauromorph reptiles. *Journal of Systematic Palaeontology* 5:465-469.

Hone DW, and Benton MJ. 2008. A new genus of rhynchosaur from the Middle Triassic of south-west England. *Palaeontology* 51:95-115.

Hsiou AS, De França MAG, and Ferigolo J. 2015. New data on the *Clevosaurus* (Sphenodontia: Clevosauridae) from the Upper Triassic of southern Brazil. *PLoS ONE* 10:1-21. 10.1371/journal.pone.0137523

Hsiou AS, Nydam RL, Simões TR, Pretto FA, Onary S, Martinelli AG, Liparini A, de Vivar Martínez PRR, Soares MB, and Schultz CL. 2019. A New Clevosaurid from the Triassic (Carnian) of Brazil and the Rise of Sphenodontians in Gondwana. *Scientific Reports* 9:1-12. 10.1038/s41598-019-48297-9

Huene FRv. 1902. Übersicht über die Reptilien der Trias. *Geologische und Paläontologische Abhandlungen (Neue Serie)* 6:1-84.

Huene FRv. 1905. Über die Trias-Dinosaurier Europas. *Zeitschrift der Deutschen Geologischen Gesellschaft* 57:345-349.

Huene FRv. 1908. Die Dinosaurier der europäischen Triasformation mit Berücksichtigung der aussereuropäischen Vorkommnisse. *Geologische und Paläontologische Abhandlungen Supplement* 1:1-419.

Huene FRv. 1911. Über *Erythrosuchus*, Vertreter der neuen Reptil-Ordnung Pelycosimia. *Geologische und Paläontologische Abhandlungen* 10:1-60.

Huene FRv. 1931. Über *Tanystropheus* und verwandte Formen. *Neues Jahrbuch für Geologie und Paläontologie, BB* 67:65-86.

Huene FRv. 1946. Die grossen Stämme der Tetrapoden in den geologischen Zeiten. *Biologisches Zentralblatt* 65:268-275.

Huene FRv. 1954. Ein neuer Protorosauride. *NEues Jahrbuch für Geologie und Paläontologie, Monatshefte* 5:228-230.

Hutchinson M, Skinner A, and Lee M. 2012. *Tikiguania* and the antiquity of squamate reptiles (lizards and snakes). *Biology Letters* 8:665-669.

Huxley TH. 1871. *A manual of the anatomy of vertebrated animals*. London: J. & A. Churchill.

Irmis RB, Mundil R, Martz JW, and Parker WG. 2011. High-resolution U–Pb ages from the Upper Triassic Chinle Formation (New Mexico, USA) support a diachronous rise of dinosaurs. *Earth and Planetary Science Letters* 309:258-267.

Ivakhnenko MF, and Kurochkin EN. 2008. *Fossil Reptiles and Birds Part 1*. Moscow: GEOS.

Jalil N-E. 1990. Sur deux crânes de petits Sauria (Amniota, Diapsida) du Trias moyen d'Algérie. *Comptes rendus de l'Académie des sciences Série 2, Mécanique, Physique, Chimie, Sciences de l'univers, Sciences de la Terre* 311:731-736.

Jalil N-E. 1997. A new prolacertiform diapsid from the Triassic of North Africa and the interrelationships of the Prolacertiformes. *Journal of Vertebrate Paleontology* 17:506-525. 10.1080/02724634.1997.10010998

Jalil N-E. 1999. Continental Permian and Triassic vertebrate localities from Algeria and Morocco and their stratigraphical correlations. *Journal of African Earth Sciences* 29:219-226.

Jalil N, and Knoll F. 2002. Is *Azendohsaurus laaroussii* (Carnian, Morocco) a dinosaur? *Journal of Vertebrate Paleontology* 22:70A.

Jaquier VP, Fraser NC, Furrer H, and Scheyer TM. 2017. Osteology of a New Specimen of *Macrocnemus* aff. *M. fuyuanensis* (Archosauromorpha, Protorosauria) from the Middle Triassic of Europe: Potential Implications for Species Recognition and Paleogeography of Tanystropheid Protorosaurs. *Frontiers in Earth Science* 5. 10.3389/feart.2017.00091

Jaquier VP, and Scheyer TM. 2017. Bone Histology of the Middle Triassic Long-Necked Reptiles *Tanystropheus* and *Macrocnemus* (Archosauromorpha, Protorosauria). *Journal of Vertebrate Paleontology*. 10.1080/02724634.2017.1296456

Jiang D-Y, Rieppel O, Fraser NC, Motani R, Hao W-C, Tintori A, Sun Y-L, and Sun Z-Y. 2011. New information on the protorosaurian reptile *Macrocnemus fuyuanensis* Li et al., 2007, from the Middle/Upper Triassic of Yunnan, China. *Journal of Vertebrate Paleontology* 31:1230-1237. 10.1080/02724634.2011.610853

Jiang D, Motani R, Hao W, Rieppel O, Sun Y, Tintori A, Sun Z, and Schmitz L. 2009. Biodiversity and sequence of the Middle Triassic Panxian marine reptile fauna, Guizhou Province, China. *Acta Geologica Sinica-English Edition* 83:451-459. 10.1111/j.1755-6724.2009.00047.x

Kearney M, and Rieppel O. 2006. Rejecting "the given" in systematics. *Cladistics* 22:369-377.

Kuhn-Schnyder E. 1947. Der Schädel von *Tanystropheus*. *Eclogae Geologicae Helvetiae* 40:390.

Kuhn-Schnyder E. 1954. Über die Herkunft der Eidechsen. *Endeavour* 13:215-221.

Kuhn-Schnyder E. 1959. Hand und Fuss von *Tanystropheus longobardicus* (Bassani). *Eclogae Geologicae Helvetiae* 52:921-941.

Kuhn-Schnyder E. 1962. Ein weinterer Schädel von *Macrocnemus bassanii* Nopsca aus der anisischen Stufe der Trias des Monte San Giorgio (Kt. Tessin, Schweiz). *Paläontologische Zeitschrift* 36:110-133.

Kuhn-Schnyder E. 1963. Wege der Reptiliensystematik. *Paläontologische Zeitschrift* 37:61-87.

Kuhn-Schnyder E. 1967. Das Problem der Euryapsida. *Éditions du Centre national de la recherche scientifique* 163:335-348.

Kuhn-Schnyder E. 1974. Die Triasfauna der Tessiner Kalkalpen. *Vierteljahresschrift der naturforschenden Gesellschaft in Zürich, Neuljahrsblatt* 118:1-119.

Kuhn O. 1971. *Die Saurier der Deutschen Trias*. Altötting: Geiselberger.

LaBarbera MC, and Rieppel O. 2005. Suction feeding in a Triassic protorosaur? Response. *Science* 308:1113.

Lane H. 1945. New mid-Pennsylvanian reptiles from Kansas. *Transactions of the Kansas Academy of Science* 47:381-390.

Langer MC, and Schultz CL. 2000. A new species of the Late Triassic rhynchosaur *Hyperodapedon* from the Santa Maria Formation of south Brazil. *Palaeontology* 43:633-652.

Legler B, and Schneider JW. 2008. Marine ingressions into the Middle/Late Permian saline lake of the Southern Permian Basin (Rotliegend, Northern Germany) possibly linked to sea-level highstands in the Arctic rift system. *Palaeogeography, Palaeoclimatology, Palaeoecology* 267:102-114.

Lehman J-P. 1971. Nouveaux vertébrés fossiles du Trias de la Série de Zarzaitine. *Annales de Paléontologie (Vertébrés)* 57:71-93.

Lessner EJ, Parker WG, Marsh AD, Nesbitt SJ, Irmis RB, and Mueller BD. 2018. New insights into Late Triassic dinosauromorph-bearing assemblages from Texas using apomorphy-based identifications. *PaleoBios* 35.

Li C. 2003. First Record of Protorosaurid Reptile (Order Protorosauria) from the Middle Triassic of China. *Acta Geologica Sinica* 77:419-423. 10.1111/j.1755-6724.2003.tb00122.x

Li C. 2007. A juvenile *Tanystropheus* sp. (Protorosauria, Tanystropheidae) from the Middle Triassic of Guizhou, China. *Vertebrata PalAsiatica* 45:41.

Li C, Fraser NC, Rieppel O, and Wu X-C. 2018. A Triassic stem turtle with an edentulous beak. *Nature* 560:476-479. 10.1038/s41586-018-0419-1

Li C, Fraser NC, Rieppel O, Zhao L-J, and Wang L-T. 2017a. A new diapsid from the Middle Triassic of southern China. *Journal of Paleontology*:1-7. 10.1017/jpa.2017.12

Li C, Rieppel O, and Fraser NC. 2017b. Viviparity in a Triassic marine archosauromorph reptile. *Vertebrata PalAsiatica* 55:210-217.

Li C, Rieppel O, and LaBarbera MC. 2004. A Triassic aquatic protorosaur with an extremely long neck. *Science* 305:1931.

Li C, Zhao L-J, and Wang L-T. 2007. A new species of *Macrocnemus* (Reptilia: Protorosauria) from the Middle Triassic of southwestern China and its palaeogeographical implication. *Science in China Series D: Earth Sciences* 50:1601-1605. 10.1007/s11430-007-0118-5

Liu J, Organ CL, Benton MJ, Brandley MC, and Aitchison JC. 2017. Live birth in an archosauromorph reptile. *Nature communications* 8:14445. 10.1038/ncomms14445

Liutkus-Pierce CM, Fraser NC, and Heckert AB. 2014. Stratigraphy, sedimentology, and paleontology of the Upper Triassic Solite Quarry, North Carolina and Virginia. Elevating Geoscience in the Southeastern United States: New Ideas about Old Terranes—Field Guides for the 2014 GSA Southeastern Section Meeting, Blacksburg, Virginia: Boulder, CO, Geological Society of America. p 255-269.

Lucas SG. 2010. The Triassic timescale based on nonmarine tetrapod biostratigraphy and biochronology. *Geological Society, London, Special Publications* 334:447-500. 10.1144/SP334.15

MacDougall MJ, Tabor NJ, Woodhead J, Daoust AR, and Reisz RR. 2017. The unique preservational environment of the Early Permian (Cisuralian) fossiliferous cave deposits of the Richards Spur locality, Oklahoma. *Palaeogeography, Palaeoclimatology, Palaeoecology* 475:1-11.

Menning M, and Hendrich A. 2016. Deutsche Stratigraphische Kommission: Stratigraphische Tabelle von Deutschland 2016.

Merck J. 1997. A phylogenetic analysis of the euryapsid reptiles. *PhD dissertation, University of Texas at Austin, Austin, Texas*:785 p.

Meyer Hv. 1830. *Protorosaurus*. *Isis von Oken*:517-519.

Meyer Hv. 1832. Palaeologica zur Geschichte der Erde und ihrer Geschöpfe. *S Schmerber*.

Meyer Hv. 1855. Die Saurier des Muschelkalkes mit Rücksicht auf die Saurier aus buntem Sandstein und Keuper. In: Keller H, ed. *Zur Fauna der Vorwelt, zweite Abtheilung*. Frankfurt a.m.: Heinrich Keller.

Meyer Hv. 1856. Zur Fauna der Vorwelt–Saurier aus dem Kupferschiefer der Zechstein-Formation. *Keller*:24 p.

Miedema F, Spiekman SNF, Fernandez V, Reumer JWF, and Scheyer TM. 2020. Cranial morphology of the tanystropheid *Macrocnemus bassanii* unveiled using synchrotron microtomography. *Scientific reports* 10:12412. 10.1038/s41598-020-68912-4

Modesto SP, and Sues H-D. 2004. The skull of the Early Triassic archosauromorph reptile *Prolacerta broomi* and its phylogenetic significance. *Zoological Journal of the Linnean Society* 140:335-351.

Montefeltro FC, Langer MC, and Schultz CL. 2010. Cranial anatomy of a new genus of hyperodapedontine rhynchosaur (Diapsida, Archosauromorpha) from the Upper Triassic of southern Brazil. *Earth and Environmental Science Transactions of the Royal Society of Edinburgh* 101:27-52.

Müller J. 2004. The relationships among diapsid reptiles and the influence of taxon selection. *In Recent advances in the origin and early radiation of vertebrates, by Arratia G, Wilson MVH, and Cloutier R, eds Verlag Dr Friedrich Pfeil, München*:379-408.

Muscio G. 1996. Preliminary note on a specimen of Prolacertiformes (Reptilia) from the Norian (Late Triassic) of Preone (Udine, North-Eastern Italy). *Gortania - Atti del Museo Friulano di Storia Naturale* 18:33-40.

Nesbitt SJ. 2011. The early evolution of archosaurs: relationships and the origin of major clades. *Bulletin of the American Museum of Natural History* 352:292 p. 10.1206/352.1

Nesbitt SJ, Butler RJ, Ezcurra MD, Barrett PM, Stocker MR, Angielczyk KD, Smith RM, Sidor CA, Niedźwiedzki G, and Sennikov AG. 2017a. The earliest bird-line archosaurs and the assembly of the dinosaur body plan. *Nature* 544:484. 10.1038/nature22037

Nesbitt SJ, Flynn JJ, Pritchard AC, Parrish JM, Ranivoharimanana L, and Wyss AR. 2015. Postcranial anatomy and relationships of *Azendohsaurus madagaskarensis*. *Bulletin of the American Museum of Natural History* 398:1-126. 10.1206/amnb-899-00-1-126.1

Nesbitt SJ, Stocker MR, Ezcurra MD, Fraser NC, Heckert AB, Marsh A, Parker W, Mueller B, and Pritchard AC. 2017b. The 'strange reptiles' of the Triassic: the morphology, ecology, and taxonomic diversity of the clade Allokotosauria illuminated by the discovery of an early diverging member. *SVP Program and Abstracts 2017*:168.

Nopsca FB. 1923. Neubeschreibung des Trias-Pterosauriers *Tribelesodon*. *Paläontologische Zeitschrift* 5:161-181.

Nopsca FB. 1930. Notizen über *Macrochemus Bassanii* nov. gen. et spec. *Centralblatt für Mineralogie, Geologie und Paläontologie B* 7:252-255.

Nosotti S. 2007. *Tanystropheus longobardicus* (Reptilia, Protorosauria): Re-interpretations of the anatomy based on new specimens from the Middle Triassic of Besano (Lombardy, northern Italy). *Memorie della Società Italiana di Scienze Naturali e del Museo Civico di Storia Naturale di Milano* 35:1-88.

Ochev VG. 1979. New Lower Triassic archosaurs from the eastern part of the European USSR. *Palaeontological Journal* 1:104-109.

Olsen PE. 1979. A new aquatic eosuchian from the Newark Supergroup (Late Triassic-Early Jurassic) of North Carolina and Virginia. *Postilla* 176:1-14.

Olson EC, and Broom R. 1937. New genera and species of tetrapods from the Karroo beds of South Africa. *Journal of Paleontology*:613-619.

Ortlam D. 1966. Fossile Böden als Leithorizonte für die Gliederung des Höheren Buntsandsteins im nördlichen Schwarzwald und südlichen Odenwald. *Geologisches Jahrbuch* 84:485-590.

Osborn HF. 1903. The reptilian subclasses Diapsida and Synapsida and the early history of the Diaptosauria. *Memoirs of the American Museum of Natural History* 1:449-519.

Otschev VG. 1986. Concerning the Middle Triassic reptiles from the southern Cis-Ural region. *Ezhegodnik Vsesoyuznogo Paleontologicheskogo Obshchestva* 29:171-179.

Owen R. 1842. Description of parts of the skeleton and teeth of five species of the genus *Labyrinthodon* (*Lab. leptognathus*, *Lab. pachygnathus*, and *Lab. ventricosus*, from the Coton-end and Cubbington Quarries of the Lower Warwick Sandstone; *Lab. Jaegeri*, from Guy's Cliff, Warwick; and *Lab.*

scutulatus, from Leamington); with remarks on the probable identity of the *Cheirotherium* with this genus of extinct batrachians. *Transactions of the Geological Society, London* 2:515-543.

Padian K. 1997. Pterosauromorpha. *In Encyclopedia of dinosaurs, by Currie, PJ, and Padian, K, eds San Diego, Academic Press*:617-618.

Padian K, and Chiappe LM. 1998. The origin and early evolution of birds. *Biological Reviews* 73:1-42.

Parker WG, and Martz JW. 2010. The Late Triassic (Norian) Adamanian–Revueltian tetrapod faunal transition in the Chinle Formation of Petrified Forest National Park, Arizona. *Earth and Environmental Science Transactions of the Royal Society of Edinburgh* 101:231-260. 10.1017/S1755691011020020

Parks P. 1969. Cranial anatomy and mastication of the Triassic reptile *Trilophosaurus* MSc. University of Texas at Austin.

Parrington FR. 1935. On *Prolacerta broomi*, gen. et sp. n. and the origin of lizards. *Annals and Magazine of Natural History Series 10* 16:197-205.

Parrington FR. 1956. A Problematic Reptile from the Upper Permian. *The Annals and magazine of natural history; zoology, botany, and geology* 12:333-336.

Parrish JM. 1992. Phylogeny of the Erythrosuchidae (Reptilia: Archosauriformes). *Journal of Vertebrate Paleontology* 12:93-110.

Peabody FE. 1952. *Petrolacosaurus kansensis* Lane, a Pennsylvanian reptile from Kansas. *University of Kansas Paleontological Contributions - Vertebrata*:1-41.

Peecook BR, Smith RM, and Sidor CA. 2019. A novel archosauromorph from Antarctica and an updated review of a high-latitude vertebrate assemblage in the wake of the end-Permian mass extinction. *Journal of Vertebrate Paleontology* 38. 10.1080/02724634.2018.1536664

Peters D. 2000. A reexamination of four Prolacertiformes with implications for pterosaur phylogenesis. *Rivista Italiana di Paleontologia e Stratigrafia* 106:293-336.

Peters D. 2005. Suction feeding in a Triassic protorosaur? *Science* 308:1112.

Peyer B. 1930. *Tanystropheus longobardicus* Bass. sp. (Vorläufige Mitteilung). *Cbl Miner usw*:336-337.

Peyer B. 1931. Die Triasfauna der Tessiner Kalkalpen II. *Tanystropheus longobardicus* Bass. sp. *Abhandlungen der Schweizerischen Paläontologischen Gesellschaft* 50:9-110.

Peyer B. 1937. Die Triasfauna der Tessiner Kalkalpen XII. *Macrocnemus bassanii* Nopsca. *Abhandlungen der Schweizerischen Paläontologischen Gesellschaft* 54:1-87.

Pinheiro FL, França MA, Lacerda MB, Butler RJ, and Schultz CL. 2016. An exceptional fossil skull from South America and the origins of the archosauriform radiation. *Scientific Reports* 6:22817.

Pinheiro FL, Simão-Oliveira DD, and Butler RJ. 2019. Osteology of the archosauromorph *Teyujagua paradoxa* and the early evolution of the archosauriform skull. *Zoological Journal of the Linnean Society* XX:1-40. 10.1093/zoolinnean/zlz093

Pinna G. 1980. *Drepanosaurus unguicaudatus*, nuovo genere e nuova specie di Lepidosauro del trias alpino (Reptilia). *Atti della Società italiana di scienze naturali e del Museo civico di storia naturale di Milano* 121:181-192.

Pinna G. 1984. Osteologia di *Drepanosaurus unguicaudatus*, Lepidosauro triassico del Sottordine Lacertilia. *Atti della Società Italiana Scienze Naturali* 124:7-28.

Pinna G. 1986. On *Drepanosaurus unguicaudatus*, an Upper Triassic Lepidosaurian from the Italian Alps. *Journal of Paleontology* 60:1127-1132.

Pinna G. 1993. The Norian Reptiles from Northern Italy. *Paleontologia Lombarda Nuova* Serie 2:115-124.

Premru E. 1991. Beschreibung eines neuen Fundes von *Macrocnemus bassanii* Nopsca (Reptilia, Squamata, Prolacertiformes) aus der Grenzbitumenzone (Anis/Ladin) des Monte San Giorgio (Besano, I). *Diplomarbeit an der Philosophischen Fakultät II der Universität Zürich*.

Pritchard AC, Gauthier JA, Hanson M, Bever GS, and Bhullar B-AS. 2018. A tiny Triassic saurian from Connecticut and the early evolution of the diapsid feeding apparatus. *Nature communications* 9:1213.

Pritchard AC, and Nesbitt SJ. 2017. A bird-like skull in a Triassic diapsid reptile increases heterogeneity of the morphological and phylogenetic radiation of Diapsida. *Royal Society Open Science* 4.

Pritchard AC, and Sues H-D. 2019. Postcranial remains of *Teraterpeton hrynewichorum* (Reptilia: Archosauromorpha) and the mosaic evolution of the saurian postcranial skeleton. *Journal of Systematic Palaeontology* 17:1745-1765. 10.1080/14772019.2018.1551249

Pritchard AC, Turner AH, Irmis RB, Nesbitt SJ, and Smith ND. 2016. Extreme Modification of the Tetrapod Forelimb in a Triassic Diapsid Reptile. *Current Biology* 26:1-8.

Pritchard AC, Turner AH, Nesbitt SJ, Irmis RB, and Smith ND. 2015. Late Triassic tanystropheids (Reptilia, Archosauromorpha) from Northern New Mexico (Petrified Forest Member, Chinle Formation) and the biogeography, functional morphology, and evolution of Tanystropheidae. *Journal of Vertebrate Paleontology*:e911186. 10.1080/02724634.2014.911186

Rauhut OWM, Heyng AM, López-Arbarello A, and Hecker A. 2012. A New Rhynchocephalian from the Late Jurassic of Germany with a Dentition That Is Unique amongst Tetrapods. *PLoS ONE* 7.

Reisz R, Modesto S, and Scott D. 2000. *Acanthotoposaurus bremneri* and the origin of the Triassic archosauromorph reptile fauna of South Africa. *South African Journal of Science* 96:443-445.

Reisz RR. 1977. *Petrolacosaurus*, the Oldest Known Diapsid Reptile. *Science* 196:1091-1093.

Reisz RR. 1981. A diapsid reptile from the Pennsylvanian of Kansas. *Special Publication of the Natural History Museum, University of Kansas* 7.

Reisz RR, Berman DS, and Scott DM. 1984. The Anatomy and Relationships of the Lower Permian Reptile *Araeoscelis*. *Journal of Vertebrate Paleontology* 4:57-67.

Reisz RR, Heaton MJ, and Pynn BR. 1982. Vertebrate fauna of late Pennsylvanian rock lake shale near Garnett, Kansas: Pelycosauria. *Journal of Paleontology*:741-750.

Reisz RR, Laurin M, and Marjanović D. 2010. *Apsisaurus witteri* from the Lower Permian of Texas: yet another small Varanopsid Synapsid, not a Diapsid. *Journal of Vertebrate Paleontology* 30:1628-1631.

Reisz RR, Modesto SP, and Scott DM. 2011a. A new Early Permian reptile and its significance in early diapsid evolution. *Proc R Soc B* 278:3731-3737.

Reisz RR, Modesto SP, and Scott DM. 2011b. A new Early Permian reptile and its significance in early diapsid evolution. *Proceedings of the Royal Society B* 278:3731–3737.

Renesto S. 1994a. *Megalancosaurus*, a possibly arboreal archosauromorph (Reptilia) from the Upper Triassic of northern Italy. *Journal of Vertebrate Paleontology* 14:38-52.

Renesto S. 1994b. A new prolacertiform reptile from the Late Triassic of Northern Italy. *Rivista Italiana di Paleontologia e Stratigrafia* 100:285-306.

Renesto S. 1994c. A reinterpretation of the pectoral girdle and anterior limb of *Drepanosaurus unguicaudatus* (Reptilia, Diapsida). *Zoological Journal of the Linnean Society* 111:247-264.

Renesto S. 2000. Bird-Like Head on a Chameleon Body: New Specimens of the Enigmatic Diapsid Reptile *Megalancosaurus* from the Late Triassic of Northern Italy. *Rivista Italiana di Paleontologia e Stratigrafia* 106:157-180.

Renesto S. 2005. A new specimen of *Tanystropheus* (Reptilia Protorosauria) from the Middle Triassic of Switzerland and the ecology of the genus. *Rivista Italiana di Paleontologia e Stratigrafia* 111:377-394.

Renesto S, and Avanzini M. 2002. Skin remains in a juvenile Macrocnemus bassanii NOPCSA (Reptilia, Prolacertiformes) from the Middle Triassic of northern Italy. *Neues Jahrbuch für Geologie und Paläontologie Abhandlungen*:31-48.

Renesto S, and Binelli G. 2006. *Vallesaurus cenensis* Wild, 1991, a Drepanosaurid (Reptilia, Diapsida) from the Late Triassic of Northern Italy. *Rivista Italiana di Paleontologia e Stratigrafia* 112:77-94.

Renesto S, and Dalla Vecchia FM. 2000. The unusual dentition and feeding habits of the prolacertiform reptile *Langobardisaurus* (Late Triassic, Northern Italy). *Journal of Vertebrate Paleontology* 20:622-627. 10.1671/0272-4634(2000)020[0622:tudafh]2.0.co;2

Renesto S, and Dalla Vecchia FM. 2005. The skull of the holotype of *Megalancosaurus preonensis* (Diapsida, Drepanosauridae) from the Upper Triassic of Northern Italy. *Rivista Italiana di Paleontologia e Stratigrafia* 111:247-257.

Renesto S, and Dalla Vecchia FM. 2007. A revision of *Langobardisaurus rossii* Bizzarini and Muscio, 1995 from the Late Triassic of Friuli (Italy). *Rivista Italiana di Paleontologia e Stratigrafia* 113:191-201.

Renesto S, Dalla Vecchia FM, and Peters D. 2002. Morphological evidence for bipedalism in the Late Triassic prolacertiform reptile *Langobardisaurus*. *Palaeobiodiversity and Palaeoenvironments* 82:94-106.

Renesto S, and Paganoni A. 1995. A new *Drepanosaurus* (Reptilia, Neodiapsida) from the Upper Triassic of Northern Italy. *Neues Jahrbuch für Geologie und Paläontologie Abhandlungen* 197:87-99.

Renesto S, Spielmann JA, Lucas SG, and Spagnoli GT. 2010. The taxonomy and paleobiology of the Late Triassic (Carnian-Norian: Adamanian-Apachean) drepanosaurs (Diapsida: Archosauromorpha: Drepanosauromorpha): Bulletin 46. *New Mexico Museum of Natural History and Science* 46.

Rieppel O. 1989. The hind limb of *Macrocnemus bassani* (Nopsca) (Reptilia, Diapsida): Development and functional anatomy. *Journal of Vertebrate Paleontology* 9:373-387.

Rieppel O. 1994. Osteology of *Simosaurus* and the interrelationships of stem-group Sauropterygia (Reptilia, Diapsida). *Fieldiana, Geology, New Series* 28:1-28.

Rieppel O. 2001. A new species of *Tanystropheus* (Reptilia: Protorosauria) from the Middle Triassic of Makhtesh Ramon, Israel. *Neues Jahrbuch für Geologie und Paläontologie Abhandlungen* 221:271-287.

Rieppel O. 2002. Feeding mechanics in Triassic stem-group sauropterygians: the anatomy of a successful invasion of Mesozoic seas. *Zoological Journal of the Linnean Society* 135:33-63.

Rieppel O, Fraser NC, and Nosotti S. 2003. The monophyly of Protorosauria (Reptilia, Archosauromorpha): a preliminary analysis. *Atti della Società italiana di scienze naturali e del Museo civico di storia naturale di Milano* 144:359-382.

Rieppel O, and Gronowski RW. 1981. The loss of the lower temporal arcade in diapsid reptiles. *Zoological Journal of the Linnean Society* 72:203-217.

Rieppel O, Jiang D-Y, Fraser NC, Hao W-C, Motani R, Sun Y-L, and Sun Z-Y. 2010. *Tanystropheus* cf. *T. longobardicus* from the early Late Triassic of Guizhou Province, southwestern China. *Journal of Vertebrate Paleontology* 30:1082-1089. 10.1080/02724634.2010.483548

Rieppel O, and Kearney M. 2007. The poverty of taxonomic characters. *Biology & Philosophy* 22:95-113.

Rieppel O, Li C, and Fraser NC. 2008. The skeletal anatomy of the Triassic protorosaur *Dinocephalosaurus orientalis*, from the Middle Triassic of Guizhou Province, southern China. *Journal of Vertebrate Paleontology* 28:95-110. 10.1671/0272-4634(2008)28[95:tsaott]2.0.co;2

Rieppel O, Mazin J-M, and Tchernov E. 1999. Sauropterygia from the Middle Triassic of Makhtesh Ramon, Negev, Israel. *Fieldiana, Geology, New Series* 40:1-85.

Rigo M, Galli M, and Jadoul F. 2009. Late Triassic biostratigraphic constraints in the Imagna Valley (western Bergamasc Alps, Italy). *Albertiana* 37:39-42.

Romer AS. 1956. Osteology of the Reptiles. *Chicago: University of Chicago Press*:772 p.

Romer AS. 1966. Vertebrate paleontology. *Chicago: University of Chicago Press* 3rd edition:468 p.

Romer AS. 1968. Notes and Comments on Vertebrate Paleontology. *The University of Chicago Press*.

Rubidge BS. 2005. Re-uniting lost continents–fossil reptiles from the ancient Karoo and their wanderlust. *South African Journal of Geology* 108:135-172.

Rubidge BS, Erwin DH, Ramezani J, Bowring SA, and de Klerk WJ. 2013. High-precision temporal calibration of Late Permian vertebrate biostratigraphy: U-Pb zircon constraints from the Karoo Supergroup, South Africa. *Geology* 41:363-366.

Saller F, Renesto S, and Dalla Vecchia FM. 2013. First record of *Langobardisaurus* (Diapsida, Protorosauria) from the Norian (Late Triassic) of Austria, and a revision of the genus. *Neues Jahrbuch für Geologie und Paläontologie Abhandlungen* 268:83-95.

Sanz JL, and López-Martínez N. 1984. The prolacertid lepidosaurian *Cosesaurus aviceps* Ellenberger & Villalta, a claimed «protoavian» from the Middle Triassic of Spain. *Geobios* 17:747-755.

Scheyer TM, Spiekman SNF, Butler RJ, Ezcurra MD, Sues H-D, and Jones MEH. 2020a. *Colobops*, a juvenile rhynchocephalian reptile (Lepidosauromorpha), not a diminutive archosauromorph with an unusually strong bite. *Royal Society Open Science* 7:1-14. 10.1098/rsos.192179

Scheyer TM, Wang W, Li C, Miedema F, and Spiekman SNF. 2020b. Osteological re-description of *Macrocnemus fuyuanensis* (Archosauromorpha, Tanystropheidea) from the Middle Triassic of China. *Vertebrata PalAsiatica* 58:169-187. 10.19615/j.cnki.1000-3118.200525

Schmidt M. 1928. *Die Lebewelt unserer Trias*. Öhringen: Hohenlohe'sche Buchhandlung.

Schmidt M. 1938. *Die Lebewelt unserer Trias (Nachtrag)*. Öhringen: Hohenlohe'sche Buchhandlung.

Sen K. 2003. *Pamelaria dolichotrachela*, a new prolacertid reptile from the Middle Triassic of India. *Journal of Asian Earth Sciences* 21:663-681.

Sengupta S, Ezcurra MD, and Bandyopadhyay S. 2017. A new horned and long-necked herbivorous stem-archosaur from the Middle Triassic of India. *Scientific Reports* 7:8366.

Sennikov AG. 1997. An enigmatic reptile from the Upper Permian of the Volga River Basin. *Paleontological Journal* 31:94-101.

Sennikov AG. 2005. A new specialized prolacertilian (Reptilia: Archosauromorpha) from the Lower Triassic of the Orenburg Region. *Paleontological Journal* 39:199-209.

Sennikov AG. 2011. New tanystropheids (Reptilia: Archosauromorpha) from the Triassic of Europe. *Paleontological Journal* 45:90-104. 10.1134/s0031030111010151

Senter P. 2004. Phylogeny of Drepanosauridae (Reptilia: Diapsida). *Journal of Systematic Palaeontology* 2:257-268.

Sharov AG. 1970. [Unusual reptile from the Lower Triassic of Fergana]. *Paleontologicheskii Zhurnal* 1:127-131.

Sharov AG. 1971. [New flying reptiles from the Mesozoic of Kazakhstan and Kirgizstan.]. *Trudy Paleontologicheskogo Instituta AN SSSR* 130:104-113.

Shishkin MA, and Sulej T. 2009. The Early Triassic temnospondyls of the Czatkowice 1 tetrapod assemblage. *Palaeontologia Polonica* 65:77.

Simões TR, Caldwell MW, Palci A, and Nydam RL. 2016. Giant taxon-character matrices: quality of character constructions remains critical regardless of size. *Cladistics* 33:198-219.

Simões TR, Caldwell MW, Tałanda M, Bernardi M, Palci A, Vernygora O, Bernardini F, Mancini L, and Nydam RL. 2018. The origin of squamates revealed by a Middle Triassic lizard from the Italian Alps. *Nature* 557:706.

Skawiński T, Tałanda M, and Sachs S. 2015. *Megacnemus* – a forgotten reptile, presumably from the Triassic of Poland. *EAVP Poster*.

Skawiński T, Ziegler M, Czepiński Ł, Szermański M, Tałanda M, Surmik D, and Niedźwiedzki G. 2017. A re-evaluation of the historical ‘dinosaur’remains from the Middle-Upper Triassic of Poland. *Historical Biology* 29:442-472. 10.1080/08912963.2016.1188385

Smith R, Rubidge B, and Van der Walt M. 2012. Therapsid biodiversity patterns and paleoenvironments of the Karoo Basin, South Africa. In: Chinsamy-Turan A, ed. *Forerunners of Mammals: Radiation, Histology, Biology Indiana University Press, Bloomington, Indiana*. Bloomington, Indiana: Indiana University Press, 30-62.

Smith RMH, and Evans SE. 1996. New material of *Youngina*: evidence of juvenile aggregation in Permian diapsid reptiles. *Palaeontology* 39:289-303.

Sobral G, and Müller J. 2019. The braincase of *Mesosuchus browni* (Reptilia, Archosauromorpha) with information on the inner ear and description of a pneumatic sinus. *PeerJ* 7:e6798.

Sobral G, Sookias RB, Bhullar B-AS, Smith RMH, Butler RJ, and Müller J. 2016. New information on the braincase and inner ear of *Euparkeria capensis* Broom: implications for diapsid and archosaur evolution. *Royal Society Open Science* 3.

Sookias RB. 2016. The relationships of the Euparkeriidae and the rise of Archosauria. *Royal Society Open Science* 3.

Sookias RB, and Butler RJ. 2013. Euparkeriidae. *Geological Society, London, Special Publications* 379:SP379. 376.

Sookias RB, Sennikov AG, Gower DJ, and Butler RJ. 2014. The monophyly of Euparkeriidae (Reptilia: Archosauriformes) and the origins of Archosauria: a revision of *Dorosuchus neoetus* from the Mid-Triassic of Russia. *Palaeontology* 57:1177-1202.

Spener CM. 1710. Disquisitio de crocodilo in lapide scissili expresso, aliisque Lithozois. *Misc Berol ad increment sci, ex scr Soc Regiae Sci exhibits* 1:92-110.

Spiekman SNF. 2018. A new specimen of *Prolacerta broomi* from the lower Fremouw Formation (Early Triassic) of Antarctica, its biogeographical implications and a taxonomic revision. *Scientific Reports* 8:17996. 10.1038/s41598-018-36499-6

Spiekman SNF, Bleeker R, Dorst M, de Haan R, Winkelhorst H, and Voeten DFAE. 2019. Tanystropheids from the Winterswijkse Steengroeve – rare but recurring elements in the Vossenveld paleoassemblage. *Grondboor & Hamer (Staringia 16)* 73:208-215. 10.5167/uzh-182944

Spiekman SNF, Neenan JM, Fraser NC, Fernandez V, Rieppel O, Nosotti S, and Scheyer TM. 2020. Aquatic habits and niche partitioning in the extraordinarily long-necked Triassic reptile *Tanystropheus*. *Current Biology* 30:1-7. 10.1016/j.cub.2020.07.025

Spiekman SNF, Neenan JM, Fraser NC, Fernandez V, Rieppel O, Nosotti S, and Scheyer TM. submitted. The cranial morphology of *Tanystropheus hydroides* (Tanystropheidae, Archosauromorpha) as revealed by synchrotron microtomography. *PeerJ*

Spiekman SNF, and Scheyer TM. 2019. A taxonomic revision of the genus *Tanystropheus* (Archosauromorpha, Tanystropheidae). *Palaeontologia Electronica* 22:1-46. 10.26879/1038

Spielmann JA, Heckert AB, and Lucas SG. 2005. The Late Triassic archosauromorph *Trilophosaurus* as an arboreal climber. *Rivista Italiana di Paleontologia e Stratigrafia* 111:395-312.

Spielmann JA, Lucas SG, Hunt AP, and Heckert AB. 2006. Reinterpretation of the holotype of *Malerisaurus langstoni*, a diapsid reptile from the Upper Triassic Chinle Group of West Texas. *New Mexico Museum Natl Hist Sci Bull* 37:543-547.

Spielmann JA, Lucas SG, Rinehart LF, and Heckert AB. 2008. The Late Triassic archosauromorph *Trilophosaurus*. *New Mexico Museum Naturall History and Science Bulletin* 43:1-177.

Stockar R. 2010. Facies, depositional environment, and palaeoecology of the Middle Triassic Cassina beds (Meride Limestone, Monte San Giorgio, Switzerland). *Swiss Journal of Geosciences* 103:101-119. 10.1007/s00015-010-0008-2

Stocker MR, Zhao L-J, Nesbitt SJ, Wu X-C, and Li C. 2017. A short-snouted, Middle Triassic phytosaur and its implications for the morphological evolution and biogeography of Phytosauria. *Scientific Reports* 7:46028.

Sues H-D, and Olsen PE. 2015. Stratigraphic and temporal context and faunal diversity of Permian-Jurassic continental tetrapod assemblages from the Fundy rift basin, eastern Canada. *Atlantic Geology* 51:139-205. 10.4138/atlgeol.2015.006

Sullivan C, Reisz RR, and May WJ. 2000. Large dissorophoid skeletal elements from the Lower Permian Richards Spur fissures, Oklahoma, and their paleoecological implications. *Journal of Vertebrate Paleontology* 20:456-461.

Szulc J, Racki G, and Bodzioch A. 2017. Comment on “An early Late Triassic long-necked reptile with a bony pectoral shield and gracile appendages” by Jerzy Dzik and Tomasz Sulej. *Acta Palaeontologica Polonica* 62:287-288. 10.4202/app.00352.2017

Tackett LS, and Tintori A. 2019. Low drilling frequency in Norian benthic assemblages from the southern Italian Alps and the role of specialized durophages during the Late Triassic. *Palaeogeography, Palaeoclimatology, Palaeoecology* 513:25-34. 10.1016/j.palaeo.2018.06.034

Tatarinov LP. 1978. Triassic Prolacertilians of the USSR. *Paleontological Journal* 12:88-100.

Tatarinov LP. 1989. [The systematic position and way of life of the problematic Upper Triassic reptile *Sharovipteryx mirabilis*]. *Paleontologicheskii Zhurnal* 2:110-112.

Tatarinov LP. 1994. Terrestrial vertebrates from the Triassic of the USSR with comments on the morphology of some reptiles. *In Evolution, Ecology and Biogeography of the Triassic Reptiles, by Mazin, J-M and Pinna, G, eds Paleontologia Lombarda, New Series, 2*:165-170.

Trotteyn MJ, and Ezcurra MD. 2014. Osteology of *Pseudochampsa ischigualastensis* gen. et comb. nov. (Archosauriformes: Proterochampsidae) from the early Late Triassic Ischigualasto Formation of northwestern Argentina. *PLoS ONE* 9.

Tschanz K. 1986. Funktionelle Anatomie der Halswirbelsäule von *Tanystropheus longobardicus* (Bassani) aus der Trias (Anis/Ladin) des Monte San Giorgio (Tessin) auf der Basis vergleichend morphologischer Untersuchungen an der Halsmuskulatur rezenter Echsen. *PhD thesis Universität Zürich*.

Tverdokhlebov VP, Tverdokhlebova GI, Surkov MV, and Benton MJ. 2003. Tetrapod localities from the Triassic of the SE of European Russia. *Earth-Science Reviews* 60:1-66.

Unwin DM, Alifanov VR, and Benton MJ. 2000. Enigmatic small reptiles from the Middle-Late Triassic of Kirgizstan. *In The age of dinosaurs in Russia and Mongolia, by Benton M J, Kurochkin E N, Shishkin M A, Unwin D M, eds Cambridge: Cambridge University Press*:140-159.

Vaughn PP. 1955. The Permian reptile *Araeoscelis* restudied. *Bulletin of the Museum of Comparative Zoology at Harvard College* 113:303-469.

Walker AD. 1969. The reptile fauna of the 'Lower Keuper' Sandstone. *Geological Magazine* 106:470-476.

Watson DMS. 1912. *Mesosuchus browni*, gen. et spec. nov. *Records of the Albany Museum* 2:298-299.

Watson DMS. 1917. A Sketch Classification of the Pre-Jurassic Tetrapod Vertebrates. *Journal of Zoology* 87:167-186.

Watson DMS. 1957. On *Millerosaurus* and the Early History of the Sauropsid Reptiles B. *Philosophical Transactions of the Royal Society of London B: Biological Sciences* 240:325-400.

Welman J. 1998. The taxonomy of the South African proterosuchids (Reptilia, Archosauromorpha). *Journal of Vertebrate Paleontology* 18:340-347.

Werning S, and Irmis R. 2010. Reconstructing the ontogeny of the Triassic basal archosauromorph *Trilophosaurus* using bone histology and limb bone morphometrics. *Journal of Vertebrate Paleontology* 30.

Whiteside DI, and Duffin CJ. 2017. Late Triassic terrestrial microvertebrates from Charles Moore's ‘Microlestes’ quarry, Holwell, Somerset, UK. *Zoological Journal of the Linnean Society* 179:677-705. 10.1111/zoj.12458

Whiteside DI, Duffin CJ, Gill PG, Marshall JEA, and Benton MJ. 2016. The Late Triassic and Early Jurassic fissure faunas from Bristol and South Wales: stratigraphy and setting. *Palaeontologia Polonica* 67:257-287. 10.4202/pp.2016.67_257

Whiteside DI, and Marshall JE. 2008. The age, fauna and palaeoenvironment of the Late Triassic fissure deposits of Tytherington, South Gloucestershire, UK. *Geological Magazine* 145:105-147. 10.1017/S0016756807003925

Wild R. 1973. Die Triasfauna der Tessiner Kalkalpen XXII. *Tanystropheus longobardicus* (Bassani) (Neue Ergebnisse). *Schweizerische Paläontologische Abhandlungen* 95:1-182.

Wild R. 1980a. Neue Funde von *Tanystropheus* (Reptilia, Squamata). *Schweizerische Paläontologische Abhandlungen* 102.

Wild R. 1980b. *Tanystropheus* (Reptilia : Squamata) and its importance for stratigraphy. *Mémoires de la Société Géologique de France, n s* 139:201-206.

Wild R. 1987. An example of biological reasons for extinction: *Tanystropheus* (Reptilia, Squamata). *Mémoires de la Société Géologique de France, n s* 150:37-44.

Wild R. 1991. *Aetosaurus* (Reptilia, Thecodontia) from the Upper Triassic (Norian) of Cene near Bergamo, Italy, with a revision of the genus. *Rivista Italiana di Paleontologia e Stratigrafia Museo Civico di Scienze Naturali "E Caffi" Bergamo* 14:1-24.

Wild R, and Oosterink H. 1984. Tanystropheus (Reptilia: Squamata) aus dem Unteren Muschelkalk von Winterswijk, Holland. *Grondboor en Hamer* 5:142-148.

Williston SW. 1925. Osteology of the Reptiles. *Society for the Study of Amphibians and Reptiles*.

Witmer LM. 1997. Craniofacial air sinus systems. In: Currie PJ, and Padian K, eds. *Encyclopedia of dinosaurs*. New York: Academic Press, 151-159.

Woodhead J, Reisz R, Fox D, Drysdale R, Hellstrom J, Maas R, Cheng H, and Edwards RL. 2010. Speleothem climate records from deep time? Exploring the potential with an example from the Permian. *Geology* 38:455-458.

Young C-C. 1973. The Discovery of Prolacertilia in Jimusar, Sinkiang. *Vertebrata PalAsiatica* 11:46-49.

Table 1(on next page)

Percentage of scored characters of each OTU for the character matrix used in this study.

Table 1. Percentage of scored characters of each OTU for the character matrix used in this study.

OTU	% of characters scored
Petrolacosaurus kansensis	87,3
Orovenator mayorum	47,6
Youngina capensis	90,6
Acerosodontosaurus piveteaui	31,6
Claudiosaurus germaini	64,2
Gephyrosaurus bridensis	78,2
Planocephalosaurus robinsonae	75,6
Czatkowiella harae	50,8
Protorosaurus speneri	73,3
Jesairosaurus lehmani	54,7
Macrocnemus bassanii	93,2
Macrocnemus obristi	8,1
Macrocnemus fuyuanensis	71,3
Tanystropheus hydroides	91,9
GMPKU P1527 *T. cf. hydroides*	24,4
Tanystropheus longobardicus	79,8
Tanystropheus conspicuus	4,6
"Tanystropheus antiquus"	5,2
Sclerostropheus fossai	4,9
Raibliania calligarisi	9,4
Augustaburiania vatagini	8,8
Langobardisaurus pandolfii	49,5
Amotosaurus rotfeldensis	45,9
AMNH FARB 7206	6,2
Tanytrachelos ahynis	37,1
Ozimek volans	31,3
Elessaurus gondwanoccidens	8,1
Pectodens zhenyuensis	45,6
Fuyuansaurus acutirostris	25,7
Dinocephalosaurus orientalis	64,8
Prolacerta broomi	96,7
Pamelaria dolichotrachela	59,3
Azendohsaurus madagaskarensis	94,5
Trilophosaurus buettneri	89,3
Mesosuchus browni	89,3
Howesia browni	46,6
Eohyosaurus wolvaardti	25,7
Teyujagua paradoxa	47,9
Proterosuchus fergusi	56,0
Proterosuchus alexanderi	74,9
Euparkeria capensis	90,2
Erythrosuchus africanus	84,4

3

Figure 1

Selected phylogenetic hypotheses for “protorosaur” relationships.

(*A*) Ezcurra 2016. (*B*) Pritchard et al. 2015. (*C*) Rieppel et al. 2003, which represent a compilation of the matrices of Benton & Allen (1997), Jalil (1997), and Dilkes (1998).

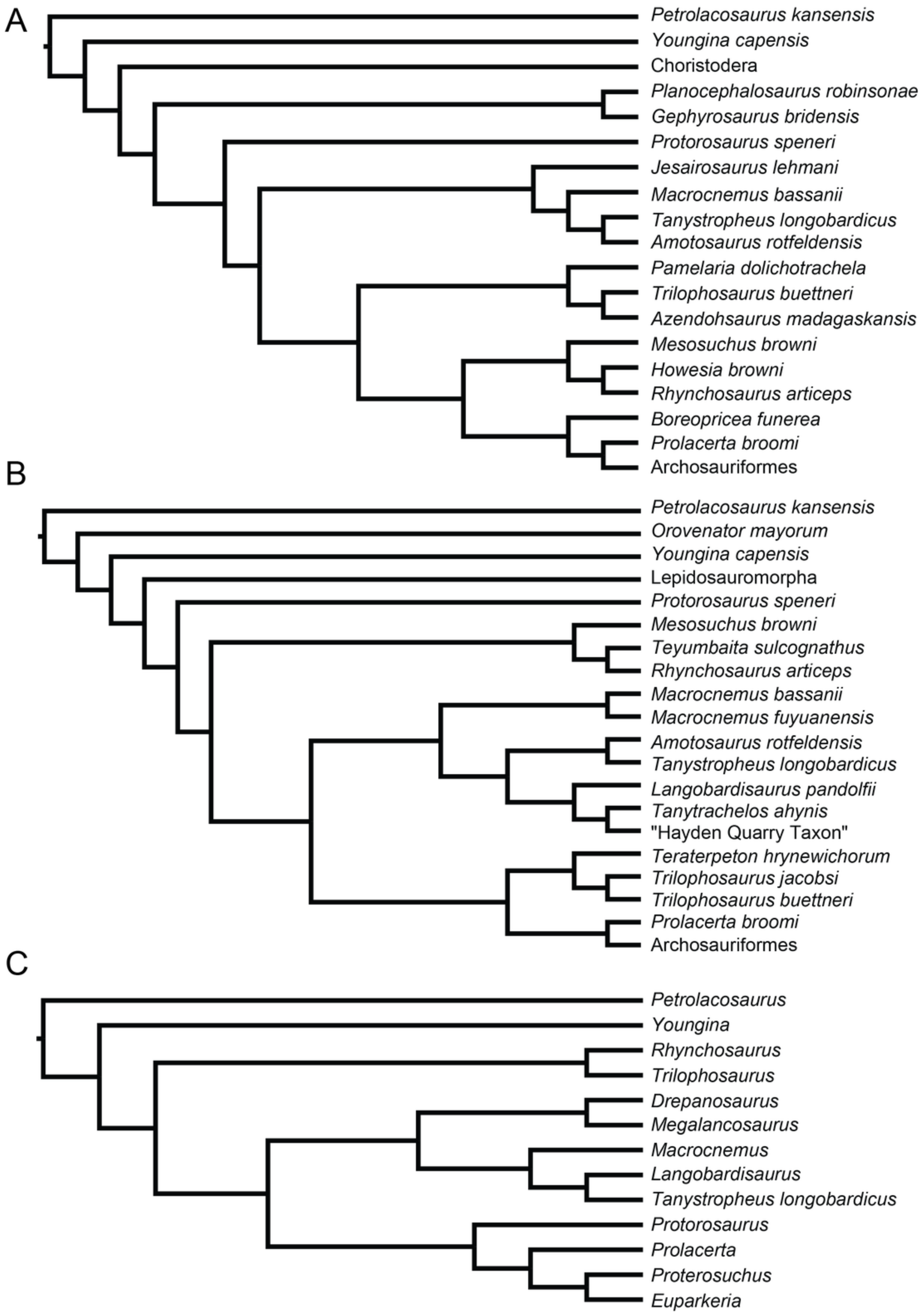
A
Petrolacosaurus kansensis
Youngina capensis
Choristodera
Planocephalosaurus robinsonae
Gephyrosaurus bridensis
Protorosaurus speneri
Jesairosaurus lehmani
Macrocnemus bassanii
Tanystropheus longobardicus
Amotosaurus rotfeldensis
Pamelaria dolichotrachela
Trilophosaurus buettneri
Azendohsaurus madagaskansis
Mesosuchus browni
Howesia browni
Rhynchosaurus articeps
Boreopricea funerea
Prolacerta broomi
Archosauriformes
B
Petrolacosaurus kansensis
Orovenator mayorum
Youngina capensis
Lepidosauromorpha
Protorosaurus speneri
Mesosuchus browni
Teyumbaita sulcognathus
Rhynchosaurus articeps
Macrocnemus bassanii
Macrocnemus fuyuanensis
Amotosaurus rotfeldensis
Tanystropheus longobardicus
Langobardisaurus pandolfii
Tanytrachelos ahynis
"Hayden Quarry Taxon"
Teraterpeton hrynewichorum
Trilophosaurus jacobsi
Trilophosaurus buettneri
Prolacerta broomi
Archosauriformes
C
Petrolacosaurus
Youngina
Rhynchosaurus
Trilophosaurus
Drepanosaurus
Megalancosaurus
Macrocnemus
Langobardisaurus
Tanystropheus longobardicus
Protorosaurus
Prolacerta
Proterosuchus
Euparkeria

Figure 2

Illustration of character 17.

(*A*) State 0 in *Prolacerta broomi* (BP/1/5880, anterior snout in left lateral view). (*B*) State 1 in a digital reconstruction of *Tanystropheus hydroides* (PIMUZ T 2790, anterior snout in left lateral view). (*C*) State 3 in *Erythrosuchus africanus* (BP/1/4526, isolated right premaxilla in lateral view). (*D*) State 4 in a digital reconstruction of *Macrocnemus bassanii* (PIMUZ T 2477, anterior snout in right lateral and medial view).

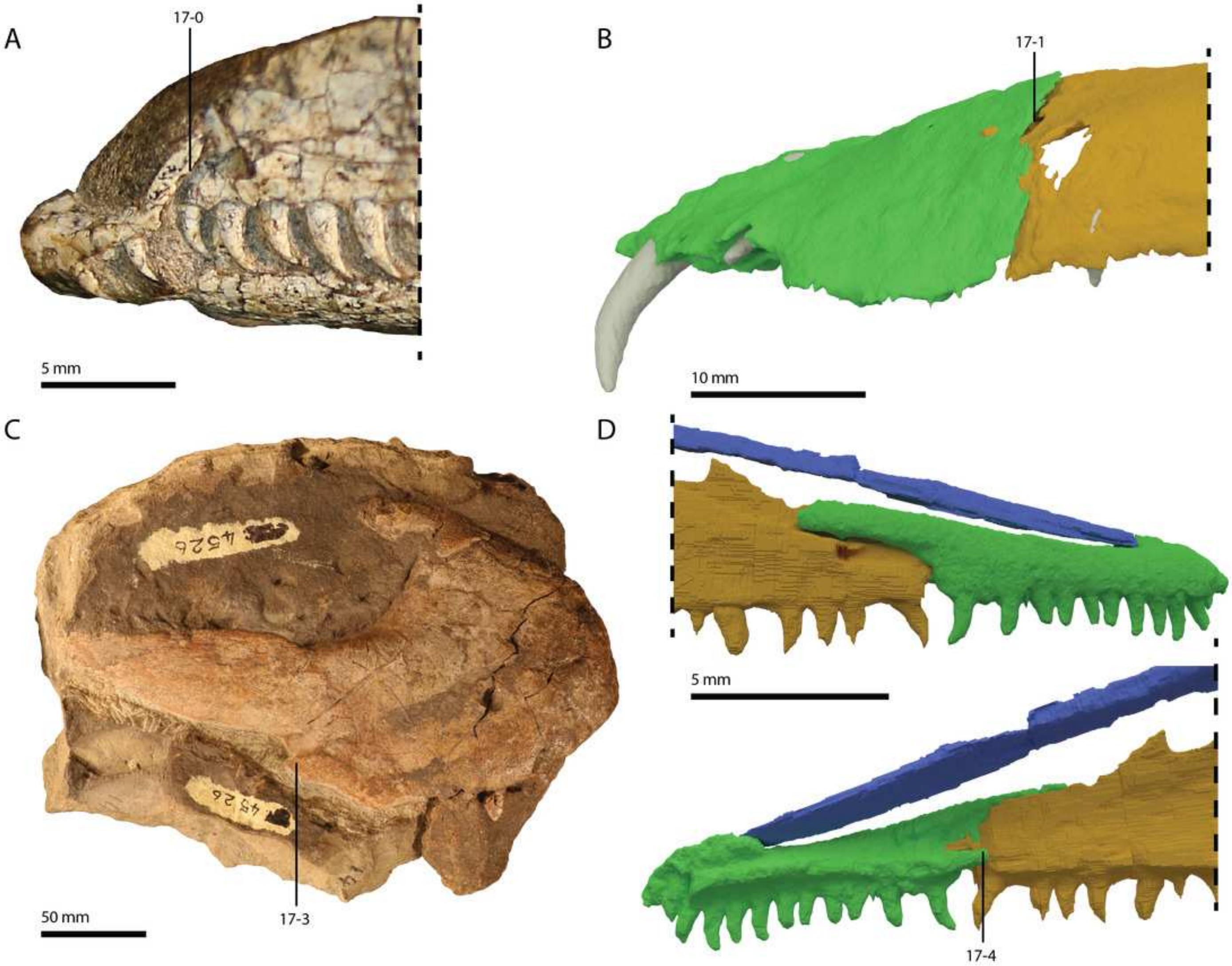

Figure 3

Illustration of character 20.

(*A*) State 0 in *Protorosaurus speneri* (NMK S 180, anterior part of the skull in right laterodorsal view). (*B*) State 1 in *Amotosaurus rotfeldensis* (SMNS 50830, right maxilla in medial view). (*C*) State 0 in *Youngina capensis* (AMNH FARB 5561, skull in right lateral view). (*D*) State 1 in *Macrocnemus fuyuanensisi* (PIMUZ T 1559, disarticulated skull with right maxilla visible in lateral view).

Figure 4

Illustration of character 23.

(*A*) State 0 in *Macrocnemus bassanii* (PIMUZ T 4822, skull in left lateral view). (*B*) State 1 in *Dinocephalosaurus orientalis* (IVPP V13767, anterior part of the skull in right laterodorsal view).

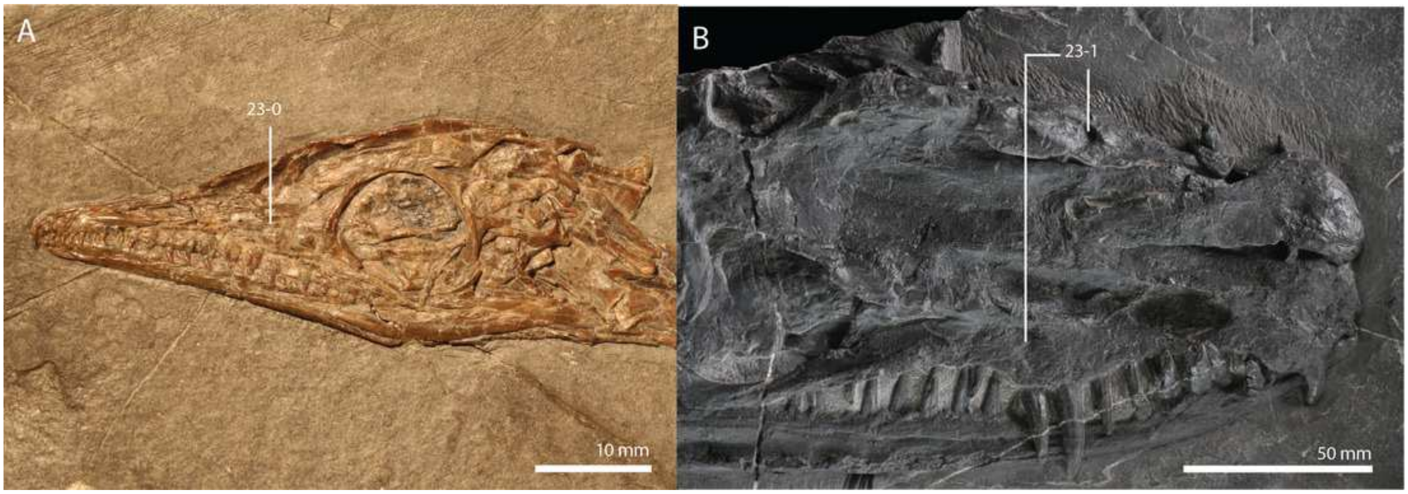

Figure 5

Illustration of character 25.

(*A*) State 0 in a digital reconstruction of *Tanystropheus hydroides* (PIMUZ T 2790, skull in right lateral view). (*B*) State 1 in a digital reconstruction of *Macrocnemus bassanii* (PIMUZ T 2477, skull in left lateral view). (*C*) State 2 in *Euparkeria capensis* (SAM-PK-5867, skull in right lateral view). (*D*) State 4 in *Dinocephalosaurus orientalis* (IVPP V13767, skull in right dorsolateral view).

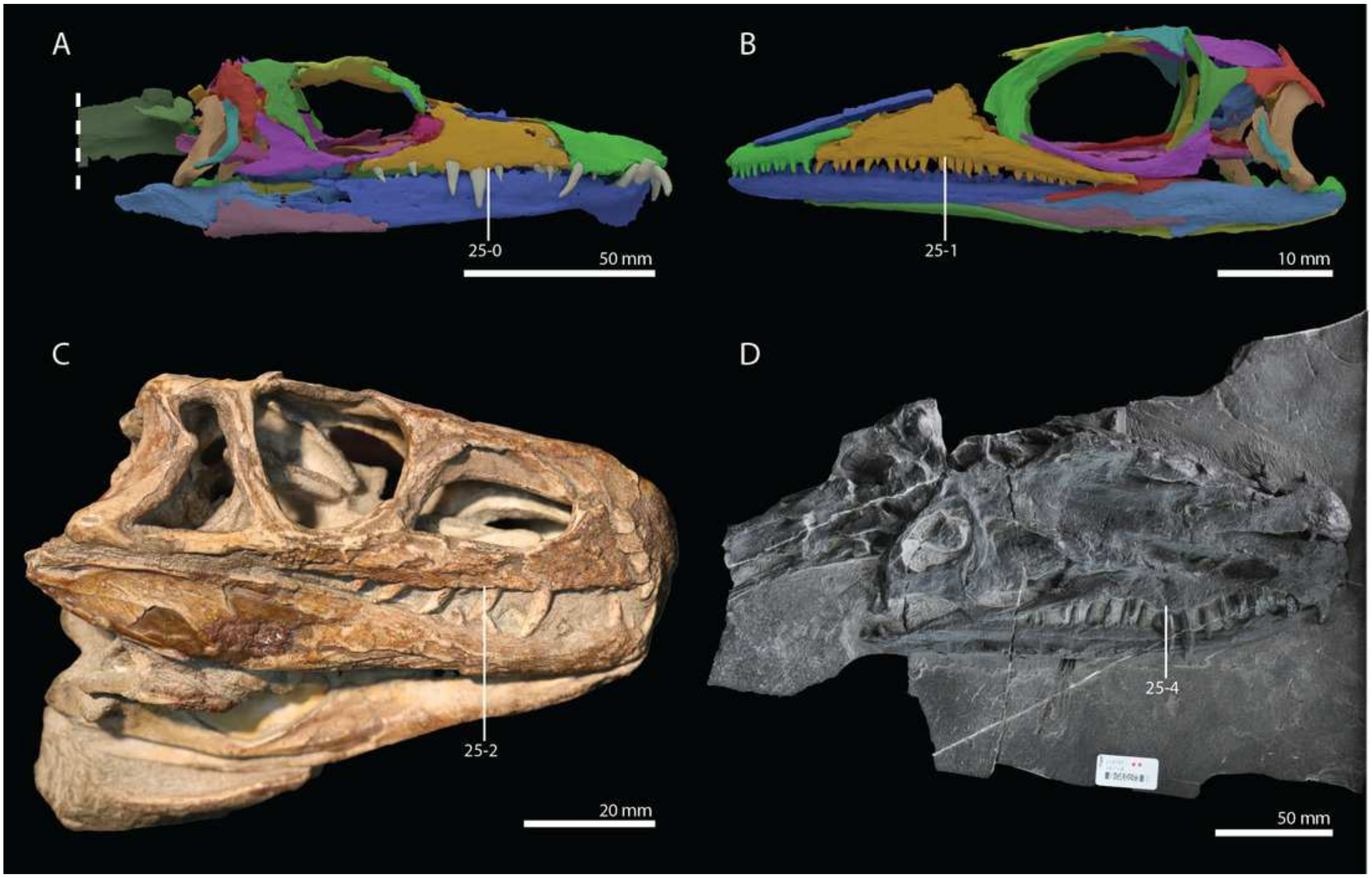

Figure 6

Illustration of character 31.

(*A*) State 0 in *Youngina capensis* (SAM-PK-K7578, skull in dorsal view). (*B*) State 1 in *Pectodens zhenyuensis* (IVPP V18578, skull in right lateral view).

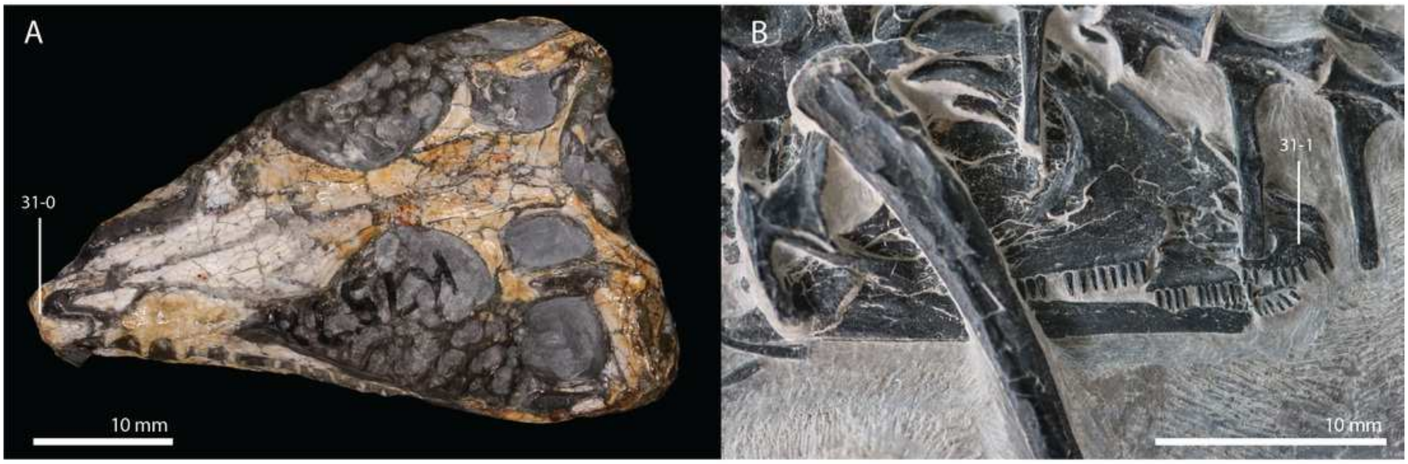

Figure 7

Illustration of character 33.

(*A*) State 1 in *Dinocephalosaurus orientalis* (IVPP V13767, anterior part of the skull in right dorsolateral view). (*B*) State 1 in *Tanystropheus hydroides* (PIMUZ T 2819, anterior part of the skull in dorsal view). (*C*) State 0 in *Mesosuchus browni* (SAM-PK-6536, skull in dorsal view). (*D*) State 0 in *Euparkeria capensis* (SAM-PK-5867, skull in dorsal view).

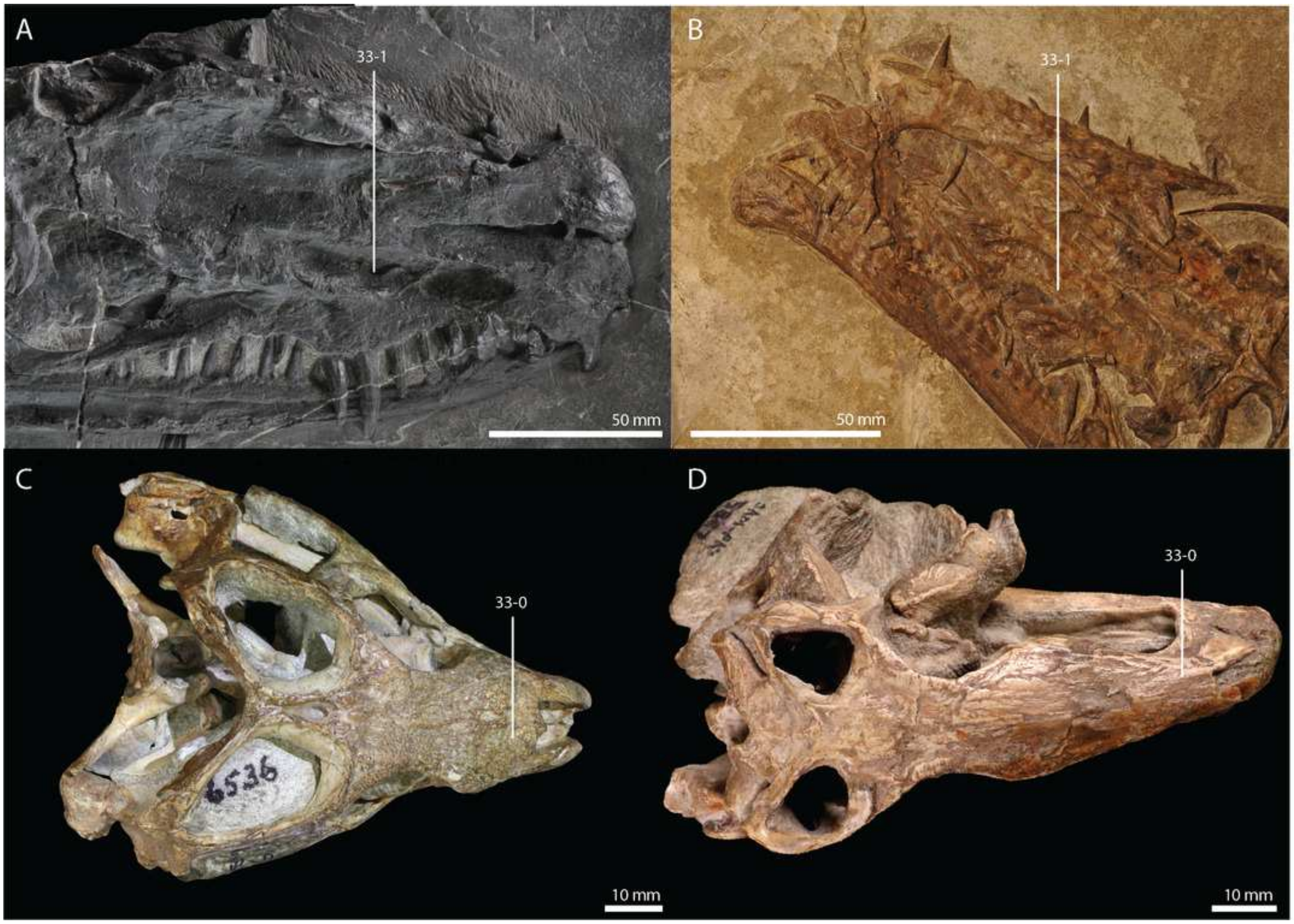

Figure 8

Illustration of characters 38 and 39.

(*A*) 38-1 and 39-0 in *Euparkeria capensis* (SAM-PK-5867, skull in left lateral view). (*B*) 38-1 and 39-1 in *Erythrosuchus africanus* (BP/1/5207, skull in right lateral view). (*C*) 38-0 and 39-1 in *Proterosuchus alexanderi* (NM QR 1484, skull in right lateral view). Image of *Proterosuchus alexanderi* courtesy of Martín Ezcurra.

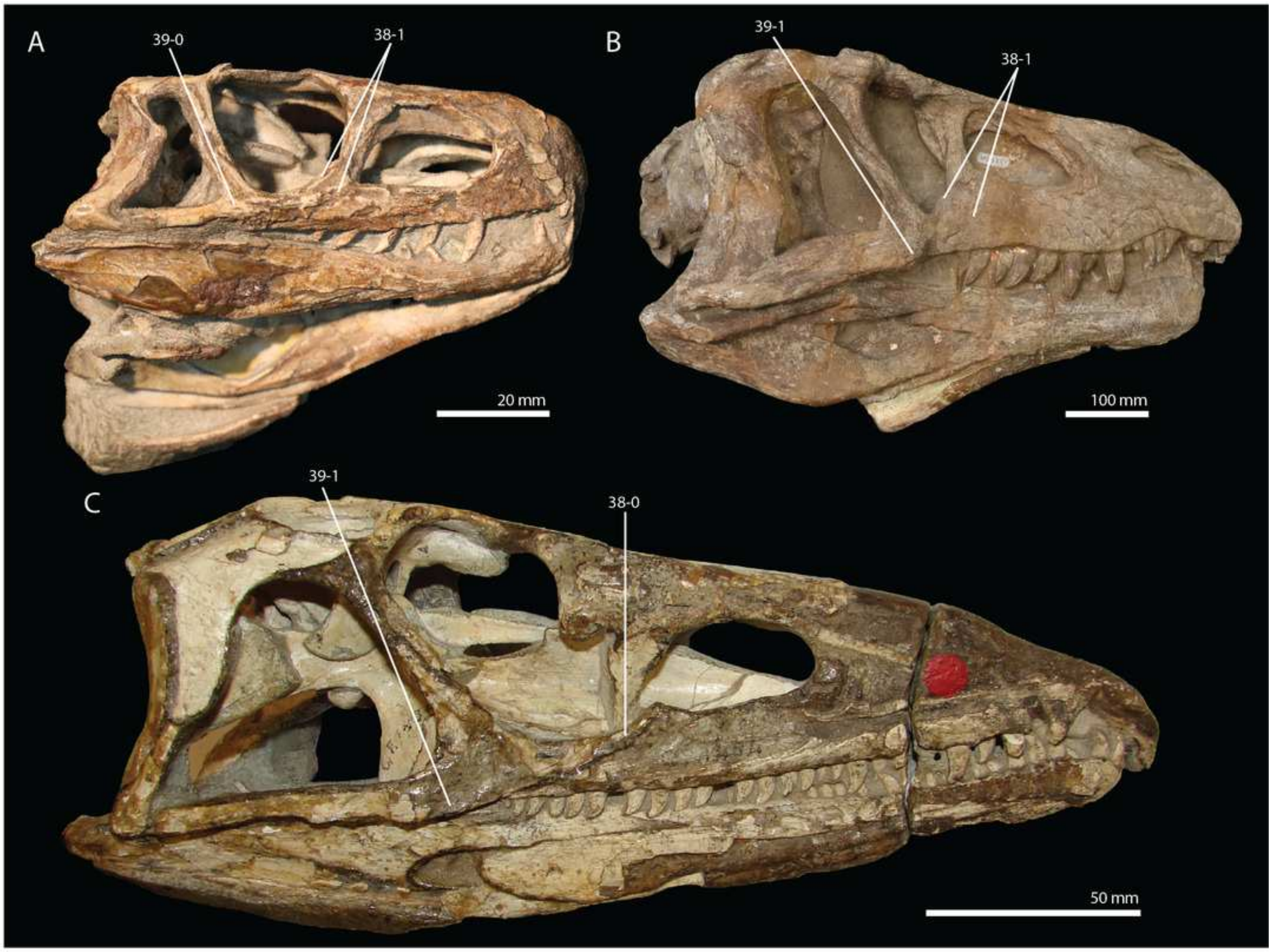

Figure 9

Figure 9. Illustration of character 42

(*A*) State 0 in *Tanystropheus longobardicus* (PIMUZ T 3901, skull in left lateral view). (*B*) State 1 in *Dinocephalosaurus orientalis* (IVPP V13767, skull in right laterodorsal view).

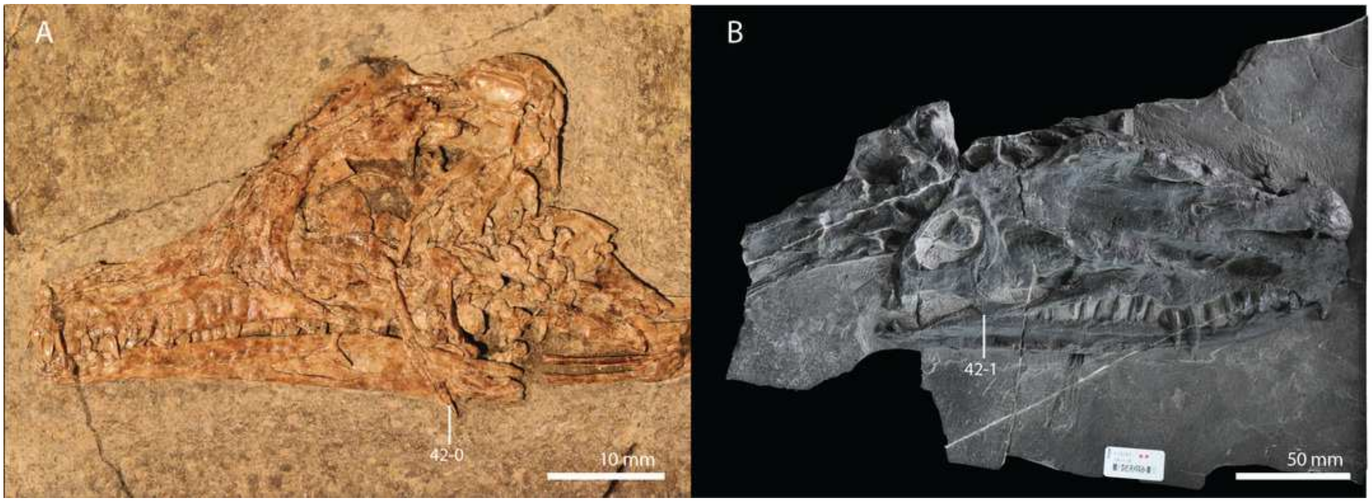

Figure 10

Illustration of character 55.

(*A*) State 1 in a digital reconstruction of *Tanystropheus hydroides* (PIMUZ T 2790, skull in dorsal view). (*B*) State 1 in *Tanystropheus longobardicus* (PIMUZ T 2484, frontal, parietal, and postfrontal in dorsal view). (*C*) State 0 in a digital reconstruction of *Macrocnemus bassanii* (PIMUZ T 2477, skull in dorsal view). (*D*) State 0 in *Prolacerta broomi* (BP/1/471, skull in dorsal view).

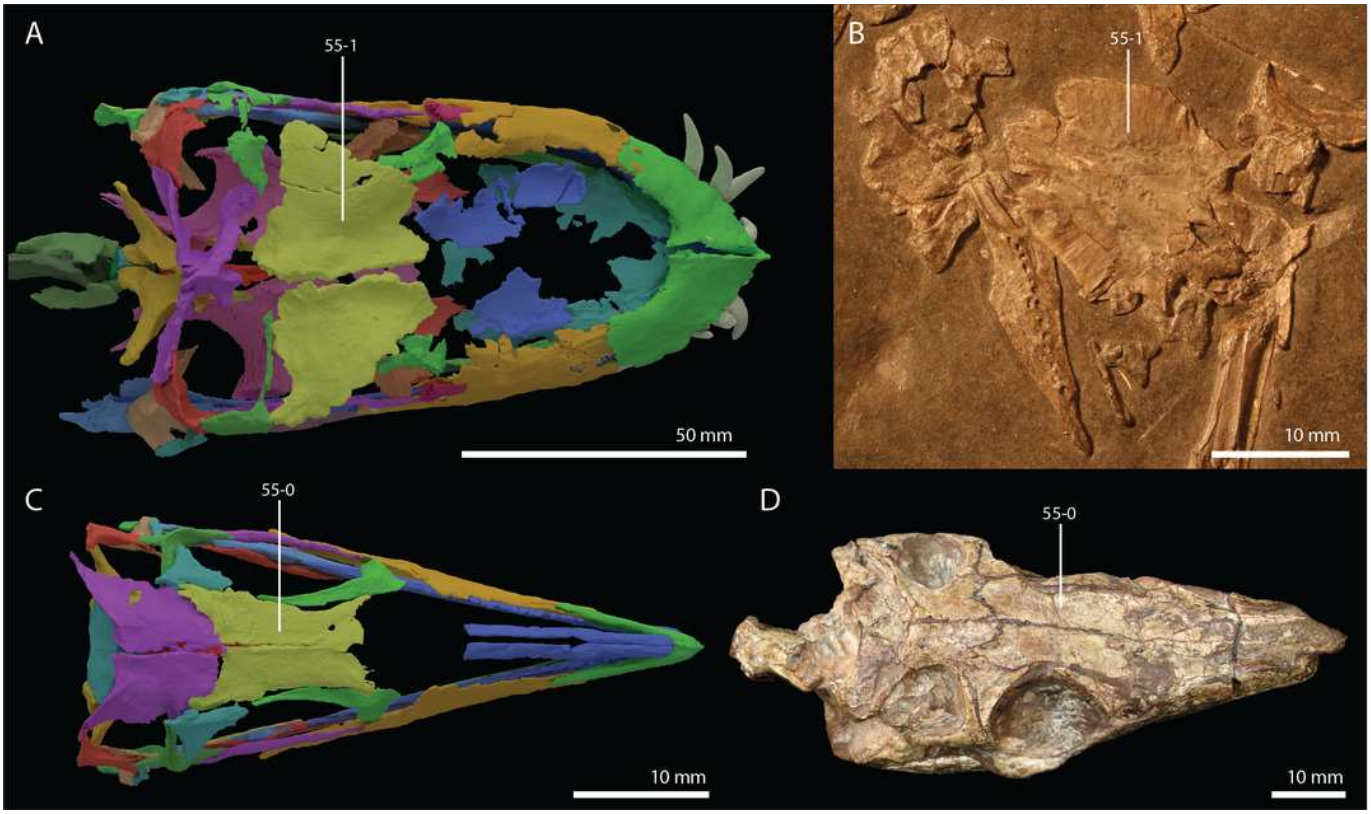

Figure 11

Illustration of character 57.

(*A*) State 0 in a digital reconstruction of *Macrocnemus bassanii* (PIMUZ T 2477, skull in dorsal view). (*B*) State 1 in *Tanystropheus longobardicus* (PIMUZ T 2484, frontal, parietal, and postfrontal in dorsal view). (*C*) State 2 in *Proterosuchus alexanderi* (NM QR 1484, skull in dorsal view). Image of *Proterosuchus alexanderi* courtesy of Martín Ezcurra.

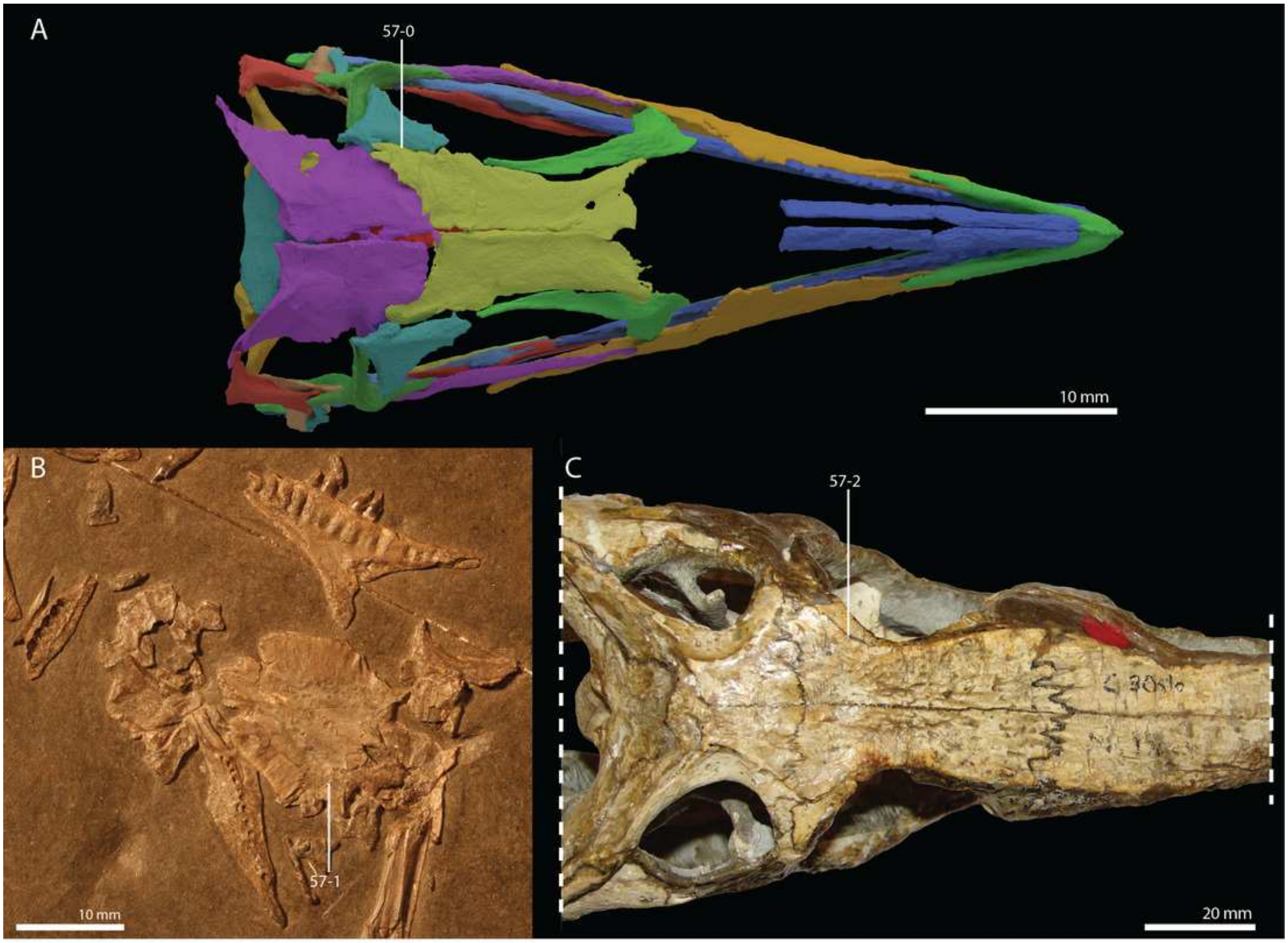

Figure 12

Illustration of characters 67 and 71.

(*A*) 67-0 in *Prolacerta broomi* (BP/1/5375, partial skull in left lateral view). (*B*) 67-1 in a digital reconstruction of *Tanystropheus hydroides* (PIMUZ T 2790, posterior part of the skull in right lateral view). (*C-D*) 67-0 and 71-0 in a digital reconstruction of *Macrocnemus bassanii* (PIMUZ T 2477, right squamosal in (*C*) lateral and (*D*) angled oblique anteromedial view). (*E-F*) 67-1 and 71-1 in a digital reconstruction of *Tanystropheus hydroides* (PIMUZ T 2790, right squamosal in (*E*) lateral and (*F*) anterior view.

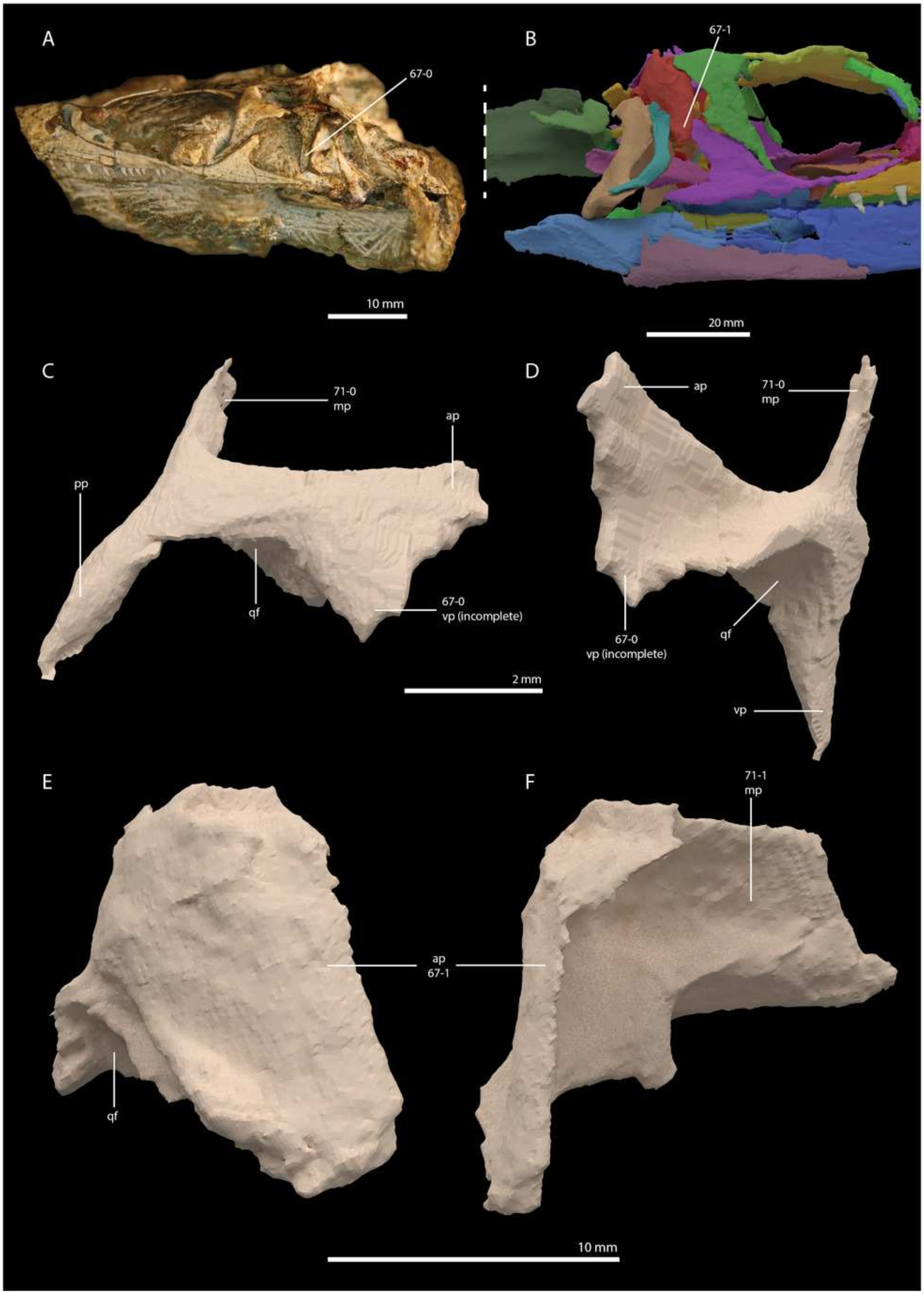
A
67-0
10 mm
B
67-1
20 mm
C
71-0
mp
ap
pp
qf
67-0
vp (incomplete)
2 mm
D
ap
71-0
mp
67-0
vp (incomplete)
qf
vp
E
qf
ap
67-1
F
71-1
mp
10 mm

Figure 13

Illustration of characters 76, 79, 81, and 83

(*A*) 76-0, 79-1, 81-1, 83-0 in *Youngina capensis* (SAM-PK-K7578, posterior part of the skull in dorsal view). (*B*) 79-1, 81-0 in a digital reconstruction of *Macrocnemus bassanii* (PIMUZ T 2477, posterior part of the skull in dorsal view). (*C*) 76-0, 79-0, 81-1, 83-2 in *Tanystropheus hydroides* (PIMUZ T 2819, posterior part of the skull in dorsal view). (*D*) 76-1, 79-1, 81-1, 83-1 in *Dinocephalosaurus orientalis* (IVPP V13767, posterior part of the skull in right laterodorsal view).

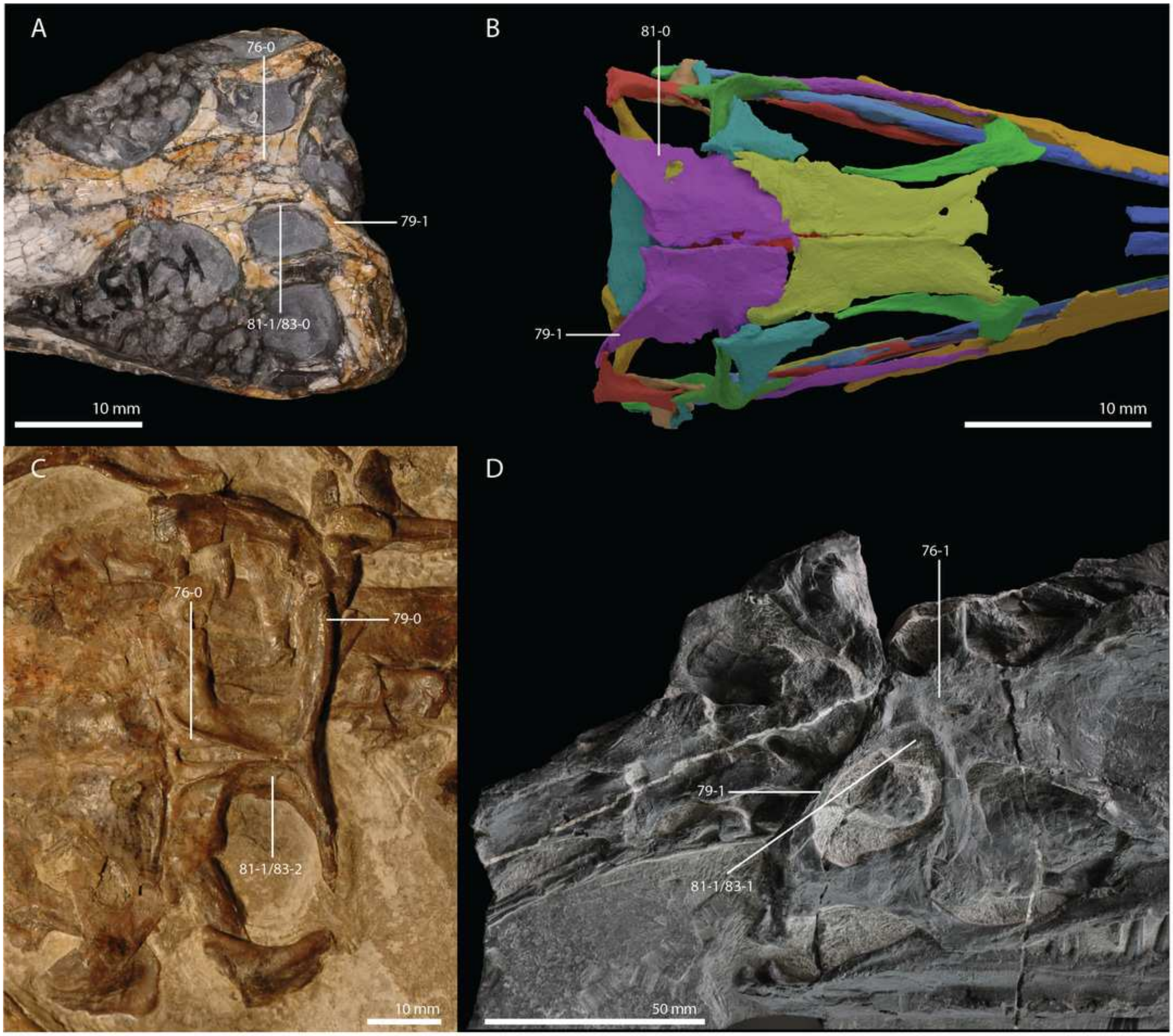
A
76-0
79-1
81-1/83-0
10 mm
B
81-0
79-1
10 mm
C
76-0
79-0
81-1/83-2
10 mm
D
76-1
79-1
81-1/83-1
50 mm

Figure 14

Illustration of characters 92, 93, and 94.

(*A-B*) 92-0, 93-1, 94-1 in a digital reconstruction of *Tanystropheus hydroides* (PIMUZ T 2790, right quadrate in (*A*) posterior and (*B*) medial view). (*C*) 94-0 in *Macrocnemus fuyuanensis* (PIMUZ T 1559, right quadrate in anterior view). (*D*) 92-0 and 93-0 in *Proterosuchus alexanderi* (NM QR 1484, left side of the skull in posterior/occipital view). Image of *Proterosuchus alexanderi* courtesy of Martín Ezcurra.

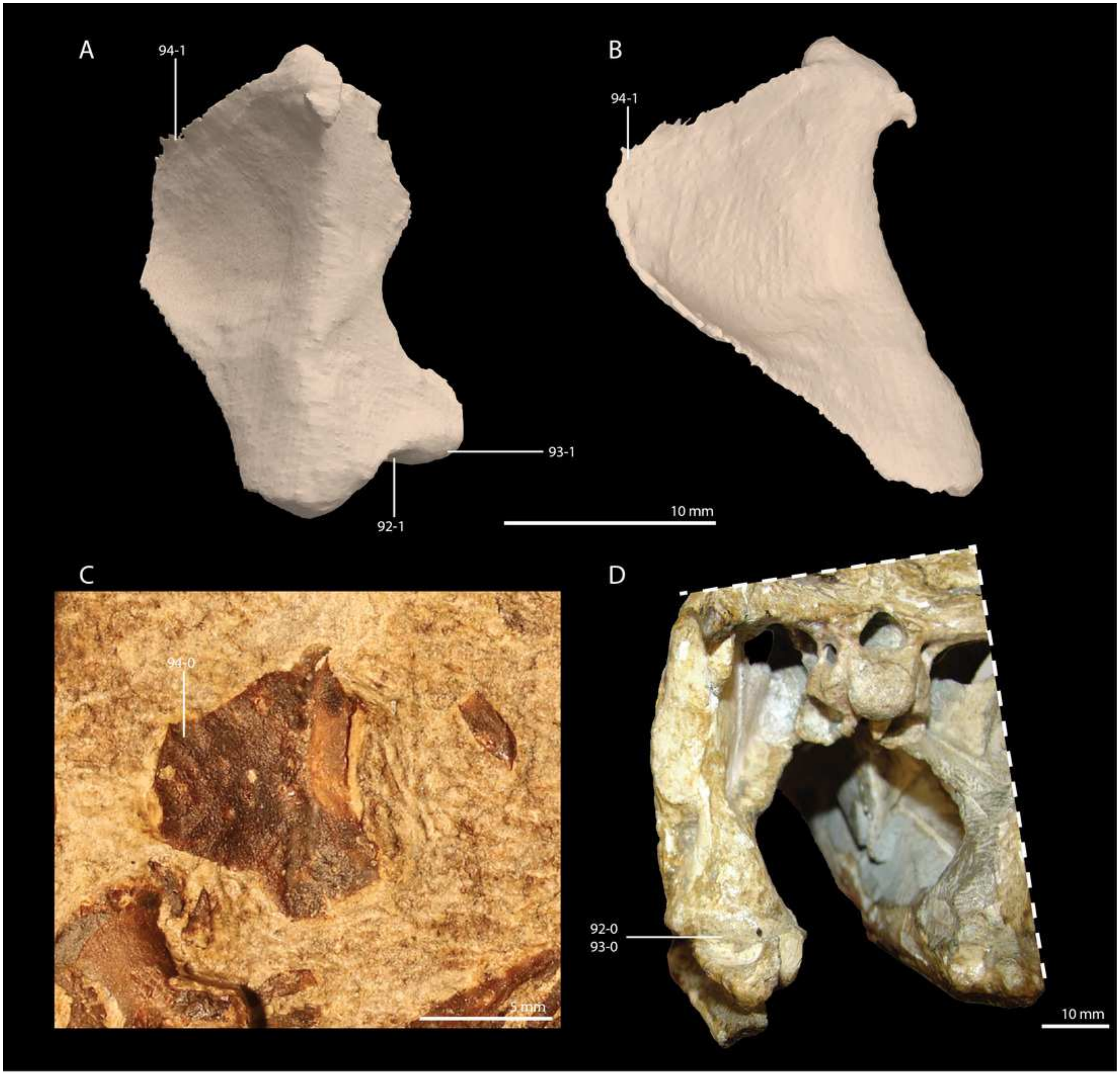
A
94-1
93-1
92-1
B
94-1
10 mm
C
94-0
5 mm
D
92-0
93-0
10 mm

Figure 15

Illustration of characters 97, 101, 105, 108, 109, and 110.

(*A*) 105-0, 108-0, 109-0, and 110-1 in *Macrocnemus fuyuanensis* (palatal reconstruction, modified from Scheyer et al. 2020b). (*B*) 97-1, 101-1, 105-1, 108-0, 109-0, and 110-0 in *Azendohsaurus madagaskarensis* (palatal reconstruction, modified from Flynn et al. 2010). (*C*) 97-0, 101-1, 105-0, 108-0, and 109-1 in *Tanystropheus longobardicus* (palatal reconstruction, modified from Spiekman et al. 2020). (*D*) 97-1, 108-1, 109-1, and 110-0 in *Tanystropheus hydroides* (palatal reconstruction, modified from Spiekman et al. 2020).

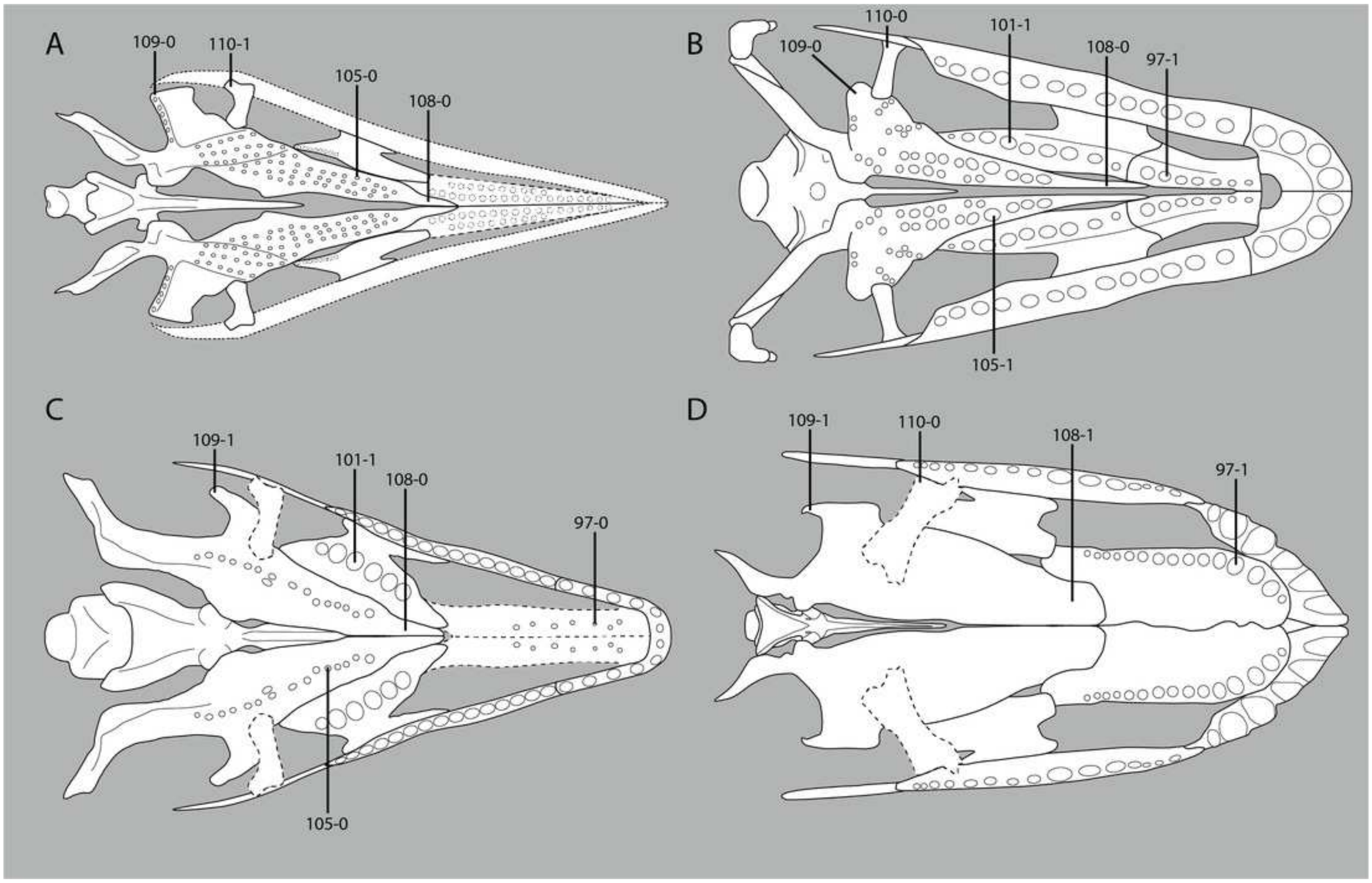

Figure 16

Illustration of characters 124 and 128.

(*A*) 124-0 and 128-1 in a digital reconstruction of *Macrocnemus bassanii* (PIMUZ T 2477, skull in posterior/occipital view). (*B*) 124-0 and 128-2 in *Erythrosuchus africanus* (BP/1/3893, partial braincase in posterior/occipital view). (*C*) 124-1 in a digital reconstruction of *Tanystropheus hydroides* (PIMUZ T 2790, skull in posterior view).

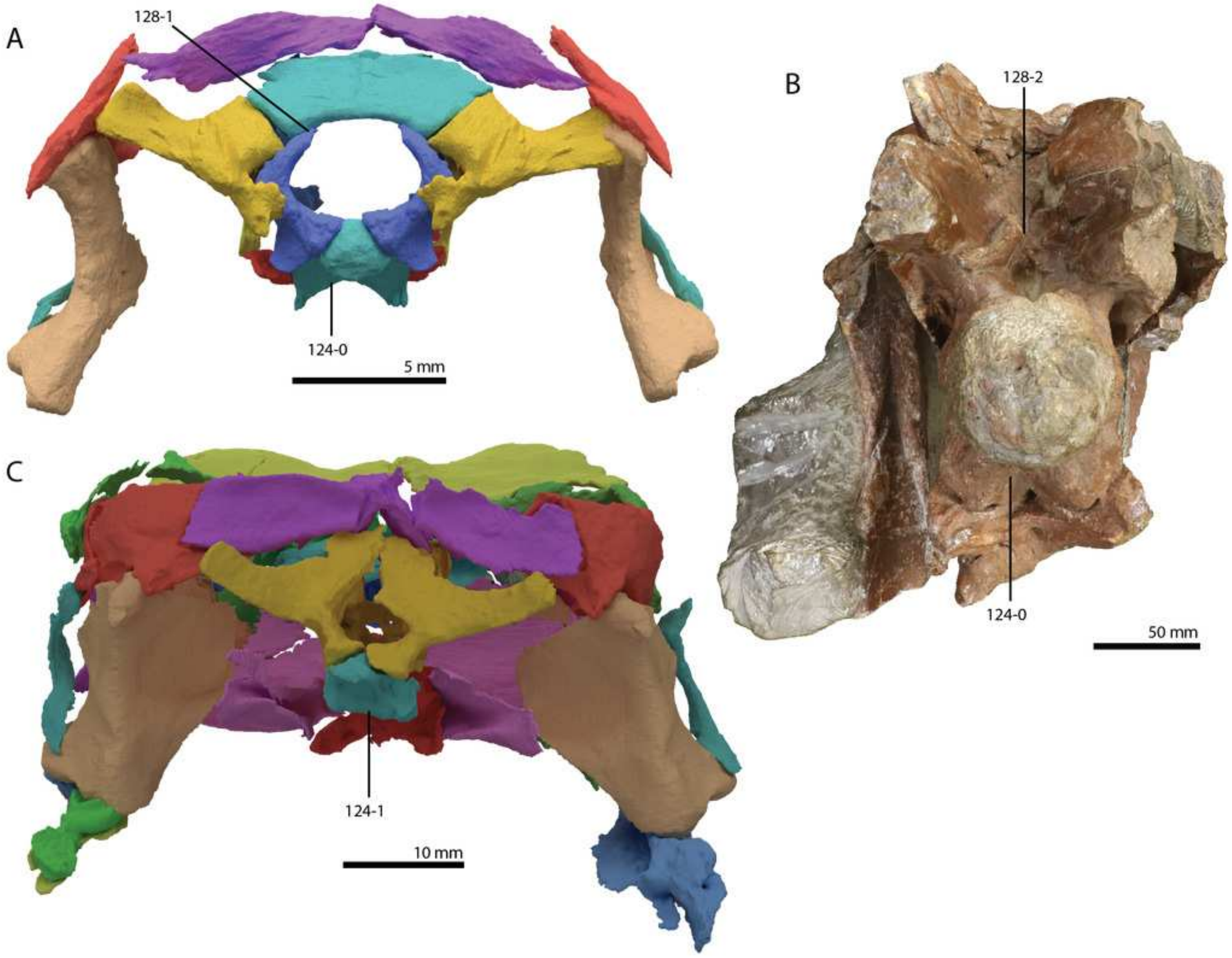

Figure 17

Illustration of characters 133, 137, 138, 139, and 140

(*A*) 133-1 in *Prolacerta broomi* (BP/1/2675, partial braincase in angled right lateroposteroventral view). (*B*) 133-3, 137-1, 138-1, 139-1, 140-2 in *Erythrosuchus africanus* (BP/1/3893, partial braincase in angled right lateroposterior view). (*C*) 133-2, 137-0, 138-1, 139-0, 140-0 in a digital reconstruction of *Macrocnemus bassanii* (PIMUZ T 2477, braincase right lateral view). (*D*) 133-2, 137-0, 138-1, 139-1, 140-1 in a digital reconstruction of *Tanystropheus hydroides* (PIMUZ T 2790, braincase right lateral view).

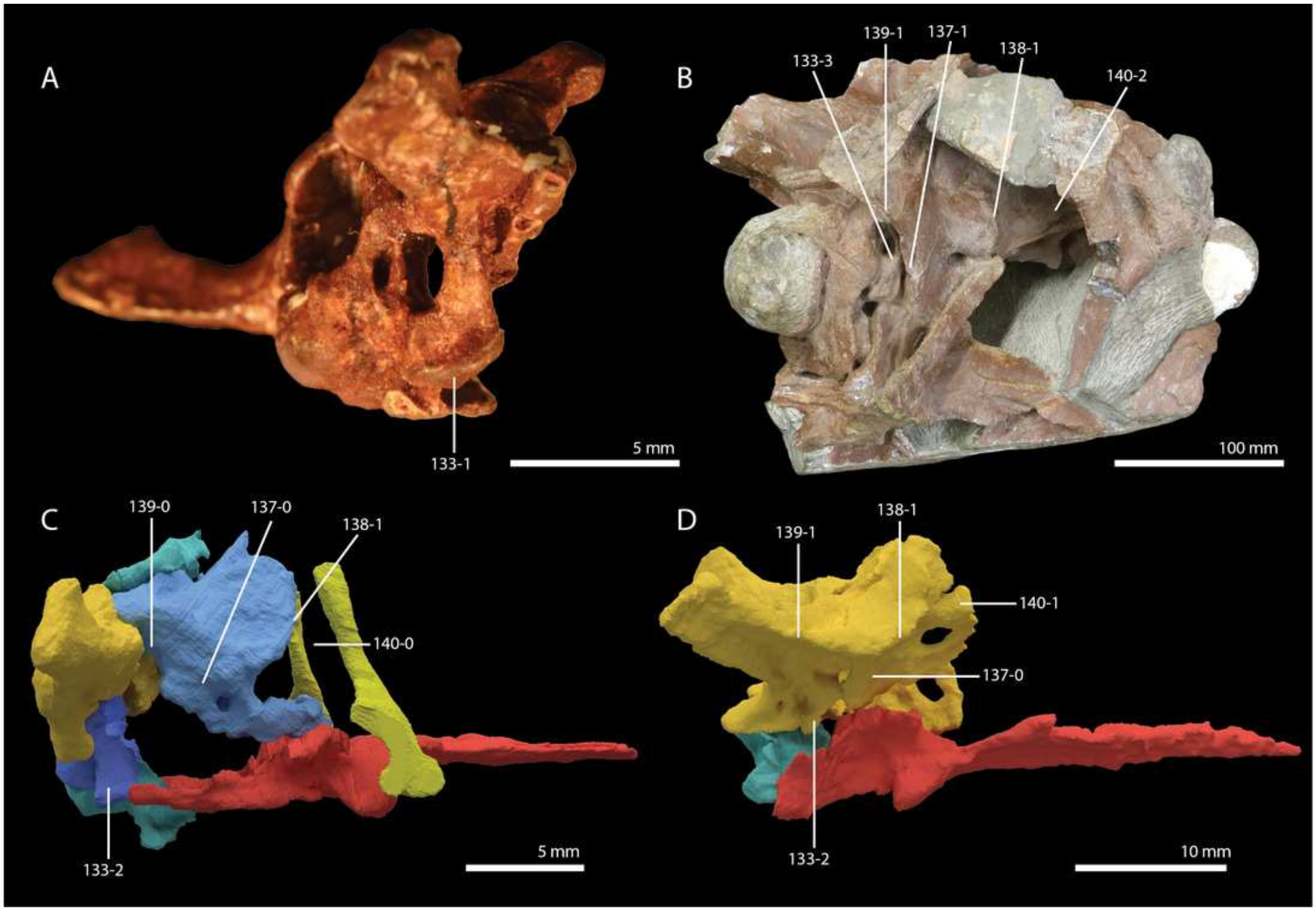

Figure 18

Illustration of characters 146, 158, 159, 161, and 165.

(*A*) 146-0, 158-0, 159-2, 161-0, and 165-0 in a digital reconstruction of *Macrocnemus bassanii* (PIMUZ T 2477, right lower jaw in lateral view). (*B*) 146-1, 158-1, 159-1, 161-1, and 165-1 in a digital reconstruction of *Tanystropheus hydroides* (PIMUZ T 2790, left lower jaw in lateral view).

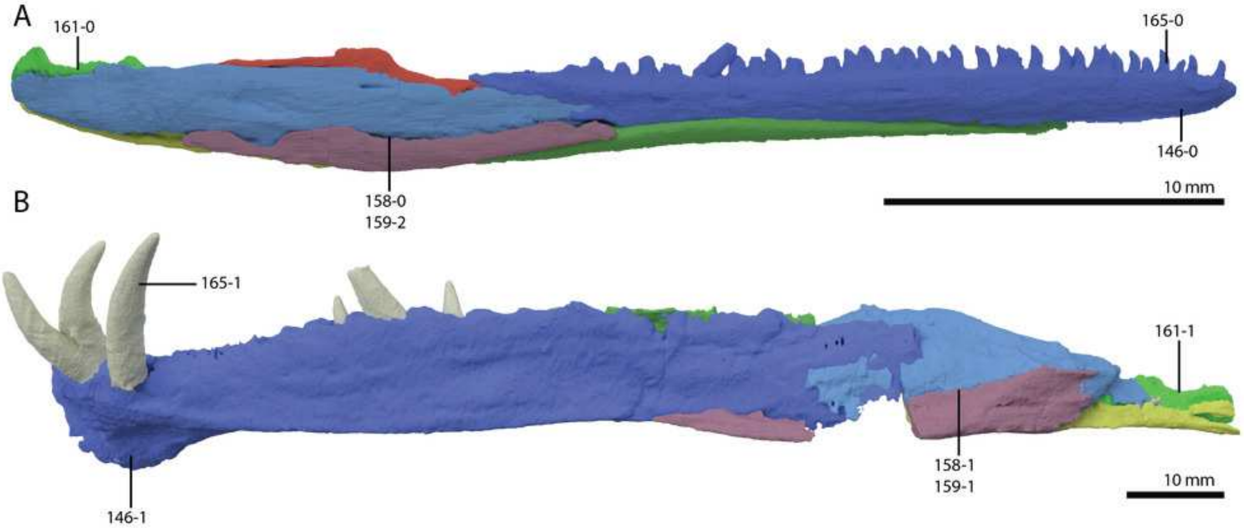

Figure 19

Illustration of character 178.

(*A*) State 4 in *Sclerostropheus fossai* (MCSNB 4035, mid-cervical vertebra in right lateral view). (*B*) State 3 in *Tanystropheus hydroides* (PIMUZ T 2819, mid-cervical vertebrae in left lateral view). (*C*) State 2 in *Fuyuansaurus acutirostris* (IVPP V17983, mid-cervical vertebrae in left lateral view). (*D*) State 0 in *Youngina capensis* (BP/1/3859, anterior cervical vertebrae right lateral view).

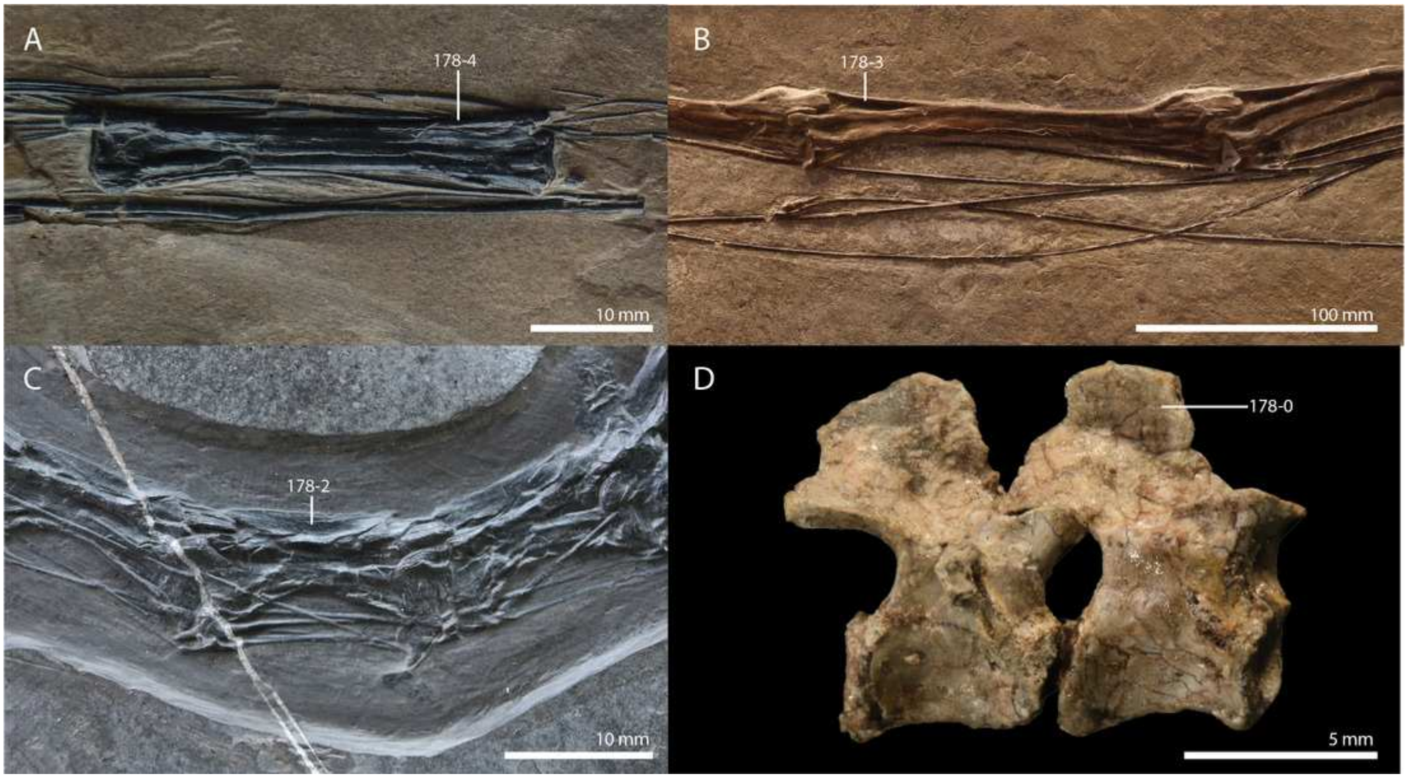

Figure 20

Illustration of characters 179 and 180.

(*A*) 179-1 and 180-2 in *Macrocnemus fuyuanensis* (IVPP V15001, anterior cervical vertebrae in right lateral view). (*B*) 179-0 and 180-0 in *Mesosuchus browni* (SAM-PK-5882, anterior cervical vertebrae in left lateral view).

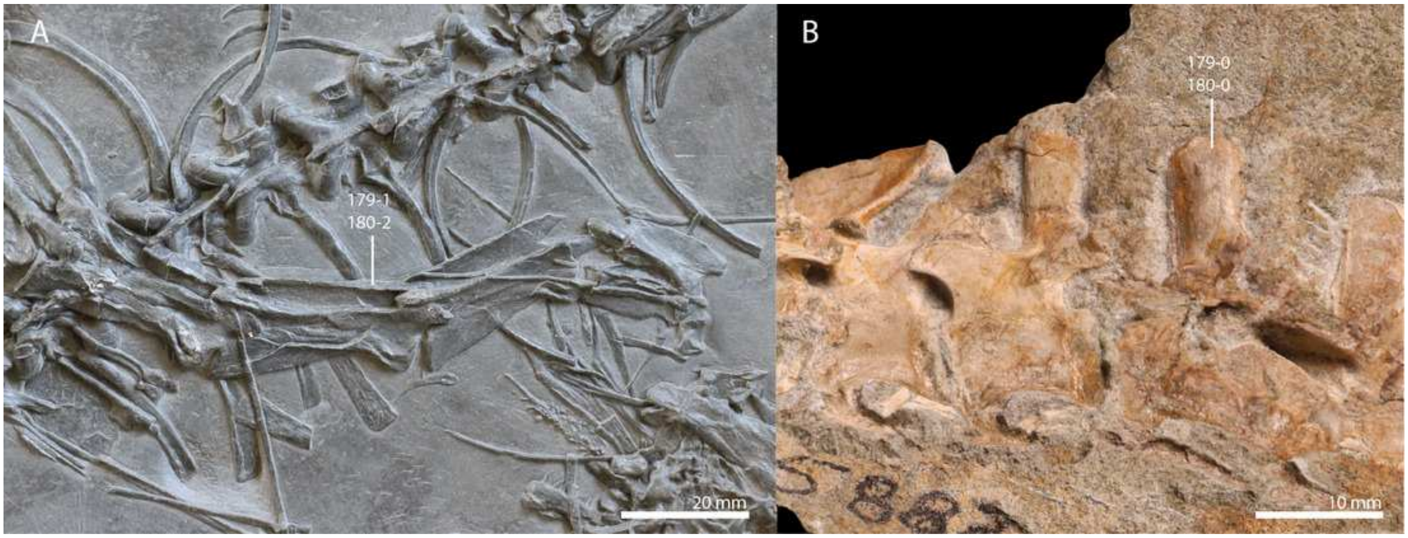

Figure 21

Illustration of character 184.

(*A*) State 1 in a digital reconstruction of *Tanystropheus hydroides* (PIMUZ T 2790, atlas-axis complex in right lateral view). (*B*) State 0 in a digital reconstruction of *Macrocnemus bassanii* (PIMUZ T 2477, atlas-axis complex in left lateral view).

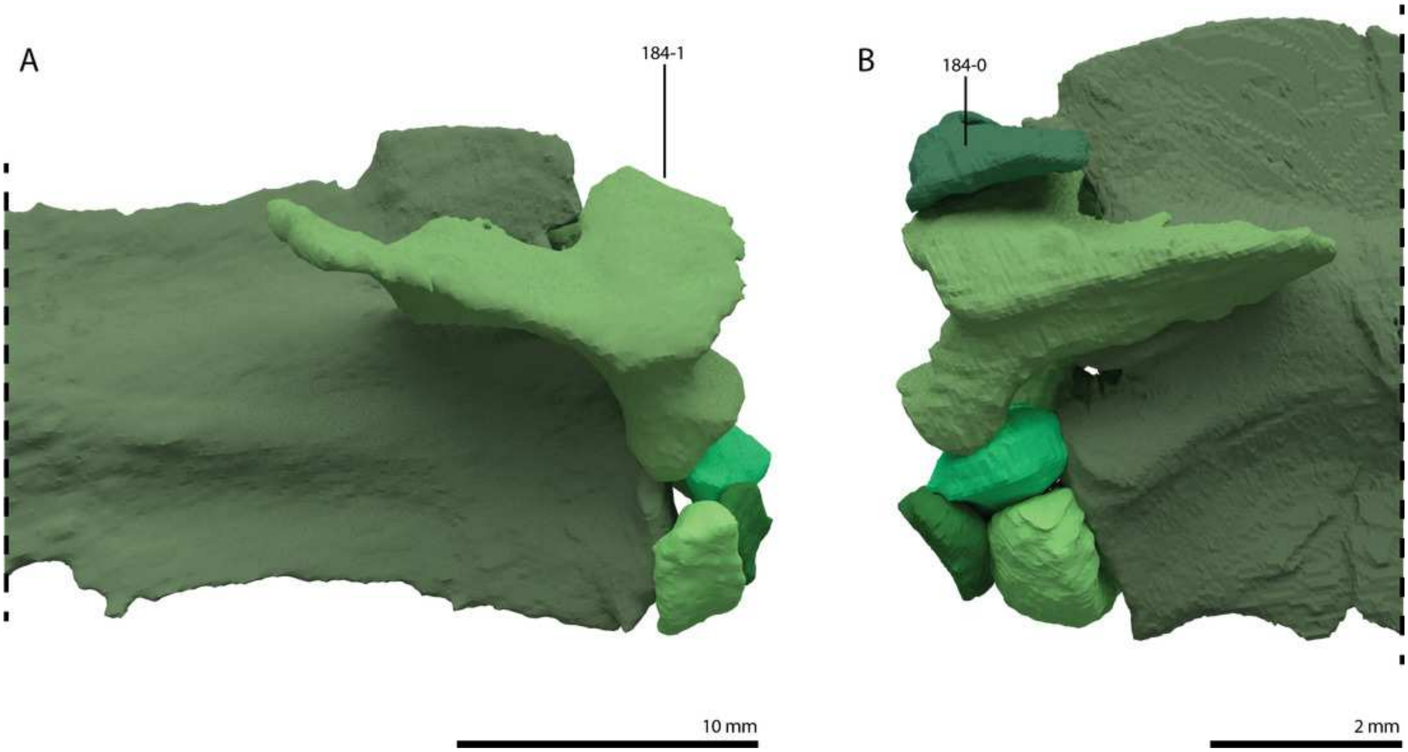

Figure 22

Illustration of character 191.

(*A*) State 0 in *Protorosaurus speneri* (WMsN P 47361, posterior cervical vertebrae in right lateral view). (*B*) State 1 in *Tanystropheus "conspicuus"* (U-MO BT 733, posterior part of mid-cervical vertebra in right lateral view).

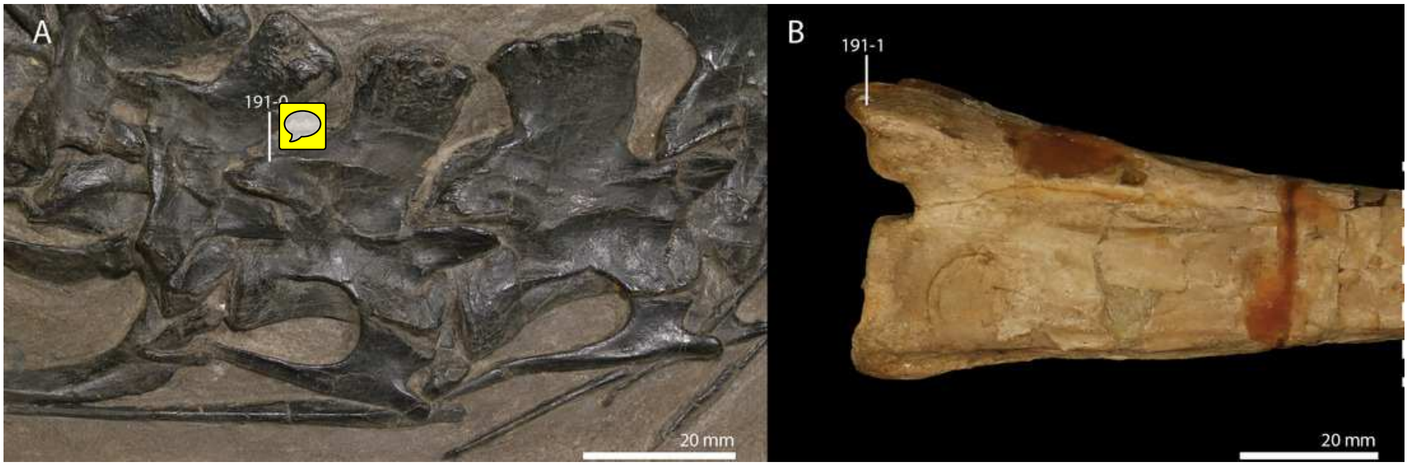

Figure 23

Illustration of character 192.

(*A*) State 0 in *Pamelaria dolichotrachela* (ISIR 316, anterior cervical vertebra in dorsal view). (B) State 1 in *Tanystropheus "conspicuus"* (U-MO BT 740, posterior part of mid-cervical vertebra in dorsal view). Image of *Pamelaria dolichotrachela* courtesy of Martín Ezcurra.

Figure 24

Illustration of character 196.

(*A*) State 0 in *Youngina capensis* (BP/1/3859, anterior cervical vertebra in ventral view). (*B*) State 1 in *Tanystropheus “conspicuus”* (U-MO BT 733, partial cervical vertebra in ventral view).

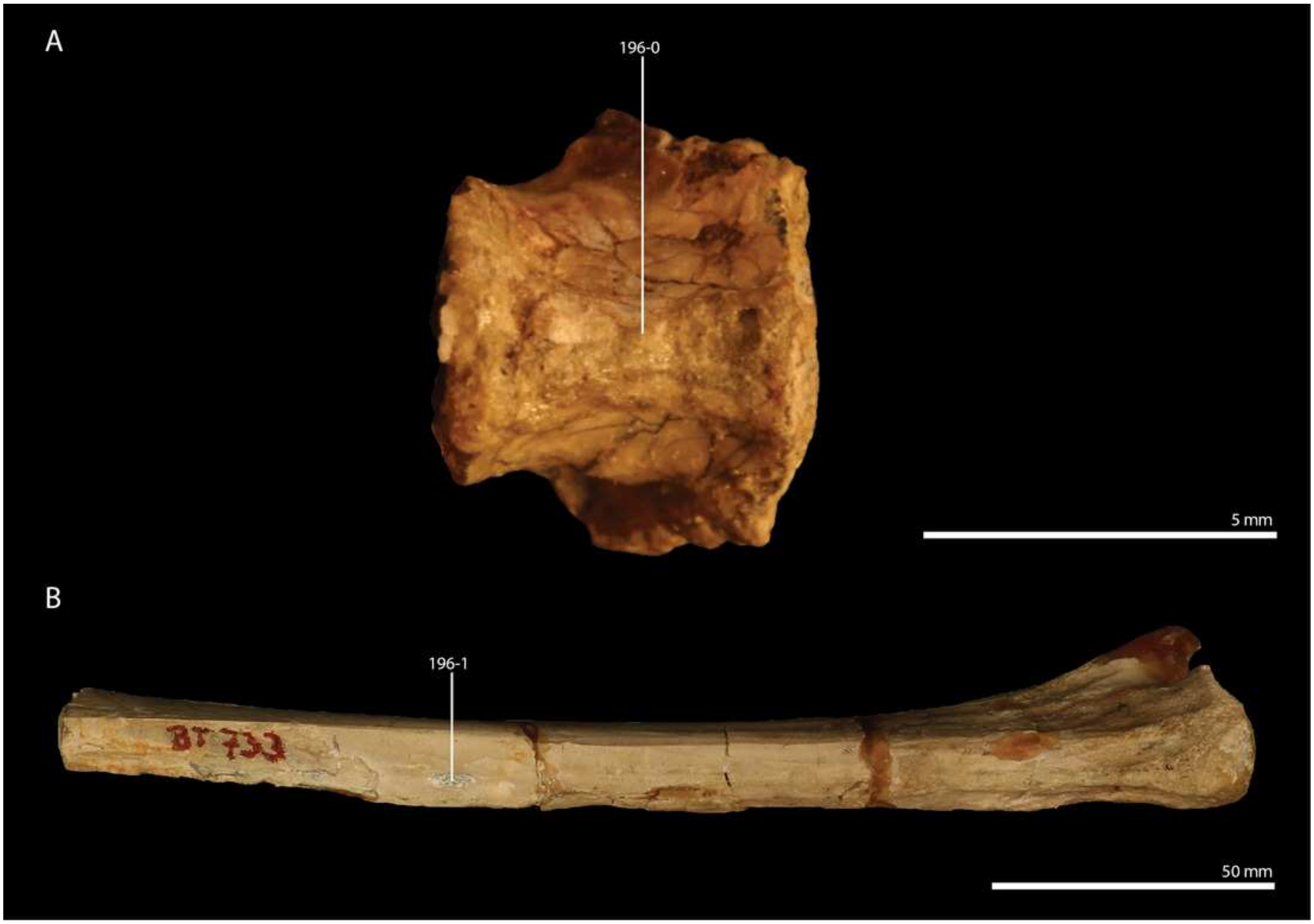

Figure 25

Illustration of characters 199 and 200.

(*A*) 199-2 and 200-1 in *Tanystropheus longobardicus* (PIMUZ T 3901, skull and partial cervical column in left lateral view). (*B*) 199-1 and 200-2 in *Tanytrachelos ahynis* (VMNH 120346a, partial skeleton including cervical column, cervical column in left lateral view). (*C*) 199-2 and 200-2 in *Pectodens zhenyuensis* (IVPP V18578, skull and cervical column in right lateral view).


A
200-1
199-2
20 mm
B
199-1
200-2
10 mm
C
199-2
200-2
10 mm

Figure 26

Illustration of characters 202 and 203.

(*A*) 202-1 and 203-2 in *Tanystropheus longobardicus* (PIMUZ T 1277, disarticulated anterior dorsal vertebrae, indicated vertebra in angled left dorsolateral view). (*B*) 202-0 and 203-1 in *Mesosuchus browni* (SAM-PK-6046, dorsal vertebral column in left lateral view). (*C*) 202-0 and 203-0 in *Euparkeria capensis* (SAM-PK-6047A, dorsal vertebral column in right lateral view).

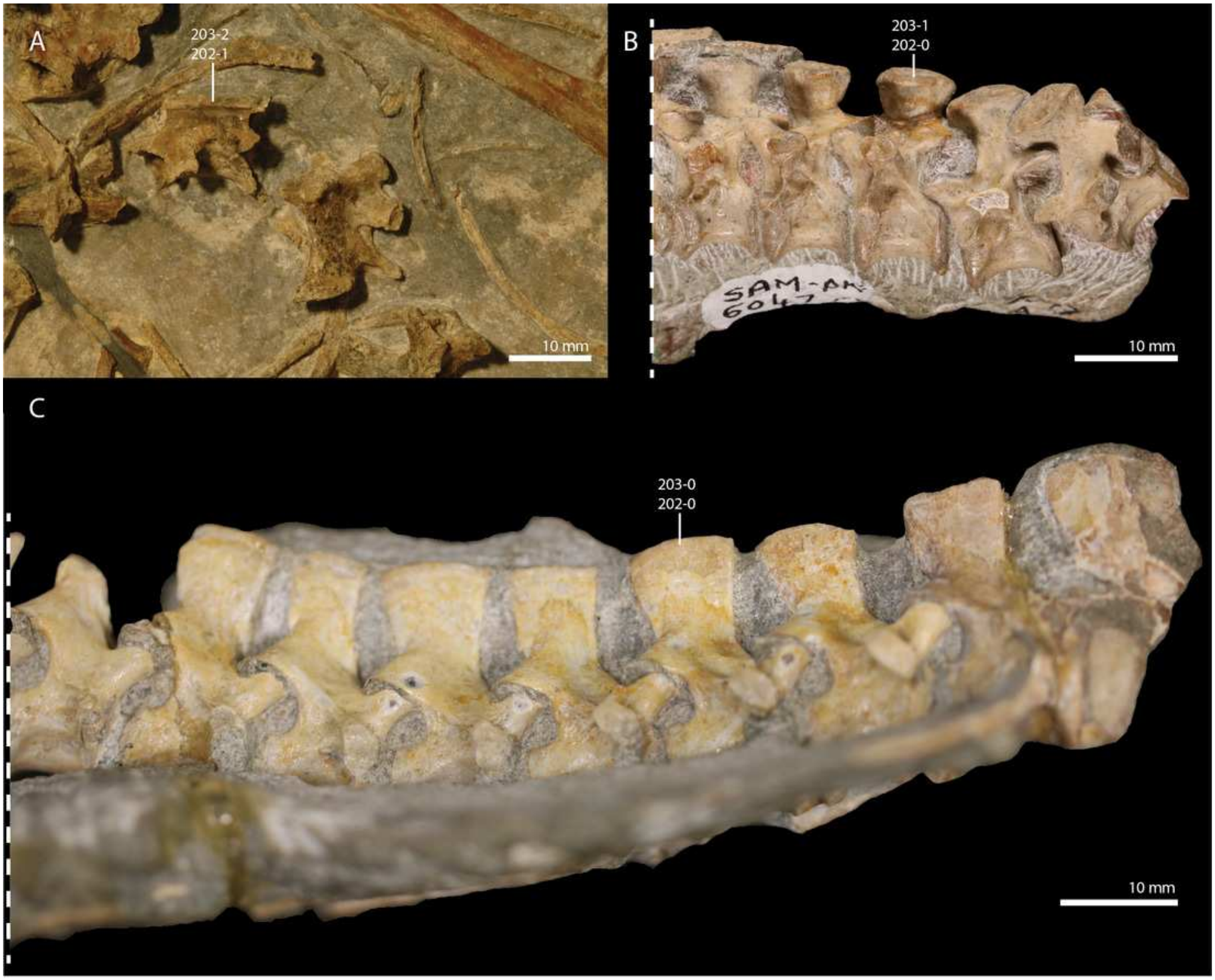

Figure 27

Illustration of character 224

(*A*) State 0 in *Protorosaurus speneri* (WMsN P 47361, largely complete skeleton in right lateral view, scale bar in cm). (*B*) State 1 in *Pectodens zhenyuensis* (IVPP V18578, largely complete skeleton, largely in ventral view).

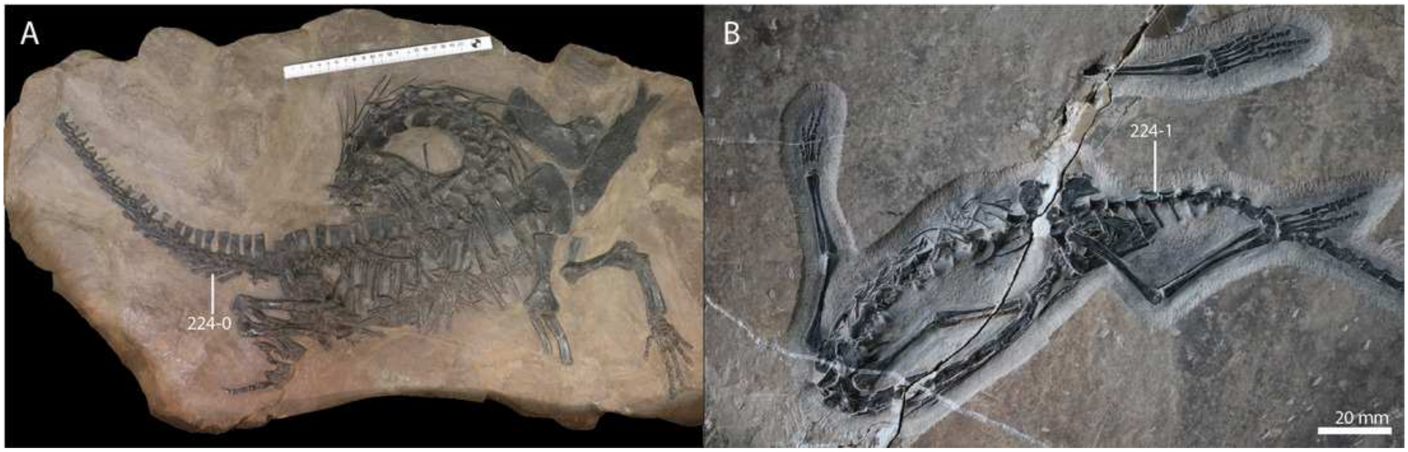

Figure 28

Illustration of character 225 state 1 in *Tanytrachelos ahynis* (VMNH 120013, largely complete skeleton exhibiting heterotopic bones).

Figure 29

Illustration of characters 227 and 228.

(*A*) 227-2 and 228-1 in *Tanystropheus longobardicus* (PIMUZ T 1277, left scapulocoracoid in medial view). (*B*) 227-0 and 228-0 in *Protorosaurus speneri* (WMsN P 47361, right scapulocoracoid in lateral view). (*C*) 227-1 and 228-0 in *Euparkeria capensis* (SAM-PK-5867, partial articulated skeleton including pectoral girdle in angled right lateroventral view).


A
228-1
227-2
10 mm
B
228-0
227-0
50 mm
C
228-0
227-1
50 mm

Figure 30

Illustration of characters 266 and 278.

(*A*) 266-0 and 278-1 in *Macrocnemus fuyuanensis* (IVPP V15001, right half of the pelvic girdle in medial view). (B) 266-1 in *Tanystropheus longobardicus* (PIMUZ T 1277, right ilium in medial view). (C) 278-0 *Tanystropheus hydroides* (PIMUZ T 2817, ischia in lateral view).

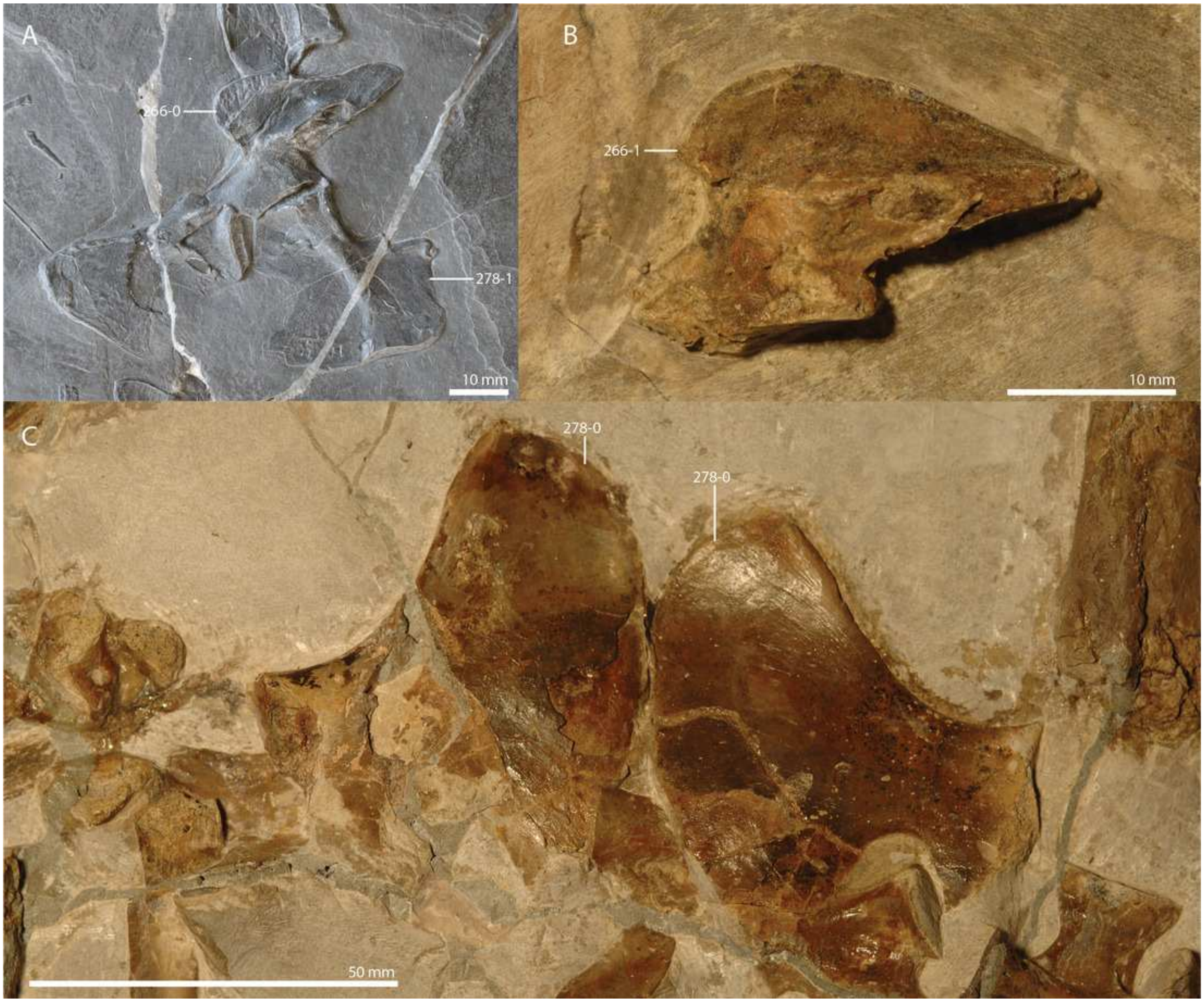

Figure 31

Strict consensus trees of analysis 1 (specified characters ordered; all taxa included in iteration A and all taxa except for "*Tanystropheus antiquus*" included in iteration B).

(A) Strict consensus tree of 1132 MPTs with 1177 steps of analysis 1 including "*Tanystropheus antiquus*". *(B)* Strict consensus tree of 587 MPTs with 1173 steps of analysis 1 excluding "*Tanystropheus antiquus*". Bremer values above 1 and Bootstrap frequencies above 50% are provided above and below each node, respectively.

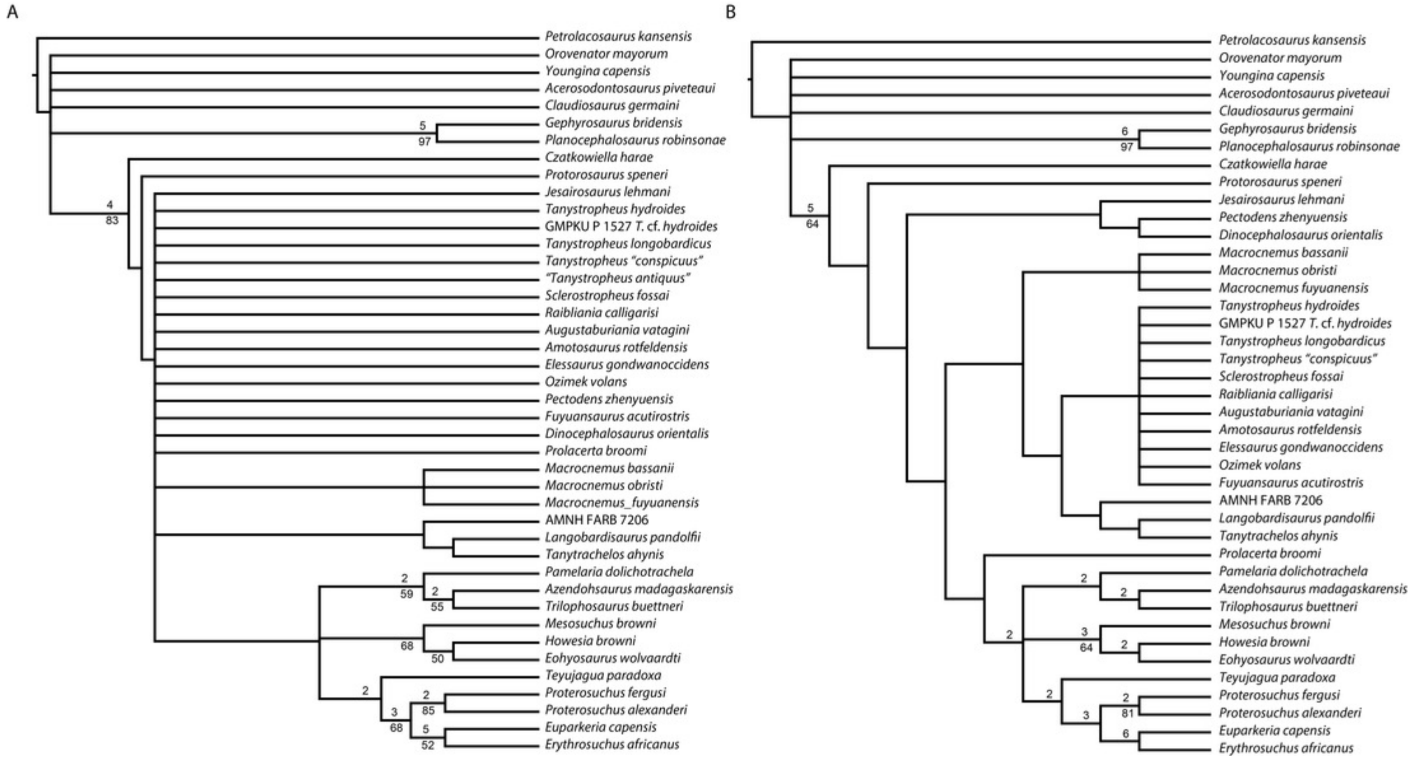

Figure 32

Strict consensus trees of analysis 2 (all characters unordered and ratio characters have been excluded; all taxa included in iteration A and all taxa except for "*Tanystropheus antiquus*" included in iteration B).

(A) Strict consensus tree out of 1646 MPTs with 974 steps of analysis 2 including "*Tanystropheus antiquus*". *(B)* Strict consensus tree of 1996 MPTs with 971 steps of analysis 2 excluding "*Tanystropheus antiquus*". Bremer values above 1 and Bootstrap frequencies above 50% are provided above and below each node, respectively.

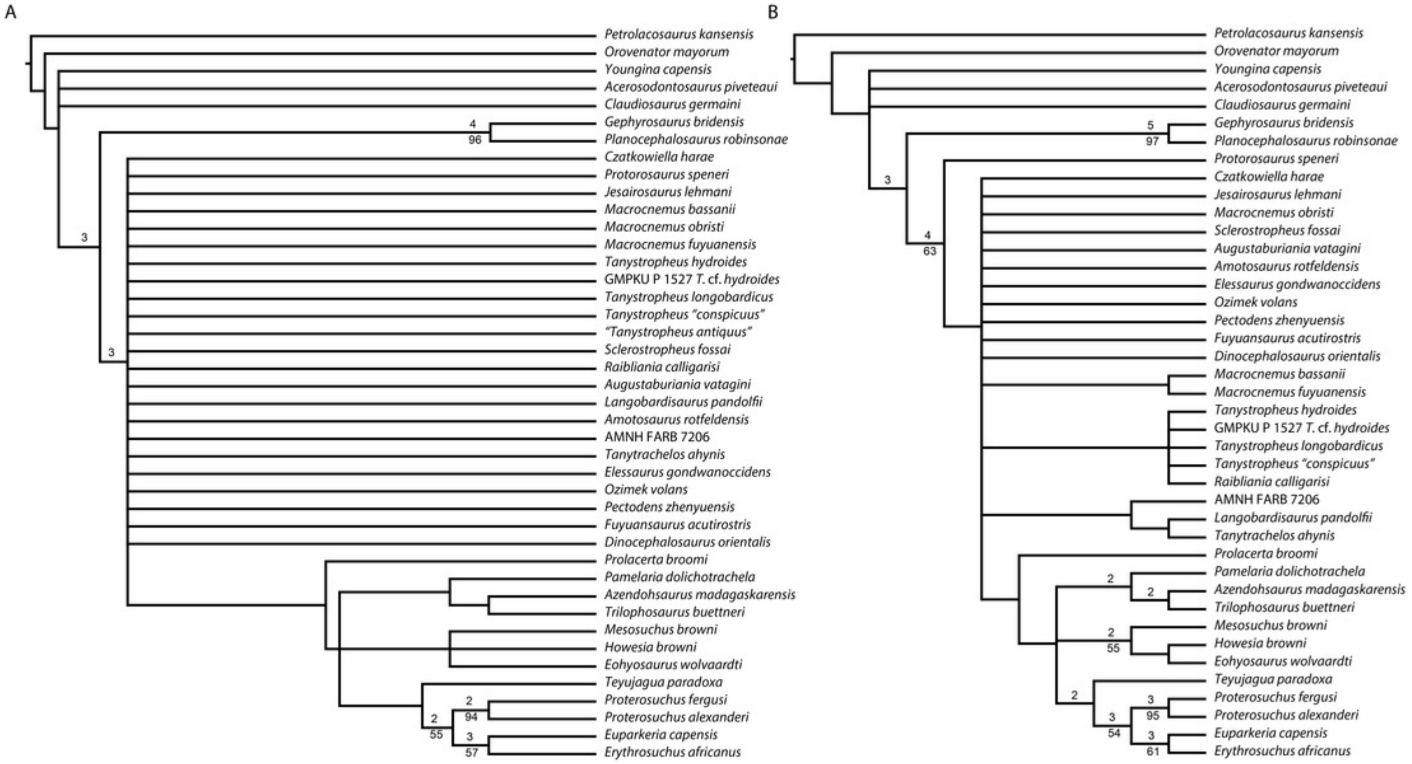

Figure 33

Strict consensus tree out of 11 MPTs with 1096 steps of analysis 3 (specified characters ordered; specified taxa pruned).

Bremer values above 1 and Bootstrap frequencies above 50% are provided above and below each node, respectively.

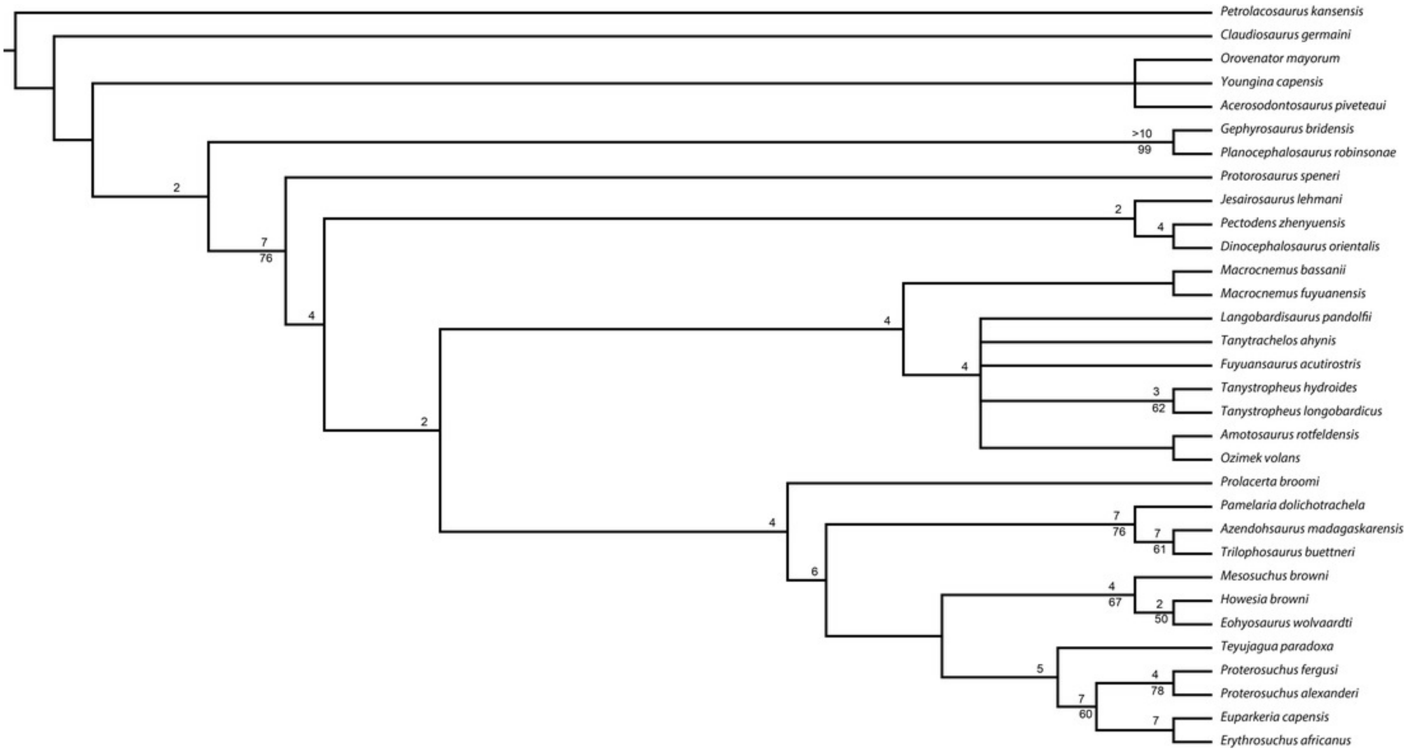

Figure 34

Strict consensus tree out of a single MPT with 934 steps of analysis 4 (all characters unordered and ratio characters have been excluded; specified taxa pruned).

Bremer values above 1 and Bootstrap frequencies above 50% are provided above and below each node, respectively.

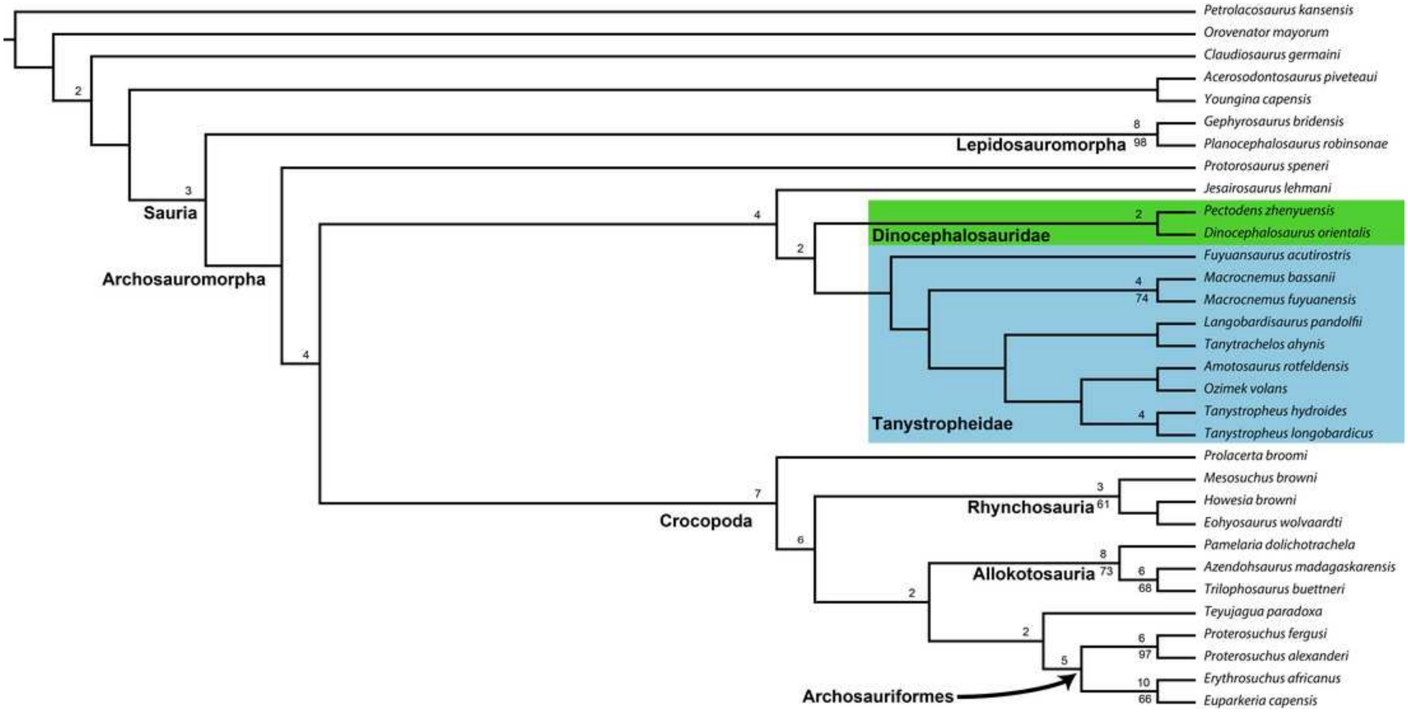

Figure 35

Time-calibrated phylogenetic tree based on the relationships recovered in analysis 4.

The black boxes indicate the possible temporal range of each OTU based on the available stratigraphic information (e.g. the age of Member II of the Guanling Formation, from which the only known specimen of *Pectodens zhenyuensis* is known, cannot be further restricted than being of Anisian age, and therefore the possible temporal range of *Pectodens zhenyuensis* covers the complete Anisian). The non-saurian diapsid taxa *Petrolacosaurus kansensis* and *Orovenator mayorum* from the Carboniferous and Early Permian, respectively, are not indicated to since they are considerably older than the other taxa of this study. Their phylogenetic position is indicated in Figure 34. The timescale based on the International Chronostratigraphic Chart of the International Commission on Stratigraphy (accessed May 2020).